University of Bath

PHD

Lectin affinity chromatography of monosaccharides

Santori, Fabio

Award date:
2002

Awarding institution:
University of Bath

Link to publication

Alternative formats
If you require this document in an alternative format, please contact:
openaccess@bath.ac.uk

Copyright of this thesis rests with the author. Access is subject to the above licence, if given. If no licence is specified above, original content in this thesis is licensed under the terms of the Creative Commons Attribution-NonCommercial 4.0 International (CC BY-NC-ND 4.0) Licence (https://creativecommons.org/licenses/by-nc-nd/4.0/). Any third-party copyright material present remains the property of its respective owner(s) and is licensed under its existing terms.

Take down policy
If you consider content within Bath's Research Portal to be in breach of UK law, please contact: openaccess@bath.ac.uk with the details. Your claim will be investigated and, where appropriate, the item will be removed from public view as soon as possible.

Download date: 06. May. 2023

To My Grandfather

Lectin Affinity Chromatography of Monosaccharides

Submitted by Fabio Santori

For the degree of PhD

To the University of Bath

2002

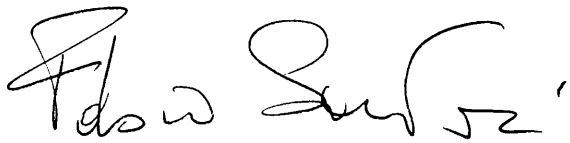

COPYRIGHT

Attention is drawn to the fact that the copyright of this thesis rests with its author. This copy of the thesis has been supplied on the condition that anyone who consults it understood to recognise that its copyright rests with its author and that no quotation from the thesis and no information derived from it may be published without the prior written consent of the author.

This thesis may be available for consultation within the University Library and may be photocopied or lent to other libraries for the purpose of consultation.

UMI Number: U601810

All rights reserved

INFORMATION TO ALL USERS
The quality of this reproduction is dependent upon the quality of the copy submitted.

In the unlikely event that the author did not send a complete manuscript
and there are missing pages, these will be noted. Also, if material had to be removed,
a note will indicate the deletion.

UMI U601810
Published by ProQuest LLC 2013. Copyright in the Dissertation held by the Author.
Microform Edition © ProQuest LLC.
All rights reserved. This work is protected against
unauthorized copying under Title 17, United States Code.

ProQuest LLC
789 East Eisenhower Parkway
P.O. Box 1346
Ann Arbor, MI 48106-1346

UNIVERSITY OF BATH
LIBRARY
75 20 NOV 2002
Ph.D.

Acknowledgements

I would like to thank my supervisor Dr. John Hubble for his invaluable help, professional advice, support and encouragement throughout my work.

My thanks are also due to the Department of Chemical Engineering as a whole, administrative and technical staff; in particular Ms. Elaine Odgers and Mr. Fernando Acosta for their constant support, as well as all my fellow students and friends I met during the time spent in Bath. The author is grateful to Dr. Maurizio Varrone and Dr. Dimitrios Hatziantoniou for the interesting and constructive scientific conversations.

The generous financial support, provided by the project sponsor DANISCO (Cultor), is also gratefully acknowledge.

Abstract

This project investigates the potential of a new technology for the separation of low molecular weight carbohydrates, based on lectins as a specific adsorption media.

The basis of Lectin Affinity Chromatography (LAC) for monosaccharide separation and the mechanism of lectin-monosaccharide interactions are investigated using Concanavalin A (ConA), a widely studied legume lectin, purified from jack bean.
These studies showed that lectin-monosaccharide interactions lie in the weak affinity and low capacity range. The system was successfully exploited for chromatographic monosaccharide separation under isocratic conditions and increased capacities were also observed in comparison with theoretical values.

The final objective was to evaluate the possibility of using LAC integrated in a bio-refining process, to add value by allowing the purification of rare sugars from sugar beet waste streams. The target is a rare aldohexose, L-fucose, which has a number of potentially useful applications. To this end, one L-fucose binding lectin was chosen; Lotus Tetragonolobus (LTA) was purified from winged beans and its interaction with L-fucose characterised.
On an analytical column chromatography scale, immobilised LTA was effective for L-fucose separation.

LTA was also used as a specific carrier in a size exclusion column operating in desalting mode. This approach named Low Affinity Pair Size Exclusion Chromatography (LAPSEC) offers a low cost alternative to packed bed affinity chromatography.
A simple multi-stage equilibrium model was developed to examine the potential of LAPSEC and to identify the key parameters involved. The simulations show good agreement with the experimental results and predict the range of applicability of the LAPSEC approach.

Speculations on the feasibility of these processes for application on a preparative scale and attempts to outline a simple scale up procedure were made. Productivity was estimated and the system capacity and mobile phase flow rate identified as key parameters for productivity and throughput optimisation.

Contents

Table of Symbols

a	[mm^{-1}], Interface area per void volume of particles.
a_{ir}	Activity coefficient.
A_s	Peak asymmetry.
c	Wiseman parameter (ITC).
C *or* C_m	[M], Solute concentration in the mobile phase.
C_o	[M], loading solute conc. in frontal chromatography.
C_s	[M], Solute concentration in the stationary phase.
D_m	[$mm^2 \cdot s^{-1}$], Solute Diffusivity in the mobile phase.
D_x	[$mm^2 \cdot s^{-1}$], Axial dispersion coefficient.
d_p	[mm], Particle diameter.
f_a	Sugar injection volume fraction.
F_i	Fractions of solute bound to i^{th} binding site population.
f_p	Lectin injection volume fraction.
F_r	[$ml \cdot min^{-1}$], Volumetric flow rate.
G	[$cal \cdot mol^{-1}$], Gibbs free energy.
H	[cm], High equivalent to a theoretical plate.
K	Equilibrium constant.
K_f	Freundlich isotherm adsorption constant.
K_p	Partition coefficient.
K_a	[M^{-1}], Association constant.
K_{ai}	[M^{-1}], Apparent association constant, multiple binding site system.
K_{ai}^o	[M^{-1}], Intrinsic association constant, multiple binding site system.
K_d	[M], Dissociation constant.
k_{on}	[$l \cdot mol^{-1} \cdot s^{-1}$], Adsorption rate constant.
k_{off}	[s^{-1}], Desorption rate constant.
k'	Capacity factor.
k_1'	Capacity factor of first eluted solute.
k_2'	Capacity factor of second eluted solute.
k_f	[$mm \cdot s^{-1}$], Interface mass transfer coefficient.
k_o	Ratio of intraparticle void volume on external void volume.
L	[mm], Column bed length.
L_s	Number of loading steps.
M	[M], Macromolecule concentration
M_t	[M], Bound and free Macromolecule concentration
N	Number of Theoretical Plates.
N_{eff}	Effective Number of Theoretical Plates.
n	Number of binding site per promoter or Stoichiometry of binding.
n_s	Moles of solute in the stationary phase.
n_m	Moles of solute in the mobile phase.
n_i	Final number of moles after adsorption.
n_{io}	Initial number of moles.
nf	Freundlich isotherm adsorption constant.
P	[$M \cdot s^{-1}$], Productivity.
q	[M], adsorbate concentration per volume unit of adsorbent.
q_{max}	[M], maximum binding capacity.
Q_r	Purity ratio
Q	[$cal \cdot mol^{-1}$], Isothermal heat of binding.
Q_a	[$cal \cdot mol^{-1}$], Adiabatic heat of binding.

R	Resolution.
R	Constant = 1.986 cal·mol^{-1} ·K^{-1}.
R^{SPR}	[RU], SPR response.
$R^{SPR}_{\max}$	[RU], Maximum binding capacity in SPR units
$R^{SPR}_{eq.}$	[RU], SPR equilibrium response.
s	Radius of gyration.
T	[°C], Temperature.
t_{cycle}	Time required to complete one entire chromatographic cycle.
t_e	Retention time relative to the external void volume (V_e).
t_{nr}	Retention time for non-retained solute.
t_r	Retention time for retained solute.
u_s	[cm·h^{-1}], Mobile phase superficial velocity.
u_{si}	[cm·h^{-1}], Solute superficial velocity.
V_{bed}	[ml], Column bed volume.
V_{cell}	[ml], Cell Volume (ITC).
V_e	[ml], External void volume.
V_{inj}	[ml], Injection volume.
V_m	[ml], Mobile phase volume.
V_{nr}	[ml], Retention volume for non retained solute.
V_p	[ml], Pores void volume.
V_r	[ml], Retention volume for retained solute.
V_s	[ml], Stationary phase volume.
W	[min or ml], Base peak width.
X	[M], Ligand concentration.
X_t	[M], Bound and free Ligand concentration
Y	Occupied binding sites fraction.
ΔC_p	[cal· mol^{-1} ·K^{-1}], Excess of heat capacities.
ΔG	[cal· mol^{-1}], Gibbs free energy of binding.
ΔH	[cal·mol^{-1}], Enthalpy of binding.
ΔS	[cal·mol^{-1} ·K^{-1}], Entropy of binding.
Φ_o	Universal Constant.
α or α_{21}	Separation factor or selectivity.
α_s	Stationary phase volume fraction (=1-ε)
γ	Obstruction factor.
ε	Interparticle (mobile phase) void fraction.
ε_p	Intraparticle void fraction.
η	[cp], Viscosity.
$[\eta]$	Intrinsic viscosity.
λ	Particle geometric factor.
ν	[cm^2/s], Kinematic viscosity.
μ_i	Single species potential.
ξ	Extent of adsorption reaction.
ρ	[mg·l^{-1}], Solution density.
σ	Standard deviation.
σ^2	Variance.
χ^2	Least-square norm.
ω	Porosity function.

Abbreviations

AAL	Aleuria Aurantia Lectin
AC	Affinity Chromatography
Ara	Arabinose
c.e.	Crude Extract
ConA	Concanavalin A Lectin
BSA	Bovine Serum Albumin
DC	Displacement Chromatography
EDC	N-ethyl-N'-(dimethyl-aminopropyl)-carbodiimide
EDTA	Ethylenediaminetetraacetic acid
FC	Frontal Chromatography
FPLC	Fast Protein Liquid Chromatography
Fru	Fructose
Fuc	Fucose
Gal	Galactose
Glc	Glucose
GlcNAc	N-Acetylgalactosamine
HETP	Height Equivalent to a Theoretical Plate
HPLC	High Performance Liquid Chromatography
HPMA	N-(2-hydroxypropil) methacrylamide
ITC	Isothermal Titration Calorimeter
LAPSEC	Low Affinity Pair Size Exclusion Chromatography
LAC	Lectin Affinity Chromatography
LTA	Lotus Tetragonolobus Lectin
Man	Mannose
mdg	metyl-α-D-glucopyranoside
mdm	metyl-α-D-mannopyranoside
MW	Molecular weight
NHS	N-hydroxysuccinimide
papf	p-aminophenil α-L-fucopyranoside
PBS	Phosphate Buffer Saline
pnpa	p-nitrophenil α-L-arabinopyranoside
pnpf	p-nitrophenil α-L-fucopyranoside
pnpg	p-nitrophenil α-D-glucopyranoside
pnpm	p-nitrophenil α-D-mannopyranoside
RI	Refractive Index
RU	SPR units
SDS	Sodium Dodecyl Sulphate.
SEC	Size Exclusion Chromatography
SPR	Surface Plasmon Resonance
SSL	Sulphite Spent Liquor
UEA I	Ulex Europeus Lectin
WAC	Weak Affinity Chromatography
Xyl	Xylose
ZC	Zonal Chromatography

Chapter I

Project Introduction and Objectives

1.1 Sugar beet

All plants contain sugar, but the sugar beet contains especially high levels and it is the only plant from which it is profitable to extract sugar in Europe. Beets were originally used directly as food until the end of the 18th century, when man began to extract sucrose from them. Sugar beets with higher sugar contents were cultivated by plant breeding, and the sugar beet became a raw material for industrial sucrose manufacture. Sucrose (α-D-glucopyranosyl-β-D-fructofuranoside) is commonly known as sugar, it is a disaccharide consisting of two monosaccharides, glucose and fructose (Figure 1.1), bound by a glycosydic link and is the most commonly used sweetener, both domestically and industrially. Saccharides with 2-9 monosaccharides are called oligosaccharides while polysaccharides (e.g.: starch and cellulose) are those with more than 10 units.

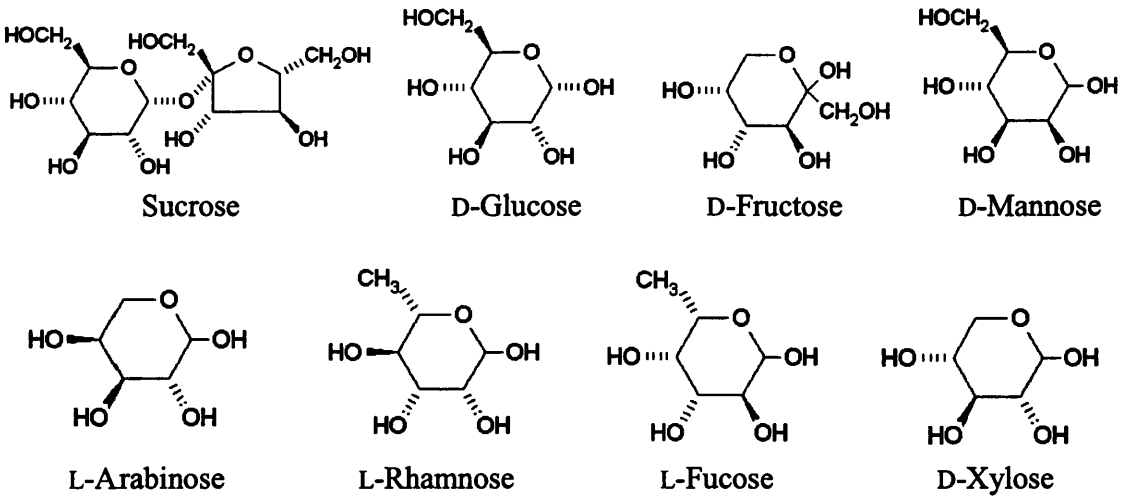

Figure 1.1: Planar structure of common sugars; sucrose and monosaccharides and some rare monosaccharides Five atom sugar ring name is ending with furanose, six atom rings are named by the ending pyranose.

1.2 Rare sugars: purification and market

Rare sugars are identified as small saccharides, naturally occurring in relatively low amounts. Some of those sugars (Figure 1.1) are monosaccharides (arabinose, rhamnose, fucose, xylose and xylitol, etc.) commercialised in either pure crystalline form or as blends in corresponding syrups. Some of them have already become very common, e.g. xylitol (sugar alcohol, hydrogenated form of xylose) with a well-established purification process and related market (chewing-gum, tooth paste, etc.). Xylitol has one-third fewer calories than conventional sugar and the same sweetening power, is mainly produced from bio-refining of Sulphite Spent Liquor (SSL) generated from cooking process of lignosolphonate.

Due to an increasing number of applications, rare sugars are gaining importance particularly within the flavour and pharmaceutical industry and improving the access to rare sugars is becoming a prominent goal. Biotechnology companies are raising capital to fund their bio-refinery to further process sugar beet pulp to produce sugar beet pectin, L-fucose, L-arabinose, carboxymethyl cellulose and other rare carbohydrates. Despite the low concentration of the target, the design of separation processes to manufacture and market these high-value added sugars, is potentially very attractive. Hemicellulose containing L-arabinose and L-fucose, in combination with the pectin fraction can be sold as a functional food additive and can be further processed to purify rare sugar and create more value. Van Thorre (2002) has recently patented a process by which L-arabinose is purified from hydrolysed sugar beet pulp hemicellulose using a chiral stationary phase within a continuous chromatographic process.

1.3 Chromatography for sugar separation

Candidates for generally dealing with oligosaccharides side streams are batch or column chromatography processes. The dark thick syrup, obtained from the crystallisation of sucrose, is known as molasses. It is a by-product of beet sugar manufacture containing 50% of sucrose. In 1983 Heikkilä published a simple method based on ion exchange

chromatography for the extraction of sucrose, with a capability of 50000 m.t./yr of molasses, 85-90% fraction recovery and with a low power consumption.
Although sugars present a challenge in terms of separation because of the small differences in their chemical and physical properties, there are several well-developed methods used today based on ion exchange, partition, reversed-phase and size exclusion chromatography. On the other hand, when the separation needs to be focused on one particular sugar present at low concentration in a complex mixture the easiest procedure is either to adsorb the target on a highly selective resin or to use a less selective adsorbent to bind the majority of the contaminants. High selectivity or specificity is the most important characteristic of affinity chromatography.

1.4 Lectins: a selective sugar targeting agent

Specific interactions form the basis of Affinity Chromatography and a large family of glycoproteins known as lectins offer the most attractive high-specificity carbohydrate binding agents currently available commercially (Merkle and Cummings, 1984). Immobilised lectins are used already in separation technologies for carbohydrates, glyconjugates, enzymes, immunoglobulines and cells (Singh *et al.*, 1999). Lectins are an heterogeneous group of proteins first described in 1888 by P. H. Stillmark who discovered haemagglutinating activity in castor bean extracts. Later, it was demonstrated that the agglutination properties of lectins were based on their specific recognition of, and reversible binding to, carbohydrates (mono- or oligosaccharides). Since then, numerous lectins have been isolated from plants, animals and micro-organisms and classified on the base of their carbohydrate specificity (Sharon and Lis, 1998). Carbohydrates interact with lectins through hydrogen bonds, metal coordination, van der Waals and hydrophobic interaction (Elgavish and Shaanan, 1997). Lectins are generally made up of one or more subunits in a multimer. If the subunits are identical the lectin has multiple binding sites recognising specific saccharides.

Legume lectins are a large family of homologous carbohydrate binding proteins that are found mainly in the mature seeds of most legume plants. They strongly differ from each other with respect to their carbohydrate-binding specificity (Sharon and Lisi, 1990). In fact

they have several different carbohydrate-binding specificities and on this basis a common classification is made (Liener *et al.*, 1986, Van Damme *et al.*, 1998):

- Mannose/glucose specific lectin.
- Galactose/N-acetylgalactosamine specific lectins.
- Chitobiose specific lectins.
- L-Fucose specific lectins.
- Finally there are examples of legume lectins which do not bind to any simple sugar but interact only with oligosaccharides.

The structure of legume lectins can present different degree of glycosylation. Their structure is based on subunits (monomers), which possess divalent cations, held in place by interactions with specific amino acid residues and essential for the carbohydrate binding activity (Lonnerdal *et al.*, 1983).

1.5 L-Fucose: production and uses

Fucan is a sulphated polysaccharide located in the cell walls of brown seaweed. Fucan extracts are viscous structurally very heterogeneous, generally with high molecular weights and composed of 3-branched (1 - 2) or (1 - 3) linked alpha-L-fucose-4-sulphate units (Chapman and Chapman 1980). Fucoidan is a high molecular weight fucan, found in the intercellular mucilage of rockweeds, the general formula is $(C_6H_9O_3SO_4Ca_{1/2})_n$, but several structural variations have been considered. A common methodology to obtain L-fucose is by hydrolysis of this polysaccharide extracted in acid conditions from seaweed (Takemura *et al.*, 1988). Chemical (Sarbajana *et al.* 1995) and enzymatic (Wong *et al.*, 1995) syntheses have also been reported. Microorganisms producing extra-cellular polysaccharides rich in L-fucose include a broad range of bacteria, fungi and algae as reported by Vanhoren and Vandame (1999) who investigated the production of L-fucose during submerged fermentation.

The growing effort around this monosaccharide and its sources is due to its numerous biological properties. For example, it has been shown that tumor cell colonisation of the

lung can be significantly inhibited using L-fucose or fucodian, for its specificity of pulmonary cell (Keida and Monsigny, 1986). L-fucose is also an indicator of colon carcinoma and brest cancer since it is over expressed in these malignancies (Listinsky *et al.*, 2001). It posses antithrombic, anti-inflammatory and antiviral activities, it plays important roles in memory formation-potentiation and in cosmetic it decreases the product's allergenic effects (Vanhoren and Vandame, 1999, Marquardt *et al.*, 1999, Matthies *et al.*, 2000).

1.6 Aim of the project

This project was conceived to investigate the possibility of using Lectin Affinity Chromatography (LAC) as a rare sugar purification technology. To this end, the biological foundation of lectin- monosaccharide interactions must be identified and the exploitation in chromatography investigated with process viability and productivity.

The project target is the purification of a rare monosaccharide L-fucose (6-deoxy-galactose, structure in Figure 1.1) by LAC from a defined mixture containing monosaccharides.

Chapter II

Theoretical Background

2.1 Summary

In this section, a theoretical introduction to those subjects and principles that are used in experimental work involved in this project, are described. Chromatography is the main area of interest with particular focus on affinity chromatography. Basic principles of chromatography and affinity chromatography are summarised with some of the most important literature reports. As biomolecular interactions represent the topic under investigation, equilibrium and thermodynamics of these interactions in chromatographic systems are described. Other systems used for studying and characterising these binding processes (isothermal titration micro-calorimeters and surface plasomn resonance) are also described. In summary this chapter focuses on describing the main tools used to identify and investigate lectin monosaccharide interactions with the introduction of simple mathematical approaches employed.

2.2 Chromatography: principles and methods

A mixture of substances to be separated is applied in solution (liquid) to a support medium. This may be paper, a layer of silica or a column packed with an adsorbent (solid or liquid). This work is focused on liquid chromatography using columns packed with solid adsorbent. Liquid column chromatography is a separation process whereby the liquid mixture carried by a mobile phase flows through a column filled with adsorbent or molecular sieve gel (stationary phase).

A brief classification of the phenomena used in chromatography is given in Table 2.1, pointing out five main principles on which separation can be achieved (Cozzi *et al.*, 1987). The separation is based on the different partition for each mixture component between the two phases involved; if q is the solute stationary phase concentration, and C the mobile phase concentration, the partition coefficient K_p is defined as follows;

$$K_p = \frac{q}{C} \tag{2.1}$$

Table 2.1: Main separation principles of Chromatography

ADSORPTION	Interaction between the solute and a functional group present on the surface of a solid adsorbent.
PARTITION	Solutes partition themselves between the two usually liquid phases based on their individual partition coefficients.
ION EXCHANGE	Charged solutes are reversibly adsorbed on to an immobilised ion exchange group of opposite charge (IEC).
EXCLUSION	It is based on the size of sample in solution; larger molecules move faster, excluded from the pores of the packing material, smaller ones diffuse in and out the pores and move slower (SEC).
AFFINITY	Substances are selectively adsorbed onto an insoluble adsorbent by biospecific interactions with a particular functional group or whole-immobilised molecule (AC).

2.2.1 Practical methods and chromatographic techniques

Column chromatography can be carried out following three different methodologies:

1) Zonal Elution Method (ZC). Solute concentration is raised with a small amount of sample mixture fed into the column as a discrete slug. Separation is achieved in the form of "bands" and depends on the differential migration rate of the mixture components, i.e. selective retardation due to different degrees of solute affinity for the stationary phase.
It is used widely at analytical scale. As only a small fraction of the adsorbent capacity is occupied during separation, longer columns are usually required to achieve the separation

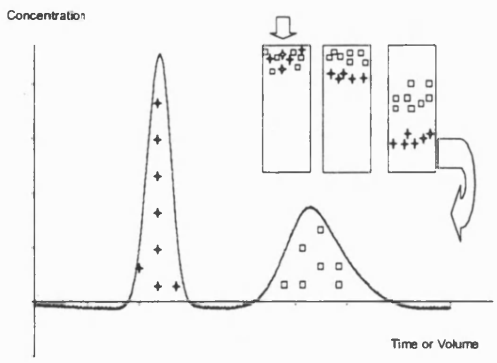

Figure 2.1: Separation of a bi-component mixture with chromatogram.

(Jonsson, 1987). HPLC (High Pressure Liquid Chromatography) and GC (Gas Chromatography) applications are two of the most common systems used for sample analysis, component mixture identification and quantification. Figure 2.1 shows the dynamic separation of a mixture of two solutes throughout the column and the resulting chromatogram of the two solute bands eluted from the column outlet.

2) Frontal Elution Method (FC). The stationary phase in the column is loaded with a constant feed solute concentration, solute is suddenly raised and maintained at a constant value until the chromatographic media is saturated and a complete breakthrough occurs (Figure 2.2).

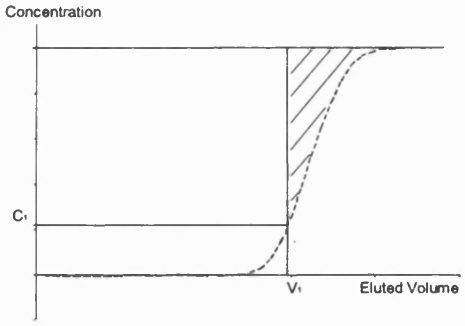

Figure 2.2: Sigmoid concentration profile of a typical breakthrough-curve.

The loaded column is then washed to remove unbound and weakly bound impurities. Finally the product is eluted by changing physical or chemical parameters in the system. This technique is used for large-scale separation since it allows extensive use of resin capacity and allows a smaller column.

Typically, to minimise the product loss, loading is terminated when the outlet concentration is only a fraction of the feed concentration (Dantigny *et al.*, 1991).

As shown for instance in Figure 2.2, after an eluted volume V_1, the total amount of solute loaded into the column is $V_1 \times C_1$, while the area underneath the curve represents what is lost in the column outlet, the red dotted area above the breakthrough is unused bed capacity. A different balance between losses and unused capacity is required depending on the situation.

3) Displacement Elution Method (DC). A relatively small sample is fed into the column, with the column capacity almost saturated during this step.

Then elution starts with a competitor containing eluent which has a higher affinity for the adsorbent than the sample. The sample component is forced out, or displaced, from the stationary phase and subsequently eluted highly concentrated. This approach is a good candidate for preparative purposes when the enrichment of trace substances is required (Freitag, 1999).

In analytical and semi preparative scale chromatography the emphasis is to acquire as much data as possible from the production of small amount of pure material. In preparative scale the process stream is usually well characterised and the emphasis shifts towards the purification of large amounts of material.

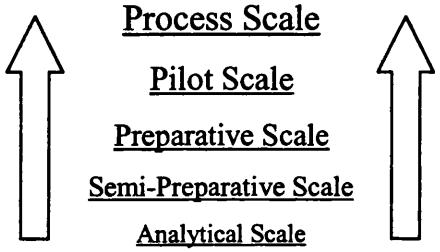

Figure 2.3 Chromatography working scales

Pilot and process scales deal with larger amounts of material and this is when costs become the major factor to be considered.

All preparative separations start with an analytical run (Figure 2.3), it is very important to evaluate at this stage the key parameters and features that describe the separation for use in scale up design.

2.2.2 Physical aspects and key parameters

Solid packing material can be porous or non-porous, the former is more common as it offers high capacity per unit volume. High porosity and large surface areas per gram of sorbent are the main characteristics of materials used commercially in chromatography. Considering a column operating in ZC, where the components of the mixture applied are separated depending on their size (SEC), their elution is identified by the time (t_r) or volume (V_r) required to pass through the bed. For porous packing materials, the total column bed volume (V_{bed}), the inter-particles liquid void volume (V_e) and the volume occupied by the stationary phase (solid + pores; $V_s = V_{bed} - V_e$) must be defined and ε, the column voidage, which mainly depends on the particle size, shape and column packing procedure, calculated.

$$\varepsilon = \frac{V_e}{V_{bed}} \tag{2.2}$$

Solutes, which can diffuse in and out the pores of the stationary phase, access a larger fraction of the bed volume and so are slower moving (t_r or V_r) than solutes which are totally excluded and elute earlier, carried by the mobile phase throughout the column void volume (t_e or V_e). The solute mass distribution between the stationary and mobile phase (n_s / n_m) is called the capacity factor, k' and can be expressed as the ratio of the time (or volume) that the average molecule spends in the two phases:

$$k' = \frac{n_s}{n_m} = \frac{t_r - t_e}{t_e} = \frac{V_r - V_e}{V_e} \tag{2.3}$$

Combining 2.1, 2.2 and 2.3 a practical expression for the partition or distribution coefficient is obtained;

$$k' = \frac{V_s}{V_e} \cdot \frac{q}{C} = \frac{1-\varepsilon}{\varepsilon} \times K_p \qquad \Rightarrow \qquad K_p = \frac{V_r - V_e}{V_s} = \frac{V_r - V_e}{V_{bed} - V_e} \tag{2.4}$$

With a gel as stationary phase, it is common practice to use the latter expression (Laurent and Killander, 1963) with K_p representing the solute available stationary phase fraction.
For small molecules the retention volume approaches the total bed volume ($K_p=1$) while larger, totally excluded, molecules move with the mobile phase ($K_p=0$).
If $K_p>1$, there is obviously an interaction between solute and support, which is not only due to a molecular sieve effect.
The fraction of free solute in the mobile phase decreases as the system capacity factor increases. The relative retention of the two solutes (1 and 2) by the stationary phase and their partition against a constant mobile phase composition is a thermodynamic factor called selectivity (separation factor) $\alpha_{2,1}$. The higher $\alpha_{2,1}$ the better and easier the separation.
k_1' and k_2' are respectively the capacity factors of the first (1) and second (2) eluted solute,

$$\alpha_{2,1} = k_2'/k_1' \tag{2.5}$$

2.2.3 Adsorption chromatography

When mobile phase and solute flow in the void volume outside the particles, the solute diffuses through an external film to the particle and may be adsorbed on the external surface or diffuse into the stagnant fluid into the pores and be adsorbed. The adsorption process is determined by electrical, physical or chemical interactions between a functional group or whole molecule present on the stationary phase. If it is reversible, the solute can desorb and diffuse through the pores across the external film into the moving fluid. This can occur many times; the solute in the moving fluid is carried along the column bed at the fluid speed until it diffuses into another particle and the whole process is repeated.

Adsorption chemistry and column performance are based on equilibrium and solute mass balance. Having a defined equilibrium relationship is fundamental for a chromatographic investigation since it determines the extent of the process. Equilibrium data are available as adsorption isotherms and plotted with the solute concentration in the mobile phase C in abscissa and the solute concentration adsorbed on the stationary phase q in ordinate.
The easiest case is described by a linear relationship between the two concentrations described by a constant partition coefficient,

$$q = K_p \cdot C \qquad (2.6)$$

The most common deviation from linear adsorption is an upward convex curve which can be described by the Langmuir isotherm (equation 2.7, Figure 2.4), in which q_{max} is the maximum binding capacity (maximum moles of adsorbate per unit volume of adsorbent) K_d (M) is the equilibrium dissociation constant and K_a (M^{-1}) is the equilibrium association constant ($1/K_d$). The Langmuir isotherm expresses favourable adsorption in contrast to an unfavourable concave upward equilibrium adsorption trend (Figure 2.4). There are many other forms of adsorption isotherm like for instance the Freundelich isotherm ($q = K_f \cdot C^{1/nf}$) used to describe liquid-solid systems.

$$q = \frac{q_{max} \cdot C}{K_d + C} = \frac{q_{max} \cdot K_a \cdot C}{1 + K_a \cdot C} \qquad (2.7)$$

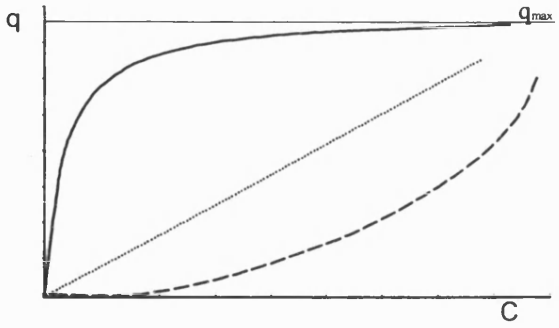

Figure 2.4: Typical hyperbolic favorable Langmuir isotherm (continuous line), linear adsorption (dotted line), unfavorable adsorption (dashed line).

In dilute systems ($C<<K_d$) with Langmuir behaviour, q becomes proportional to C and a linear adsorption isotherm is a reasonable approximation.

The adoption of the Langmuir model assumes a monolayer adsorption surface, that all sites are energetically equivalent and independent and that there are no interactions between adsorbed molecules. From (2.7) the analogy with the Michaelis Menten (1913) equation describing the kinetics of a single substrate enzyme reaction is evident. A simple derivation of the Langumuir isotherm is realised with the expressions (2.8) - (2.11), where q and C are respectively represented by the concentration of filled binding sites and concentration of free solute in the mobile phase, k_{on} and k_{off} are the rate constants of adsorption and desorption (Belter *et al.*, 1988). The higher the association constant (or the lower the dissociation constant) the stronger the affinity and vice versa.

$$[\text{free solute}] + [\text{free binding sites}] \underset{k_{off}}{\overset{k_{on}}{\rightleftharpoons}} [\text{filled sites}] \qquad (2.8)$$

$$\underline{\text{Dissociation constant}}: K_d = \frac{k_{off}}{k_{on}} = \frac{[\text{free solute}] \times [\text{free binding sites}]}{[\text{filled sites}]} \qquad (2.9)$$

$$[\text{free binding sites}] = [\text{Total binding sites}] - [\text{filled sites}] \qquad (2.10)$$

$$[\text{filled sites}] = \frac{[\text{Total binding sites}] \times [\text{free solute}]}{K_d + [\text{free solute}]} \qquad (2.11)$$

The movement of adsorbed solute (adsorption wave or band) occurs at lower speed than the velocity of the mobile phase and an increase in the number of solute moles loaded with the mobile phase $\bullet n_m$, implies an incremental change $\bullet n_s$ in the adsorbed number of moles on the stationary phase. The superficial velocity u_s is defined as the ratio of volumetric flow rate to empty column cross-section (Horvarth and Lin, 1976) and for a large number of solute molecules, carried by the mobile phase moving at u_s, the average speed u_{si} is determined from the fraction of time these molecules are in the mobile phase (equilibrium fraction of solute in the mobile phase),

$$u_{si} = u_s \cdot \frac{\Delta n_m}{\Delta n_m + \Delta n_s} = \frac{u_s}{1 + \left(\frac{1-\varepsilon_e}{\varepsilon_e}\right) \cdot \frac{\Delta q}{\Delta C}} \tag{2.12}$$

A linear equilibrium isotherm $\left(\frac{\Delta q}{\Delta C} = K_p\right)$ implies a limit in solute speed, independent of concentration and dependent only on the thermodynamic variables changing K_p.

The distance x travelled along the column, versus time t, is a line with constant slope equal to the solute velocity. Therefore for a pulse feed, two solutes with independent isotherms move with two different constant velocities, resulting in the outlet as two uncoupled waves.

In the most common cases of non-linear systems as Langmuir adsorption isotherm, differentiating equation (2.7), the following is obtained,

$$\frac{\Delta q}{\Delta C} \approx \frac{\partial q}{\partial C} = \frac{q_{\max} \cdot K_a}{(1 + K_a \cdot C)^2} \tag{2.13}$$

which substituted in equation 2.12 shows that the more concentrated solute is faster moving. Displacement of a concentrated solution by a dilute one, implies that the solute outlet concentration is decreasing continuously in proportion to the column length (proportional pattern). With the opposite displacement, a more concentrated solution overtakes the dilute one, an intermediate elution velocity occurs independently of the column length once that local equilibrium is achieved (constant pattern).

This approach to chromatographic separation analysis is known as the solute movement theory and is described in more detail by Wankat (1986).

Proportional and constant patterns are recognised in FC respectively for unfavourable and favourable adsorption isotherms and described in detail by Vermeulen *et al.* (1973).

2.2.4 Chromatographic theories

The theories used to describe chromatography can be divided into two major categories: the plate theory and the rate theory (Yang and Tsao, 1982a). Without a rigorous mathematical derivation, the fundamental principles of these theories can be summarised.

The Plate theory. In a classical paper on liquid-liquid chromatography Martin and Synge (1941) developed a Plate Theory, analogous to the theory applied to distillation processes, explaining solute band spreading. This method is widely used to quantify chromatographic column performances. The column is thought of as a succession of N well-mixed stages (plates) where is assumed that:

- Equilibrium between the two phases is always reached in each stage.
- Diffusion of solute between plates is negligible.
- K_p is constant (linear isotherm).
- Solutes do not compete or interact with each other.

For each component i and stage j the mass balance for an infinitesimal bed element dV is:

$$C_{i,j-1}dV - C_{i,j}dV = V_e dC_{i,j} + V_s dq_{i,j} \xrightarrow{lin.adsorp.} \frac{dC_{i,j}}{dV} = \frac{C_{i,j-1} - C_{i,j}}{V_e + K_p \cdot V_s} \qquad (2.14)$$

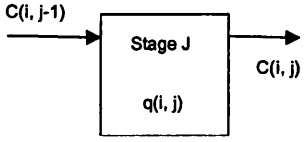

Figure 2.5: equilibrium stage j

which, solved for a pulse of n_i moles, results in a Gaussian expression form for a large number of stages. For a column length L, with N plates, each one height of H, therefore $N = L/H$.

The height H of a single stage (Height Equivalent of a Theoretical Plate, HETP), defined for a single component, serves as a measure of band broading and column efficiency.
It can be defined as the minimum thickness of a column bed portion which the solute leaves, carried by the mobile phase, in equilibrium with the stationary phase.
The number of stages and therefore the HETP are experimentally determined from the retention time or volume of material processed and W, the eluted peak width (Figure 2.6).

$$N = 16 \cdot \left(\frac{t_r}{W}\right)^2 = 16 \cdot \left(\frac{V_r}{W}\right)^2 \qquad (2.15)$$

The Gaussian distribution describing the solute elution after N equilibrium stages has standard deviation $\sigma = \sqrt{N}$, therefore the peak width (band spreading, W) is proportional to the square root of column length. Under conditions assumed in the Plate theory, the solute retention time or volume is independent of the sample size and Gaussian distributions describe chromatographic peaks well, providing they are symmetric.

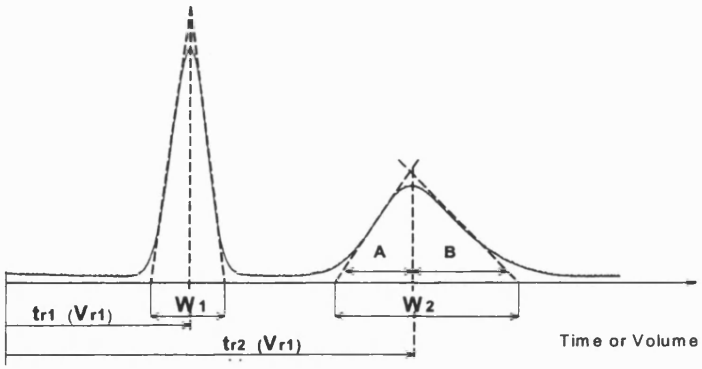

Figure 2.6: Chromatogram representing the elution of two components with the parameters needed for the evaluation of the separation achieved. The Gaussian shape is recogniseble particularly for the first peak

Therefore a peak asymmetry factor A_s = B/A (Figure 2.6) can be adopted to verify the theory hypothesis of linear equilibrium. Skewed peaks result from non-linear distribution isotherms and non-achievement of equlibrium. For instance, in the case of adsorption

isotherms, tailing peaks ($A_s>1$) show a typical convex upward (favourable) Langmuir isotherm while fronting peaks ($A_s<1$) show concave upward (unfavourable) isotherm.
The ability to separate two solutes of a chromatographic column is expressed in terms of resolution R which measure the peaks overlap;

$$R=\frac{2\cdot\left(t_{r2}-t_{r1}\right)}{\left(W_1+W_2\right)} \tag{2.16}$$

Assuming the same peak widths, R can be obtained as a function of the other chromatographic parameters mentioned so far.

$$R=\frac{1}{4}\sqrt{N}\cdot\left(\frac{\sigma_{21}-1}{\sigma_{21}}\right)\cdot\left(\frac{k_2'}{k_2'+1}\right) \tag{2.17}$$

R is proportional to the square root of column length, increases with decreasing HETP and obviously depends on the system thermodynamics (σ_{21}). For higher selectivity less plates are required to achieve good resolution.

Rate theories. Starting from the fact that equilibrium is seldom achieved in real operations, a more rigorous approach to fixed bed adsorption is represented by the Rate Theory of chromatography, based on solute material balance equations with appropriate boundary and initial conditions applied to an infinitesimal element of the bed.
The equation describing the changes in the liquid phase concentration of adsorbate is

$$D_x\cdot\left(\frac{\partial^2 C}{\partial x^2}\right)-\frac{u_s}{\varepsilon}\cdot\left(\frac{\partial C}{\partial x}\right)=\left(\frac{\partial C}{\partial t}\right)+\frac{1-\varepsilon}{\varepsilon}\cdot\left(\frac{\partial q}{\partial t}\right) \tag{2.18}$$

where on the left hand side the rate of axial dispersion (first term, D_x is the solute axial dispersion coefficient) in contrast to the rate of solute movement with the flow along the axial x-axis of the column (second term) equals the accumulation rate of solute (right hand side) in the interstices (third term) and by adsorption (forth term). Theoretically (2.18) can

be solved to provide the effluent concentration as a function of time. However the solution is usually very difficult particularly because the adsorption isotherms are generally not linear. Moreover the overall rate of adsorption is influenced by a number of resistances; mass transfer within the liquid, interface and solid phase and the actual adsorption process. The diversity of the existing rate theories is in the identification of the rate-determining step; an important simplification is obtained when the overall rate of mass transfer and adsorption is written by a single equation. For instance, when surface adsorption is rate controlling, Thomas (1944) solved the mass balance neglecting all dispersion effects considering a second order rate of adsorption and first order rate of desorption (k_{on} and k_{off} are the rate adsorption, desorption constants):

$$\frac{\partial q}{\partial t} = k_{on} C(q_{\max} - q) - k_{off} q \tag{2.19}$$

When the slowest step is the transfer of the solute through the film between the two phases, a linear driving force, determined by the distance the system is from equilibrium, is defined as;

$$\frac{\partial q}{\partial t} = \frac{k_f a}{1-\varepsilon}(C - C^*) \tag{2.20}$$

where $k_f a$ is the interface mass transfer coefficient times the specific area of adsorbent and C^* is the free solute concentration in equilibrium with the adsorbate (at the interface). If local and linear equilibrium is assumed ($q = K_p C^*$) a further simplification is obviously obtained.

Detailed analysis of rate theories on adsorption in packed bed operations is reported in the works of Ruthven (1984) and Tien (1994).

2.2.5 HETP expression

In 1956, comparing the result from the Plate theory with that from the Rate theory approach of Lapidus and Amundson (1952) van Deemter *et al.* (1956) established a resulting expression for the height equivalent to a theoretical plate, function of the mobile phase flow rate F_r.

$$H = A + \frac{B}{F_r} + C \times F_r \qquad (2.21)$$

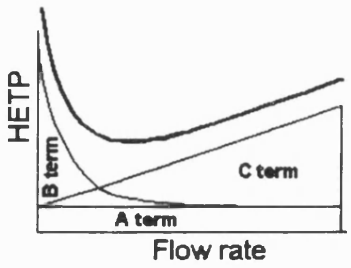

Figure 2.7: Graphical presentation of the effect of increasing flow rate on the three contributions to zone spreading.

A, B, C, are constants for a specific system. A (eddy dispersion) is the contribution to the band broadening that depends only on the packing material and column packing manufacture. B/F_r is the axial dispersion contribution that decreases when F_r increases. Finally, $C \times F_r$ accounts for the contribution from film mass transfer, particle diffusion, and increases at higher flow rate (Figure 2.7). It is apparent that there is an optimum velocity at which HETP is minimised, this minimum value disappears if axial dispersion is negligible. Many studies of zone spreading, including adsorption/desorption kinetics, both for linear and non-linear systems, have expanded the van Deemter equation and many others have found similar expressions following different paths (Giddings, 1965, Horvart and Lin, 1978).

2.3 Affinity Chromatography

Affinity chromatography (AC) was introduced about 34 years ago by Cuatrecasas *et al.* (1968). Since then it has been improved and thousands of different molecules have been purified using this method thanks to the rapid development of support media and chemical coupling schemes.

AC is based on biospecific interactions, in which biochemicals coupled to a solid support are able to recognise, with extreme selectivity, particular structure elements of another substance. AC comprises a number of bio-specific systems such as antibody-antigen, enzyme-substrate, lectin-sugar in which the ligand has an highly specific binding site, recognising the 3-dimensional conformation of the molecule to be bound, and the presence and orientation of key chemical groups within this region.
Usually each affinity packing or adsorbent contains three structural elements:

- The solid support or matrix (porous or non porous).
- The spacer group, which links the ligand to the support at a defined distance.
- The ligand chemically bound through the spacer to the matrix.

These represent a typical arrangement when for instance a macromolecule such as a lectin needs to be purified from a crude extract using AC, with the affinity media based on the immobilised specific sugar (ligand). Obviously following the same principle the lectin can be immobilised and the relative specific sugar purified from a mixture of impurities.

2.3.1 The matrix

The solid support should be insoluble, permeable, and hydrophilic and have no intrinsic charged groups that could cause non-specific adsorption. It should also possess good mechanical-chemical stability properties, resistance to microbial or enzymatic degradation and if porous, the pores must be large enough to allow easy transfer of adsorbate into and out of the particle. Common matrix materials are: porous glass or silica, cellulose, agarose, dextran, and polyacrilamide. The most popular matrix in AC is based on agarose (Wilchek and Miron, 1999), polysaccharides obtained from seaweed (Chapman and Chapman, 1980) consisting of alternating 1,3-linked β-D Galactopyranose and 2,4-linked 3,6-anhydro-α-L Galactopyranose. Commercial products contain between 4 to 6 % (w/v) of agarose. Sepharose, for instance is a bead formed of agarose gel and is widely used because of its very large open-pore structure and low non-specific adsorption. It shows minimal channelling in the bed (Yang and Tsao, 1982b) however as a hydrogel it has significant

mechanical limitations. Its modest rigidity can be improved by cross-linking the gel but this reduces porosity and the availability of covalent attachment sites.

2.3.2 Activation and coupling

Hydroxyl groups on the matrix residue are the usual candidates to be derivatised for the covalent attachment of a ligand. First of all these groups need to be activated which means introducing an anchor (spacer) with a reactive terminating group.

The purpose of the spacer is to reduce steric interference but occasionally it can contribute to non-specific adsorption phenomena (O'Carra *et al.*, 1973).

In the case of agarose gel, the most frequently used method is the cyanogen bromide-activation, which leads to a highly reactive cyanate ester. Subsequent coupling of ligand to the activated matrix results in an isourea linkage. The latter is unstable under alkaline conditions and can lead to slow leakage of ligand, it is also protonated at physiological pH, which might imply ionic non-specific interactions (Yang and Tsao, 1982b).

Other common techniques in the chemistry of activation and coupling are based on bis-oxirane, carbonyldiimidazole, periodate, glutaraldehyde and divinyl Sulfone and a suitable method, to ensure stability, minimal modification of the coupled ligand, and to avoid hydrophobic and ionic interference, must be chosen in different situations (Lowe and Dean, 1974, Dean *et al.*, 1985). The ligand density (moles of ligand per unit volume of support) is an important parameter to be optimised in order to maximise the active capacity of the affinity packing. Often this does not correspond to the highest level of ligand density achievable on the solid support (Harris and Angal, 1989).

2.3.3 Solute adsorption-elution and chromatographic media regeneration

Standard batch or column applications with high affinity systems ($K_d < 10^{-5} M$) are basically on/off procedures, used for protein, enzyme and antibody purification.

Chemical parameters such as pH, composition and ionic strength of the mobile phase, thermodynamic and physical factors such as flow rate and temperature are crucial for

system performance and they are equilibrium characterising. Best conditions must be experimentally set to optimise specific adsorption while minimising interference and undesirable interactions. Once the product has been loaded and washed from weaker adsorbed contaminants, the elution can start by changing one or more chemical of physical parameters. Ligate elution may be achieved for instance, adding an excess concentration of a free ligand competing compound (biospecific elution), changing mobile phase salts concentration, pH, temperature as gradient or step elution, sometime also by partial reversible denaturation of the purified species (Yarmush and Colton, 1985). AC offers high selectivity, hence high resolution and usually also high capacity for the protein or general adsorbed species of interest. During AC processes, fouling is a serious problem, therefore after a few runs the adsorbent must be regenerated and washed of all the impurities accumulated. Gels are usually carefully washed with alternating acid and basic buffers and finally equilibrated with the buffer used in adsorption conditions. However, procedures vary according to type of sample and medium (Janson and Hedman, 1982).

2.3.4 Weak Affinity Chromatography (WAC)

When affinities are weak and lie typically in the mM range ($K_d = 10^{-2} - 10^{-4}$ M, Zopf and Ohlson, 1990) chromatographic separation can be operated in a zonal mode where differences in dissociation constants between immobilised receptors and adsorbate species moderate the rate of transport through an adsorbent bed. The goal of this technique (WAC), first introduced and developed by Ohlson *et al.* (1988), is that the separation can be achieved under mild isocratic conditions. The basic theoretical approach is very similar to what has been introduced previously as solute movement theory. A pulse of solutes with weak affinity for the stationary phase will not be properly adsorbed but only slowed down. Competition for the binding sites among the solutes makes the more strongly bound substance pushing the less strongly bound one ahead. Due to ligand capacity limitations, these effects are useful when a trace component is weakly bound in the presence of a higher concentration of a contaminant more strongly adsorbed. Athough competition effects limit adsorbent capacity, they offer the possibility of using a competitive displacement effect to promote the elution of bound solutes.

After loading the weaker solute a combination of higher concentration and affinity of a displacer solution can elute the weakly bound component significantly concentrated.
Analytical applications reported by Leickt *et al.* (1997) and Ohlson *et al.* (1998) separated small saccharides using immobilised wheat germ agglutinin lectin in WAC mode and separated steroids containing sample on a IgM immobilised antibody column (Strandh *et al.*, 1998). Computer simulations were made by Wilkstrom and Ohlson (1992) for single component elution under linear and non-linear weak adsorption conditions. They observed that the main reasons for the peak spreading are: slow kinetics of adsorption and desorption, large particle size (however considered less important than slow kinetics), strong affinity interaction and too high an immobilised ligand density. They also observed the typical reduction of retention with tailing peak, when injected solute concentration is high. Later, Hubble (2001) has provided a model, based on an equilibrium-stage and discontinuous loading process (feed treated incrementally) assuming a non-linear isotherm, describing the elution of two competing solutes. He showed that the elution of two solutes, under zonal and frontal WAC, was characterised by displacement of the more weakly bound component by the more strongly bound, depending on concentrations and equilibrium constants.

2.3.5 Quantitative aspects

In AC favourable isotherms are usually encountered and systems are more complicated than conventional gas or liquid chromatography due to factors not always accessible for evaluation. Bed flow distribution, swelling, shrinking for soft gels during gradient elution, plus non-specific adsorption interference often make the process complex and irreproducible (Yang and Tsao, 1982b). The potential use of AC systems can be evaluated using characteristic measurements such as the media capacity, equilibrium and rate constants of adsorption and desorption. This can be done by traditional kinetic (relaxation studies, Bernasconi, 1976), equilibrium studies (equilibrium dialysis, Sheehan, 2000), gel filtration (Hummel and Dreyer, 1962) and zonal or frontal affinity chromatography (Andrew *et al.* 1973, Nichol *et al.*, 1974) methods. The latter approach allows the study of the interaction with the immobilised ligand and practically with the same system, which would then be adopted for chromatographic application. Therefore if the biological

interaction is under investigation to examine its potential in AC application, this method is the best candidate. Later in this Chapter relatively modern techniques developed for biomolecular interaction studies are described to assess and validate chromatographic applications (Isothermal Tritration Micro-Calorimeter (ITC) and a Surface Plasmon Resonance (SPR) equipment).

2.3.6 Ligand capacity and equilibrium constant determinations

How AC can be used for quantitative biomolecular interaction analysis is fairly intuitive. Looking at equation (2.4) in fact, the solute partition between the two phases (bound, free solute ratio) is obtainable from its retention volume. Under linear equilibrium conditions, the same approach is independent of sample concentration in zonal or frontal studies (Arnold *et al.* 1986). For non-linear systems it is not so straightforward. Arnold and Blanch (1986) assumed local equilibrium, considered mass transfer and kinetic limitations and presented solutions for zonal and frontal applications. However, while in FC the concentration is known and will be the same everywhere in the column at equilibrium, in ZC it is constantly changing along the column, therefore the FC approach is preferred. The determination of the equilibrium partition isotherm can be achieved with great accuracy when the column is brought to quasi-equilibrium with the solution in frontal chromatography (Jaulmes and Vidal-Madjar, 1989). Once the plateau is reached, the column is in a state of dynamic equilibrium, and the situation is reduced to a simple equilibrium problem with a constant solute concentration C_o. The retention volume V_r is obtainable integrating the breakthrough curve

$$V_r = \frac{1}{C_o} \cdot \int_0^{C_o} V(C)dC, \qquad (2.22)$$

V_{nr}, the elution volume for a non-retained solute, is independent of its loading concentration and the total specifically adsorbed solute is equal to $C_o \cdot (V_r - V_{nr})$ as shown in Figure 2.8.

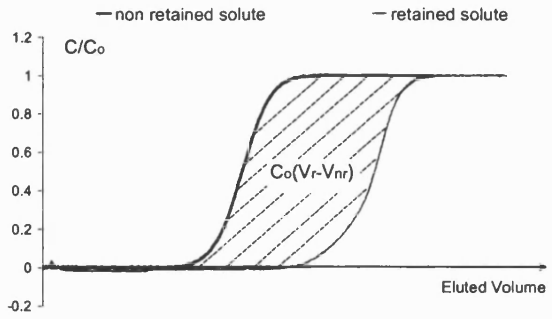

Figure 2.8: Breakthrough curves for a non retained solute and a retained solute, the dotted area represents the amount of retained solute bound to the stationary phase in equilibrium with the loading concentration C_o.

From the reciprocal form of the Langmuir equation (2.7) the following is obtained,

$$\frac{1}{q}=\frac{V_s}{C_o\cdot(V_r-V_{nr})}=\frac{K_d}{q_{\max}}\cdot\frac{1}{C_o}+\frac{1}{q_{\max}} \qquad (2.23)$$

When a single identical population of binding sites independent to each other and binding a solute with stoichiometry 1 to 1 can be described by a Langmiur isotherm, the FC approach and the double reciprocal plot (Lineweaver and Burk, 1934) $1/C_o\cdot(V_r-V_{nr})$ versus $1/C_o$, provides the system dissociation constant and the maximum binding capacity.

In 1986 Kasai and Oda using this approach concluded that AC could be studied at the same level of enzyme-substrate and showed how when C_o increases, V_r becomes smaller approaching V_{nr} for infinite C_o. They also presented a method for calculating the dissociation constant (K_i) of inhibitors (counter ligands present in the mobile phase), through their ability to diminish the elution volume of ligates following the work presented by Nicol *et al.* 1974, under linear conditions. However a simple ligand-ligate system FC investigation does not need linear equilibrium assumption to identify the effective active number of moles of ligand and the dissociation constant for the AC system.The affinity media efficiency can be defined as $\frac{workingcapacity}{theroret.capacity}\times 100$, where,

Theoretical capacity = immobilized ligand concentration × number of binding sites, assuming unitary stoichiometry of binding.

Ligand efficiencies of 1% or even less are common for small ligands, on the other hand, macromolecular ligands, such as monoclonal antibodies, often show efficiencies in excess of 10 % (Harris and Angal, 1989).

2.3.7 Experimental data evaluation, cooperative effects and the Adair model

When the equilibrium points of an affinity system are found with the FC approach the Lineweaver-Burk plot is not satisfactory mainly because it gives too much weight to measurements made at high concentration. The Eadie-Hofstee plot, obtained through a different manipulation of the Langmuir isotherm represents an alternative:

$$q = -K_d \cdot \left(\frac{q}{C}\right) + q_{\max} \tag{2.24}$$

In 1949 Scatchard observed that when a single ligand binds to an oligomer protein with identical and non-interacting binding sites, a graph in which the ratio of the concentrations of bound and free ligand plotted against the concentration of bound ligand will be linear. This is basically the situation described in equation (2.24).

These and other graphical methods were commonly adopted to describe experimental results. More recently numerical methods mainly based on linear and non-linear least square algorithms have replaced them for a direct and more robust evaluation of regression parameters through experimental data fitting procedures. However graphical approaches are still useful as indicators of model assumptions viability (Johnson and Faunt, 1992). A non-linear Scatchard plot provides an indication of something wrong in the model assumption. In fact, it can usually be used in the investigation of cooperative effects among different populations of binding sites.

Positive cooperativity is characterised by the binding of solute to a first binding site promoting the following binding to a second site, while in negative cooperativity, the binding to one binding site inhibits the binding to the successive one. The Hill plot (Hill,

1910) obtained again by equilibrium assumption $M + nX = MX_n$, makes the most famous empirical cooperativity analysis between general receptor M and n molecules of a ligand X.

$$K_a = \frac{MX_n}{M \cdot X^n} \qquad \Rightarrow \qquad \frac{Y}{1-Y} = \frac{MX_n}{M} = K_a \cdot X^n \tag{2.25}$$

$$\Rightarrow \quad Log\left(\frac{Y}{1-Y}\right) = h \cdot Log(X) + Log(K_a) \tag{2.26}$$

Y is the fraction of occupied binding sites, X is the ligand concentration, and h is the Hill coefficient, equivalent to the number of interacting population of binding sites. Negative cooperativity produces Hill coefficients smaller than one and concave Scatchard plots, instead convex Scatchard plots and sigmoidal adsorption isotherms, resulting from experimental data, indicate positive cooperativity, however those plots are not always readily interpretable and usable for cooperativity identification and quantification (Creighton, 1993).

First of all, for a two binding site receptor the real association constants (intrinsic constant K_{a1}^o and K_{a2}^o) must be distinguished from the measured ones (K_{a1} and K_{a2}) which include statistical possibility factor influencing binding to the i^{th} site.

$$K_{ai} = \frac{n-i+1}{1} K_{ai}^o \tag{2.26}$$

Therefore in terms of intrinsic association constant cooperativity effects can be identified: for identical binding site acting independently $K_{a1}^o = K_{a2}^o$, while if there is positive cooperation $K_{a1}^o < K_{a2}^o$ and $K_{a1}^o > K_{a2}^o$ in the case of negative cooperation (Cornish-Bowden, 1979).

At the beginning of the 19th century the scientific focus on haemoglobin uptake of oxygen drove Adair (1925) to discover that the protein is made up of four identical subunits with one oxygen binding site each, working in four separate steps, with four different affinities.

Following Adair's approach, in general if M is the acceptor subunit with a dimeric structure, X the ligand, Y the fraction of occupied binding sites,

$$Y = \frac{MX}{MX + M} \tag{2.27}$$

$$K_{a1} = \frac{M_2X}{M_2 \cdot X} \tag{2.28}$$

$$K_{a2} = \frac{M_2X_2}{M_2X \cdot X} \tag{2.29}$$

with $MX = M_2X+2M_2X_2$ and $M=2M_2+M_2X$, the following equations expressing Y in function of apparent and intrinsic association constants are obtained

$$Y = \frac{K_{a1}X + 2K_{a1}K_{a2}X^2}{2 \cdot (1 + K_{a1}X + K_{a1}K_{a2}X^2)} \tag{2.30}$$

$$Y = \frac{K^o_{a1}X + K^o_{a1}K^o_{a2}X^2}{1 + 2K^o_{a1}X + K^o_{a1}K^o_{a2}X^2} \tag{2.31}$$

These are known as the Adair equations for a two binding site system and represent a more rigorous approach to investigate and quantify cooperation.

2.4 AC process scale up

AC industrial applications are mostly in the field of purification of enzymes, plasma protein, monoclonal antibodies, hormones, and vaccines (Janson and Hedman, 1982).
For on/off processes, batch operation is often suitable for use on any scale. The adsorbent can be stirred directly in the sample, or suspended on it within a "tea bag" and then washed and eluted by changing the mobile phase.
The most convenient way of handling the AC adsorbent is to keep it packed in a column during all the steps required. This is particularly true on laboratory scale where volumes are small. In any separation it is important that the system is characterised and the resolution optimised before it is scaled up. This requires testing and optimising ligand

features, ligand density, binding and elution conditions, and flow rate. For achievement of rapid high-resolution in large-scale chromatography, efficiency is sacrificed for process economy so it is common to work under overloading conditions and allow higher flow rates, increasing throughput. A practical macroscopic parameter used to quatify chromatographic processes is the productivity P, defined as the amount of product separated in one cycle time per unit bed volume,

$$P = \frac{Q_r \cdot C_o \cdot V_{inj}}{V_{bed} \cdot t_{cycle}} \tag{2.32}$$

where Q_r is the purity ratio, C_o is the sample concentration, V_{inj} is the feed volume and t_{cycle} is the whole process time (Yamamoto and Sano, 1992).

General guidelines for scale up are:

- same grade of chemicals and same gel,
- constant ratio sample volume to column,
- same superficial velocity,
- constant height bed, increasing only column diameter (Wankat, 1986)

The Van Deemter zone spreading expression (2.21) can be rewritten in a more detailed form for this situation:

$$H = 2\lambda d_p + 2\frac{\gamma D_m}{u_s} + \omega \frac{d_p^2}{D_m} u_s \tag{2.33}$$

where λ is a particle geometric factor, d_p is the particle diameter, γ is the obstruction factor, ω is a constant function of the porosity and D_m is the adsorbate diffusivity in the mobile phase. Equation (2.33) does not consider kinetic effects, if eddy and axial dispersion (respectively the first and second term) are negligible and mass transfer is the rate determining step,

$$H \propto d_p^2 \quad \Rightarrow N \propto \frac{L}{d_p^2} \tag{2.34}$$

The number of stages required will be set by the affinity media selectivity and desired resolution, using equation (2.17). It follows that by keeping the L/d_p^2 ratio constant, different columns can be considered to perform similarly.

d_p must be very small to obtain high performance, but with very small particles (d_p<10μm), pressure drop increases, mass transfer resistance is reduced and kinetic effects can become critical. Zone spreading is no longer inversely proportional to d_p^2 and equation (2.33) no longer applies. In the case of rigid packing material the pressure drop is kept constant by scaling up with constant L/d_p^2 ratio but this does not apply for gels that can be easily compressed (Janson and Hedman, 1982). Gels usually present an upper limit in flow rate applicable. The longer and narrow the column, the higher the pressure drop and the smaller the volumetric flow rate will be, although wall effects must be considered to oppose the drag force, protecting the bed from compression. However this generally leads to scale up based on keeping column length (L) small and increasing the column diameter.

Standard chromatographic theory is not always applicable to affinity systems due to the isotherm's strong non linearity, possible secondary interactions and the need for very large sample loading in preparative scale. Therefore Wankat (1974) introduced the use of a simple schematic representation of column operation based on the Martin and Synge model which allows a more accurate description of the biomolecular interaction. This multi-stage model is based on discrete transfer and equilibrium step. Fractions of liquid are transferred to the next stage at each transfer step without mixing with each other. A mass balance for the adsorbed solute is needed for each stage after each transfer (loading) step coupled with the equilibrium adsorption isotherm to obtain the final elution concentration profile.

A more complex model which led to complete characterisation of the AC systems, in terms of both equilibrium and kinetic effects, is described by Chase (1984). He takes a similar approach to the Thomas' model (equation 2.19) and obtains an essentially identical solution, including k_{on} and k_{off} , all the physical and chemical rate determining factors,

neglecting axial dispersion, and considering C_o constant (FC). Experimental and theoretical determinations of K_d, q_{max}, and k_{on} in batch adsorption were in good agreement in that the column simulations, using those values the model well fitted experimental data.

In 1985 Arnold *et al.* (1985a, 1985b), adopting a local-equilibrium theory, isolated the major effect of non linearity in zone spreading and developed a model including mass transfer and kinetic effects. They provided analytical tools for evaluating and predicting industrial scale AC column performance and obtained a useful set of design equations for adsorption, wash and elution in FC and a set of design equations with the assumption of linear equilibrium for ZC.

2.5 Adsorption and calorimetric studies

Adsorption-based separation processes, which are developed to separate or purify homogeneous mixtures, operate on the principle of differences in adsorption potential (Tien, 1994). Selective retention of a component from a liquid or gas mixture by a solid material is known as adsorption (Treybal, 1968), that component diffuses from the gas/liquid phase to the solid phase. This is an operation that involves changes in composition of solutions and belongs to the mass-transfer operations family including absorption, distillation and filtration.

Apart from the differences in the structural realisation of those unit operations, there are differences of basic principle amongst them. Absorption is a bulk phenomenon in which solubility determine extent. Distillation separates mixture components based on their differences in volatility (α) but requires energy and is impractical when differences in α are too low and finally, filtration deals with sizes of particles to be separated (Ruthven, 1984).

2.5.1 Thermodynamics

Like chemical equilibrium, for a given adsorption reaction, if ξ is the extent of the adsorption, n_{io} the initial moles of each species (m is the number of species involved) and v_i the stochiometric coefficient, the mass balance can be written,

$$n_i = n_{io} + v_i\xi \qquad i=1,2,...m \tag{2.35}$$

ξ is an internal state variable, the equilibrium condition is met when

$$\left(\frac{\partial G}{\partial \zeta}\right)_{T,P} = 0 \tag{2.36}$$

The Gibbs free energy G is defined as

$$G = \sum_{i=1}^{m} \mu_i n_i = \sum_{i=1}^{m} \mu_i (n_{io} + v_i\xi) \tag{2.37}$$

μ_i is the single specie potential, and in terms of the standard reference state μ_{iR},

$$\mu_i = \mu_{iR} + RT \cdot \ln(a_{iR}) \tag{2.38}$$

where a_{iR} is the activity coefficient at the standard reference state.

Defining $\Delta G^o = \sum v_i \mu_{iR}$ (function only of temperature) the equilibrium condition (2.36) becomes,

$$\prod_{1}^{n} (a_{iR})^{v_i} = \exp\left(-\frac{\Delta G^o}{RT}\right) = K \tag{2.39}$$

therefore,

$$\ln(K) = -\frac{\Delta G^o}{RT} = -\frac{1}{RT}\left(\Delta H^o - T\Delta S^o\right) \tag{2.40}$$

note that $\Delta G^o = \Delta H^o - T\Delta S^o$, and finally

$$\frac{d\ln(K)}{dT} = \frac{\Delta H^o}{RT^2} \quad \begin{matrix} <0 \ exothermic: & T \ increases, & K \ decreases \\ >0 \ endothermic: & T \ decreases, & K \ increases \end{matrix} \tag{2.41}$$

where, K is called equilibrium constant and changes with temperature according to the heat of reaction, in the standard state.

2.5.2 The heat of adsorption

The heat of adsorption Q is usually identified as the heat released upon the adsorption of an adsorbate by an adsorbent. If the adsorption takes place under isothermal conditions the heat of adsorption is the heat that has to be removed in order to maintain the system under isothermal conditions, while under adiabatic conditions it refers to the heat that raises the temperature of the system. These two quantities are not the same. In a system of volume V, containing n_a moles of adsorbent, n_s of adsorbed adsorbate, n_m of unadsorbed solute, isothermal and adiabatic heats of adsorption can be defined, (Ruthven, 1984). The isothermal heat of adsorption Q, is defined in the following relationship;

$$\left(\frac{\partial Q}{\partial n_s}\right)_{P,T} = -\Delta H^o \tag{2.42}$$

Where ΔH^o is the molar heat of adsorption.

In the case of adiabatic adsorption, the heat Q_a is defined as

$$Q_a = \left(c_c + n_m c_{pm} + n_s c_{ps}\right) \cdot \left(\frac{\partial T}{\partial n_s}\right)_{Adiab.} \qquad (2.43)$$

where c_c, c_{pm}, c_{ps}, are the heat capacities, respectively of the system, the adsorbed and the unadsorbed solute.

A more detailed description of the thermodynamic approach to an adsorption process and the mathematical implications, are given by Tien (1994).

2.5.3 Calorimeters

All chemical or physical processes are accompanied by a change in heat content that may be observed calorimetrically. Since the evolution of heat is proportional to the extent of the process, quantitative analytical information can be gained from it.
Calorimeters and microcalorimeters are today well-developed instruments by which various thermodynamic quantities such as free energy, enthalpy and entropy changes, partial molar heat capacities can be determined.

The attention of this work is focused on adsorption/desorption processes involved in biochemical interactions; particularly protein, small ligand interactions; this means low concentration (micromolar) systems, low enthalpy (micro-nanomolar), and extremely small amounts of heat generated.

The high sensitivity required is provided by Isothermal Titration Calorimeters (ITC) and Differential Scanning Calorimeters (DSC). ITC technology will be described in greater detail, since it is the thermochemical instrument most suitable for the study of bio-adsorption reactions.

Biological reactions can easily be conducted isothermally, therefore ITC applications are far wider than DSC applications (Freire, 1990) also ITC provides a comprehensive description of the binding phenomena in terms of

- Number of binding sites or stoichiometry (n).
- Strength of association (K_a).
- Cooperative effects characterisation.
- Enthalpic-Entropic contributions to the free energy of binding.
- Dependence on environmental conditions.

In a DSC two cells are mounted in a cylindrical adiabatic environment connected with the outside through narrow access tubes. Thermoelectric devices measure the temperature difference between the two cells and between the cell and the jacket.
Scanning up in temperature, DSC continuously measures excess heat capacity (ΔC_p) from the total heat generated as function of temperature. Several DSC applications of protein folding, stability and formulation, conformational energetics of biopolymers are today available (Connelly, 1994, Jelesarov and Bosshard, 1999).

In a ITC, there are again two cells enclosed in an adiabatic jacket, a syringe containing a ligand solution is titrated to a cell containing a solution of the macromolecule at constant temperature. As the two substances interact, heat is released (exothermic reaction) or adsorbed (endothermic reaction) in direct proportion to the amount of binding. A constant power is applied to the titration cell and a reference cell kept at the same temperature. This means that if for instance an exothermic reaction is happening in the sample cell, a feedback control system will decrease the power supplied to this cell to re-establish $\Delta T = 0$ between the two cells. As the macromolecule in the cell becomes saturated with added ligand, the heat signal diminishes until only background heat of dilution and mixing is observed. Control experiments are needed for real binding heat identification. A typical ITC exothermic interaction experiment generates the graph of Figure 2.9. The total heat associated with each ligand injection is the time integral of the differential power adsorbed represented by the area of each peak.

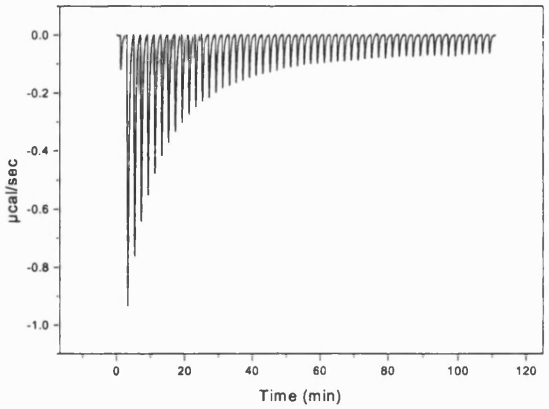

Figure 2.9: ITC experiment, negative heat developed each injection is the area of the peak, function of the volume, concentration of the titrant injected. The exothermic effect decreases as saturation is approached increasing the volume titrated (number of injections).

ITC has a wide number of applications and its importance in biomedical research (e.g. in the selection of suitable drug candidates) is well recognised; the future of ITC will develop with more sensitive equipment and the development of kinetic theories for describing the calorimetric data (Holdgate, 2001, Thompson, 2000).

2.5.4 Mathematical approach to ITC data

For an interaction one to one of macromolecule M and ligand X, at equilibrium,

$$M + X = MX \tag{2.44}$$

the equilibrium can be described by the association constant K_a,

$$K_a = \frac{MX}{M \cdot X} \tag{2.45}$$

The mass balances for the total ligand and macromolecule are:

$$X_t = X + MX \tag{2.46}$$

$$M_t = MX + M \tag{2.47}$$

Eliminating X and M from the three equations (2.45, 2.46, 2.47) and rearranging, gives a quadratic equation that can be solved in MX. The resulting expression for MX is differentiated with respect to X_t to give the rate of complex formation as a function of the total ligand concentration in the cell. The latter is related to the heat evolved (equation 2.42) to give a differential expression for the heat developed after each solute injection. This can be integrated to provide an expression for Q as a function of X_t / M_t, K_a and ΔH^o. The Q value can be calculated at the end of the i^{th} injection (Q_i) or the change of heat from the *i-1* to the i^{th} injection ΔQ_i can be measured

$$\Delta Q_i = Q_i - Q_{i-1} \tag{2.48}$$

With this differential approach, a non-linear least-square data analysis simulation reported by Wiseman *et al.* (1989), plotting $\frac{\Delta Q}{\Delta X_{tot}}$ *versus* $\frac{X_{tot}}{M_{tot}}$, defined the best condition to be adopted during the ITC experiment for a meaningful solution of the regression parameters on the base of one parameter "*c*".

$$c = n \cdot M_t \cdot K_a \tag{2.49}$$

Figure 2.10 reports Wiseman's results. For a tight binding ($c \to \infty$), all ligand added to the cell is bound and the isotherm is rectangular of height ΔH^o. When c is smaller ($1 < c < 1000$), ΔH^o and the other regression parameters (stoichiometry of binding n and association constant K_a) can be calculated by deconvolution of the area under the curve. Out of the indicated c-range, extremely vertical or horizontal isothermal traces yield less precise information.

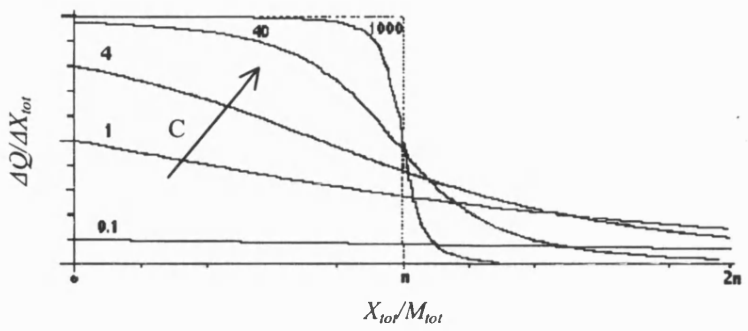

Figure 2.10: Simulated-binding isotherms varying the c parameter (defined in equation 2.49), differential approach by Wiseman *et al.* (1989).

In 1991 Sigurskjold *et al.* compared the regression analysis using the differential and integral heat expressions and observed that the two non linear least square fits do not yield the same results (except for ΔH^o), particularly in terms of the standard deviation associated to them. For more reliable association constant determination the integral mode is more accurate while for the determination of the exact cell concentration the differential mode is better. Sigurskjold *et al.* (1991) choose the receptor concentration in the cell as a regression parameter instead of the stoichiometry of binding, introducing a method for an exact quantification of the active binding site independent from receptor conformation and valence.

2.5.5 Basic models for ITC data interpretation

One and two sets of independent binding site and two sequential and interacting identical sets of binding site are commonly accommodated in commercial ITC data evaluation software.

In a single set of identical binding sites, K_a is the binding equilibrium association constant, n is the stoichiometry of binding, Y is the fraction of occupied sites, V_{cell} the Volume of the ITC cell and the system of following equations is solved,

$$\begin{cases} K_a = \dfrac{Y}{(1-Y)\cdot X} & (2.50) \\ X_t = X + n\cdot Y\cdot M_t & (2.51) \\ Q = n\cdot Y\cdot M_t\cdot \Delta H^o\cdot V_{cell} & (2.52) \end{cases}$$

This yields the final expression for Q:

$$Q = \frac{nM_t\Delta H^o V_{cell}}{2}\left[1+\frac{X_t}{nM_t}+\frac{1}{nK_aM_t}-\sqrt{\left(1+\frac{X_t}{nM_t}+\frac{1}{nK_aM_t}\right)^2-\frac{4X_t}{nM_t}}\right] \quad (2.53)$$

Q_i can be calculated at the end of each injection for a set of values n, K_a and ΔH^o and corrected according to (2.48). The data fitting procedure would calculate these values and compare them with the experimental results, improving the parameters n, K_a and ΔH^o by standard non-linear least square methods.

In a two set of independent binding sites, K_{a1}, K_{a2} are the binding equilibrium association constants, n_1, n_2 are the stoichiometries of binding, Y_1, Y_2 are the independent fractions of occupied sites, the system of equations becomes more complicated:

$$\begin{cases} K_{a1} = \dfrac{Y_1}{(1-Y_1)\cdot X} & (2.54) \\ K_{a2} = \dfrac{Y_2}{(1-Y_2)\cdot X} & (2.55) \\ X_t = X + M_t\cdot(n_1Y_1 + n_2Y_2) & (2.56) \\ Q = M_t\cdot V_{cell}(n_1Y_1\Delta H_1 + n_2Y_2\Delta H_2) & (2.57) \end{cases}$$

In the two sequential and interacting binding sites model, the two apparent association constants are defined as follows

$$K_{a1} = \frac{M_2 X}{M_2 + X} \tag{2.58}$$

$$K_{a2} = \frac{M_2 X_2}{M_2 X + X} \tag{2.59}$$

and the total amount of ligand in the cell is

$$X_t = X + 2 \cdot MX \tag{2.60}$$

Where the fraction of adsorbed solute Y is given by the Adair equation (2.30). A bisection algorithm is necessary to solve for X and finally obtain an expression for the total heat developed while the ligand is binding to the macromolecule.

$$Q = M_t V_{cell} \cdot [F_1 \Delta H_1 + F_2 (\Delta H_1 + \Delta H_2)] \tag{2.61}$$

with the fractions of bound ligang F_1 and F_2 expressed using equation 2.58 and 2.59

$$F_1 = \frac{M_2 X}{M_2 + M_2 X + M_2 X_2} = \frac{K_{a1} X}{1 + K_{a1} X + K_{a1} K_{a2} X^2} \tag{2.62}$$

$$F_2 = \frac{M_2 X_2}{M_2 + M_2 X + M_2 X_2} = \frac{K_{a1} K_{a2} X}{1 + K_{a1} X + K_{a1} K_{a2} X^2} \tag{2.63}$$

A summary of the models and their features available in commercial ITC for data analysis are summarised in table 2.2. They are based on the mathematical approaches described and on the concepts introduced in 2.3.7. The situation with more than one population of binding site is simplified to a number of 2.

Table 2.2: Possible binding models summary based on intrinsic and apparent association constants

Possible approaches	Features
1 set of site	All sites energetically identical, the equilibrium is expressed by the Langmuir isotherm
2 set of sites	▪ No Cooperation: $K_{a1}^{o} = K_{a2}^{o}$ ➢ Reduce to 1 set of site with stoichiometry = 2 Identical: ▪ Cooperation: $K_{a1}^{o} \gtrless K_{a2}^{o}$ ➢ Positive: $K_{a1}^{o} < K_{a2}^{o}$ ➢ Negative: $K_{a1}^{o} > K_{a2}^{o}$ Different and independent $K_{a1}^{o} \neq K_{a2}^{o}$

2.6 Surface adsorption and Plasmon Resonance effect

Bio-molecular interactions between one species (ligand or receptor) immobilised on an optically active surface and the other flowing over it (analyte), can be investigated with Surface Plasmon Resonance (SPR) biosensor.

"Biosensors are analytical devices that respond selectively to analytes in an appropriate sample and convert their concentration into an electrical signal via a combination of a biological recognition system and a physico-chemical transducer" (Lowe *et al.*, 1990).

At the interface of two transparent media with different refractive indices (RI), incoming light is partially reflected and partially refracted. Above a certain critical angle of incidence no light is refracted and an electromagnetic field penetrates the medium. In SPR at the interface between a glass surface and the biological surface in touch with the liquid (water) there is a thin layer of metal (gold). The monochromatic light reflected at a specific angle (SPR angle) of incidence is markedly reduced, exciting the metal delocalised electrons at the metal-biomaterial interface, this phenomenon is known as plasmon resonance (Homola *et al.*, 1999).

The SPR angle is extremely sensitive to the RI of the medium adjacent to the metal surface and it changes if something is binding to that surface. Therefore if the bio-surface is prepared to bind specifically one analyte, monitoring the angle at which resonance occurs provides an SPR adsorption profile (sensogram) with which changes in the surface concentration can be measured (Green *et al.*, 2000).

This technique allows qualitative and quantitative analysis of biomolecular interactions in terms of following a molecule through purification for instance, studying equilibrium and kinetics of biomolecular interactions and determining the concentration of a particular active species (Rich and Myszka, 2000).

As in Affinity Chromatography there is a "matrix", this time a biosurface (the most common for routine analysis is carboxylated dextran, commercially available as CM5 microchip), must be activated for a specific ligand to be coupled. Progress in biomaterials, activation and coupling procedures are the basis of the success of this technique in a wider field of applications.

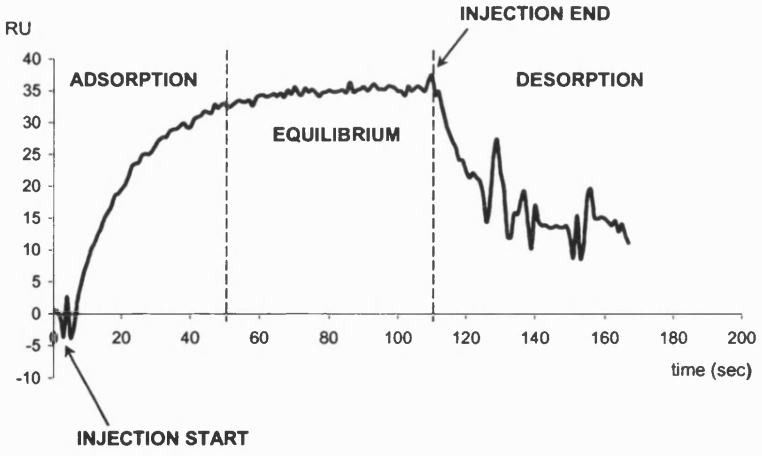

Figure 2.11: Typical SPR response (sensogram), where adsorption, equilibrium and desorption phases are shown.

The SPR response (R^{SPR}) is expressed in an arbitrary unit RU, which has been related to the specific amount of bound material with the equation 1000 RU=1ng of analyte per mm^2 of surface (Stenberg *et al.*, 1991).

Analyte M is injected into the cell as a finite pulse at a certain flow rate. In the cell ligand X is present immobilised on the surface of a microchip. The interaction between the two is monitored in real time. During the analyte injection, the SPR signal will increase as the adsorbate material increases, finally reaching a plateau, equilibrium between the concentration of injected analyte and activated surface. At the end of the injection, buffer will wash away the bound analyte and the SPR signal will decrease (Figure 2.11).

The maximum binding capacity ($R_{\max}^{SPR}$) can be evaluated from the total ligand sites available on the surface (linked to the resulting response after ligand coupling) and analyte molecular weight,

$$R_{\max}^{SPR} = \frac{analyteMW}{ligandMW} \times ligand\ response\ after\ coupling \times valence\ of\ binding \qquad (2.64)$$

Adsorption, equilibrium and desorption can therefore be monitored as they occur,

$$M_{bulk} \xleftrightarrow{k_f} M_{surface} + X \underset{k_{off}}{\overset{k_{on}}{\rightleftarrows}} MX \qquad (2.65)$$

k_f is the mass transfer coefficient relating the movement of analyte from the bulk solution (M_{bulk}) to the active surface, k_{on} and k_{off} are the adsorption, desorption rate constants.

If k_f is high, the transfer of analyte from the bulk solution to the bioactive surface is very fast and the first step of 2.65 can be neglected in the kinetic analysis.

Equilibrium determination can be carried out independently based on the plateau response (R_{eq}^{SPR}) obtained at different injected analyte concentrations. If the interaction is one to one the experimental data can be written with a Langmiur isotherm as follows

$$K_a = \frac{MX}{M \cdot X} = \frac{R_{eq}^{SPR}}{M(R_{\max}^{SPR} - R_{eq}^{SPR})} \qquad (2.66)$$

The adsorption and desorption rate equations can be written as follows and easily integrated

$$\frac{dR}{dt} = k_{on} M\left(R_{\max}^{SPR} - R^{SPR}\right) - k_{off} R^{SPR} \qquad (2.67)$$

$$\frac{dR^{SPR}}{dt} = -k_{off} R^{SPR} \qquad (2.68)$$

The main limitations on kinetic analysis are mass transfer effects. In fact the *M-X* interaction is firstly mediated by the transfer of *M* from the bulk solution to the surface, therefore if this process is very slow equations (2.67) and (2.68) are not valid and must be replaced by

$$\frac{dR^{SPR}}{dt} = k_f M_{bulk} \qquad (2.69)$$

The higher the diffusion coefficient of the analyte and flow rate with which the latter is taken through the cell, the more k_f and mass transfer effects are less likely to be the rate determining step. Also, low surface concentration of binding site (immobilised ligand) affects the kinetics of adsorption decreasing k_{on} and making the mass transfer rate negligible with respect to the slow rate of adsorption.

Any SPR investigation aimed at kinetic analysis must consider mass transfer limitations and choose conditions to reduce their effects.

Low capacity surfaces are particular important for minimising mass transport effects but even under optimal experimental conditions, it might mot be possible to neglect these effects. Hence they must be considered in the rate equation as well as the kinetics of adsorption (Rich and Myszka, 2000). On the other hand, if mass transport is the only limiting factor the binding signal is proportional to the concentration of active analyte, which can then be determined, if its molecular weight and the diffusion coefficient are known, without standard instrument calibration.

In 1993 Karlsson *et al.* measured antibody concentration, immobilising a large amount of ligand and using a calibration curve, later also more complicated mathematical approaches when mass transfer is only partially limiting step have been introduced for concentration measurement with no calibration requirement (Christensen, 1997, Richalet-Secordel, *et al.* 1997).

In protein concentration determination, spectrophotometric procedures are hardly applicable to unpurified samples, as they do not distinguish between active and inactive molecules. SPR is a valid alternative detection method to specifically identify the concentration of active species (Zeder-Lutz *et al.*, 1999). Plasmon resonance principle based detectors are already replacing RI and UV or light scattering detectors in some HPLC analytical investigation (Castillo et al., 1993, Cepria and Castillo, 1997) and SPR has also been employed on larger scale applications (Disley *et al.*, 1999, Bracewell, D. G., 2001) in monitoring and control of bioproducts.

Chapter III

Preliminary Studies on Sugar-Lectin Interactions with Concanavalin A

3.1 Summary

Legume lectins generally consist of two or more subunits in a multimeric arrangement with each monomer usually considered to bind one specific monosaccharide. In this chapter results obtained for interaction between Concanavalin A (ConA) and monosaccharides using Frontal Chromatography (FC) and Isothermal Titration Calorimetry (ITC) suggest that each lectin monomer might well be capable of binding more than one monosaccharide. FC was conducted with ConA immobilised on Sepharose 4B as the chromatographic media, using pnp-D-glucopyranoside (pnpg) and pnp-D-mannopyranoside (pnpm) as the adsorbing species. In the ITC experiments ConA solutions were titrated with D-mannose (D-Man) or D-glucose (D-Glc) solutions. Immobilised and free ConA interactions with monosaccharides were characterised and shown to lie in the range of weak affinity interactions (dissociation constant in the order of 10^{-4} M). ConA-Sepharose was tested as an affinity matrix for monosaccharide fractionation in Zonal Chromatography (ZC) mode under isocratic conditions. Initial studies using media prepared by ConA immobilisation onto an anion exchanger cellulose (GDC-resin) were unsuccessful. However, commercial ConA-Sepharose 4B, packed in small columns, confirmed the possibility of using weak lectin/monosaccharides interactions for isocratic sugar separation.

3.2 Introduction

Concanavalin A (ConA) is a legume lectin which, at ambient temperature and neutral pH, comprises of four subunits of 26-27 kDa held together by non-covalent interactions.

Each subunit or monomer contains a single specific sugar binding site coordinated with one Ca^{2+} and one Mg^{2+} with one hydrophobic cavity adjacent to the carbohydrate site (Liener *et al.*, 1986). ConA will specifically bind both terminal α-linked D-glucose and N-acetylglucosamine; however, higher affinity is exhibited for D-mannose and its glycosides especially trimannoside (Van Damme *et al.*, 1998). Mannose and glucose interactions with ConA have been widely investigated using different techniques and are usually quantified in terms of a binding dissociation constant, K_d typically in the order of 10^{-4} M. In 1981 Clegg *et al.*, using florescence techniques and temperature relaxation studies reported equilibrium and adsorption–desorption rate constants and binding enthalpies for p-nitrophenyl-D-mannopyranoside (pnpm), methyl-D-mannoside (mdm), methyl-D-glucoside (mdg) and ConA in solution. More recent isothermal titration calorimetric studies are also available on ConA titrated with D-Man and its oligomers (Swaminathan *et al.*, 1998, Gupta *et al.*, 1997). From these studies, D-Man and its derivatives are characterised by K_d values between 1 and 4×10^{-4} M with $k_{on} \approx 4\text{-}5\ M^{-1}\ s^{-1}$, $k_{off} \approx 6\text{-}12\ s^{-1}$ and $\Delta H^{o} \approx 4\text{-}9$ kcal/mol while for D-Glc and its derivatives $K_d > 6\times10^{-4}$ M, $k_{on} \approx 5\ M^{-1}\ s^{-1}$, $k_{off} \approx 30\ s^{-1}$, at 20-25°C.

Oda *et al.* (1981) studied the same biomolecular interactions investigating the elution breakthrough of ConA solutions throughout a column packed with p-aminophenyl-β-D-Glucopyranoside-Sepharose when competing ligand saccharides are present. K_d values of those soluble sugars and their derivatives for ConA are related to their ability to diminish the lectin elution volume, they are reported in Table 3.1 under their abbreviation (see table of abbreviations). These values show good agreement with previous findings, although the order of magnitude value for K_d show wider variation; from 10^{-3} M (D-Glc) to 10^{-5} M (pnpm).

Table 3.1: Dissociation constants for ConA-sugars interactions, from Oda *et al.* (1981) work

Sugar	pnpm	mdm	D-Man	mdg	D-Glc	GlcNAc	D-Gal	D-Xyl	D-Fuc
K_d (mM)	0.014	0.47	0.2	0.22	1.5	7.2	260	300	510

Quantitative performance of immobilised ConA on CNBr activated Sepharose-4B has been investigated by Ohyama *et al.* (1985) with pnpm α and β and respectively $K_d = 1.8\times10^{-5}$ M and $K_d = 1\times10^{-4}$ M were determined using a FC approach. Further studies on the separation and affinities achievable with an affinity support based on ConA, have been conducted by others, using an HPLC system with the lectin immobilised on small (10-50 μm) silica particles using glutaraldehyde activation. Muller and Carr (1984 and 1986) studied the elution of pnpm pulses in presence of different concentration of an inhibitor Methyl-D-Mannoside (mdm) and found K_d value (0.6×10^{-4}M) in agreement with previous work. However they also obtained distribution isotherms for pnpm using the breakthrough method that led to a concave upward final Scatchard plot, a sign of heterogeneous interactions. The stronger affinity population was identified with the dissociation constant K_d=1.3×10^{-5} M, extrapolated from the same Scatchard plot. Using the approach first introduced by Horvat and Lin (1976, 1978) for linear system, Muller and Carr (1984, 1986) considered HETP influenced only by adsorption-desorption kinetics according to the following expression

$$HETP = H_{kin} = \frac{2 \cdot k' \cdot u_s}{\varepsilon \cdot (1 + k_o) \cdot (1 + k')^2 \cdot k_{off}} \tag{3.1}$$

where k' is the capacity factor, k_o is the ratio between intraparticle and interparticle volumes and k_{off} is the dissociation rate constant. From experimental *HETP* values, particularly low values for dissociation rate constants ($k_{off} < 1\ s^{-1}$) were found. Anderson *et al.* (1986) and Anderson and Walters (1986) worked on the same system of Muller and Carr with frontal and zonal applications arguing that the underestimation of k_{off} was probably a consequence of overestimation of H_{kin}. They believed that the contributions to the plate height of slow diffusion in the stagnant pores mobile phase were larger. Although they achieved equilibrium constants close to the ones obtained by Muller and Carr, their isotherms did not level off at high sugar concentration, therefore they assumed a second group of non-specific weaker sites simply adding a second term to the standard Langmuir equation.

Immobilised ConA is now widely recognised as an effective system for fractionating and characterising N-linked sugar chains of glycoproteins (Merkle and Cummings, 1984, Kobata, 1992) and is also employed in large-scale applications (Janson *et al.*, 1982).
These are used in frontal procedures, exploiting the strong mono or multivalent interaction ($K_d < 10^{-6}$ M) between the lectin and usually trimannoside terminal group(s).

So far, nobody used immobilised lectins for simple monosaccharide separations and very few of these kind of applications lie in the general isocratic elution chromatography range of weak interactions (Ohlson *et al.*, 1998, Strandh *et al.*, 1998). Therefore the use of lectin affinity chromatography for small rare saccharides purification can be approached with an investigation of a system based on ConA, characterising the interactions with the specific monosaccharide and the effectiveness achievable in its purification.

3.3 Materials

Concanavalin A immobilised on Sepharose 4B was purchased from Amersham Pharmacia Biotech. (Buckinghamshire, U.K.). P-nitrophenyl-α-D-glucopyranoside (pnpg), -D-mannopyranoside (pnpm) -L-arabinopyranoside (pnpa), D-glucose (D-Glc), D-mannose (D-Man), L-fucose (L-Fuc), L-arabinose (L-Ara), lyophilised Concanavalin A (ConA) type IV highly purified from jack bean, salts, buffers, cellulose dialysis tubes (12 kDa cut off), Bradford reagent and BSA standards were obtained from Sigma Chemicals Ltd (Poole, UK). For protein concentration determination, a UV-1601 detector (Schimadzu, Wolverton, U.K.) was used. PVDF/PE syringe filters 0.22 μm bought from Millipore (Watford, U.K.), the solvent was always ultrapure water from an ELGA Purelab Option Unit (Bucks U.K.) and GDC-resin, a DEAE-cellulose matrix, was a gift from DANISCO-Cultor (Kantvic, Finland).

Chromatographic experiments were conducted with two systems: an automated FPLC from BioRad (Hertfordshire, U.K.) with integrated acquisition and elaboration data software and a manual HPLC system from Anachem (Luton, U.K.) equipped with VisiDaq acquisition data card and software from Advantech (Southampton, U.K.).

Isothermal titration microcalorimetric (ITC) experiments were performed using OMEGA Microcalorimeter VP-ITC from MicroCal (Northampton, USA) supplied with a thermostated samples degassing unit (ThermoVac), 290 µl automatic syringe and Origin Software for data analysis.

3.4 Interactions characterisation: Methods

Concanavalin A interactions with monosaccharides; D-Man and D-Glc were determined in solution titrating the lectin with the sugars using the isothermal microcalorimeter.
Due to the importance of knowing ConA concentration during ITC experiments, a brief investigation of methods for the measurement of protein concentration was carried out. Finally the affinity interactions between the two monosaccharides and ConA, immobilised onto Sepharose 4B and packed in small columns were characterised using Frontal Chromatography (FC) method.

3.4.1 Total protein concentration determination

Calibration of the spectrophotometer was performed at 280 nm for raw protein solutions and at 595 nm with the Bradford assay (Bradford, 1976).
BSA standards and ConA powders were dissolved in Phosphate buffer pH 7.4, containing 150 mM NaCl and 0.02 % NaN_3 and were diluted and used for the instrument calibration.
Wavelength adsorption scanning procedures, for one ConA sample (1 mg/ml) and one p-nitrophenyl-α-D-Glucopyranosyde (10 µM) were run and results compared.

3.4.2 ITC experiments

The OMEGA ITC reference cell was filled with water and the instrument calibrated firstly using standard electrical pulses as described in the manual and then using a calibration kit containing ribonuclease A and cytidine 2-monophosphate supplied by the manufacture.

The buffer used in these application was 50 mM MOPS buffer pH 7.2-7.4 containing 0.5 mM $CaCl_2$, 0.5 mM $MnCl_2$, 0.5 mM $MgCl_2$, 150 mM NaCl and 0.02% NaN_3. Solid ConA was dissolved in that buffer then dialysed against the same buffer at 4°C, filtered with PVD/PE syringe filters and monomer concentration adjusted to 0.15 mM.. Titrant sugar samples of D-Mannose and D-Glucose were diluted to a final concentration of 12.2 and 24.4 mM respectively. Titration were run at 20°C and all the samples degassed at 15°C with a ThermoVac unit, while the cells were thermostated at 18°C to allow buffers in the cell and syringe equilibrated to the same temperature at the start of the experiment. Titration started with a first equilibration 2 µl injection to eliminate diffusion effects, which might have taken place at the bottom of the syringe needle. Then 54 injections of 5 µl of sugar solution were automatically added at 2 minutes intervals into the lectin solution stirred at 300 rpm. The heat evolved after each injection is measured by the cells feedback network as differential heat effects between sample and reference cell.

Control experiments were carried out by identical sugar injections into a cell containing buffer without protein and the relative heats of dilution and mixing subtracted from the heats of binding relative to the real titration experiment.

Final experimental results, represented by heat developed versus cell ligand/lectin ratio, are fitted using one and the two sequential binding sites per monomer models, available in Origin ITC Data Analysis Software, based on a non linear least square curve fitting procedure, Levenberg-Marquardt algorithm (Marquardt, 1963).

3.4.3 FC experiments

Two 3 × 100 mm columns were slurry packed with commercial ConA–Sepharose-4B, pnpm and pnpg affinity for this affinity media was investigated by Frontal Chromatography, by loading them (feed concentration range between 1.7 and 0.02 mM) at 0.1 ml/min. Experiments were carried out at room temperature (≈20°C), using 20 mM Tris buffer pH 7.2-7.4 containing 0.5 mM $CaCl_2$, 0.5 mM $MnCl_2$, 0.5 mM $MgCl_2$, 150 mM NaCl and 0.02% Thimerosal as the mobile phase. The column used for pnpm was operated in an automated BioRad FPLC system with Biologic Optics Module OM-10 at 280 nm and

AV7-3 injection valve. The second column for pnpg FC experiments was operated with a manual HPLC; pump, Rheodyne injection loop and a continuous flow cell UV 116 detector at 305 nm; frontal loading was realised using large injection loops.

The breakthrough curves response from frontal loading was normalised to the plateau value for each run and the dimensionless output C/C_o obtained. The retention volume V_r was calculated integrating the breakthrough curves as described in Chapter II. Different concentrations of p-nitophenyl-arabinopyranoside (pnpa), chosen as non specific sugar, have been applied to the two columns to calculate the non-retained solute elution volume (V_{nr}), columns voidage was not experimentally determined but it is assumed to be 0.32, based on commonly reported values. For each loading concentration C_o the amount of bound sugar at equilibrium is therefore easily calculated by $C_o(V_r-V_{nr})$ and dissociation constant (K_d) and maximum binding capacity (q_{max}) identified for the two affinity systems, fitting the data with Langmuir equation using non linear least square algorithm with a commercial software package (Scientist Micromath, Ltd).

ConA-Sepharose sites heterogeneity was investigated from Scatchard plots and speculations on the possible cooperativity among two populations of binding sites, made. The equilibrium data; Y (= q / q_{max}) versus C_o were also fitted using a two sequential binding site model (equation 2.31). The two resulting microscopic association constant were the model regression parameters and were subsequently used as input values in a simple multi-sectional equilibrium model of column performance, where the column is treated as a series of N equilibrium stages in which the mass balance for each stage (Figure 3.1) can be written as in equation (3.2). Coupling the mass balance (3.2) with the Langmuir isotherm (3.3), the concentrations of adsorbed and free solute in equilibrium at each stage are obtained in (3.4) and in (3.5). In Figure 3.1, the subscript i indicate the equilibrium stage, j expresses the initial condition (*1*), and equilibrium conditions (*2*). In the mass balance, ε is the external void volume fraction and α_s is the stationary phase volume fraction ($1-\varepsilon$).

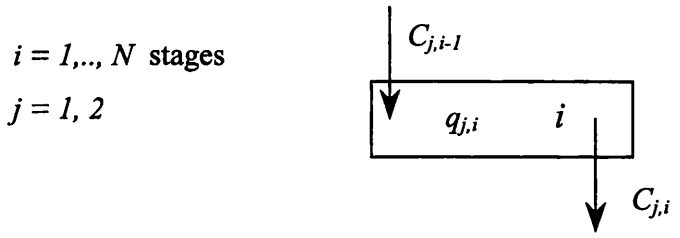

Figure 3.1: Single equilibrium adsorption stage adopted in the multi-sectional model, schematic representation.

$$C_{Tot} = \varepsilon \cdot C_{j,i-1} + \alpha_s \cdot (C_{j,i} + q_{j,i}) \tag{3.2}$$

$$q_{2,i} = \frac{C_{2,i} \cdot q_{\max}}{K_d + C_{2,i}} \tag{3.3}$$

$$C_{2,i} = \frac{C_{Tot} - K_d - \alpha \cdot q_{max} + \sqrt{C_{Tot}^2 + 2 \cdot C_{Tot} \cdot K_d - 2 \cdot \alpha_s \cdot C_{Tot} \cdot q_{max} + K_d^2 + 2 \cdot \alpha_s \cdot K_d \cdot q_{max} + \alpha_s^2 \cdot q_{max}^2}}{2} \tag{3.4}$$

$$q_{2,i} = \frac{C_{Tot} - C_{2,i}}{\alpha_s} \tag{3.5}$$

When the isotherm (3.3) is the Adair equation the problem can be solved with a bisection algorithm, the model was coded in Power Basic (listing in Appendix A).

The number of equilibrium stages was determined experimentally from the pnpg elution peak. The resulting C/C_o profile was compared with that obtained using the same model based on a single binding site equilibrium Langumiur equation (program listing in Appendix A) and with the experimental profile.

3.5 Immobilised ConA for monosaccharides Chromatography: Methods

Concanavalin A interactions with monosaccharides have been characterised and classified in the range of weak biomolecular interaction with K_d values between 10^{-2} and 10^{-4} M.
A Weak Affinity Chromatography (WAC) approach, first introduced by Zopf and Ohlson (1990), would therefore enable rapid separations throughout an immobilised ConA column bed, between similar molecules (monosaccharides) under isocratic elution conditions.

Two affinity media were tested based on ConA; the first one was obtained immobilising ConA on a DEAE anion exchanger cellulose resin and the second was a commercial preparate of ConA covalently immobilised onto Sepharose 4B using cyanogen bromide activation and coupling.

3.5.1 ConA immobilised on an anion exchanger

A number of buffers were tested over a range of pH values between 4.5 to 8, and buffer capacities between 2.5 to 20 mM to optimise the ionic adsorption of Con A onto GDC-carrier, a DEAE-cellulose resin. 50 ml of buffer was placed in a stirred tank and temperature controlled by a water bath. 0.1 ml of highly concentrated ConA solution (50 mg/ml) was added in the stirred tank with 1 ml of resin, gently stirred. Protein concentration was monitored using a UV-Detector previously calibrated (280 nm) linked to a personal computer. Trace quantities of $MnCl_2$ and $CaCl_2$ are included in the binding buffer and in some cases 1 mM of D-Mannose was added, to protect ConA affinity binding sites. A glass column 6 × 450 mm was then slurry packed with GDC-resin. As suggested by Danisco the column was washed with four bed volumes of 2% caustic soda, 25-30 bed volumes of deionised water, 3 bed volumes of 0.25 M sodium acetate buffer (pH 4.5), and again several deionised water bed volumes. Finally equilibrated with the binding buffer (2.5 mM Bis-Tris pH7.4 with 0.02% of sodium azide and 1 mM of $CaCl_2$ and $MnCl_2$). The column was loaded with ConA at room temperature and with a flow rate of 1 ml/min and final ConA concentration: 5, 10, 15, 20 mg per ml of resin were obtained and investigated. Sugar samples of 50-200 µl were injected through the column with and without lectin at flow rates between 0.2 ml/min and 1 ml/min. Concentrations between 0.04 to 1 mg/ml of D-Man, D-Glc and D-Fru, both singly and in a mixture, were injected and the concentration in the column effluent monitored using an RI detector.

3.5.2 Commercial ConA-Sepharose.

The biospecific adsorbent ConA-Sepharose 4B supplied by Pharmacia Biotechnology was prepared, packed, stored and regenerated in accordance with manufacturer's recommendations. The binding buffer was 20 mM Tris-HCl, pH 7.4 containing 150 mM NaCl, 0.5mM of $MnCl_2$ $CaCl_2$ and $MgCl_2$ and 0.01 % of Thimerosal as preservative.
Gel storage was at 4°C with 0.1 M acetate buffer pH 6 containing 1 M NaCl, 1mM $CaCl_2$, 1mM $MnCl_2$, 1 mM $CaCl_2$ and Thimerosal 0.02%. Usually after four-six weeks of use, ConA-Sepharose was regenerated for re-use by washing the gel alternatively with 3 column volumes of 0.1 M Tris Buffer pH 8.5 and 0.1 M acetate buffer pH 4.5 both containing 0.5 M NaCl. This cycle was repeated 3 times followed by equilibration in binding buffer as suggested in the Pharmacia instruction sheet. To avoid bed compression the manufacturer suggested 75 cm/h as maximum superficial velocity. Using a Shimadzu HPLC, two, slurry packed under mild vacuum, ConA-Sepharose stainless steel columns (4×114 mm and 4.4×250 mm) were tested using zonal elution experiments at room temperature and relatively high flow rates. Injections of different monosaccharide combinations were made using 20, 10 and 5 µl loops with flow rates between 0.20 and 0.5 ml/min to allow the possibility of sugar separation under isocratic conditions to be investigated.

3.6 Protein concentration determination: Results and Discussion

Absorbance at 280 nm gave the same calibration curve for BSA and ConA standards, represented by points and linear regression shown in Appendix B, evidence of the very close extinction coefficient for the two proteins. Calibration curves using the dye-binding assay (Appendix B) gave different results for the two proteins. Bradford assay results can vary with the amino acid composition and can be influenced by glyco-groups (Harris and Angal, 1989) likely present in protein molecules. Thus BSA was probably not the best standard in this case, also due to different level of glycosylation the use of a different lectin for calibration is not ideal.

Difficulties in expressing lectin molar concentration are due to a number of factors; principally these glycoproteins are usually a mixture of different subunit aggregates in

equilibrium with each other (monomer/dimer, dimer/tetramer etc.), in terms of sugar specificity, only part of the total protein may be active in solution and ideally that fraction needs to be known. Lectin sample relative activity can be quantified as the number of active binding sites (or active monomer × stoichiometry *n* of binding) per total content of protein.

Although at physiological pH and room temperature ConA is predominantly a tetramer, its concentration is expressed in terms of monomer concentration with the monomer molecular weight of 27.000 Da, (Liener *et al.*, 1986, Van Damme *et al.*, 1998).
For ConA concentration determination simple UV adsorption was used and therefore the relative instrument calibration employed. To remove very small fragments and large aggregates, samples were firstly dialysed (10 kDa cut off) against the same buffer, then filtered through a PVDF/PE syringe filter 0.22 μm.

In Appendix B the absorbance at variable wavelength for ConA and p-nitrophenyl-glucopyranoside equimolar solution are also reported and compared. This highlights that at 305 nm the lectin has much lower absorbance than the pnp-derivative and provides a basis for the UV detection of pnp-derivative in the presence of lectin.

3.7 ITC experiments: Results and Discussion

To be effectively detected, low affinity binding requires high protein concentration (*C*) as well as high ligand (titrant) concentrations. The ideal conditions for reliable determination of affinity should be chosen with the concentration of the protein around the dissociation constant K_d value and with the *c* parameter ($c = C \cdot K_d \cdot n$) between 5 and 100, however for weak interactions this is not always possible due to macromolecule solubility and aggregation limits, (Holdgate, 2001). Expecting a K_d value of circa 10^{-4} M, 0.15 mM ConA in the ITC cell seemed reasonable despite the low value for *c* (assuming unitary stochiometry of binding, $n=1$). This requires high concentration of titrants: 12.2 mM for D-Man and 24.4 mM for D-Glc for appreciable heat developments.

While resultant experimental conditions do not lie on the ideal titration range (Wiseman *et al.*, 1989) they resulted in excellent raw ITC plots where binding of monosaccharides is evident throughout the titration towards complete saturation.

Figure 3.2 shows ConA titration with 54 injections of 12.2 mM D-Man solution with data fitted with one (Figure 3.2, left) and two sequential set of biding sites (Figure 3.2, right). The single binding site model gave a good fit with reasonable values for the thermodynamic and affinity constants except that the stoichiometry value n was greater than 1. From the data obtained after each injection it is possible to calculate the amount of bound ligand and generate a Scatchard plot (Figure 3.4, left) whose non perfect linearity suggests the existence of an heterogeneous population of binding sites, (Zierler, 1989). Data generated from ITC-Origin software and calculated points for Scatchard plots relative to D-Man titration are reported as example in Appendix C, all the others titrations in this work are of the same format and follow the same logic. Using a two sequential binding site model, the results, reported on the right hand side of Figure 3.2 in terms of K_{a1} and K_{a2} are apparent binding constant, therefore the intrinsic constants can be evaluated with the statistical factors and they result to be $K_{a1}^{o} = 3519M^{-1}$ and $K_{a2}^{o} = 2018M^{-1}$ which shows negative cooperation.

Similar results are obtained when ConA is titrated with D-Glc solutions. The single binding site model gives a good fit (Figure 3.3, left) but again the final stoichiometry n is larger than 1. The final K_d value of 4×10^{-3} M seems to be particularly high (extremely weak interaction) and the Scatchard plot (Figure 3.4 right) is not again very helpful for verifying the model assumption or identify any cooperation effects. The second fit with the set of two sequential binding site model reported in Figure 3.3 (right) might be a more reasonable interpretation of the results. Negative cooperativity is again observed as in D-Man titration, from the values of intrinsic constants ($K_{a1}^{o} = 480M^{-1}$ and $K_{a2}^{o} = 308M^{-1}$) calculated using the statistically modified apparent values.

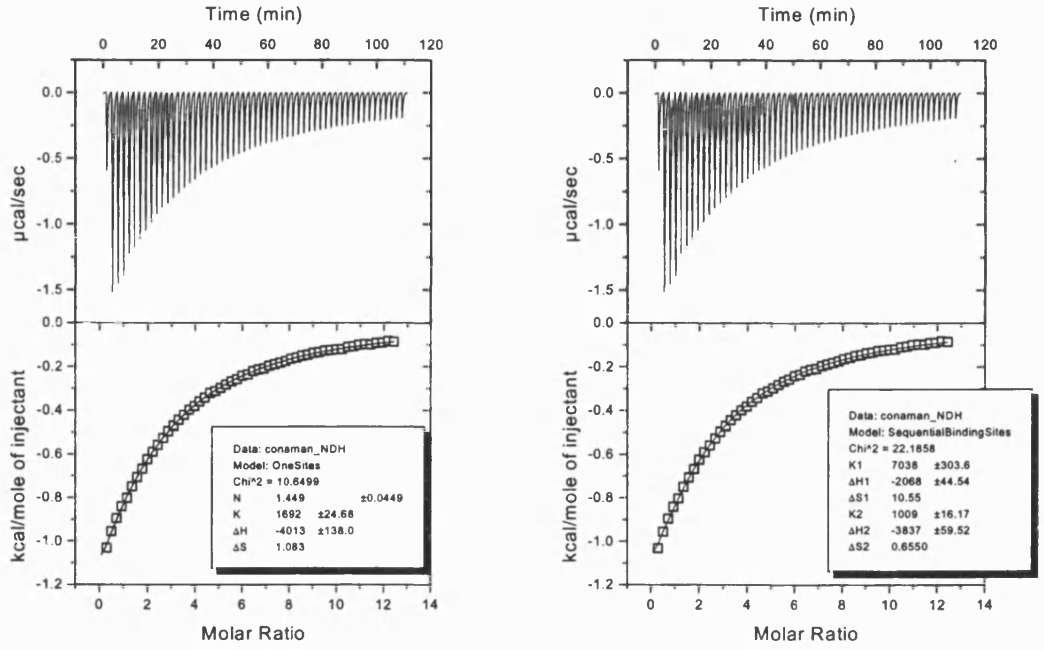

Figure 3.2: 0.15 mM of ConA titrated with D-Man (12.2 mM) at 20 C. Left: One single binding site model. Right: Two sequential binding site model. The parameter results and relative errors are summarised: N (Stoichiometry), K (association constant [M^{-1}]), ΔH (Enthalpy [cal mol^{-1}]), ΔS (Entropy [cal mol^{-1} K^{-1}])

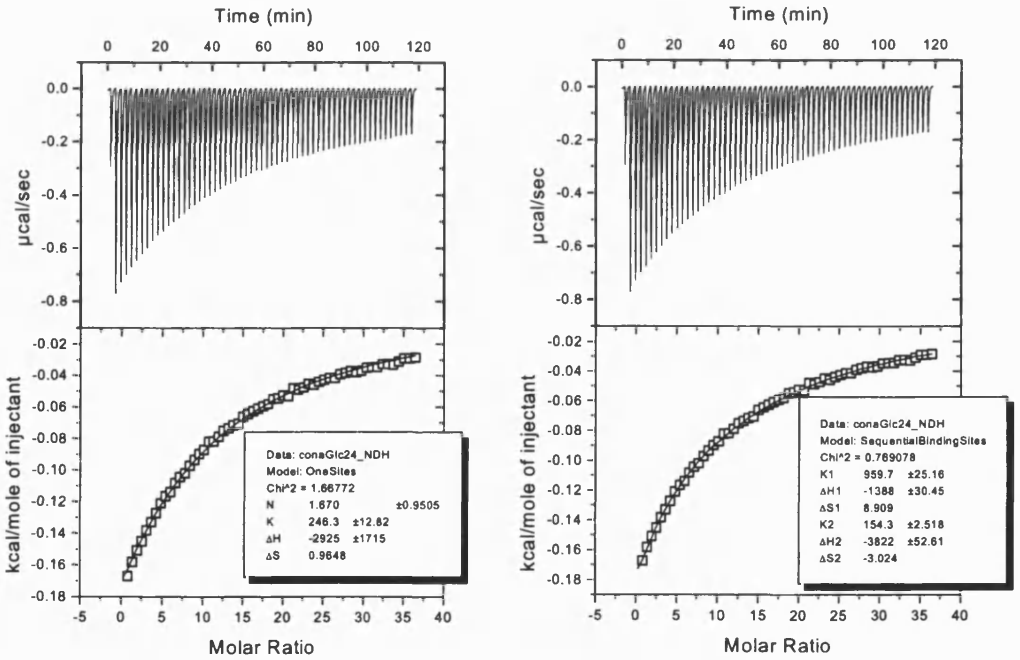

Figure 3.3: 0.15 mM of ConA titrated with D-Glc (24.4 mM) at 20°C. Left: One single binding site model. Right: Two sequential binding site model. The parameter results and relative errors are summarised: N (Stoichiometry), K (association constant [M^{-1}]), ΔH (Enthalpy [cal mol^{-1}]), ΔS (Entropy of [cal mol^{-1} K^{-1}]).

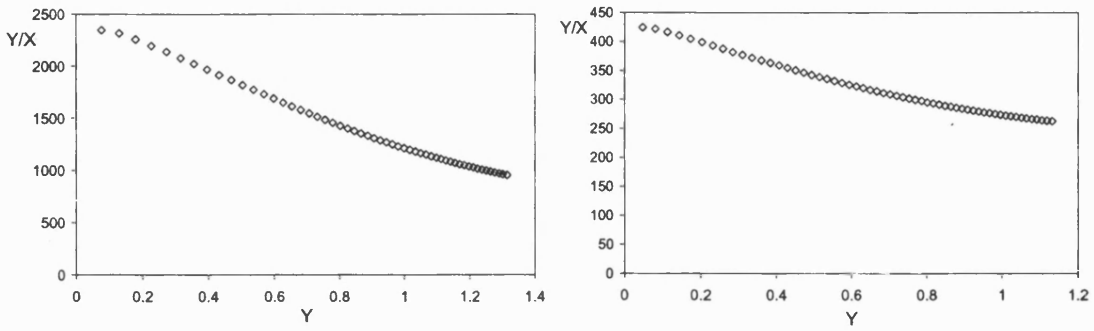

Figure. 3.4: Left: Scatchard plots for D-Mannose titration. Right: Scatchard plot for D-Glucose titration. After each injection, Y is the fraction of occupied sites over the total number of binding site and X is the total free ligand concentration.

The very high ligand/receptor molecular ratio needed to achieve saturation, compared to common values of maximum 2.5 for a *c* parameter below 10 (ITC user manual) and the lack of perfect linearity of Scatchard plots, suggest that the assumption of a single population of weak binding sites, described by a standard Langmuir adsorption isotherm, is not valid. However, the possibility of poor purity of commercial ConA could have affected results and must be considered as well.

Although between 5 to 9 hydrogen bonds (directly or through water molecules) are usually involved in monosaccharide-legume lectin binding, generally in the case of protein-ligand interactions, these are mainly mediated by hydrophobic nature (Srinivas *et al.*, 1999). A two step association consisting of the mutual penetration by the ligand of hydration layers causing disordering of the solvent followed by short-range specific interactions (Ross and Subramanian, 1981) could provide a realistic description of the phenomena observed here. In fact the positive high entropy values (ΔS_1=10.6 cal mol^{-1} K^{-1}, for D-Man ΔS_1=8.9 cal mol^{-1} K^{-1} for D-Glc) associated with the first population of binding site with respect to the lower values (ΔS_2= 0.7 cal mol^{-1} K^{-1}, for D-Man. ΔS_2= -3 cal mol^{-1} K^{-1} for D-Glc) for the second, shows the energetic importance of solvent molecule reorganisation at the start of the interaction. According to this concept when the first binding "step" is over with the most of solvent reorganisation around the protein established, some ConA promoter would

be able to accommodate another monosaccharide probably with more hydroxyl groups available for binding, since $|\Delta H_2| > |\Delta H_1|$.

Derewenda *et al.* (1989) and Loris *at al.* (1989) elucidated, at atomic resolution, the crystal structure of both ConA-methyl-α-D-mannopyranoside and ConA-trimannoside complexes. These results identified all the key features of binding in terms of the linkages between one sugar molecule carbons and key lectin aminoacids. However since the binding site can accommodate a trimannoside molecule, it is possible that more than one small monosaccharide molecule could be bound with weaker affinity. An isothermal calorimetric titration study with ConA carried out by Williams *et al.* (1992) suggests that binding can occur through a number of distinct sites instead of a single high affinity site. In any case, according to the assumptions made, a monomer with one "large" binding site or more than one standard binding site results in a system stoichiometry greater than 1.

3.8 FC experiments: Results and Discussion

Frontal loadings of a number of different concentrations of pnpm and pnpg through two 3 × 100 mm ConA-Sepharose 4B columns are shown respectively in Figure 3.5 and 3.6.
From these breakthrough curves the retention volume V_r relative to each concentration loaded C_o is calculated. The non-retained elution volume $V_{nr} \approx 0.85$ ml does not change with injected pnpa concentration in the first column (Appendix B). The bed volume is 0.7 ml and the higher value of retention for pnpa is likely to be mainly due to extra-column effects rather than to non-specific interaction. For the second column operating with different equipment, the extra column void effect is even higher due to the longer internal tubing of the UV 116 respect to the smaller FPLC optical unit, employed for the first system. 0.37 mM of pnpa was eluted with a retention of 0.91 ml. However if the extra column dead volume affects the breakthrough curve shape, it has the same effect on the final value of retention volumes and no influence on the final amount of adsorbed solute $C_o(V_r-V_{nr})$ in equilibrium with C_o.

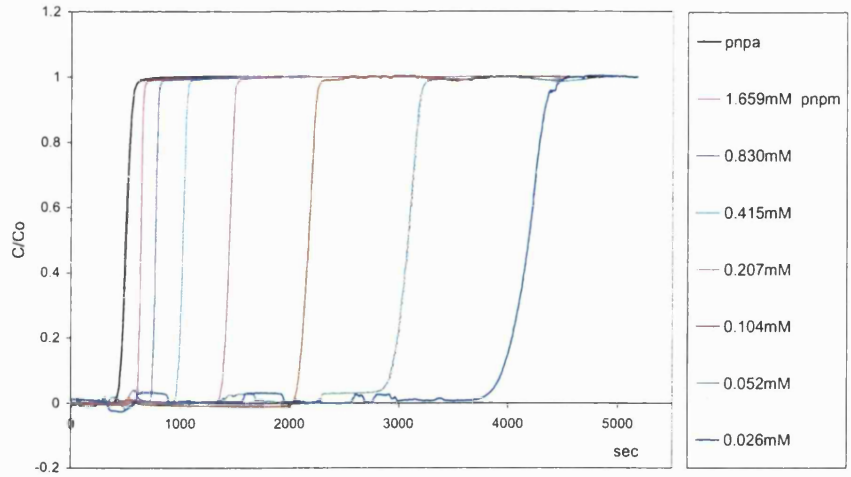

Figure 3.5: FC curves for 3×100 mm ConA-Sepharose 4B glass column. Non retained pnpa breakthrough curve first on the left and 7 breakthrough curves for pnpm at different loading concentration (in the legend).

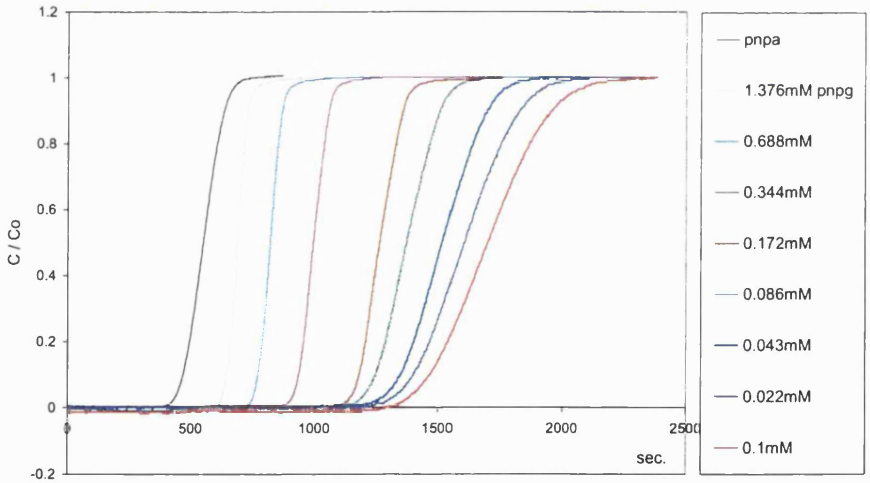

Figure 3.6: FC curves for 3×100 mm ConA-Sepharose 4B glass column. Non retained pnpa breakthrough curve first on the left and 8 breakthrough curves for pnpg at different loading concentration (in the legend).

All data and calculated results relating to these experiments are given in Appendix B. The final results: experimental equilibrium points *(q, C)* and relative Langmiur isotherm fits are summarised for pnpa and pnpg in Figure 3.7.

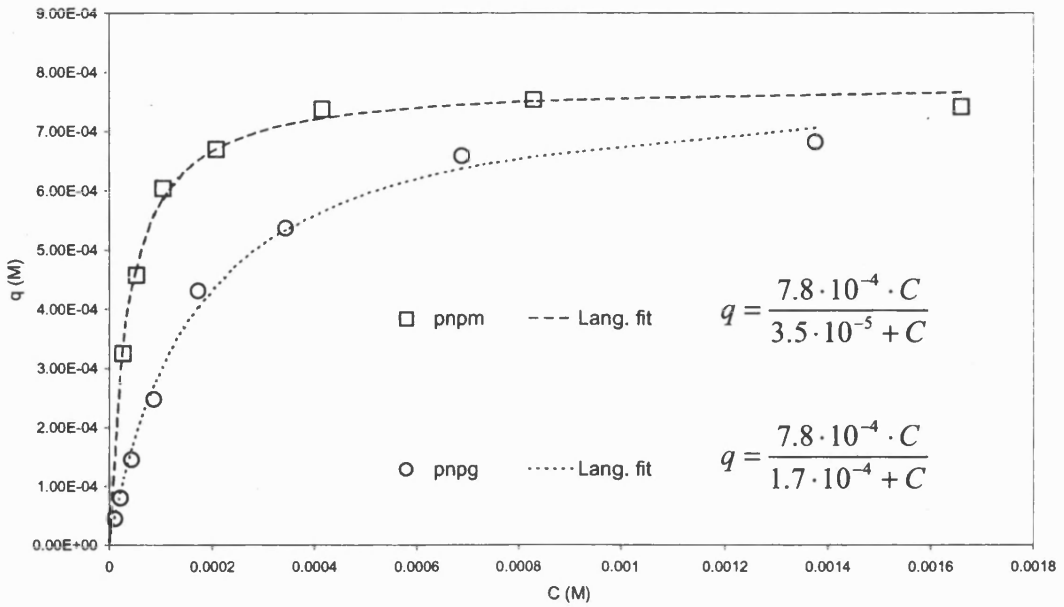

Figure 3.7: Pnpm and pnpg experimentally calculated adsorption equilibrium points from FC method and Langmiur fitting curves calculated with Scientiest software package.

The suggested capacity for ConA-Sepharose (between 3 and 7×10^{-5} M), given on the manufacturer's data sheet is more than 10 times lower than the value determined here, but this was determined for a larger adsorbate molecule (porcine thyroglobulin, MW=660.000 Da). Assuming ConA immobilised on the gel is 100 % active and assuming (from manufacturer's specification) 15 mg of ConA per ml of Sepharose, based on ConA monomer and one binding site per monomer, the theoretical maximum binding capacity is approximately 6×10^{-4} M. The experimentally calculated maximum binding capacity (in close agreement for both systems) was 30 % higher than the maximum theoretical value. This over capacity could be related either to hydrophobic interactions of sugar derivative phenyl group with ConA, which however were not enough to delay non-specific pnpa elution, or to a partially extended specificity of ConA monomer. The fact that the voidage ε was not measure and assumed to be 0.32, could have affected the final results as well as other experimental errors such as flow rate accuracy, however as the different systems give similar results this is unlikely. The dissociation constants obtained, $K_d = 3.5\times10^{-5}$ M for pnpm and $K_d = 1.7\times10^{-4}$ M for pnpg are lower than ITC results, reported in the previous

section, also lower than other solution values found in the literature for the interaction of ConA with D-Man and D-Glc amd summarised in the introduction of this chapter. On the other hand they show closer agreement with the literature chromatographic results for immobilised ConA- pnp-monosaccharides interactions. This reinforces the view that the phenyl group might play a role in binding when associated with some other specificity. It also appears that the overall biochemical selectivity of ConA is not altered by immobilisation on agarose based gels.

The Scatchard plots (q/C_o *vs.* q, Figures 3.8) suggests the possibility of a cooperativity within an heterogeneous population of binding sites, therefore the equilibrium data for pnpg; Y (q / q_{max}) versus C_o were fitted with Scientist software package adopting a two sequential binding site Adair equation (2.31). The result is a good fit reported in Figure 3.9 with the intrinsic equilibrium constants describing a positive cooperativity.

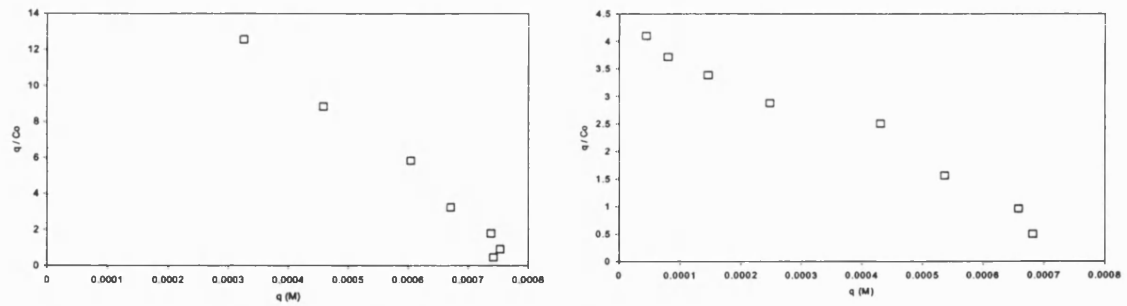

Figure 3.8: Right: Scatchard plot from FC data describing pnpm partition between ConA stationary phase and liquid mobile phase. Left: Scatchard plot from FC data describing pnpg partition between ConA stationary phase and liquid mobile phase.

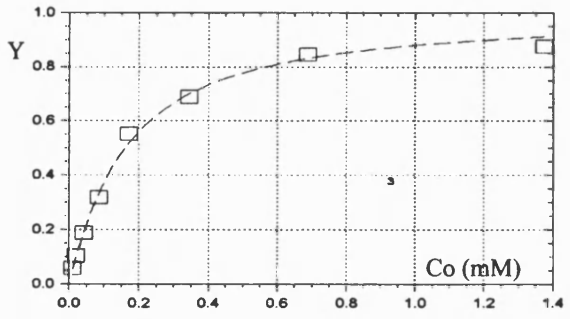

$$K^o_{a1} = 5200\ M^{-1}$$

$$K^o_{a2} = 7200\ M^{-1}$$

Figure 3.9: Two binding sites Adair model, experimental data points □ and fitting curve (dashed line). K^o_{a1}, K^o_{a2} are the resulting intrinsic association constants, fitting regression parameters.

Also, the experimental breakthrough curves for pnpg were compared with the breakthrough curves obtained using a multi-sectional equilibrium model based on a Langumiur adsorption equation with relative K_d input and based on the two binding sites Adair equation and relative K^o_{a1}, K^o_{a2} inputs. A number of 30 equilibrium stages was obtained from zonal application of diluted pnpg samples into the 3×100 mm ConA-Sepharose column and used in the multisectional model. This comparison is summarised for six different pnpg concentrations in Figure 3.10 and the Adair model gives a better fit, although at high concentrations the two predictions overlap. The same observations were not made for pnpm because the simple multisectional equilibrium model seemed not to give a good description for the stronger affinity pnpm-ConA system with both the one and two binding site model assumptions.

3.9 ITC-FC comparison

Parameters such as strength of interaction and maximum binding capacity are obviously essential for system characterisation and prediction of the viability of the separation. From both ITC titrations and FC experiments Concanavalin A showed weak specific interactions with glucose, mannose and their derivatives, associated with a certain level of binding heterogeneity. While the titrations experiments suggest a second population of weaker binding sites (negative cooperativity), FC experiments show positive cooperativity. Despite the apparent contradiction both sets of results are in line with literature data, so final absolute conclusions can not be made. Extended specificity, hydrophobicity, solvent reorganisation and any other weak side effects of biomolecular interactions are not negligible when associated to weak affinity interaction and can be influenced by the different environmental conditions. It is very difficult to find a single parameter, which can describe lectin-monosaccharide interactions, and it can be obtained only as a compromise of approximations and assumptions. It was felt that further investigation or speculation would not reach the objectives of this project. It is important though that ITC for free lectin-monosaccharide and FC for immobilised lectin-monosaccharide were shown to be quick and effective in providing a detailed picture of their biological interaction and a starting point for the design of monosaccharide separation process.

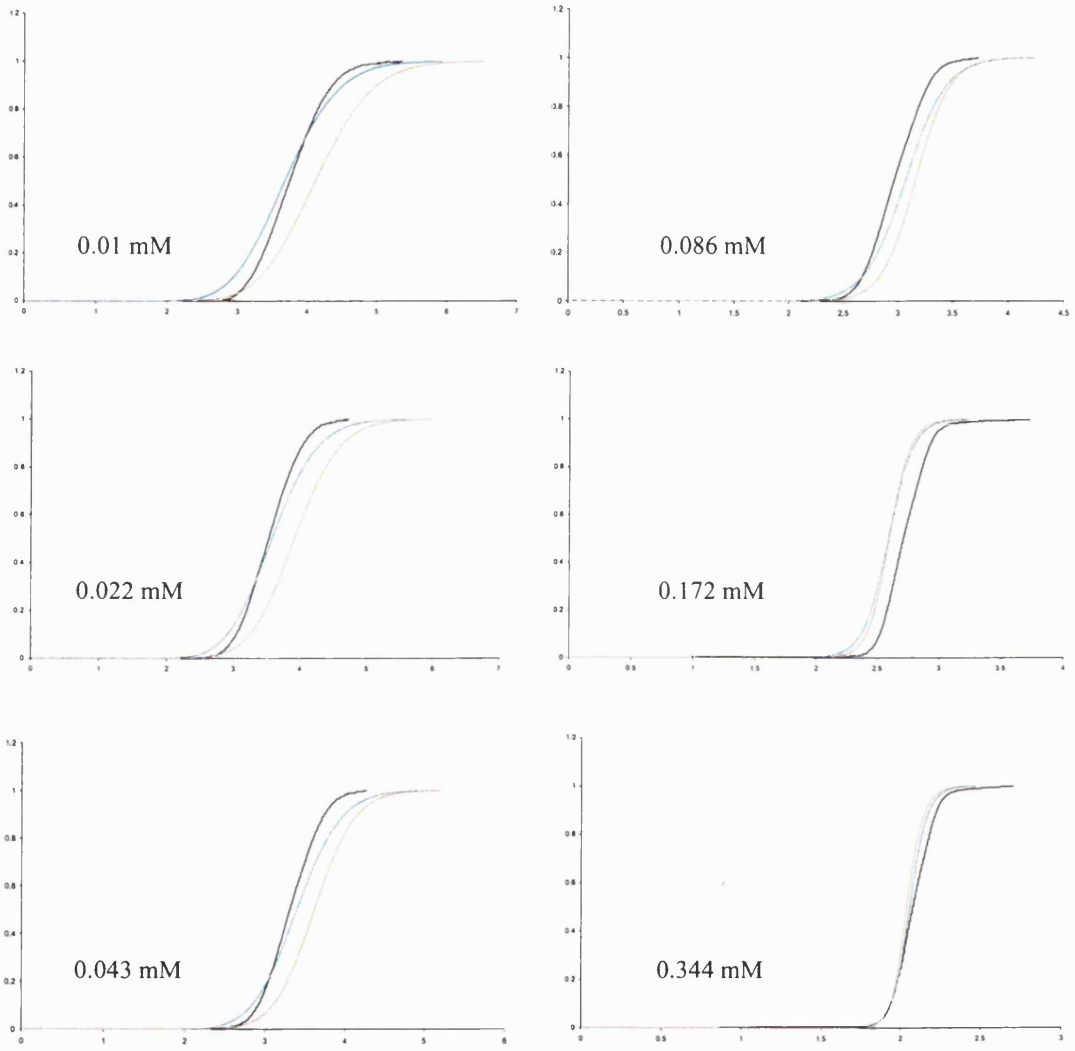

Fig.3.10: Experimental breakthrough curves of different pnpg concentrations loaded into Con A-Sepharose 4B column (black curves) and multi sectional model results adopting one binding site Langmuir equation (orange curves) and two sequential binding sites Adair equation (blue curves). X-axis: elution volume fraction (V_r/V_{bed}), Y-axis: C/C_o.

3.10 Performance of ConA-GDC resin: Results and Discussion

Agrawal and Goldstein (1968) and Pazur *et al.* (1996) investigated the physiochemical properties of ConA and reported the *pI* of ConA at pH 7.2. This is confirmed by another

study by Wang and Edelman (1978) who investigated the stability of ConA and covalently cross-linked ConA derivatives. The best ConA ionic immobilisation onto the DEAE-cellulose beads with minimum aggregation and lectin stability problems, was obtained using BisTris buffer 2.5 mM pH 7.4 containing 0.25 mM $MnCl_2$ and 0.25 mM $CaCl_2$. ConA was not significantly eluted by changes in ionic strength but pH values below 5 led to significant displacement. Ionic coupling between GDC-resin and ConA has shown a binding capacity of more than 20 mg of ConA per ml of dry cellulose during batch anion adsorption (experimental equilibrium data in Appendix B). When zonal chromatography of a monosaccharide mixture were performed, at different immobilised ConA densities, flow rates and sugar sample concentrations no separation was detected. Even when dextran was injected, its elution was unaffected by the presence of the affinity ligand. Dextran is a large polysaccharide with many specific groups, able to interact with immobilised ConA resulting in polyvalent interactions, collectively much stronger than corresponding monovalent interactions (Elgavish and Shaanan, 1997, Mammem *et al.*, 1998). Therefore if Dextran is not bound on the affinity packing it is unlikely to be active. It is clear that sugar-binding sites of ConA are directly affected by ionic interactions, so much that the lectin completely looses its sugar binding affinity. Loading of ConA onto the GDC-resin in the presence of its specific "counter-sugar" to protect the binding site did not solve the problem.

Other workers have used ConA-cellulose beads as an affinity chromatography medium (Mislovičová *et al.* 1995 and Gemenier *et al.* 1998) but in these cases the coupling between protein and cellulose support was always covalent.

3.11 Performance of ConA-Sepharose: Results and Discussion

Proof that ConA-Sepharose is an efficient affinity adsorbent for monosaccharides was demonstrated under isocratic conditions exploiting their weak interactions. Reasonable separation was obtained by decreasing the injection volume from 20 to 5 µl leading to the identification of the sample volume as a critical parameter in experimental design as generally expected in low capacity and non linear systems. With 5 µl injections quite broad peaks were obtained at a flow rate of 0.2 ml/min, increasing the flow rate to 0.25 ml/min

and then 0.3 ml/min induced a loss of resolution and efficiency. L-fucose (L-Fuc) and L-arabinose (L-Ara) were not retained, D-Man showed, as expected, the highest binding, while D-fructose (D-Fru), which was expected not to be retained, showed higher affinity than D-Glc. Some chromatograms obtained from injecting monosaccharides mixtures of 1 and 0.5 mg/ml at different flow rates are shown from Figure 3.11, to 3.14. Other chromatograms are in Appendix D and from those, retention times (t_r), peaks widths (W), for L-Ara, L-Fuc and D-Man and HETP values (H) for D-Man, are measured and the results summarised for different flow rates in Tables 3.2 and 3.3 (calculations are based on the classical equilibrium Plate theory). Early investigation with the short column (4 × 114 mm) did not give high resolutions but clearly showed differences in interactions between packed ConA-Sepharose and monosaccharides (Figure 3.11), while significant improvement was achieved with the longer column (4.6 × 250 mm), chromatograms in Figures 3.12, 3.13 and 3.14.

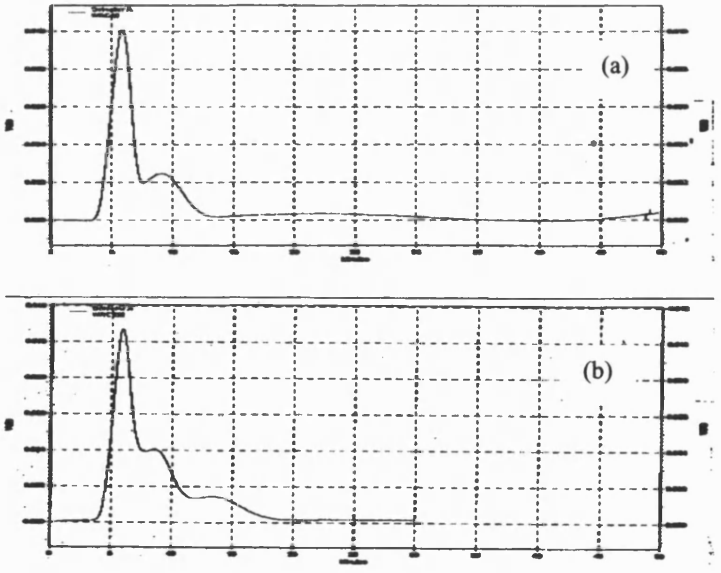

Figure 3.11: (a); Affinity chromatography of 5 µl mixture containing 0.5 mg/ml L-Fuc, 0.5 mg/ml D-Fru. (b); Affinity chromatography of 5 µl mixture containing 0.5 mg/ml L-Fuc, 0.5 mg/ml D-Fru, 0.5 mg/ml D-Man. Flow rate 0.3 ml/min, 4 × 114 mm column. Y-axis from 0 to 0.012 Volts (RI signal output).

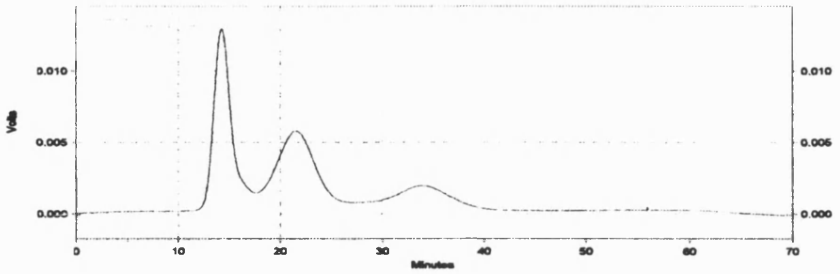

Figure 3.12: Affinity chromatography of 5 µl mixture containing in elution order 1 mg/ml of L-Ara, 1 mg/ml of D-Fru, 1 mg/ml of D-Man. Flow rate 0.3 ml/min, 4.6 × 250 mm column.

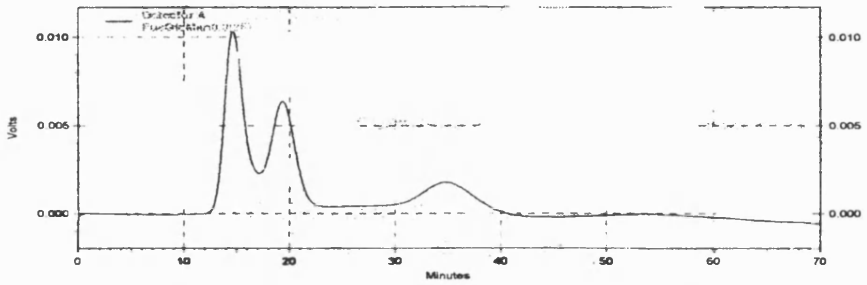

Figure 3.13: Injection of 5 µl mixture containing in elution order 1 mg/ml of L-Ara, 1 mg/ml of D-Glc, 1 mg/ml of D-Man. Flow rate 0.3 ml/min, 4.6 × 250 mm column.

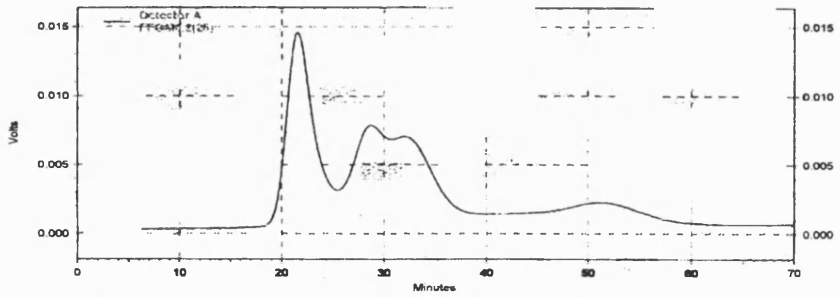

Figure 3.14: Injection of 5 µl mixture containing in elution order 1 mg/ml of L-Fuc, 1 mg/ml of D-Glc, 1 mg/ml of D-Fru and 1 mg/ml of D-Man. Flow rate 0.2 ml/min, 4.6 × 250 mm column.

Table 3.2: ConA-Sepharose 4 × 114 mm column. Data from Zonal Chromatography experiments with Shimadzu HPLC, elution of 5 µl containing L-arabinose and D-mannose (Chromatograms in Appendix D).

Flow rate ml/min	W_{Ara} min	W_{Man} min	$t_{r\,Ara}$ min	$t_{r\,Man}$ min	R	$HETP_{Man}$ cm
0.20	6	17.5	8.5	22.5	1.2	0.43
0.25	4.5	14.5	7	17.5	1.05	0.49
0.3	4	13.5	6	14.5	0.97	0.62

Table 3.3: ConA-Sepharose 4.6 × 250 mm column. Data from Zonal Chromatography experiments with Shimadzu HPLC, elution of 5 µl containing L-fucose and D-mannose (Chromatograms in Appendix D).

Flow rate ml/min	W_{Fuc} min	W_{Man} min	$t_{r\,Fuc}$ min	$t_{r\,Man}$ min	R	$HETP_{Man}$ cm
0.2	5	12	23	54	>2	0.077
0.25	4	11.5	18	45	>2	0.102
0.3	4	9.5	16	35.8	>2	0.11
0.35	3.5	8	12.8	29.5	>2	0.115
0.4	3	7.5	11	25.5	>2	0.135
0.45	3	7	10	22	>2	0.158

Figure 3.15 shows the trend of the height equivalent of a theoretical plate; *H* increases with flow rate increases. The high value of *H* is within standard values in bio-affinity chromatography particularly when dealing with slow kinetics, large macro-porous support (Sepharose-4B has an average particle diameter of 90 µm) and weak affinity.

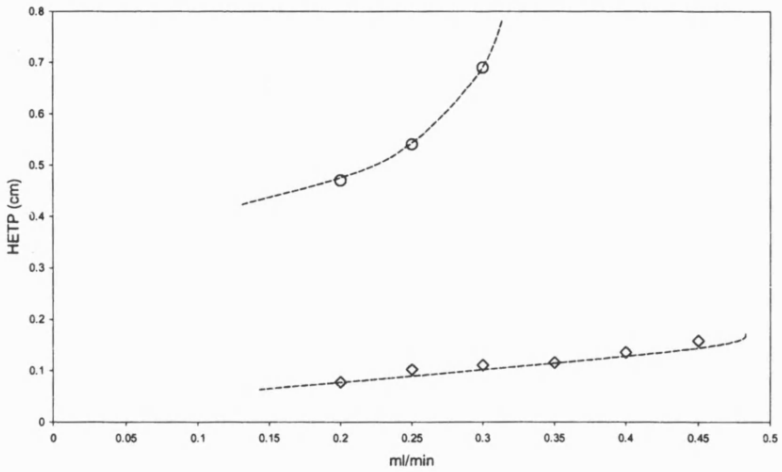

Figure 3.15: HETP function of mobile phase flow rate: ○ 4 × 125 mm Con A-Sep. column; •: 4.6 × 250 mm Con A-Sep. column.

The higher HETP values found for the first column with respect to the ones obtained for the longer column was probably related to pre and post column contribution to peak broadening, obviously more important with the smaller column. Kaltenbrunner *et al.*(1997) demonstrated that approximately 60% of the total peak broadening for a 1 ml column is caused by extra-column effects. The obtained column efficiency could appear poor compared with HPLC applications nevertheless it is well within the range of standard bio-chromatography (Jungbauer, 2000; Yamamoto, 1988).

This preliminary work on Concanavalin A has demonstrated that small differences between monosaccharides in terms of affinity interaction with the lectin based stationary phase can be successfully exploited and yield purified small sugar bands under isocratic elution. Although the apparently high molar capacity shown by ConA for monosaccharide molecules is encouraging, the unfavourable molecular weight ratio between the species involved limits the possible amount of sugar mixture processed to low concentration and volume. The obvious main drawback is that such a process will be attractive only when applied to bio-refining processes of high added value targets.

Chapter IV

Preparation and Characterisation of an L-Fucose Binding Lectin

4.1 Summary

A brief literature review of the known fucose-binding lectins is summarised in the introduction of this chapter. After these were assessed on the raw material practical availability, economics and level of specificity for L-fucose, one was chosen and purified for further chromatographic applications. This chapter reports the purification procedure of this lectin, carried out using column and stirred batch affinity chromatography onto L-fucose-Sepharose 6B and its characterisation in terms of molecular weight, activity and interaction with the monosaccharide. A number of techniques were exploited for this purpose; including typical haemaglutination tests, gel permeation chromatography, gel electrophoresis, Surface Plasmon Resonance and Isothermal Micro-Calorimetric titrations. The final purified lectin was LTA from *Lotus Tetragonolobus* (winged beans) with yields between 300 and 500 mg per 100 grams of seeds. LTA showed agglutination activity with blood-group O erythrocytes, the molecular weight of the major lectin fraction was found to be around 34 kDa with two specific binding sites (probably one binding site per monomer of 17 kDa each). The interaction for L-fucose was found to be entropy-enthalpy assisted and quantified with a dissociation constant between 3 and 8×10^{-4} M depending on the temperature.

4.2 Introduction

The major sources of fuco-lectins from animal and plant kingdoms are: seaweed, *Ulva Lactuca* (Sampaio et al. 1998); eel serum, *Anguilla Anguilla* (Desai and Springer, 1972); orange peel fungus, *Aleuria Aurantia* (Kochibe and Furukawa 1980, 1982); gorse, *Ulex*

europeus, (Osawa and Matsumoto 1972, Allen and Johnson, 1977); winged beans, *Lotus Tetragonolobus*, (Yariv *et al.*, 1972, Allen and Johnson, 1977). In Table 4.1 these lectins are summarised with the minimum concentration of L-fucose required to inhibit agglutination of O-group blood cells and equilibrium constants for the lectin-monosaccharide interaction with relative literature references.

Table 4.1: Summary of the main L-Fucose binding lectins from animal and plant kingdoms with minimum L-Fucose concentration required to inhibit O red blood cells agglutination and dissociation constant describing the binding equilibrium between L-fucose and lectin.

Source	FucoLectins	Minimum concentration (mM) of L-fucose giving complete inhibition of Agglutination of Group O Erythrocytes.	K_d (M)
Fungus	Aleuria Aurantia	0.78 (Kochibe and Furukawa, 1980)	1.6×10^{-5} (Kochibe and Furukawa, 1980)
Eel	Anguilla Anguilla	0.75 (Hořejší and Kocourek, 1978)	1.6×10^{-3} (Kelly, 1984)
Winged beans	Lotus Tetragonolobus	0.75 (Allen et al., 1977)	2.7×10^{-5} - 1.7×10^{-4} (Kalb, 1968)
Gorse	Ulex europeus	2.5 (Allen et al., 1977)	3.2×10^{-4} (this work)
Marine algae	Ulva Lactuca	25 (Sampaio et al., 1998)	-

Ulex europeus (UEA I) from gorse and *Lotus tetragonolobus* (LTA) from Asparagus pea (winged beans), are the most widely studied members of the L-fucose binding lectin class and definitely the most readily available among all the other fucolectins.

These plants are widely dispensed in Europe, belong to leguminosae plant family and the lectins have an O-blood group specificity and affinity for L-fucose and fucosyl oligosaccharides (Pereira and Kabat, 1974, Pereira *et al.*, 1978).

UEA I and LTA are not as well characterised as for instance ConA, and chemical, physical and toxicological properties have not been thoroughly investigated. Thomas and Surolia (2000) investigated the mode of molecular recognition of L-Fucose by UEA I and LTA but while the primary structure of these lectins is available (Konami *et al.*, 1990 and 1991), no crystal structures for any lectin belonging to the fucose specific group have yet been reported. Allen *et al.* (1997) compared the two lectins binding specificities by hemagglutination inhibition analysis and LTA exhibits approximately 3.5-fold higher affinity than UEA I. During microcalorimetric comparisons of commercial UEA I and LTA, Ulex lectin showed weaker binding, according to literature. Therefore the project focused on the purification and characterisation of LTA, chosen as the best candidate among the L-Fucose binding lectin.

4.3 Commercial L-fucose binding legume lectins: ITC characterisation

Materials. Lyophilised powders of UEA I lectin, purified from gorse seeds according to the method of Pereira *et al.* (1978) and LTA lectin, purified from winged beans seeds according to the method of Pereira and Kabat (1974) were purchased with the other chemicals involved in the titration experiment, from Sigma (Poole, U.K.).

Methods. OMEGA Microcalorimeter VP-ITC was adopted for these studies as already described previously. These applications were carried out in 50 mM Phosphate buffer pH 7.2-7.4 containing 150 mM NaCl and 0.02% NaN_3 and run at 20 °C.
Solid LTA and UEA I were dissolved and dialysed against the same buffer at 5°C, filtered with PVDF/PE syringe filters and monomer concentration (27000 Da) adjusted to 0.077 and 0.037 mM respectively. Titrant sugar samples of L-fucose were diluted to final concentrations of 3 mM for LTA and 12.2 mM for UEA I titration. Injections of 5 µl of sugar solution were automatically added with a 290 µl microsyringe every 3 minutes into the lectin solution stirred at 300 rpm and the heat developed after each injection measured. Final experimental results, represented by heat developed versus total ligand/lectin ratio in the cell, are fitted considering one to one binding between lectin monomer and L-fucose.

Results. From ITC experiments, in terms of association constant, Lotus lectin resulted 3.6 fold stronger than UEA I in L-Fucose binding in agreement with literature (Allen *et al.*, 1977). Figure 4.1 reports the two titrations with relative thermodynamic results for binding parameters. Dissociation constants for lectin-sugar interaction is evaluated, 9×10^{-5} M for LTA and 3.2×10^{-4} M for UEA I, also substantial differences among enthalpy and entropy of binding in the two systems represent evidence of different mechanisms involved in molecular recognition.

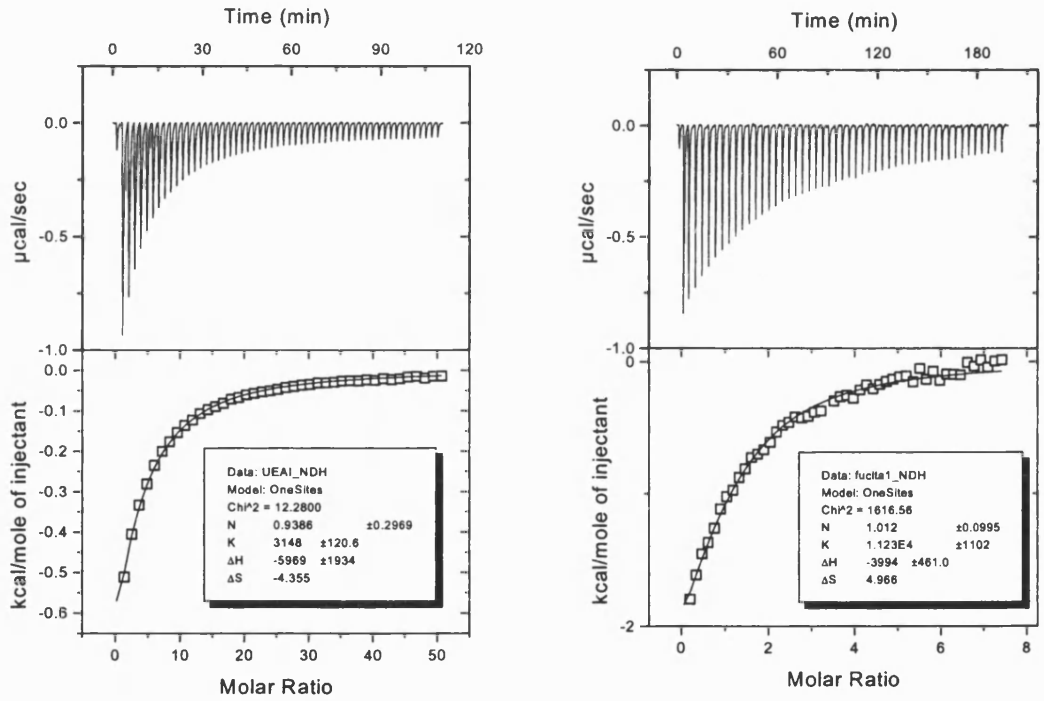

Figure 4.1: Left; Commercial UEA I (0.037 mM) isothermal titration with L-Fucose (12.2 mM) with one binding site model fitting curve and parameter results. Right; Commercial LTA (0.077 mM) isothermal titration with L-Fucose (3 mM) with one binding site model fitting curve and parameter results.

Although the Wiseman parameter *c* (2.49) is low compared to the recommended range for best titration isotherm achievement (approximately $c = 0.1$ for UEA I titration and $c = 0.9$ for LTA titration), Figure 4.1 highlights that excellent binding site saturation can be obtained using highly concentrated titrant injections. Nevertheless there is more

uncertainty on the resulting regression parameters obtained from the non linear least square data fitting algorithm in figure 4.1-left representing LTA titration, where the isotherm is obtained with lower c and higher injected L-Fucose concentration.

4.4 LTA purification and characterisation: Materials

One kilogram of seeds from *Lotus Tetragonoblobus* (Winged beans) was obtained from Thompson & Morgan Wholesale Ltd. (Ipswich, England), some of these were used to grow our own cultivation of winged beans plants. Sepharose 6B, Sephadex G-25 and Sephacryl S-100 were bought from Amersham Pharmacia Biotechnology (Buckingamshire, U.K.). divinyl Sulfone, L-fucose, p-aminophenyl-L-fucopyranoside (papf), Phosphate and Mops buffers, salts, NaN_3, proteases inhibitor cocktail, protein standards and high retention cellulose dialysis tubing were purchased from Sigma Ltd. (Poole, England). For haemagglutination experiments, blood-group O erythrocytes were purchased from the local hospital and crude papain, cysteine hydrochloride and PBS tablets from Sigma (Poole, England). LTA concentration was determined using a UV detector at 280 nm and Surface Plasmon Resonance (SPR); Biacore X, CM5 microchip, HEPES buffer, amine coupling kit purchased from Biacore (Stevenage, U.K.). Purified LTA activity in terms of capability to bind L-fucose was measured using the SPR response and also, for larger samples, using titration microcalorimetry ITC from MicoCal (Milton Keynes, U.K.), the latter technique was also used to characterise LTA-L-Fucose interactions. PVDF/PE small syringe filters 0.22 μm, Sterivex-GP filter units 0.22 μm, Millipore pump and Minitan ultrafiltration module with 4 Polysulphone membranes (10 kDa cut off) were purchased from Millipore (Watford, U.K.). The solvent used in these applications was always ultrapure water from a ELGA Purelab Option Unit (Bucks, U.K.). BioRad FPLC, BioRad (Hertfordshire, U.K.), was equipped with a workstation with two pumps, an external water bath, an auto-injection valve AV7-3, select buffer valve SV5-4, Biologic Optics module OM-10, conductivity detector, 2128 Fraction Collector with relative control and analysis software. 10-20% Tris-Glycine SDS page for polyacrylamide gel electrophoresis, sample and running buffers, pre-stained standards, staining, destaining and drying solutions were obtained from Invitrogen-Novex (Paisley, U.K.), while power supply EPS3500XL and cell Xcell II from Amersham Pharmacia Biotech. (Buckinghamshire, U.K.).

4.5 LTA purification and characterisation: Methods

The purification strategy is summarised in Figure 4.1 and was based on an Affinity Chromatography protocol developed from a procedure reported by Allen and Johnson (1977). The first step sample preparation is achieved in several sub-steps: seed grinding, liquid extraction, centrifugation, concentration, and filtration. Subsequently, capture, intermediate purification and polishing of the target lectin are carried out using an affinity chromatography approach followed by dialysis and finally sample lyophilisation. The process was initially investigated with a small-scale affinity chromatography column, larger production of LTA was carried out in a single stage stirred batch adsorption vessel. A Biacore X biosensor system equipped with a L-fucose-CM5 sensor chip was exploited in extraction, monitoring and optimisation as well as in activity (together with hemagglutination experiments) tests and concentration (together with UV assays) measurements of purified and non–purified (crude extract samples) LTA.

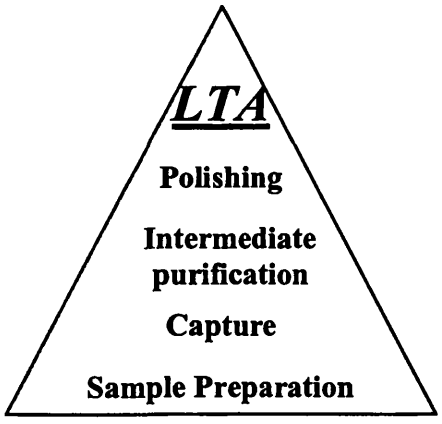

Figure 4.1: From the base to the top of the triangle the purification strategy is summarised step by step.

The protein native molecular weight was determined using Gel Permeation Chromatography (GPC) on Sephacryl S-100 columns using an FPLC, and reduced-denatured protein molecular weight determined with gel electrophoresis. Purified LTA powder was redissolved in buffer and titrated with the same L-fucose-containing buffer

using ITC at different temperatures to allow the interaction to be fully characterised in terms of enthalpy, entropy, stoichiometry and equilibrium binding constant.

4.5.1 Sample preparation

LTA seeds were ground with an electrical grinder, then stirred throughout extraction at 5°C overnight in Phosphate or Mops buffer (50 mM pH 7.2-7.4, containing 150 mM NaCl and 0.02% Sodium azide. Mops also contains 0.5 mM $CaCl_2$, $MgCl_2$ and $MnCl_2$) at a ratio of 1g of ground seeds per 10 ml of buffer. Shorter extractions were also performed and the ratio total active LTA present in the extract over time of extraction optimised. After centrifugation at 4000 rpm and 5°C, the supernatant was stored in the fridge, the solid residue was re-extracted in the same way and the second extract added to the first. 0.01 ml of protease inhibitor cocktail per ml of crude extract was added to prevent proteolitic degradation of lectin. A quick and effective concentration of the final product was carried out for small sample volumes, adding 0.1 g of Sephadex G-25 (dry matrix polymer) per ml of extract mixing for 15 minutes (Harris and Angal 1989). The swelling dry resin adsorbs water and due to the small pore size exclude big protein molucules. The supernatant was centrifuged again and finally filtered with Sterivex-GP filter units 0.22 μm; concentration and filtration were both conducted at 5°C. Extract samples bigger than 200 ml were concentrated with 4 Polysulphone membranes (10 kDa cut off), placed in series in a Minitan ultrafiltration module, the retentate LTA rich product was then filtered with Sterivex-GP filter units 0.22 μm.

4.5.2 Affinity media preparation

The biospecific L-fucose based adsorbent was made using divinyl Sulphone activation of Sepharose 6B, according to the protocol reported by Fornsted and Porath (1975) for the preparation of D-mannose-Sepharose 6B. The chemistry of this bi-functional reagent involved in matrix activation and ligand coupling can be summarised in three steps as follows:

(1) Matrix–OH + CH_2=CH–SO_2–CH=CH_2

(2) Matrix–O–CH_2–CH_2–SO_2–CH=CH_2 + R–OH

(3) Matrix–O–CH_2–CH_2–SO_2–CH_2–CH_2–O–R

This and other typical support materials activation and functionalisation in affinity chromatography are described by Lowe and Dean (1974).

100 ml of Sepharose 6B was washed with deionised water and then with 0.5 M Na_2CO_3 (pH 11), drained under mild condition and suspended in 100 ml 0.5 M Na_2CO_3 at room temperature. 10 ml of divinyl Sulfone was added and the suspension stirred gently for 70 minutes at room temperature. The resulting activated gel was washed with deionised water, drained, resuspended in 100 ml of 0.5 M Na_2CO_3 pH 10 with 20 % (*w/v*) L-fucose and stirred in the cold room for three days. Finally the gel was washed again with deionised water, drained, suspended in 100 ml 0.5 M Na_2CO_3 pH 8.5 with 2 ml of 2-Mercaptoethanol (deactivation of non reacted activated sites) and stirred for three hours at room temperature before washing with water and equilibration with phosphate buffer.

4.5.3 Column Affinity Chromatography

The filtered extract was applied to a chromatographic column packed under mild vacuum with L-fucose-Sepharose and equilibrated at 5°C with the same buffer used for the extraction. The process was first investigated in a 4 ml jacketed-glass column (6 × 15 mm) in a BioRad FPLC system at a flow rate of 0.2 ml/min. 0.5, 1, 2, 3.33, 7, and 14 ml of crude extract were injected, followed by a washing running buffer volume equal to 4 times the injection loop volume plus 30 ml. Once impurities were removed, bio-specific elution of the target lectin bound to the column was achieved by switching to running buffer containing 0.5 M L-fucose. Basic and acid pH, higher salt concentration, higher temperature and buffer containing from 0.01 to 0.1 M EDTA, were also tested as alternative step elution protocols. In all cases the process was monitored on line with UV (280 nm) and conductivity detectors.

4.5.4 Larger scale LTA purification

On a semi-preparative scale 100 ml column (50 × 50 mm) was packed with L-fucose-Sepharose. Between 30 and 60 ml of crude extract were injected at a flow rate of 0.5 ml/min, then after washing to remove impurities, LTA was eluted as described above.

The affinity purification was also run in a batch stirred tank (65 mm diameter and 200 mm high) containing approximately 100 ml of gel and the concentrated crude extract applied with or without filtering. The latter approach was carried out at 5°C, 50-200 ml of extract was stirred with the affinity matrix for two hours. The gel was then drained and washed with at least 1 litre of buffer before eluting the lectin with 2-3 fractions of 30-50 ml of buffer containing 0.5 M of L-Fucose. Each fraction was again stirred with the gel for 2 hours before collection. Fractions containing the eluted lectin were dialysed extensively against ultrapure water in the cold room and finally freeze dried to obtained LTA solid powder stored at < 1°C.

The cold room set up for LTA purification with the stirred batch adsorption unit is shown in Figure 4.2; with extraction, ultrafiltration units and dialysis tanks.

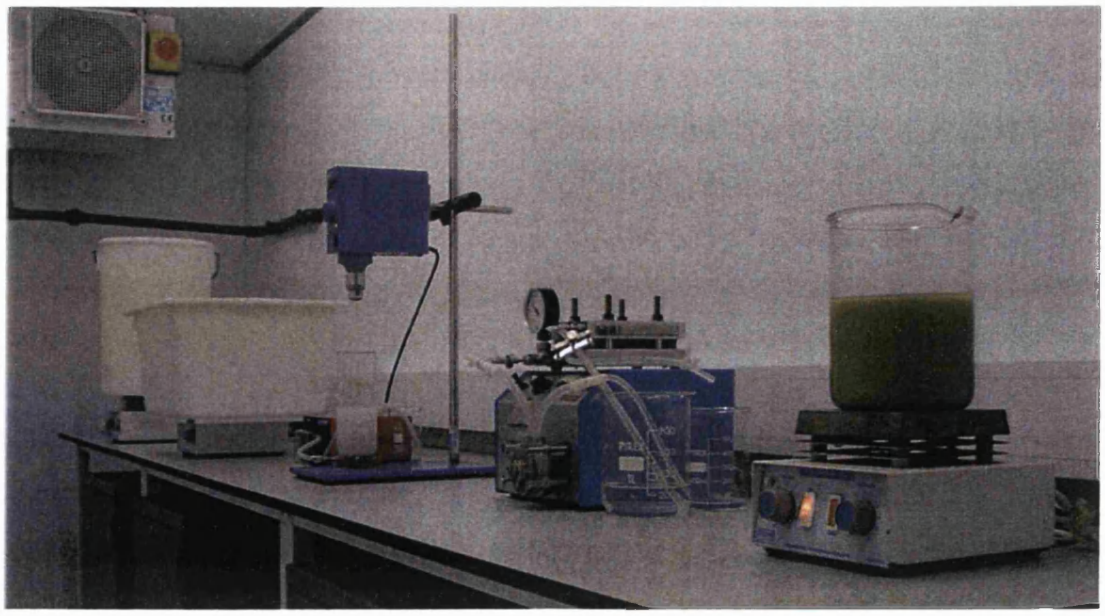

Figure 4.2: Main purification steps in semi-preparative purification of LTA from winged beans; from right to left: extraction unit, ultrafiltration module, affinity chromatography stirred batch and dialysis pools.

4.5.5 Surface Plasmon Resonance

The integrated "micro Fluidics Cartridge" in the Biacore X allows analyte to pass over two cells (Fc1 and Fc2) by which the sensor chip surface is partitioned. The carboxymethyl dextran surface of cell Fc1 on a CM5 sensor chip was activated with a pulse solution of 35 µl containing 0.05 M N-hydroxysuccinimide (NHS), 0.2 M N-ethyl-N'-(dimethyl-aminopropyl)-carbodiimide (EDC) and immediately after, p-aminophenyl-α-L-fucopyranoside (papf) was coupled to the surface by injecting 35 µl of a 2.5 mg/ml solution, excess of reactive groups are deactivated with a 35 µl pulse of 1 M ethanolamine hydrochloride, pH 8.5 (Johnsson *et al.*, 1991). The chemistry involved can be summarised as follows:

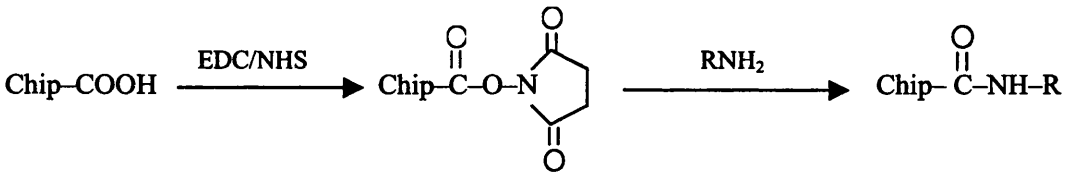

Amine activation, coupling and deactivation were carried out in 10 mM HEPES buffer pH 7.4, containing 150 mM NaCl, 3 mM EDTA, 0.005% Surfactant P20 at 5 µl/min flow rate and 20°C. The buffers used in the SPR experiments were filtered with a cellulose membrane (0.4 µm) in a vacuum glass filter unit and extensively degassed with helium. The second cell Fc-2 was set as the reference cell to compensate for changes in the refractive index of the bulk solution caused by analyte concentration, samples were filtered with PVDF/PE syringe filters (0.22 µm) and injected at 20 µl/min, sensograms recorded and analysed as Fc1-Fc2 response. Small aliqots (50 µl) of diluted samples from extraction, intermediate purification step and final purified material were injected; activity and LTA concentration monitored based upon the shape and extents of the response. Every chip after amine activation and papf coupling was calibrated with standards of previously purified LTA; the plateau response (equilibrium) reached after each sample injection, versus concentration injected, represented points for calibration curve. When the SPR response degenerated surface regeneration was performed in accordance with the manufacturer's guidelines.

4.5.6 Haemagglutination assay

Haemaglutination studies were carried out in the school of Pharmacy and Biomedical Science of Portsmouth University with help and supervision of Dr. R. V. Gibbs.
Tests were carried out with both native and papain-treated O-group human erythrocytes. Native blood cells were washed and resuspended in 0.1 M phosphate buffer saline (PBS) pH 7.4 to a final concentration of 3-5 %. Papainised erythrocytes were washed with the same buffer, incubated at 37°C for 30 min with an equal volume of papain, washed again and resuspended in PBS pH 7.4 to a final concentration of 3-5%. Papain (2 g) was soaked for 18 h in 100 ml 0.15 M PBS, pH 5.4, then heated to 37°C, mixed with 10 ml containing 0.5 M cysteine hydrochloride, 0.5 M sodium hydroxide and incubated for 1 hour. Samples from crude extract and purified LTA were prepared with serial twofold dilution to a final volume of 0.1 ml, within 10 tubes for each sample, with the last tube containing only buffer as a blank. Aliquots of blood cells suspension (0.1 ml) were added to all tubes and incubated at room temperature for 45 min. The degree of agglutination was observed at macroscopic level from complete aggregation (no free cells) to weak (granular appearance) agglutination (Gibbs, 1992).

4.5.7 Protein concentration determination

Total protein concentration was measured by ultraviolet spectrophotometer measurements at 280 nm (based on the calibration curves obtained in Chapter III) and using the response obtained from sample injection into the Biacore X SPR previously calibrated with purified lectin standards.

4.5.8 Molecular weight determination

Tris-Glycine polyacrylamide gel (10-20%, 1 mm thickness and 12 wells), based on the traditional buffer system (Laemmli, 1970), together with gel permeation chromatography columns were adopted for LTA molecular weight determination. Using a Novex X Cell II Mini-Cell, gel Electrophoresis was carried out on crude extract, intermediate and purified

LTA samples and also Concanavalin A solutions for comparison. Samples and standards were prepared with 15 µl protein solution plus 5 µl sample buffer (25 µl 2 mercaptoethanol, 250 µl Tris-Glycine SDS sample buffer, 250 µl distilled water) and boiled for 3 minutes. The running buffer placed in the cell was ultrapure water with 10 % (v:v) Tris Glycine SDS Sample Buffer. After 1 hour and 45 minutes circa at 125 V, the gel is removed and stained for at least 3 hours with a staining solution made with 110 ml ultrapure water, 40 ml Methanol, 10 ml stainer B, 40 ml stainer A from a standard Colloidal Blue Staining Kit. Gels were then washed with distilled water and dried with Gel-Dry Drying Solution.

Sephacryl S-100 gel was packed in a 26 × 600-750 mm column and used for more accurate molecular mass determination, 500 µl of sample was injected at room temperature at a flow rate of 0.8 ml/min. This column was calibrated with standard protein solution containing approximately 0.5-1 mg/ml of IgG (160 kDa), BSA (67 kDa), Ovalbumin (43 kDa), β-Lactoglobulin (35 kDa), Cytocrome C (12 kDa), DNP-Lysine (367 Da).
500 µl of filtered winged bean crude extract was also injected into the S-100 column, 10 ml fractions collected from the eluted material and analysed with the SPR as previously described to identify the molecular weight of the active fraction and compare it with that found for the purified LTA. All gel filtration experiments were run with Phosphate buffer pH 7.2-7.4 as mobile phase, containing 150 mM NaCl 0.02% NaN_3, filtered through a cellulose membrane (0.4 µm) in a vacuum glass system and degassed extensively with helium.

4.6 Results and Discussions

One example of CM5 sensor chip activation and papf (MW = 250 Da) coupling to Fc1 is shown in the sensogram of Figure 4.3. The total increase of the baseline of around 45 RU was reproducible and indicates a very high final ligand density, assuming the general relationship of 1000 RU = 1 ng/mm2 (Stenberg *et al.*, 1991). For a monovalent analyte of around 30 kDa the maximum binding capacity R_{max} was therefore over 5000 RU according to equation (2.64).

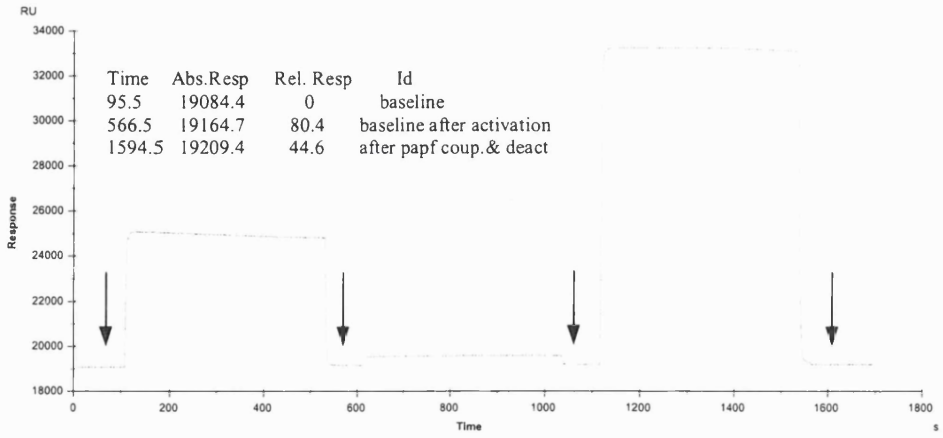

Figure 4.3: CM5-Surface preparation. The four arrows are chronologically: amine activation start, papf coupling start, deactivation start and process end. Absolute and relative responses reported.

With such a high ligand density, kinetic measurements of binding were not possible due to mass transfer limitations. However under these conditions the instrument was an invaluable tool for specific qualitative and quantitative analysis of the presence and concentration of Lotus lectin during and after purification. The sensogram grouping all the responses from standard concentration injections and relative calibration curves are summarised in Figure 4.4 and 4.5 respectively. Between 40 and 50 injections were possible after calibration before chip performance was seriously degraded. Regeneration procedures were run, but often this resulted in complete disruption of the sensor surface. Every chip was calibrated following the same procedure with reproducible results.

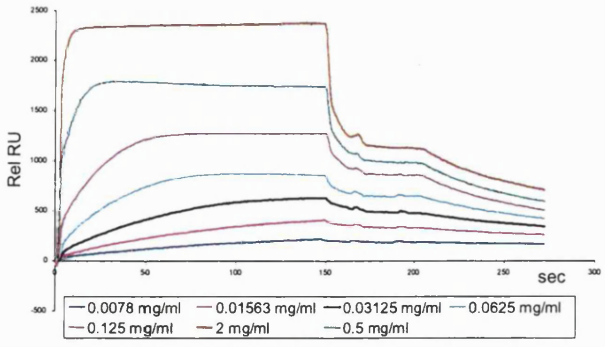

Time	AbsResp	RelResp	Id (mg/ml)
3200	2501.4	2362.9	2
4242	2288.8	2089.7	1
5169	2005.1	1788.7	0.5
6015	1578.4	1502	0.25
6383	1343.2	1269.3	0.125
7131	943.1	870.3	0.0625
7629	667.5	627.9	0.03125
8110	449.9	399.8	0.015625
8685	302.3	219.6	0.0078

Figure 4.4: Fc1-Fc2 responses at different concentrations of injected LTA solutions. The curves belong to one continuous sensogram from which time in seconds, absolute and relative responses (relative to plateau values) are reported in the table. The relative response is obtained over the baseline (RU=0) corrected before each injection.

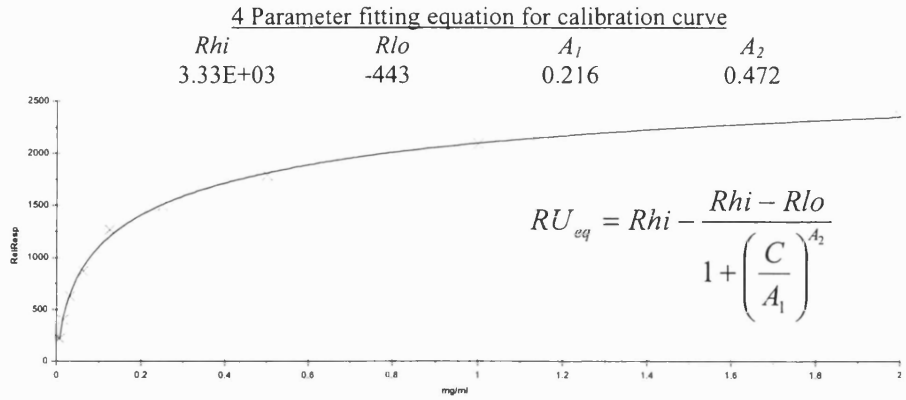

Figure 4.5: Calibration curve and equation obtained with BIAevaluation software

Figures 4.6 and 4.7 show the first example of the SPR in a qualitative application. The double extraction and two step concentration with dry matrix (Sephadex G-25) addition is monitored and compared for fresh-green LTA beans and dry beans in Figure 4.6 (left).

The results show that fresh beans yield much less LTA than the dry ones. The second extraction was very poor in activity for both samples but the dry matrix worked quite well as concentrator for small sample volume with relatively low levels of active protein loss, given that the sample volume is reduced of 50 % after each concentration step.

Seeds, naturally dried for a few weeks, show the highest L-fucose binding activity in the extract as reported in Figure 4.6 (right). These also show SPR responses of retentate and filtrate from crude extracts processed with a Minitan module containing 4 Polysolphone membranes (10 kDa cut off).

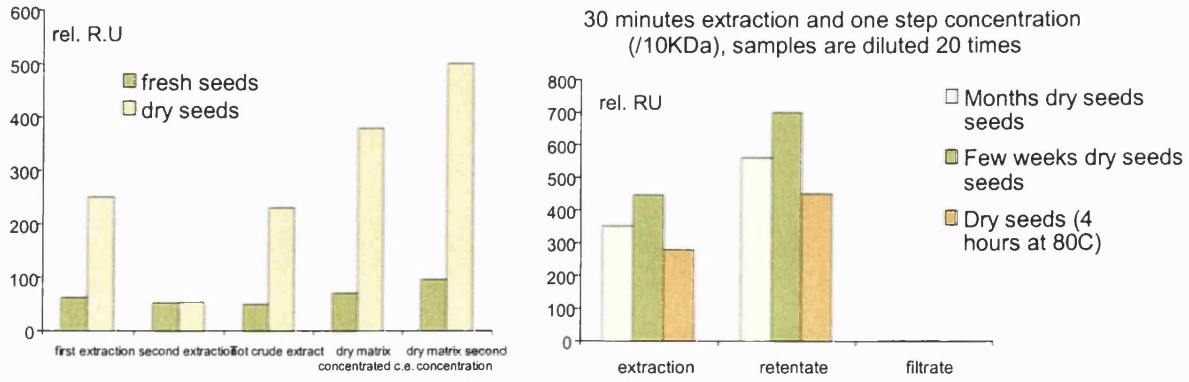

Figure 4.6: SPR monitoring of active Lotus lectin concentration during sample preparation

Using an ultrafiltration system allowed a 3-fold concentration of crude extracts within 2 hours in the cold room before protein aggregation became a problem, with negligible loss of product. Analysis of the LTA level with increasing extraction time (Figure 4.7) showed that the overnight extraction could be replaced with a 30 minutes extraction, which yielded more LTA, or at least a fraction of more highly active L-fucose binding lectin.

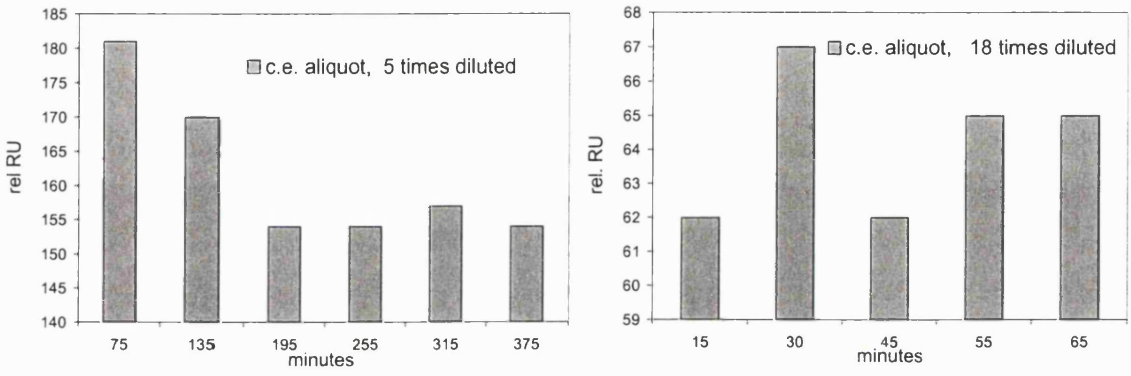

Figure 4.7: SPR monitoring of active Lotus lectin concentration during extraction.

Less high molecular weight components are present in short time extraction as shown in the chromatograms of Figure 4.8, where the elution profiles of 30 minutes and 60 minutes extracts throughout a Sephacryl S-100 gel permeation column are compared.

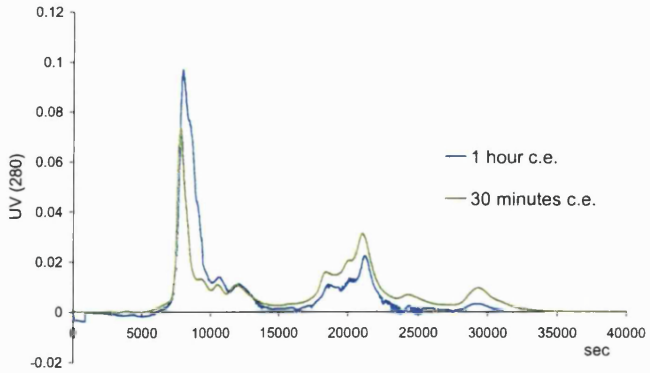

Figure 4.8: Crude extract (c.e., 0.5 ml) eluted from 26 × 700 mm Sephacryl S-100 column from 60 and 30 minutes extraction time.

At the end of the sample preparation process, extracts, analysed with SPR, generally contained 1-3 mg/ml of active LTA. For very highly concentrated crude extracts, up to 6 mg/ml of active lectin were detected. During affinity chromatography purification of LTA with the small column, step elution with buffers pH 4 and 9, EDTA, high concentration of NaCl, higher temperature were not successful. In contrast, Figure 4.9 shows tightly bound lectin eluted within a bed volume with concentrated L-fucose containing buffer (0.5 M). Similarly, Figure 4.10 reports a typical biospecific LTA elution from the 6 × 150 mm column, when 14 ml of crude extract were applied.

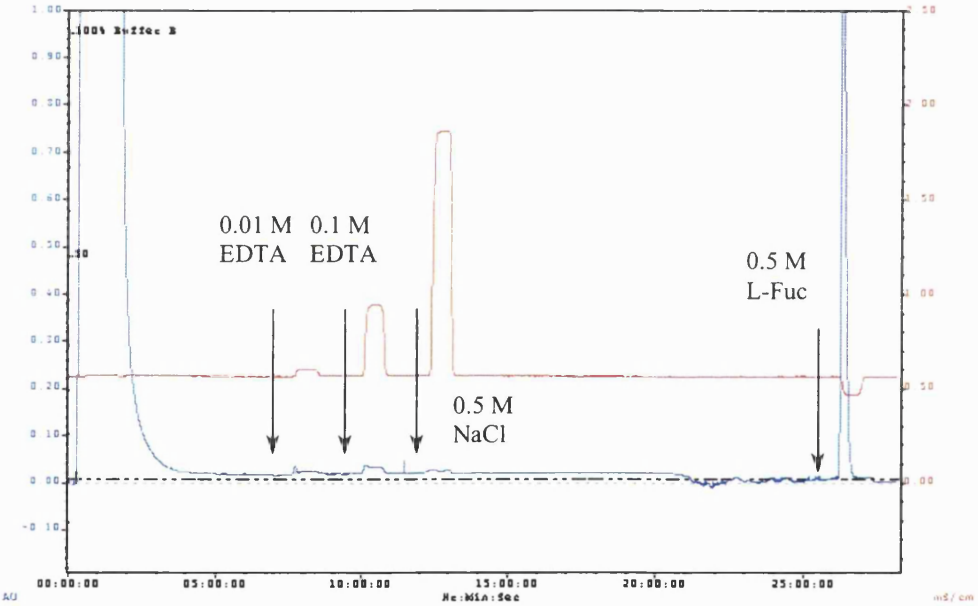

Figure 4.9: Affinity Chromatography purification from 14 ml crude extract applied to 6 × 15 mm L-fucose – Sepharose column at 5°C and 0.2 ml/min. Blue chromatogram: eluted material spectrophotometrically detected at 280 nm. Red line: eluted material conductivity (mS/cm).

L-Fucose-Sepharose gel also showed high capacity, the area of eluted peaks associated with the amount of total purified lectin, evaluated with EZ-logic BioRad software, increased with the volume of crude extract injected as reported in Figure 4.11.

It was noted that to minimise the unused bed capacity, volumes of crude extract over 3 times the column volume were required.

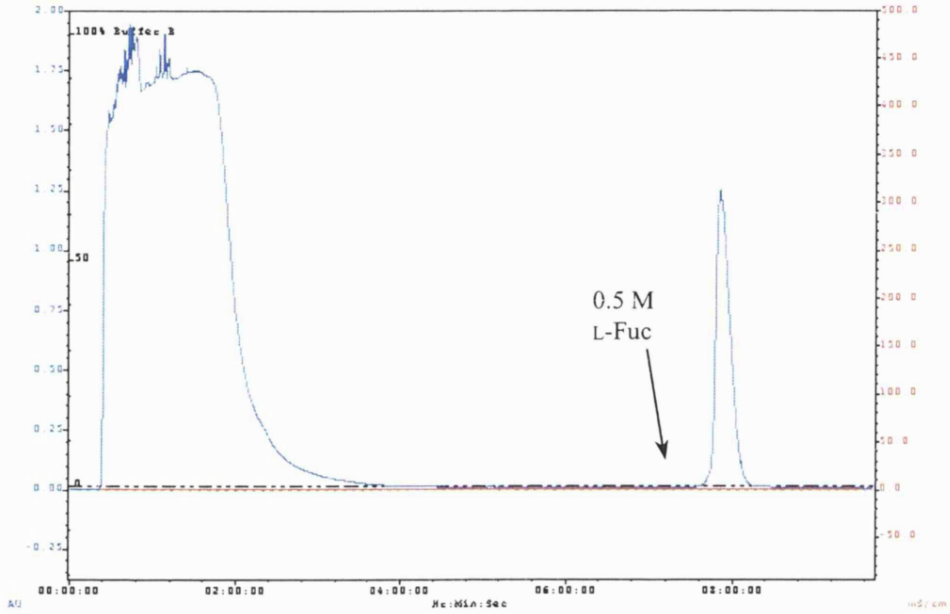

Figure 4.10: Affinity Chromatography purification from 14 ml crude extract applied to 6 × 15 mm L-fucose – Sepharose column at 5°C and 0.2 ml/min. Blue chromatogram: eluted material spectrophotometrically detected at 280 nm. Conductivity detector is off.

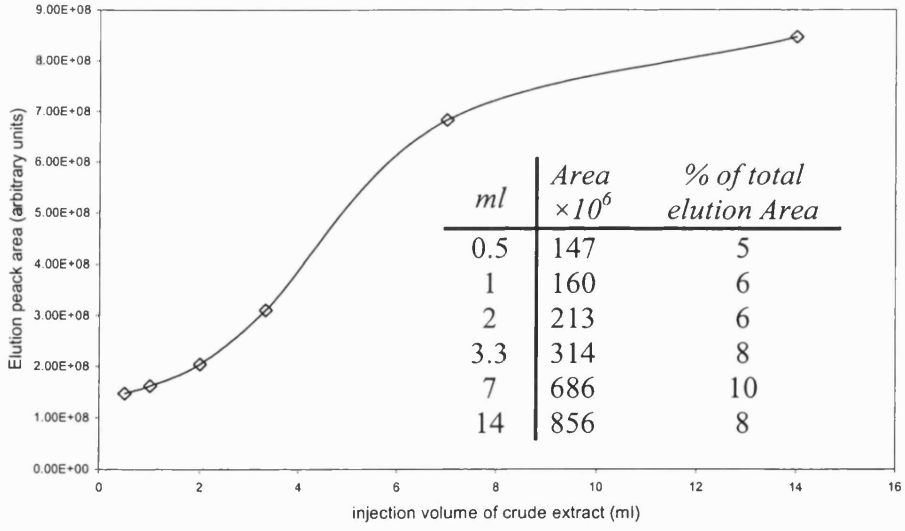

ml	*Area ×10⁶*	*% of total elution Area*
0.5	147	5
1	160	6
2	213	6
3.3	314	8
7	686	10
14	856	8

Figure 4.11: Specific eluted peak areas calculated in arbitrary unity by EZ-logic software package associated to the BioRad FPLC system, when different size injection loops are tested with the 6 × 15 mm L-fucose – Sepharose column. In the table, the % of eluted peak area is referred to the total bound and not bound eluted material area and represents an approximation of the % of target LTA over the total protein contents.

From the calculated fraction of these areas over the total area of eluted materials for each run, an approximated total content of LTA in the crude extract was identified to be around 5-10 % (Figure 4.11) of the total protein amount. Pressure problems were encountered with larger column (50 × 50 mm) operation and cycle times were excessive, therefore these were abandoned; Figure 4.12 reports two examples of large column lectin affinity purification. A stirred batch single stage adsorption unit (64 × 200 mm) was preferred mainly because of shorter cycle times. Although the process was not automated and obviously less efficient than a multi stage column adsorption, a complete purification could be carried out; from 30 minutes extraction to purified lectin fractions ready for dialysis within a day.

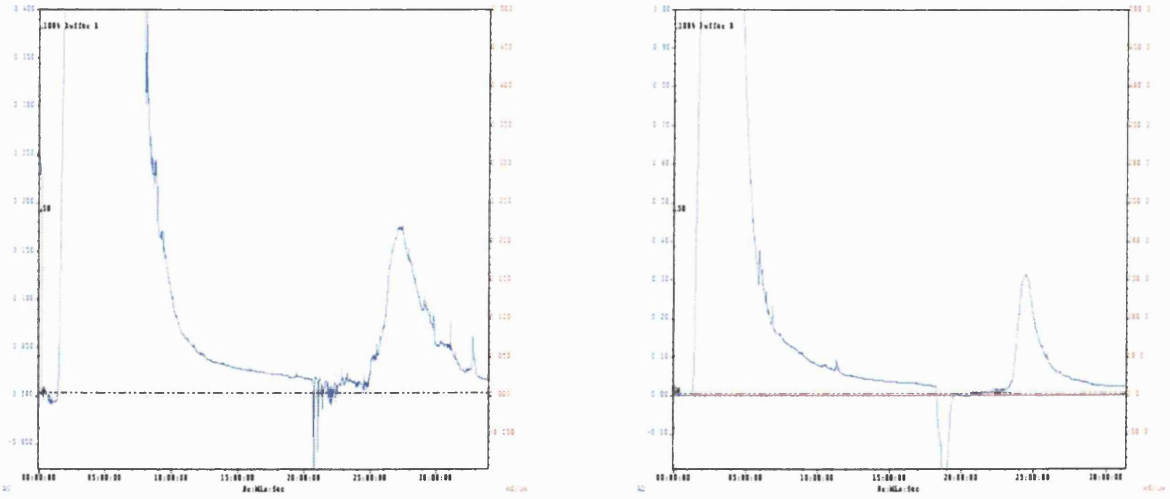

Figure 4.12: Left: LTA purification in 50 × 50 mm column, 0.5 ml/min, 50 ml crude extract injected, elution is carried out with 120 ml of buffer containing 0.3 M NaCl and 0.15 M L-Fuc. Right: LTA purification in 50 × 50 mm column, 0.5 ml/min, 30 ml crude extract injected, elution is carried out with 120 ml containing 0.5 M L-Fuc in buffer. The elution profile is detected with UV at 280 nm. Conductivity detector off.

The chief requirement for a successful batch method is that the concentration ratio of adsorbed over total target protein should be very close to one otherwise the loss would be very high (Scopes, 1994), if large volumes are processed.

However L-fucose-Sepharose did show a high binding capacity. Analysing crude extracts before and after batch purification, showed circa 98% of the total LTA was adsorbed when small (50 ml) volumes were processed. This reduced to down to 92 % for 200 ml batch

volumes. 100 grams of ground beans extracted in 1 litre of buffer and concentrated down to 300-400 ml circa yielded 300-500 mg of LTA powder when processed in 2-4 purification runs. Even though the work was carried out at 5°C the speed of the whole process was very important as high proteolitic activity was found throughout. Addiction of the protease inhibitor cocktail during extraction and sometimes also in the elution buffer proved to be crucial in maintaining product activity.

Examples of molecular weight analysis on SDS gels are shown in Figure 4.13; for samples collected throughout a number of different columns and stirred batch purification.
The LTA lectin monomer appeared to be purified to homogeneity having a molecular weight around 23.5 kDa, smaller than ConA (obtained from Sigma) monomer, 26.7 kDa, appeared to be containing some low molecular weight impurities (see Appendix B for data, calibrations and results).

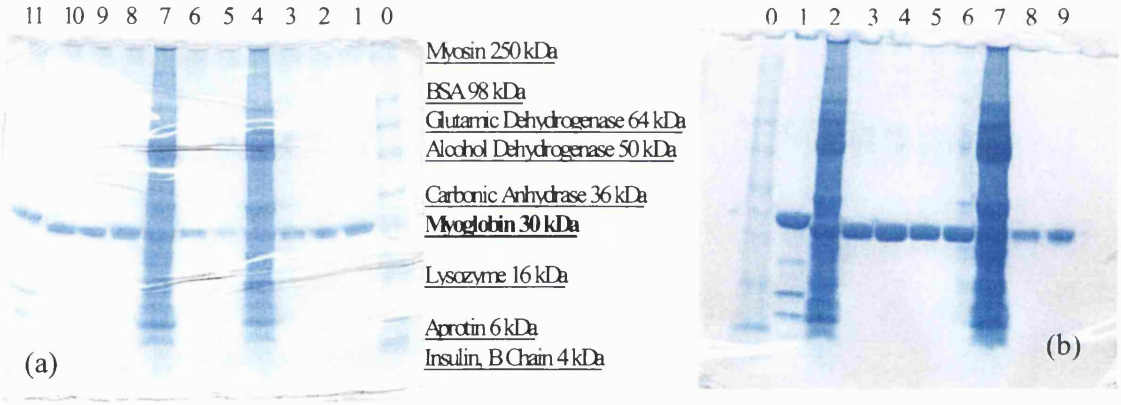

Figure 4.13: SDS Tris Gycine Gels.

(a). 0: standards. 1, 2, 3: lyophilised LTA dissolved in phosphate buffer. 4: crude extract. 5: LTA in water after dialysis. 6: eluted LTA. 7: crude extract. 8, 9, 10: third, second and first fraction of purified LTA. 11: Concanavalin A.

(b). 0: standards. 1: Concanavalin A. 2: crude extract. 3, 4, 5: first, second, third fraction of purified LTA. 6: lyophilised LTA dissolved in PBS. 7: crude extract. 8: purified LTA. 9: purified and more concentrated LTA .

The native molecular weight assessed on columns packed with Sephacryl S-100 was found to be 34 kDa after calibration with globular proteins, assuming the separation range specified by the manufacturer (1-100 kDa, Figure 4.14 and Figure 4.15).

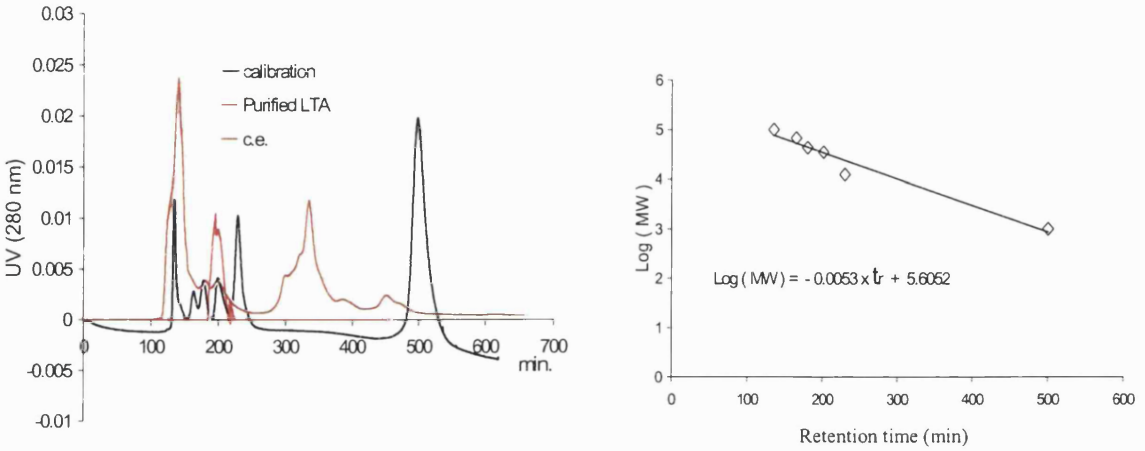

Figure 4.14: Crude extract, purified LTA from column affinity chromatography and protein standards elution profiles from 26×700 mm Sephacryl S-100 column at room temperature, 0.8 ml/min, 0.5 ml injection volume. Standard calibration for IgG (160 kDa), BSA (67 kDa), Ovalbumin (43 kDa), β-Lactoglobulin (35 kDa), Cytocrome C (12 kDa), DNP-Lysine (367 Da). MW_{LTA} = 34670 Da.

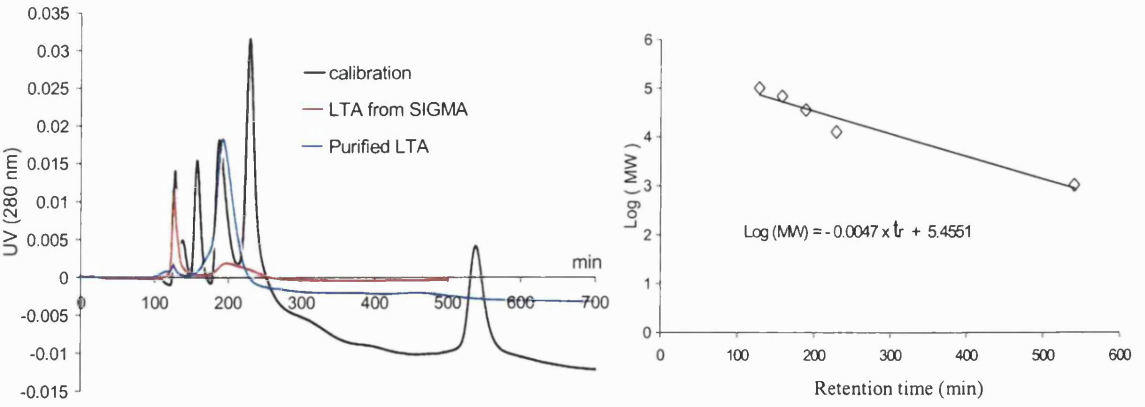

Figure 4.15: LTA from Sigma, purified LTA from column affinity chromatography and protein standards elution profiles from 26×750 mm Sephacryl S-100 column at room temperature, 0.8 ml/min, 0.5 ml injection volume. Standard calibration for IgG (160 kDa), BSA (67 kDa), β-Lactoglobulin (35 kDa), Cytocrome C (12 kDa), DNP-Lysine (367 Da). MW_{LTA} = 34190 Da.

In particular, in Figure 4.15, the elution profile (blue) of purified LTA is compared with commercial LTA chromatogram (red) and the difference in size is evident. This suggests that the two preparations yield Lotus lectin at two different degrees of aggregation; in prevalence over 100 kDa for the commercial lectin and around 34 kDa for the lectin purified in this work.

The major component size of the active LTA in the crude extract (c.e.) was again 34 kDa as demonstrated combining gel filtration and SPR.
When 10-ml fractions of crude extract, collected from the gel permeation column (Figure 4.16), were analysed, the highest activity was identified in fraction 11 (34 kDa) with also some active lectin eluted at fraction 8 (68 kDa), see Figure 4.17.

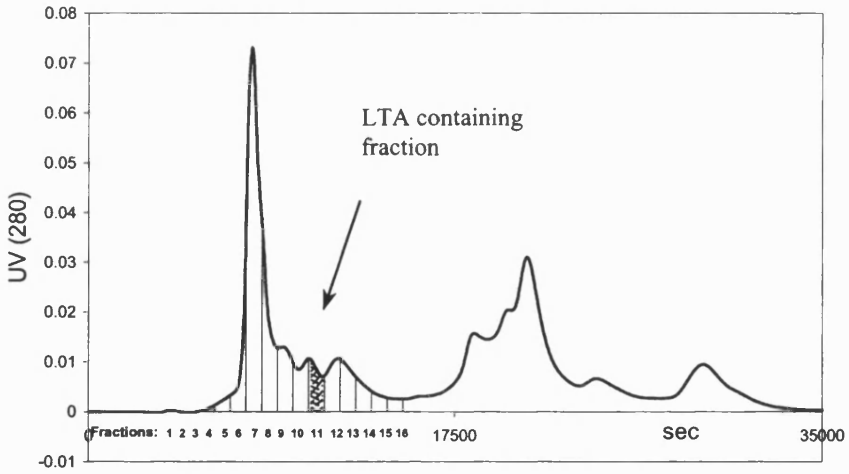

Figure 4.16: Typical elution profile of 0.5 ml of crude extract injected into a Sephacryl S-100 column. 10 ml fractions, collected and stored at 5°C.

Those results were supported also by haemaglutinin tests of O-group erythrocytes; fraction 11 showed the highest activity along with the two folds serial diluted samples.
In haemaglutinin tests, crude extract samples, purified and commercial LTA showed very weak or often no haemaglutination if the blood cells were not treated with papain.

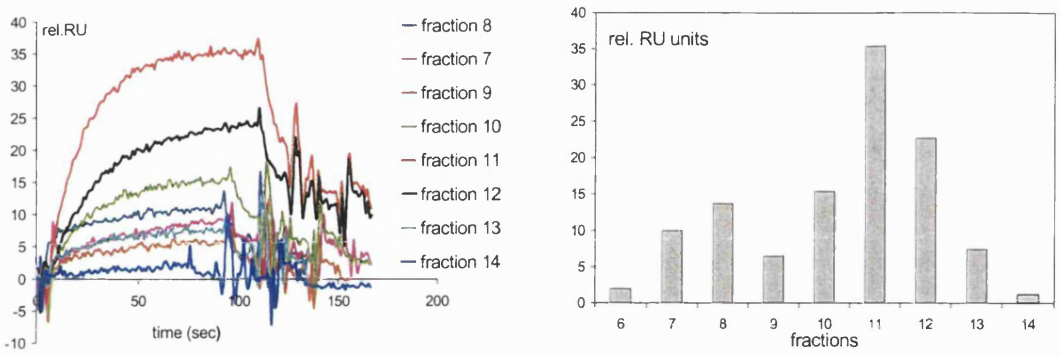

Figure 4.17: Left: Regrouped SPR responses belonging to one sensogram in which fractions of crude extract (from 7th to 14th fraction) collected from GPC column were injected. Right: a schematic representation of equilibrium SPR relative responses of pooled fractions.

Generally the use of Phosphate buffer or Mops buffer with chloride salts did not change results however the Mops buffer option gave the possibility of freezing samples where Phosphate caused the protein to be denatured (Harris and Angal, 1989).

LTA purification results were mostly in agreement with methods and results presented by Allen *et al.* in 1977 and as stated by these workers the final L-fucose binding lectin was different from that obtained using precipitation techniques and other chromatographic affinity media. Those purification methods are summarised in Table 4.2 with relevant references. The native molecular weight of the final lectin (or mixture of isolectins) product and dissociation constants for the interaction with L-fucose are also shown where available.

Basically from the literature, Lotus lectin was often found to be a mixture of glyco-isolectins according to Yariv *et al.* (1972) with similar specificities and higher molecular weight than Allen and Johnson (1977) and this work reported. Allen and Johnson (1977) obtained their result by gel filtration on Sephadex G-200 and in case lectin fractions were adsorbed by the glucosyl residues in the resin they analysed the same fractions on Ultrogel AcA 34 containing galactosyl residues, obtaining identical results. Allen and Johnson (1977) did not explain the discrepancy of their results with previous workers however they observed various degree of proteolytic degradation during purification, which probably influenced their protein aggregation final product.

Table 4.2: Some literature LTA purification methods and results

Reference	Method	Native MW	K_d
Allen and Johnson (1977)	A.C. L-fucose-Sepharose 6B, Divinyl Sulfone activation	34 Da	-
Pereira and Kabat (1974)	A.C. Insoluble polyleucyl hog blood group	110 Da, Tetramer	-
Yariv et al. (1972)	A.C. β-L-fucopyranosylammine-Sepharose 4B, Cyanogen bromide activation	A 120 Da, Tetramer B 58 Da, Dimer C 117 Da, Tetramer	$K_{dA} = 0.8\text{-}1 \times 10^{-4}$ M $K_{dB} = 1.7\text{-}2 \times 10^{-4}$ M $K_{dC} = 2.7\text{-}4.8 \times 10^{-5}$ M
Yariv et al. (1967)	Precipitation with fucosyl dye.	107 Da, Tetramer	$K_d = 0.9 \times 10^{-4}$M
This work (2002)	A.C. L-fucose-Sepharose 6B, Divinyl Sulfone activation.	34 Da	$K_d = 4 \times 10^{-4}$M (page 97)

In this work, similar features were observed, although proteolytic degradation was drastically reduced by using short extraction times, rapid batch purification and the use of a protease inhibitor cocktail. Moreover, the same native molecular weight for the major active fraction of L-fucose binding lectin was found in the fractionated crude extract with the SPR analysis.

Electrophoresis in the presence of dodecyl sodium sulfate and 2-mercaptoethanol resulted in a monomer molecular weight of around 23.5 kDa. Some studies on algal lectin suggested that with SDS-page higher values of MW may be observed; due to the glycoprotein nature of the lectins, they tend to migrate slower (Sampaio *et al.*, 1998). ConA monomer was found to be around 26.7 kDa as expected but this lectin is known to be not glycosylated (Agrawal and Goldstein, 1968) while LTA contains carbohydrate, 4-8 % (Kalb, 1968). This led to the formulation of the hypothesis that the purified 34 kDa native LTA could be a dimer of a monomer subunit of 17 kDa. Assuming, as is usual for legume lectins, one specific binding site per monomer, the purified LTA should have two binding site. This assumption of two binding sites on the purified LTA molecule was supported by

the positive haemagglutination tests; blood cell agglutination by a different molecule is obviously possible only if that molecule has more than one anchoring site. Also from column affinity chromatography it was noted that even after long periods of washing after extract application, the losses of specifically bound lectin were totally negligible; evidence of stronger multiple interaction between lectin and L-fucose-Sepharose.

LTA as purified here is a relatively small L-fucose binding lectin with two binding sites per molecule. When employing LTA in sugar separation, the fact that the molecular weight ratio lectin to ligand is smaller than expected, made use in a monosaccharide recovery process more favourable.

4.7 ITC characterisation: Methods

ITC tests and control experiments were carried out following the protocols given in previous isothermal titration materials and methods sections, the solvent used in these application was 50 mM MOPS buffer pH 7.2-7.4 containing 0.5 mM $CaCl_2$, 0.5 mM $MnCl_2$, 0.5 mM $MgCl_2$, 150 mM NaCl and 0.02% NaN_3. The purified LTA was dissolved and dialysed against the same buffer at 5°C, filtered with PVDF/PE syringe filters and monomer concentration determined on the basis of SPR response and 280 nm UV absorbance based on the promoter molecular weight equal to 17 kDa. Titrant sugar samples were prepared to obtain the final concentration of 4 mg/ml. Titrations were run in the thermostated cell at 5, 10, 20, 30, and 40°C. 57 injections of 5 µl of sugar solution were automatically added with a 290 µl microsyringe every 2 minutes into the lectin solution stirred at 300 rpm, the heat developed after each injection is measured by the cells feedback network as differential heat effects between sample and reference cell.

Final experimental results, represented by heat developed versus total ligand/lectin ratio, are fitted using one and two binding sites per monomer model, available in Origin ITC Data Analysis Software and based on a non linear least square curve fitting procedure, Levenberg-Marquardt algorithm (Marquardt, 1963).

Titrations of crude extracts before and after affinity chromatography were compared to study and estimate the activity of the lectin before purification.

4.8 ITC characterisation: Results and Discussions

During titration experiments of purified LTA under the condition described, clear evidence of binding and ongoing saturation of binding capacity was observed.
Figure 4.18 reports those titrations at different isothermal conditions, only one raw plot of the resulting peaks representing the heat developed at each injection is included.
Looking at Figure 4.18, the increasing association constant with decreasing temperature, as expected for exothermic binding (2.41), is immediately evident.

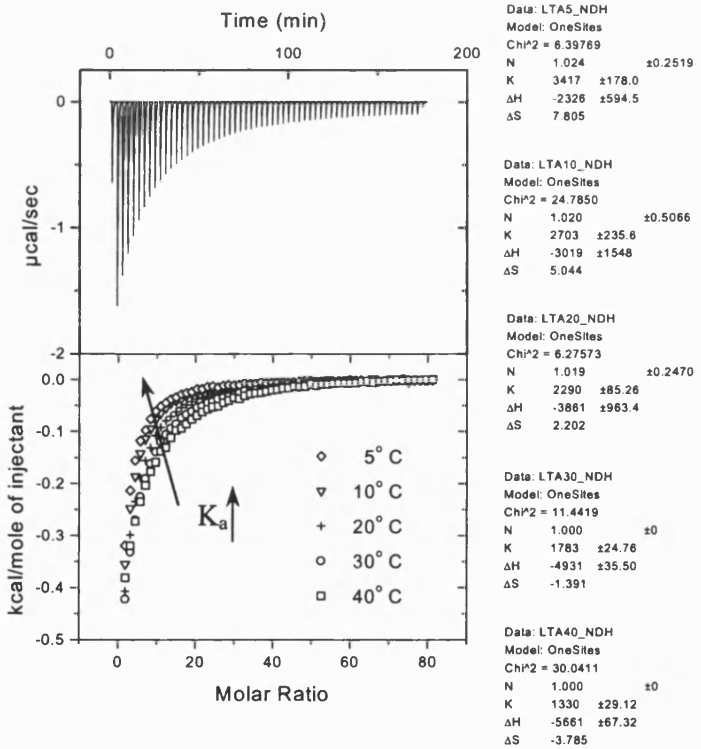

Figure 4.18: Purified powder Lotus lectin (0.01 mM) titrated with 24.4 mM L-fucose solution at different temperatures. One site binding model chosen to fit the data and resulting regression parameters are reported.

Also, as noticed during Con A titrations, the experimental conditions ($c < 1$ and high ratio of ligand concentration in the syringe over lectin concentration in the cell) were far from the optimum and clear saturation was achieved only after very high molar ligand/receptor ratio. The results for the three regression parameters; stoichiometry (n), dissociation constant (K_d), enthalpy of binding (ΔH^o) were obtained with the single binding site model and are included in Table 4.3. Errors in those parameters were around 25 % for stoichiometry and enthalpy and 3% for equilibrium constant, the non-linear least squares analysis provided good data final fitting curves with low values for the least-squares norm χ^2. Conversely in the right hand plot of Figure 4.1, where commercial LTA was titrated with L-Fucose under more ideal conditions ($c \approx 1$ and concentration ligand/receptor ratio around 20), the titration and final fitting curve was not good and the regression parameters all had errors around 10 %. An increase of ten folds for c is possible with lectin concentration above 10 mg/ml with loss of solution homogeneity and clearance due to aggregation and foaming problems.

Those results together with non linear Scatchard plots obtained from the experimental data (Figure 4.19) provided evidence that the assumption of one single population of identical binding site was not appropriate.

Table 4.3: Parameter results from ITC experimental data fitting (one binding site model). Purified LTA samples at 5, 10, 20, 30 and 40 °C and one commercial LTA sample at 20°C were titrated with L-fucose solutions. Results at 30 and 40 °C are obtained fixing the stoichiometry at 1.

T [°C]	5	10	20	30	40	20 (SIGMA)
N	1.02	1.02	1.02	1	1	1.01
$K_d \times 10^{-4}$ [M]	2.9	3.7	4.4	5.5	7.5	0.89
ΔH [cal mol^{-1}]	-2326	-3019	-3861	-4849	-5661	-3994
ΔS [cal $mol^{-1}K^{-1}$]	7.8	5	2.2	-1	-3.785	4.9

At 30 and 40 °C the stoichiometry was fixed at one during data fitting in line with previous experiments otherwise reasonable results could not be obtained in terms of enthalpy and entropy of binding (dotted line in Figure 4.20).

From this thermodynamic data a number of conclusions could be drawn; the contribution to the free energy of binding in this lectin-sugar interaction is obviously assisted by both enthalpy *H* and entropy *S* (compensatory effect), with *S* influence becoming stronger at lower temperature when hydrophobic interaction and water molecule reorganisation are energetically important.

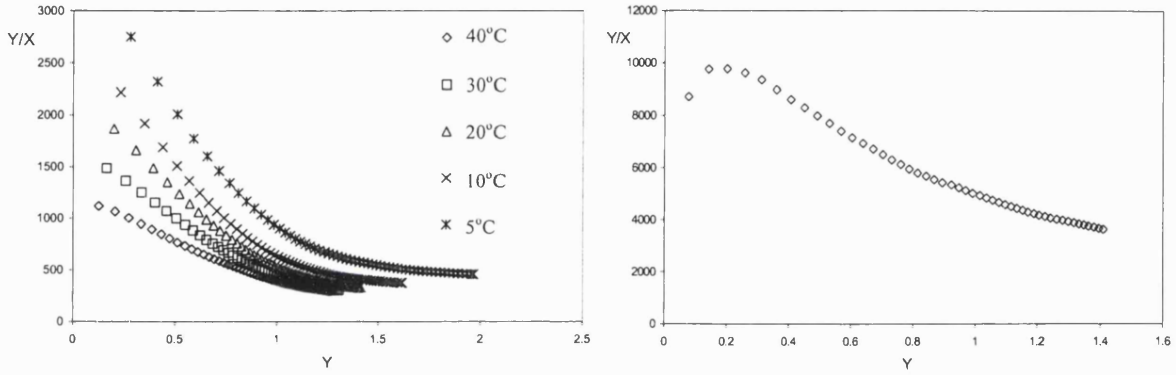

Figure 4.19: Scatchard plots for purified LTA (left) and Sigma LTA relative to titrations of figure 4.1 and 4.18.

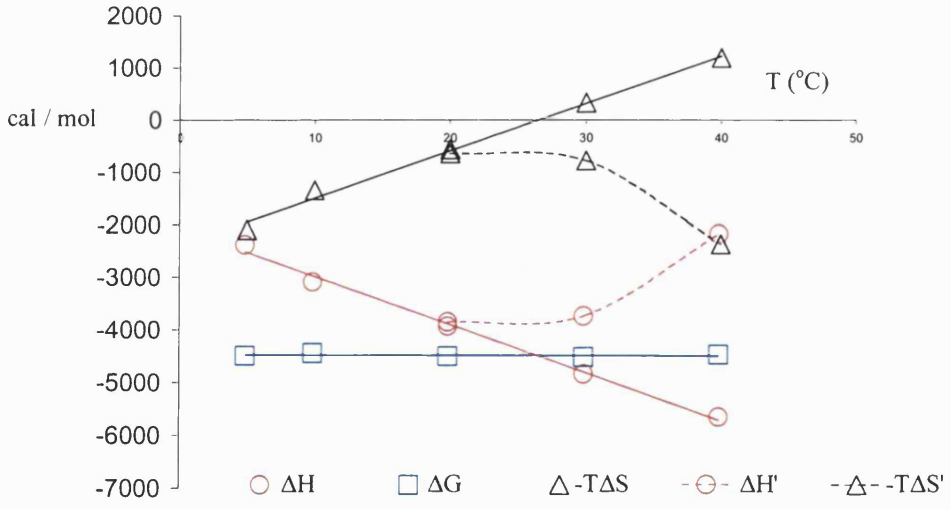

Figure 4.20: ΔH, ΔG, and -TΔS results and trend lines when at 30 and 40 °C n=1 is fixed. ΔH' and -TΔS' are results relative to normal data fitting procedure with n as one of the regression parameter.

The Sigma LTA showed an association constant one order of magnitude higher than the purified LTA. However, comparing ΔH and ΔS for the two lectins from different sources, showed similar enthalpy values therefore similar levels of specificity. However the commercial LTA had a much higher entropy value; evidence of lower purity.. Therefore the stronger binding could result from non-specific interactions. Due to the non linearity of Scatchard plots reported in Figure 4.19, a two sequential binding site model could provide a more realistic description, taking in to account all the phenomena linked to specific and non-specific binding. Table 4.4 reports the numerical results obtained fitting LTA data with the sequential sites model; the weighted sum of squared differences between fitting function and experimental data (χ^2) and association constant, enthalpy, entropy of binding for each population of binding site are summarised.

Table 4.4: Results from LTA titrations data fitting with the two sequential binding sites model; χ^2 is the least square norm and K_a, ΔH, ΔS refer to the first (subscript 1) and second (subscrip 2) population of sites.

T (°C)	5	10	20	30	40
χ^2	2.1	4	2.31	11.36	17.86
K_{a1} [M^{-1}]	13340 ± 2288	5399 ± 496	5357 ± 535	2822 ± 461	1640 ± 150
ΔH_1 [cal mol^{-1}]	-994 ± 90	-1921 ± 116	-2046 ± 145	-3241 ±443	-4329 ± 364
ΔS_1 [cal mol^{-1} K^{-1}]	15.30	10.29	10.08	5.09	0.88
K_{a2} [M^{-1}]	1628 ± 138	613 ± 90	943 ± 86	651 ± 167	488 ± 91.13
ΔH_2 [cal mol^{-1}]	-1522 ±84	-1604 ± 93	-2052 ± 140	-1612 ± 465	-836 ± 451
ΔS_2 [cal mol^{-1} K^{-1}]	9.223	7.093	6.611	7.555	9.632

Looking at the association constants (apparent) in Table 4.4, the two populations of binding sites express negative cooperation especially at low temperature. For the first population of binding site, a typical parameter temperature dependence is recognised; K_{a1}, ΔH_1 and ΔS_1 increase when temperature decreases, while for the second population, this pattern is not observed.

Generally, understanding the nature of the experimental data and associated uncertainty is the key to evaluating regression parameters. One goal of this kind of ITC study, run at high ligand concentration, was to show clearl evidence of binding and the complexity surrounding the choice of the right model to describe weak lectin-monosaccharides interactions. Awareness that experimental uncertainty on binding site concentrations and systematic errors, derived from non-specific energetic effects, influence the confidence intervals of determined parameters and their statistical significance, this use of ITC outside standards protocols was found very useful. If a lectin is to be used in a monosaccharide separation all that is needed for the preliminary design of the process is the maximum binding capacity (number of active binding site and stoichiometry of binding) and the strength of binding (equilibrium constant).

LTA, assumed to have one population of identical L-fucose binding sites, represents a simplified solution to analyse their affinity interaction, as demonstrated with the previous results. However the Langmuir based adsorption model remains very useful for a rapid and simplified picture in providing an average binding equilibrium constant and an approximate concentration of binding sites available.

Adopting a single binding site model gives the possibility of using the algorithm to quantify the amount of active macromolecule (C) placed in the ITC cell.
C is an input parameter therefore a first guess value must be given (C^*) before fitting, the results obtained for K_a and ΔH^o are the "correct" values, they strongly depend on the ligand concentration. The resulting stoichiometry n^* can then be used to calculate the real C value from $C^* \times n^*/n$ if the real stoichiometry of binding (n) is known (Sigurskjold *et al.*, 1991).

Using this approach, crude extract titration before and after affinity chromatographic removal of LTA allowed an estimation of active lectin molar concentration. In the example of figure 4.20 the crude extract resulted having 0.077 mM binding site. In other words the macromolecule solution was able to bind a maximum concentration of 0.077 mM of L-fucose.

The same sample analysed with SPR resulted containing 0.07 mM active LTA, generally this kind of double regression measurements of binding sites concentration with ITC were within ±25% of the values obtained with SPR. These measurements were carried out based on 17 kDa LTA monomer structure, containing one specific binding site and confirm the validity of the assumption.

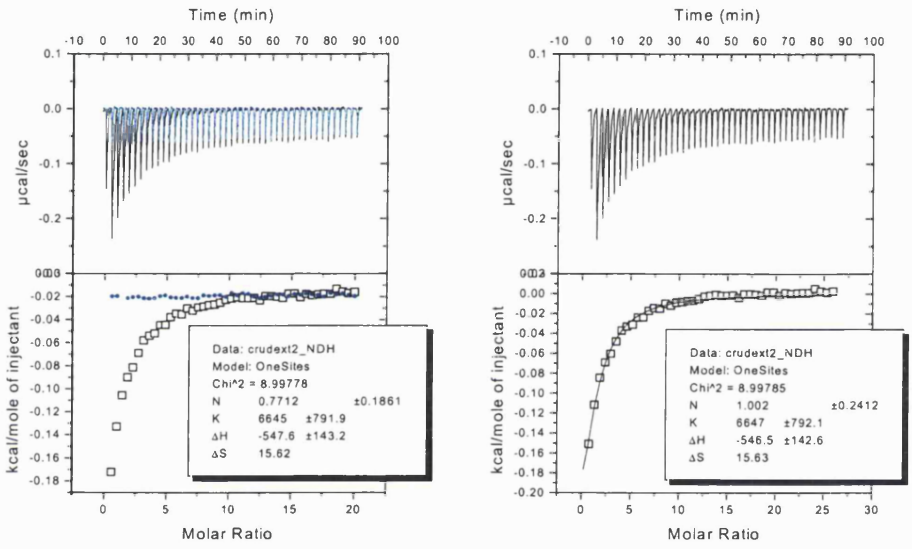

Figure 4.20: Crude extract titrated with 12 mM L-fucose solution before (black) and after affinity chromatography (blue). Left: parameters results are relative to the fitting procedure of corrected (blue titration subtracted to black one) data with input value of C = 0.1 mM. Right: Same data fitting results after C has been modified according to Sigurskjold *et al.* (1991). 0.077mM is the final concentration of active binding sites.

Chapter V

L-Fucose Separation with Immobilised LTA Affinity Chromatography

5.1 Summary

Commercial Lotus lectin (LTA) immobilised on agarose gel was characterised at 5°C and 20°C, using the FC method with p-nitrophenyl-L-fucopyranoside (pnpf) for specific interaction and p-nitrophenyl-α-D-glucopyranoside (pnpg) and α-L-arabinopyranoside (pnpa) for non specific ones. The system appeared less heterogeneous in terms of specificity than ConA-Sepharose, and pnpf purification was achieved in ZC over a range of different mixture concentrations of pnpf and pnpg at different flow rates. The packed gel void volume and porosity were also characterised on the base of elution volume of inert polymers in standard solutions. Good selectivity and resolution were achievable as well as good column efficiency. However all are strongly dependent on the volume and concentration of the sample applied, as expected for a low capacity system. Finally, in this chapter, the feasibility of this technique for rare sugar separation on a significant scale is discussed.

5.2 Introduction

The use of immobilised lectins as chromatographic media for fractionation and characterisation of various fucose-containing oligosaccharides and glycoproteins was reported by Yamashita *et al.*, (1985) who exploited the affinity between *Aleuria Aurantia lectin* (AAL) from orange peel fungi and L-fucose. In 1997 Rathi *et al.*, studied the interactions of sugars containing N-(2-hydroxypropyl) methacrylamide (HPMA) with commercial LTA immobilised on 4% beaded agarose (1-2 mg of LTA per ml of gel).

A drug delivery system based on HPMA was developed and a frontal affinity chromatography technique was used to mimic the specific cell-polymer interaction and to investigate the biospecific recognition phenomenon. Only fucosylamine containing HPMA showed specific binding to the lectin ($K_d = 2.9\times10^{-5}$ M) and HPMA group was shown to be responsible for a non specific (hydrophobic) contribution to the binding.

In 1997, high density LTA-Emphaze (Hydrazide based biosupport) columns (15 mg of LTA immobilised on 1 ml of beads) were successfully used to isolate glycans containing Lewis antigen and to analyse oligosaccharides containing L-Fucose, comparison with ConA-Sepharose columns are also reported (Yan *et al.*, 1997).

There are no other reports on immobilised LTA for chromatographic sugar separation and analysis and the possibility of using LTA biospecificity in downstream L-Fucose recovery has never been considered. Results reported in chapter III show that monosaccharide mixtures can be fractionated using a ConA–Sepharose column under isocratic conditions, depending on sugar specificity. Separation was dependent on column maximum binding capacity and total amount of mixture processed and similar principles should apply to other lectin-monosaccharide systems.

5.3 Materials

All general reagents, p-nitrophenyl-α-D-glucopyranoside (pnpg), p-nitrophenyl-α-L-arabinopyranoside (pnpa), p-nitrophenyl-α-L-fucopyranoside (pnpf), and LTA-Agarose (approximately 1-2 mg of LTA per ml of gel) were obtained from Sigma ltd (Poole, England). Standard Polyethylene oxide kit (MW range 27-920 kDa) and Pullulan (5.9 and 11.8 kDa.) for gel porosity characterisation were purchased from Phenomenex (Macclesfie Cheshire, England). Ultrapure water from a ELGA Purelab Option Unit (Bucks, U.K.) was used throughout. BioRad FPLC and Anachem HPLC used for chromatographic tests are described in the Materials and Methods sections of Chapter III.

5.4 Agarose gel porosity

Methods: Since no data were available from the gel manufacture on the gel porosity, LTA-Agarose pore structure was determined from size exclusion chromatography experiments in 50 mM Phosphate Buffer pH 7.2-7.4 containing 150 mM NaCl and 0.02% NaN_3 at room temperature using Polyethylene oxide and Pullulan standards of different molar masses.

Polyethylene oxide (920, 438, 140, 95, 51.5, 27.8 kDa) and Pullulan (5.9 and 11.8 kDa) standard solutions (≈1 mg/ml) were injected into a 3 × 100 mm glass column slurry packed under mild vacuum with LTA-Agarose gel.

Retention times for each sample were measured at the peak elution maximum, detected using the refractive index detector connected to the column outlet. Extra column effects were determined without the column from the system response.

A measurement of the effective size of a polymer molecule is the radius of gyration (*s*), defined as the root-mean-square distance of the elements of the chain from its centre of gravity (Flory, 1953). The values of the radius of gyration *s* of the polymer was estimated from the relationship

$$[\eta] = \frac{\Phi_o \cdot \left(1 - 2.63 \cdot \frac{(2 \cdot a - 1)}{3} + 2.86 \cdot \left(\frac{(2 \cdot a - 1)}{3}\right)^2\right) \cdot \left(\sqrt{6} \cdot s\right)^3}{MW} \qquad (5.1)$$

where [η] is the sample intrinsic viscosity, Φ_0 is an universal constant equal to 2.86×10^{23}, *a* is one of the constants estimated from the linear plot of *Log[η] vs. Log(MW)* obtained from Mark-Houwink-Sakurada equation $[\eta] = K \times (MW)^a$, (Schmid, *et al.;* 1991).

The sample kinematic viscosity (*v*) was measured with capillary viscometer immersed in a water bath at 20°C, measuring the time *t* for the samples and t_{water} for the buffer to drain between the two marks above the capillary tube. Samples densities are assumed not significantly different, equal to water density ρ_{water}=1g/ml, therefore numerically the kinematic viscosity *v* coincided with the dynamic viscosity η. It was also assumed $\eta_{buffer} = \eta_{water} = 1$ cp.

$$\eta = \eta_{water} \cdot \frac{t}{t_{water}} \qquad (5.2)$$

For each standard, the intrinsic viscosity $[\eta]$ is defined as

$$[\eta] = \lim_{C \to 0} \left(\frac{\eta/\eta_{water} - 1}{C} \right) \tag{5.3}$$

and is usually approximated extrapolating the experimentally determined values of $(\eta/\eta_{water} - 1)/C$ at different sample concentration C to $C = 0$. Here, one concentration per sample is used ($\approx$ 1mg/ml), assuming that this is low enough so that the correspondent $[\eta]$ is very close to the extrapolated value. The intrinsic viscosity can then be approximated as

$$[\eta] = \eta - 1 \tag{5.4}$$

The polymer hydrodynamic volume obtained from viscosimetric data was considered the only molecular parameter determining retention (Grubisic *et al.*, 1967).
The radius of gyration was set equivalent to the radius of the pore which the standard was able to diffuse into and a pore-volume distribution histogram was obtained (Schmid and Flodin, 1992).

Results: The results of sample viscosity and elution volume measurements with subsequent calculations are summarised in Table 5.1, while Mark-Houwink-Sakurada constants and the histogram representing the pore size distribution are in Figure 5.1.
The retention volume for the polyethylene standard (MW = 920 kDa) was set as void volume (V_e), column voidage of 0.355 was found and adopted in affinity chromatography experiments and calculation. From the total bed volume V_{bed} of 0.7065 ml, $V_{bed} - V_e$ equal to 0.4565 ml was calculated and set to 100% of pore volume availability.
In Table 5.1, to each sample molecular weight (MW) a value of intrinsic viscosity is associated with respective dimension (radius of gyration) and depending on the elution volume (V_r) also with the fraction of volume pores penetrable 1-$(V_{bed} - V_r)/(V_{bed} - V_e)$.
From the percentage of pores penetrable by a given sample the percentage of pores with the correspondent size is calculated and summarised in the right hand side of Figure 5.1; around 50 % of the total separating pore volume consists of pore radius > 40 Å.

Table 5.1: Viscosity and elution volume measurements with relative calculated values for intrinsic viscosity, radius of gyration, and percentage of pore volume available for the relative molecule to diffuse in.

MW (Da)	tcappil. (min)	η/η_{water}	$[\eta]$ (cm^3/g)	Log[η]	Log(MW)	Radius (Å)	V_r (ml)	% of penetrable pores.
5900	26.5	1.039	39	1.539	3.771	15	0.68	94
11800	27.5	1.078	78	1.894	4.072	25	0.605	78
27800	27.8	1.090	90	1.955	4.444	35	0.503	55
51500	29	1.137	137	2.138	4.712	49	0.413	36
95000	30	1.176	176	2.247	4.978	65	0.347	21
140000	31.5	1.235	235	2.372	5.146	82	0.317	15
438000	37.5	1.471	471	2.673	5.641	150	0.26	2
920000	49	1.922	922	2.965	5.964	242	0.253	1
water	25.5	1	-	-	-	-	-	-

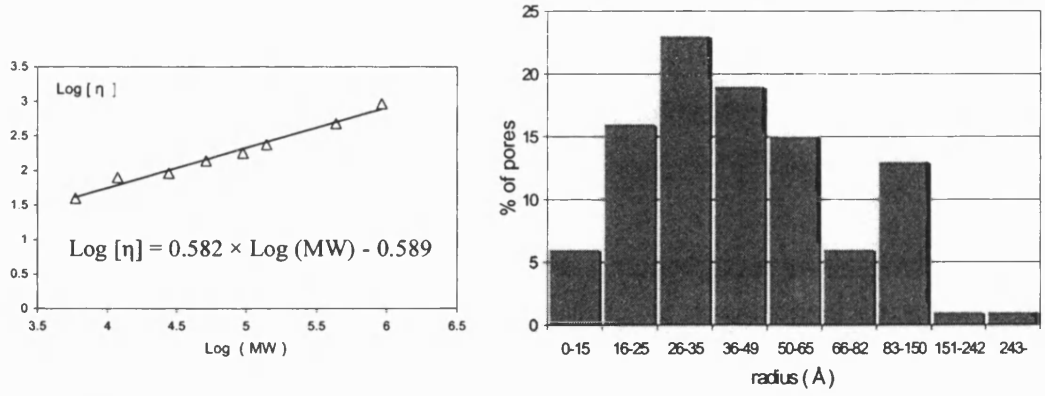

Figure 5.1: Left: linear regression of experimentally determined Log values of intrinsic viscosity against corespondent Log values of molecular weight. Right: histogram of the total % of pore size distribution.

5.5 Chromatographic Methods

Three columns, slurry packed under mild vacuum with LTA-Agarose, were used to investigate the interactions between LTA and pnpf, by chromatographic performance investigations using frontal and zonal applications with HPLC system as described in Chapter III. The p-nitrophenyl group was detected at 305 nm at different sensitivities depending on the sugar derivative concentration. The breakthrough curves, from frontal

loading, were normalised to the plateau value for each run to obtain the normalised concentration *C/Co*. Experiments were run under isothermal conditions, with buffer eluent (50 mM Phosphate buffer pH 7.2-7.4 with 150 mM NaCl and 0.02% Sodium Azide) and the column in a water bath kept at 5 and 20 °C. Frontal sample loadings were carried out using large injection loops (>7ml). Between each run, columns were extensively washed with running buffer. Adsorption isotherms were determined from the experimental breakthrough curves by the area method (Kasai and Oda, 1986, Appendix B) using the Langmuir equation for a single set of binding site model and Adair expression for a two sets of binding sites.

Frontal sample application set of tests with a 3 × 100 mm glass column, packed with fresh gel, was run at 0.1 ml/min (85 cm/h) at 5 and 20°C. A 3 × 250 mm glass column packed with LTA-Agarose was employed to investigate pnpf separation when it is pulse injected with other impurities represented by pnpg or pnpa. These experiments were performed at a flow rate of 0.1 ml/min and at temperature of 5°C. A 4×125 mm LTA-Agarose stainless steel column was also operated in ZC with relatively high flow rates. Sample injections (5 µl, containing pnpf and pnpg) were carried out at 0.2 and 0.3 ml/min and 5°C.

5.6 FC characterisation: Results and Discussion

Breakthrough curves for the 3 × 100 mm column loaded at 0.1 ml/min with a number of pnpf concentrations at 20°C and 5°C are shown respectively in Figure 5.2 and 5.3. The experimental adsorption data calculated from the breakthrough fronts (Appendix B) are well described by the Langmuir equation (Figure 5.4). The equilibrium constants are obtained from a non linear least square data fit using the Scientist package. These results are summarised with the theoretical/literature values in Table 5.1, where the theoretical maximum biding capacity ($3.7\text{-}7.4\times10^{-5}$ M) was calculated on the basis of manufacture's data (between 1 and 2 mg of LTA is immobilised per ml of Agarose gel). One binding site per monomer of 27 kDa and 1 to 1 stoichiometry of binding with L-fucose was assumed according to the manufacture's cited literature (Klab, 1968 and Yariv *et al.*, 1967), although this is not in line with the purified LTA obtained in this work (data in Chapter IV).

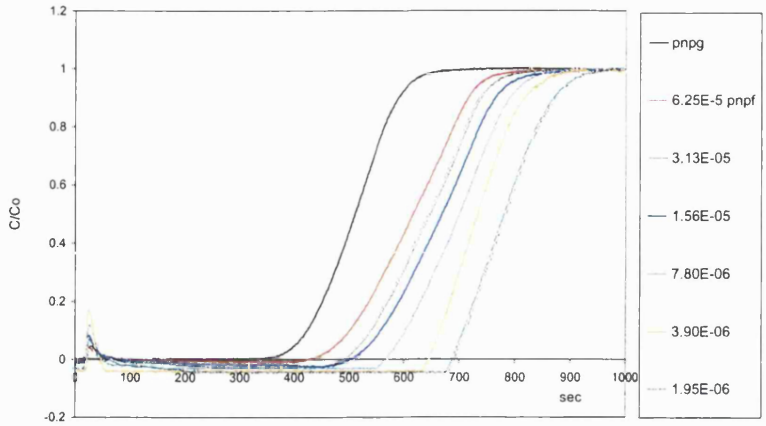

Figure 5.2: Frontal Chromatography of pnpf (molar concentrations in the legend) and pnpg (first breakthrough on the right) using 3×100 mm LTA-Agarose column at 85 cm/h and 20°C.

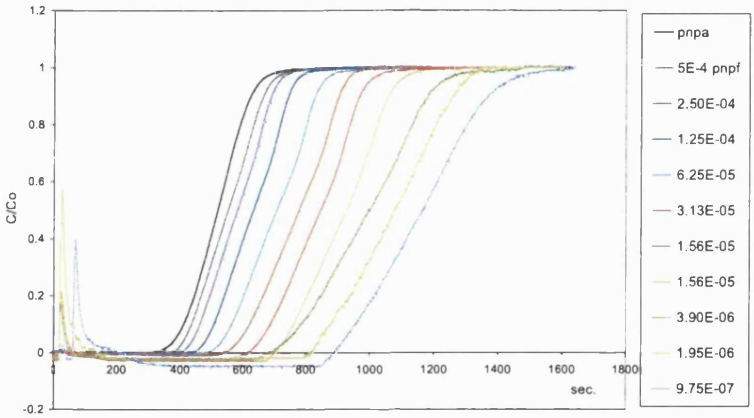

Figure: 5.3: Frontal Chromatography of pnpf (molar concentrations in the legend) and pnpg (first breakthrough on the left) using 3×100 mm LTA-Agarose column at 85 cm/h and 5°C.

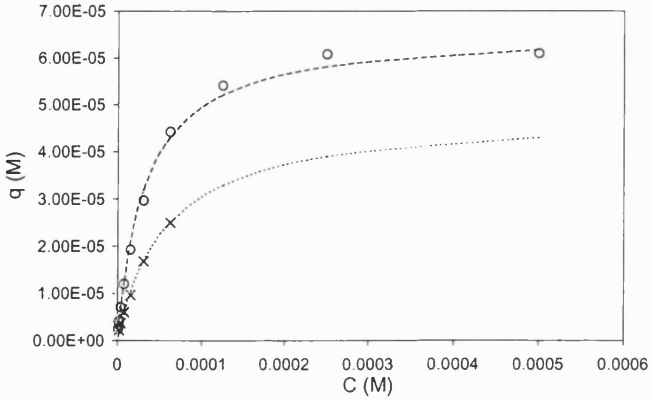

$$q = \frac{6.6 \cdot 10^{-5} \cdot C}{3.3 \cdot 10^{-5} + C}, \text{ at } 5^{\circ}C$$

$$q = \frac{4.8 \cdot 10^{-5} \cdot C}{5.8 \cdot 10^{-5} + C}, \text{ at } 20^{\circ}C$$

Figure 5.4: Experimental calculated equilibrium adsorption values from the breakthrough curves of Figure 5.2 and 5.3. Dotted and dashed lines are the best fits obtained. ×: 20°C FC experiment, ○ 5°C FC experiment.

The theoretical value for K_d in Table 5.2 is taken from the work of Rathi *et al.* (1997) which is in agreement with earlier equilibrium dialysis studies (Klab, 1968 and Yariv et al., 1967).

Table 5.2: Maximum binding capacity and dissociation constants calculated from this experimental work and theoretical values.

Langmuir constants	85 cm/h, 5°C column 3×100	85 cm/h, 20°C column 3×100	Theoretical
q_{max} (M)	6.6E-5	4.8E-5	3.7 - 7.4E-5
K_d (M)	3.3E-5	5.8E-5	2.9E-5

The strength of binding was observed to decrease, in terms of dissociation constant, with increasing temperature as expected for an exothermic interaction. The free energy of binding was calculated at 5 and 20 °C, $\Delta G^o \approx$-5680 cal/mol. As observed in the micro-calorimetric studies of Chapter IV, LTA-L-fucose interactions are enthalpy-entropy assisted (ΔG^o is constant with temperature). Especially at low temperature (5°C), ΔH^o is approximately equal to $-T\Delta S^o$ (same contribution to ΔG^o), therefore ΔH^o =-2840 cal·mol^{-1} and ΔS^o = 10 cal·mol^{-1}·K^{-1}. These are very close to the results from L-fucose titration calorimetry experiments, where ΔH^o =-2326 cal·mol^{-1} and ΔS^o = 7.8 cal·mol^{-1}·K^{-1}. The stronger affinity detected in FC experiments was likely to be due to the hydrophobic interactions of phenyl group which could also explain the higher capacity of the gel at lower temperature when those effects are particularly important.

Scatchard plot non linearity (figure 5.5) again provides evidence that the single set of binding sites model is not ideal. As done with the Con A affinity system, the experimental data were fitted with the Adair two binding sites population model (equation 2.31) and the resulting intrinsic association constants are reported on the graphs of Figure 5.6. At 5°C between the two binding sites there seems to be positive cooperation, while during ITC experiment the cooperation resulted to be negative, this discrepancy was observed for ConA as well. Hydrophobic interactions of the phenyl group might have played a significant role during FC experiments in determining a stronger secondary interaction, which decreases (as expected for this kind of interaction) when the temperature increases to 20°C.

At this temperature, the resulting intrinsic association constant values are similar i.e. no cooperation.

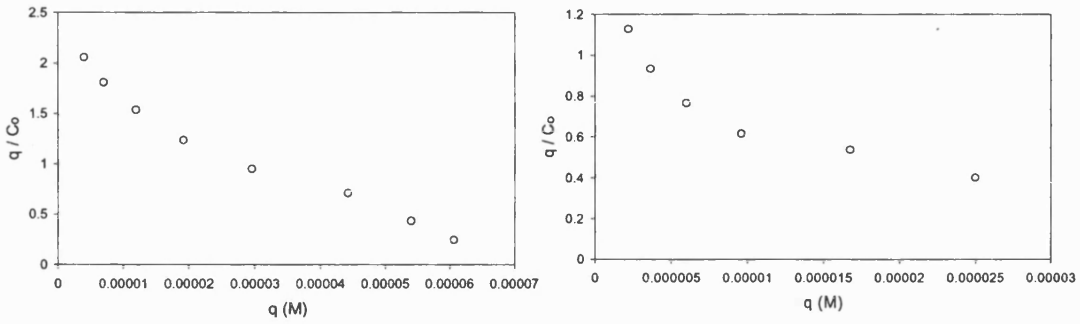

Figure 5.5: Scatchard plots from the adsorption data obtained in FC mode, for the system LTA-Agarose-pnpf at 5°C (left) and 20°C (right).

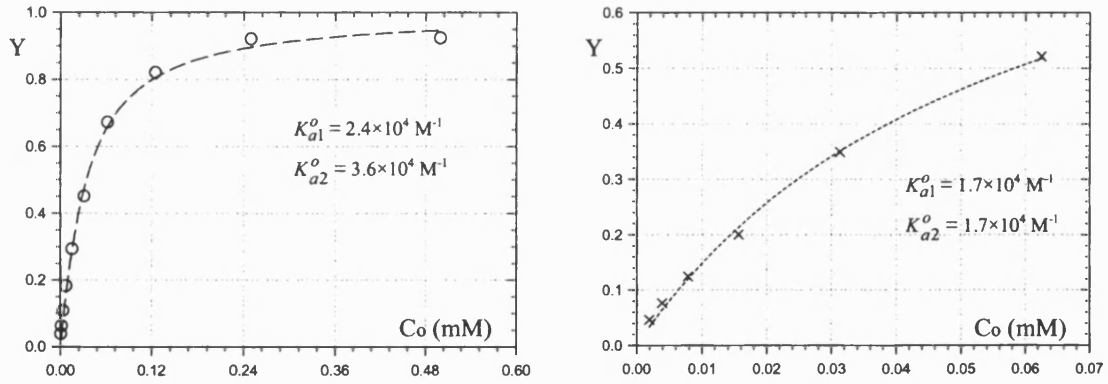

Figure 5.6: Scientiest plots obtained fitting the experimental adsorption results at 5°C (left) and 20°C (right) from the FC method with the Adair two sites binding model. The reported association constants are intrinsic values.

5.7 L-Fucose separation: Results and Discussion

The chromatograms of Figures 5.7, 5.8 and 5.9, in terms of peak Resolution (*R*) and Asymmetry (A_s) show that the separation of specifically bound pnpf sugar (second peak eluted) from pnpg (first peak eluted) is strongly concentration dependent.

Figures 5.7 and 5.8 show chromatograms obtained with the 4×125 mm HPLC column, operating at 140 and 95 cm/h, while Figure 5.9 shows those obtained with the 3×250 mm column at 85 cm/h.

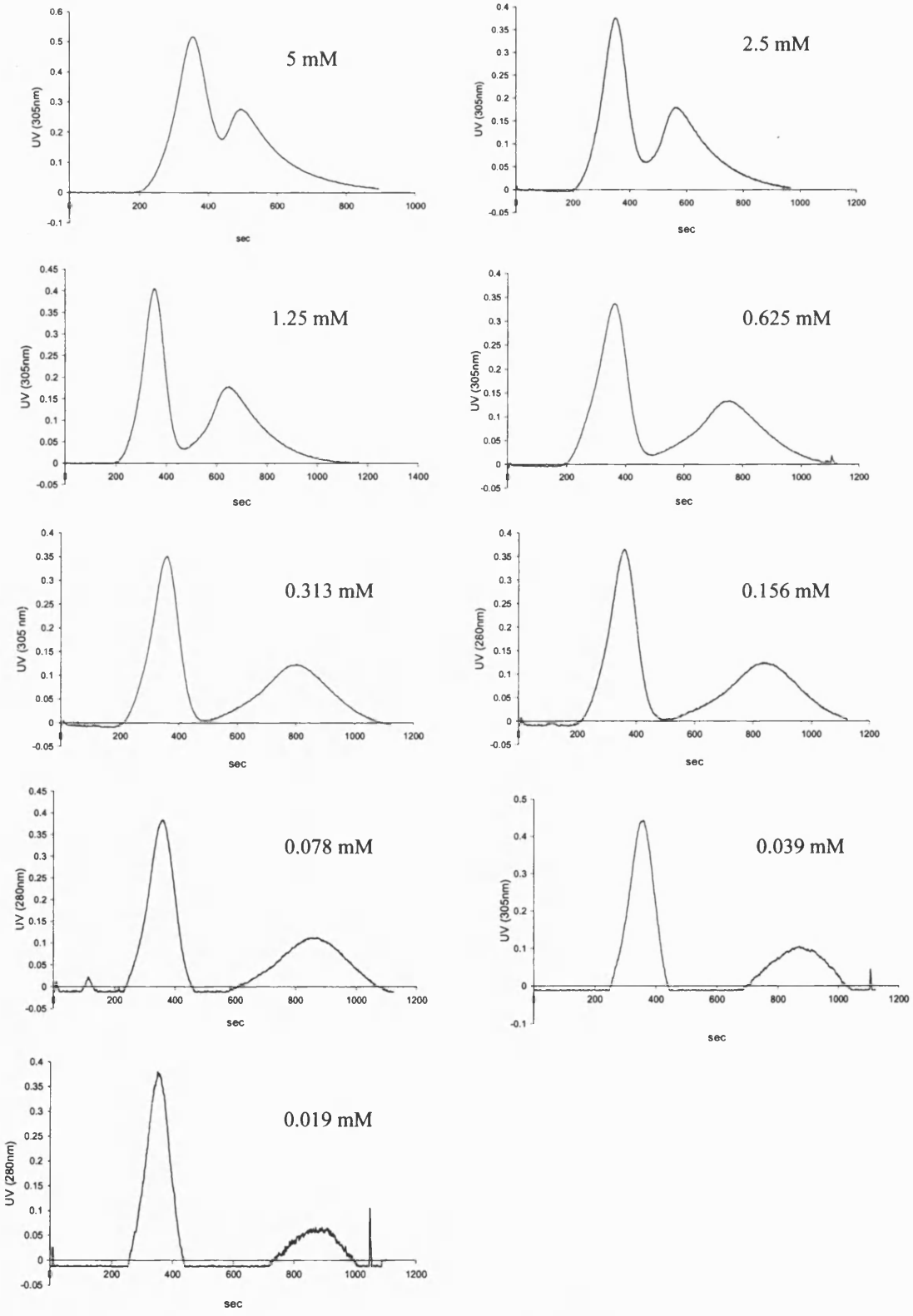

Figure 5.7: Chromatograms showing the elution profiles of 5 µl equimolar mixture of pnpf and pnpg injected into 4×125 mm LTA-Agarose column, 0.3 ml/min, 5 °C. Concentrations are indicated on each chromatogram.

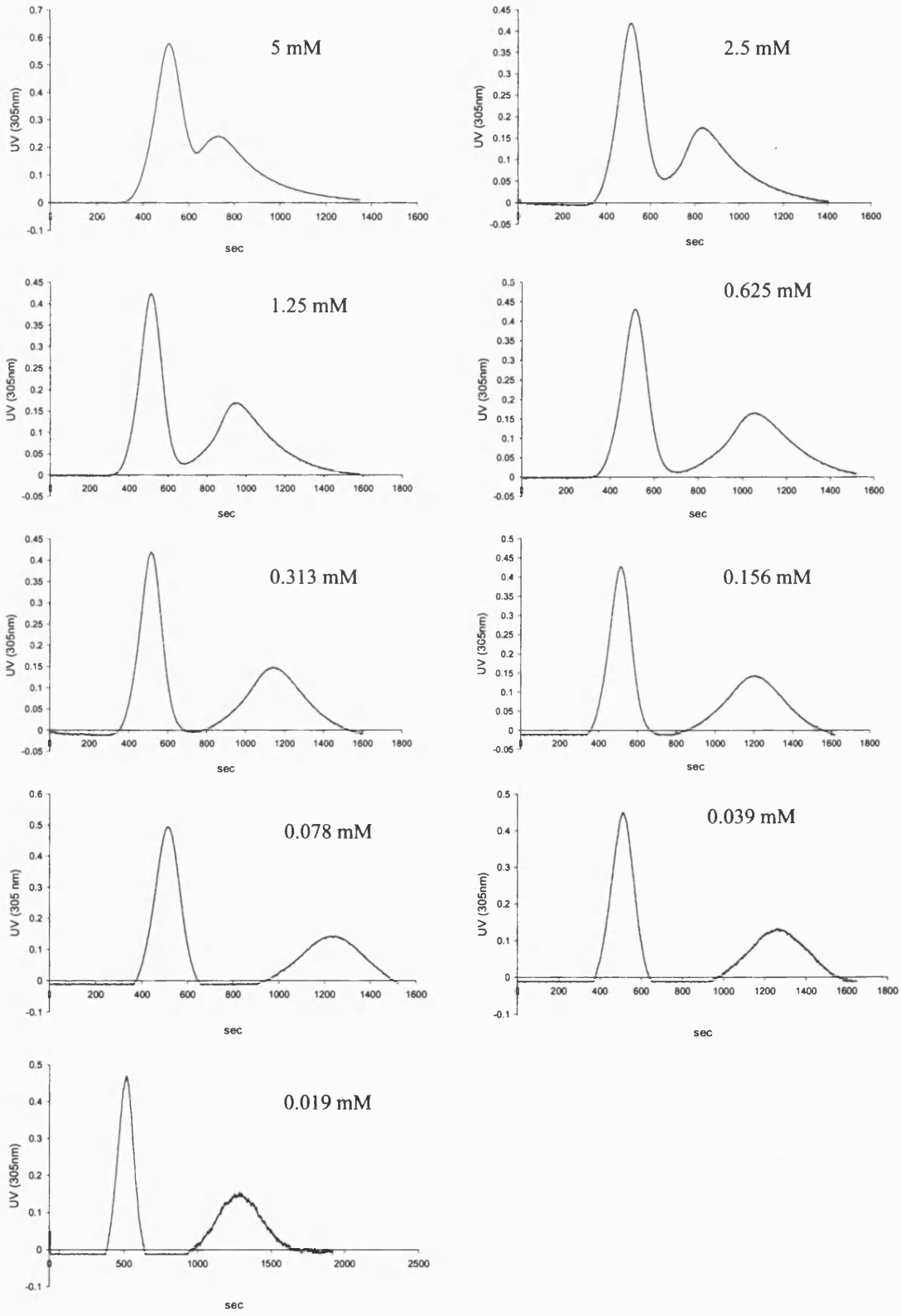

Figure 5.8: Chromatograms showing the elution profiles of 5 µl equimolar mixture of pnpf and pnpg injected into 4×125 mm LTA-Agarose column, 0.2 ml/min, 5 °C. Concentrations are indicated on each chromatogram.

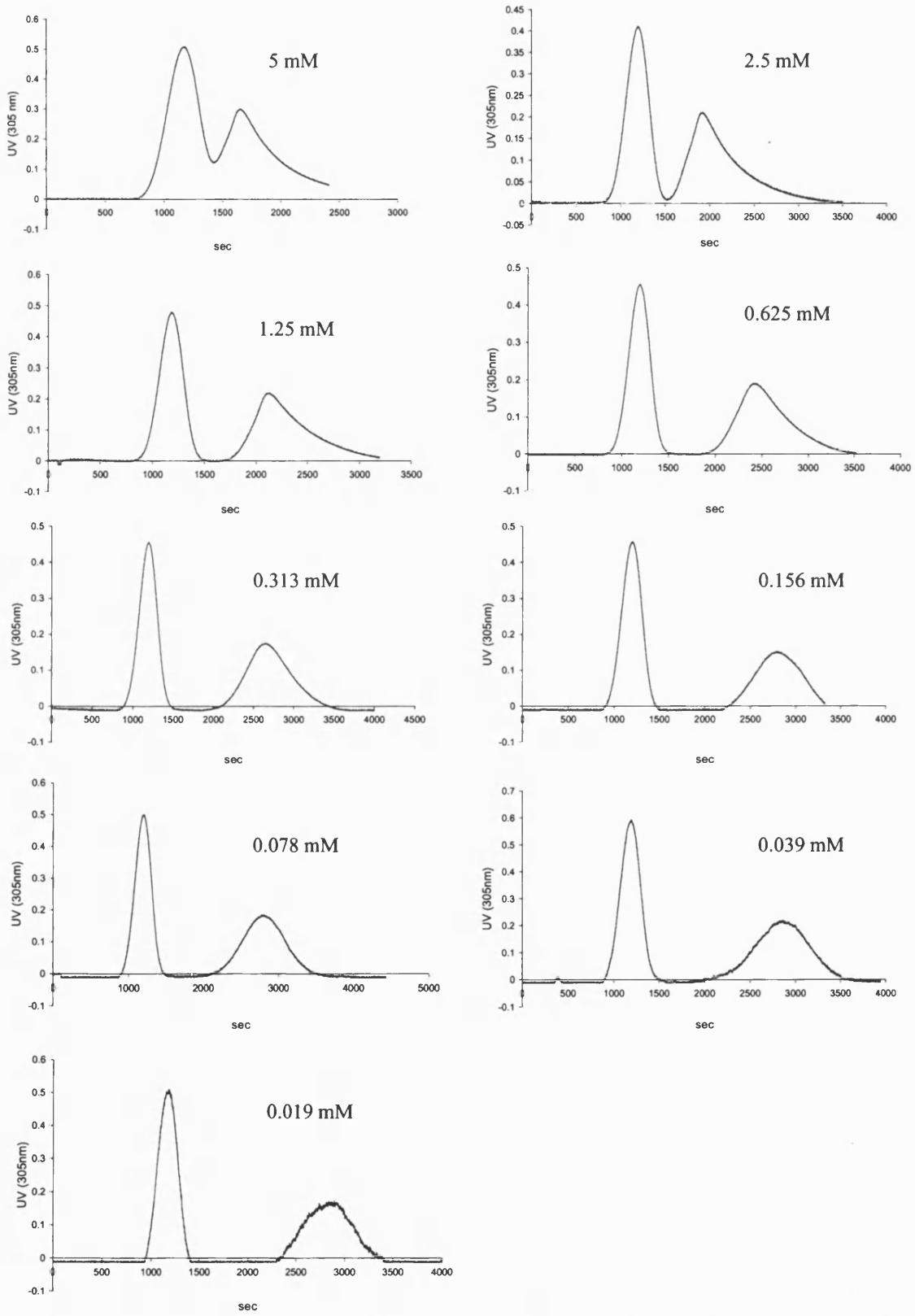

Figure 5.9: Chromatograms showing the elution profiles of 5 µl equimolar mixture of pnpf and pnpg injected into 3×250 mm LTA-Agarose column, 0.1 ml/min, 5 °C. Concentrations are indicated on each chromatogram.

It was assumed that all the columns were packed equally with a void volume fraction (V_e/V_{bed}) of 0.36 as found for the 3×100 mm column in section 5.4. Extra dead volume was determined without columns and added to the total void volume V_e. From the non-retained (first peak) and retained (second peak) elution profiles the respective capacity factors (V_{nr}-V_e)/V_e and (V_r-V_e)/V_e were calculated. The system selectivity α_{21}, defined as the ratio of the second over the first eluted peak capacity factor, was calculated with small errors values for both the column set ups, giving values over 3 at low injected concentrations (Figure 5.10). Better Resolution was achieved with the glass column that was twice the length of the HPLC column. Improvements are also probably due to the lower superficial velocity used in this case. However comparison of Resolution for the same HPLC column operating at 0.2 and 0.3 ml/min, showed little difference in separation and dynamic capacity (Jungbauer, 1993) (Figure 5.10).

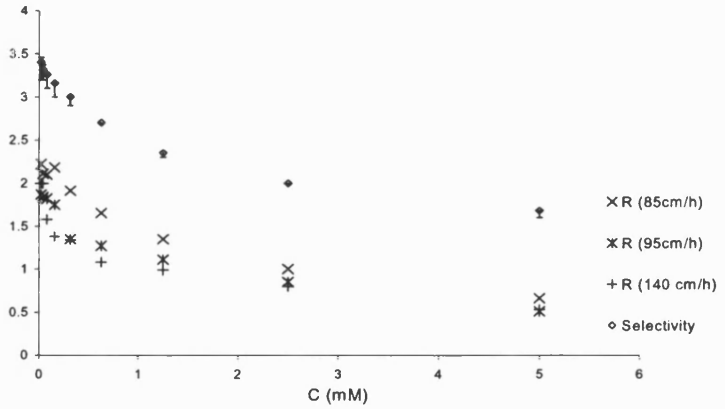

Figure 5.10: Resolution (R) and Selectivity (α_{21}) for LTA-Agarose columns when and a number of equimolar mixtures of pnpf and pnpg are injected at 140, 95 and 85 cm/hour.

The number of theoretical stages N, was calculated for the 3×250 mm column at the limit of lowest concentrations processed and it gave values between 100 and 120 theoretical equilibrium stages. This number falls 20-30 % for the effective plate number N_{eff} (Figure 5.11), defined as (Jungbauer, 2000),

$$N_{eff} = 16 \cdot \left(\frac{V_r - V_e}{W} \right)^2 \qquad (5.5)$$

Finally the height equivalent to a theoretical plate versus superficial mobile phase velocity is shown in Figure 5.12 for the 3×250-glass column, for three different concentrations injected (chromatograms in Figure 5.13).

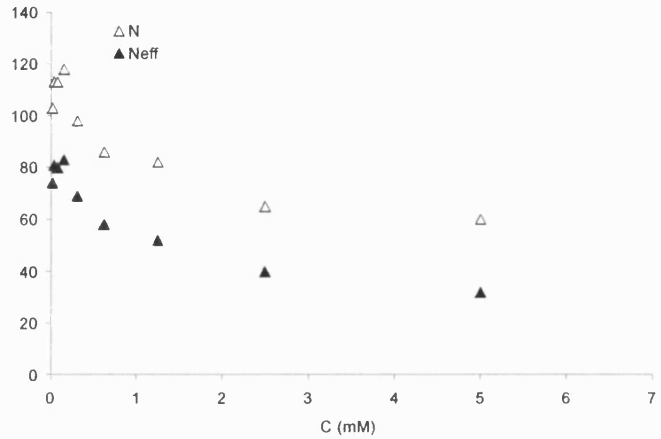

Figure 5.11: Dependency of the column number of theoretical (N) and effective (N_{eff}) plates with different sugar concentration injected, 3×250 mm LTA-Agarose column.

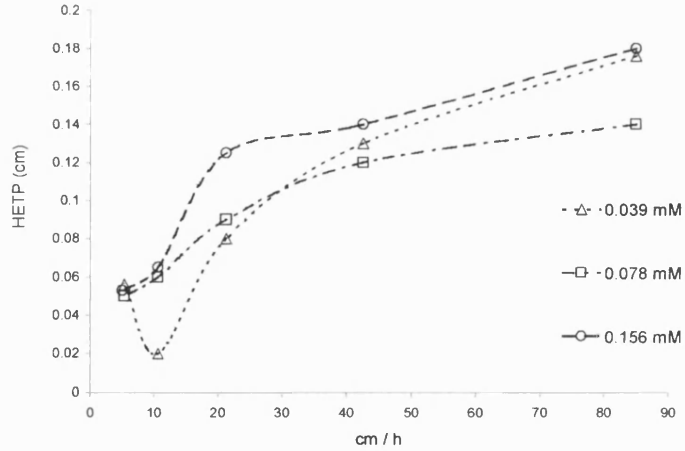

Figure 5.12: Column (3×250 mm) efficiency against superficial velocity relative to the specific elution peak of pnpf, points are based on the results of three concentrations injected 0.156 mM, 0.078 mM, 0.039 mM.

Results were well within the range of typical bioaffinity chromatographic applications, axial dispersion appears to be negligible, non-equilibrium effects due to a combination of slow mass transfer and adsorption-desorption kinetics are probably responsible of the higher HETP value at higher flows. A theoretical number of equilibrium stages up to 500

could be achieved by loading the column at 5 cm/h at the expense of a 17 fold increase in cycle time.

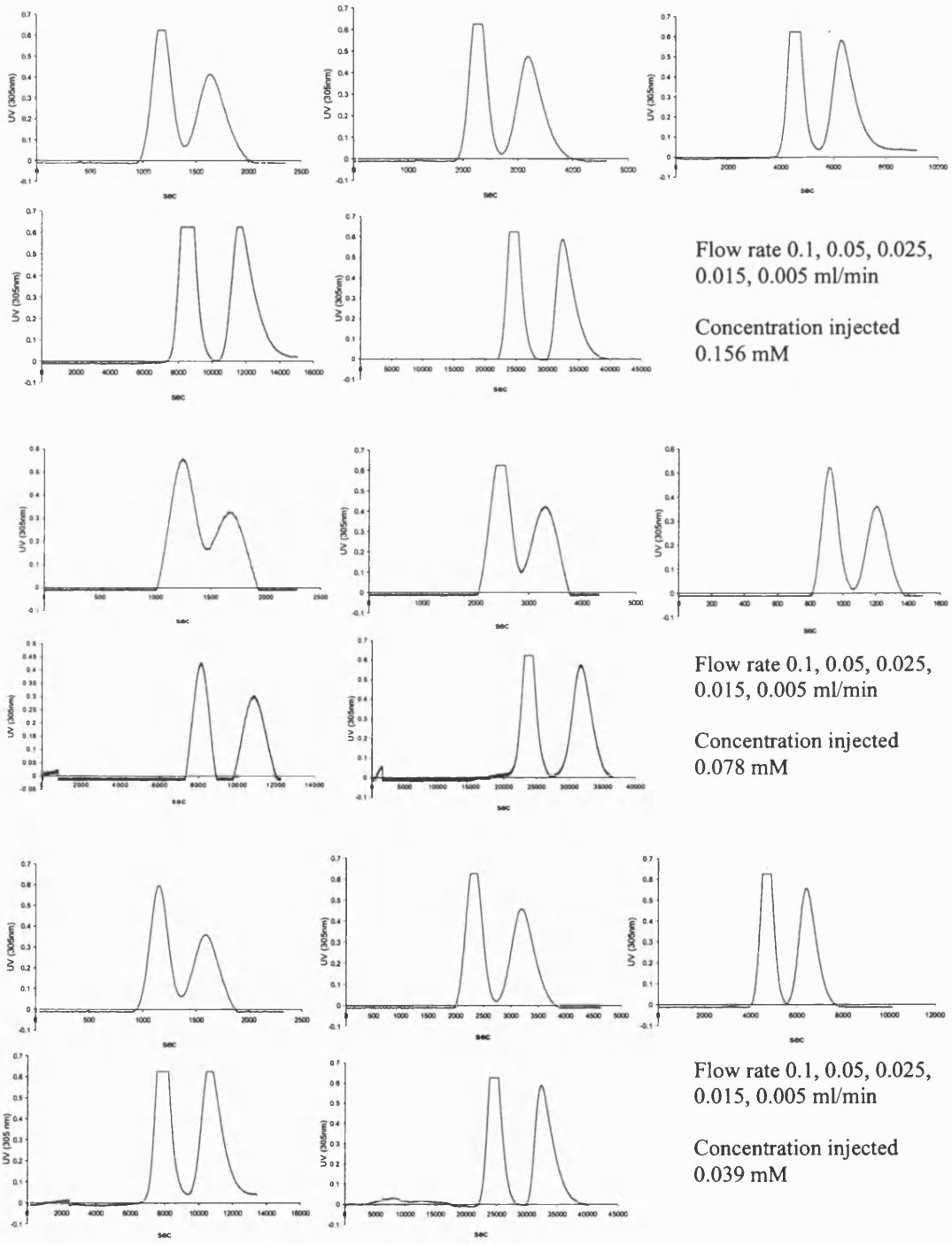

Figure 5.13: Chromatograms used to evaluate HETP versus superficial velocity summarised in Figure 5.11. Elution profiles of 5 µl containing pnpf and pnpg at 0.156, 0.078, 0.039 mM injected into 3×250 mm LTA-Agarose column, at 5 different flow rates and at 5 °C.

The performance of these columns degraded irreversibly over a period of three months. Ligand leakage and damage to the gel structure resulting from high flow rates were probably the main causes. The chromatograms used to evaluate HETP in function of flow rate in figure 5.13 were obtained with the best performance of the column already partially compromised, peaks became broader and tailing increased. This can be observed comparing the chromatograms at 0.1 ml/min of Figure 5.13 with the chromatograms relative to the same concentration mixture injected earlier, shown in Figure 5.9.

5.8 Process feasibility and scale up

"The design of a production chromatography system is a complex exercise because of the many process variables involved" (Coulson & Richardson, 1968).

To increase throughput, preparative chromatography is usually operated under extreme conditions of high flow rate and sample overloading and the obvious drawback is reduction in efficiency and resolution. In 1989 Hupe and Hoffman investigated the production rate in the case of volume or concentration overloading highlighting a linear and asymptotic increase of the production rate with increases of column cross sectional area and length. They concluded that if L_o is the length of the analytical column to perform the desired separation with infinitesimally small sample, during scale up it is convenient to increase the length up to 3/2 L_o and then increase the cross sectional area to optimise the production rate. Herbert (1991) reported an acceptable ratio of three between the efficiency of analytical and preparative columns, therefore longer columns are required at larger scale. However, it is not always possible to use longer columns to this degree. Particularly with soft gels, longer columns increase the weight of the packing and the drag force on the lower part of the bed leading to compression. Also the general assumption of pore diffusion control step i.e. N is proportional to column length over particle diameter is questionable for the weak biospecific interaction of small sugar molecules where other kinetic effects must be considered. There are always specific issues in different situations and a single formula is not available, analytical trials are essential. Generally a constant ratio L/d_p should keep resolution, throughput and pressure drops constant and is often used in scale up development (Wankat, 1986) if different particle sizes are to be used.

When physico-chemical characteristics of the chromatographic system from the laboratory to the preparative scale can be maintained constant, the conventional way to scale up is to increase the column diameter at constant length (Jangbauer, 1993).

A detailed analysis of the possible scale up of the separation described analytically in this chapter is beyond the scope of this screening study but the results allow some general observations to be made.

Taking experiments with the narrow 3×250 mm column; the flow rate (85 cm/h) was very high for the matrix and the column bed did not collapse thanks to the support from the column walls. In a larger scale application a lower flow rate would be required, therefore the efficiency would benefit and the gel compressibility effects reduced. An industrial scale column could retain similar length to that used in the laboratory scale with the column diameter increased greatly, thus from the analytical 1.7 ml column a larger scale application could be done with a 100 litres column of dimensions 720×250 mm.

In 1986 Knox and Pyper showed that to maximise the throughput, the use of concentration overloads is attractive but the sample volume could approach half of the retained elution peak volume obtained at analytical scale. This conclusion seems too optimistic in the lectin-sugar system. Here. increasing the injections volume from 5 to 20 µl seriously degraded the separation even at low concentrations. As already stated previously, in work on a small scale, extra column effects can be responsible of the majority of band spreading and this could be reduced on a larger scale. However the retained sugar contained in the 5 µl injected mixture was very diluted in the column outlet, within 1.5 ml (elution peak width). This would lead to too high injection volume based on the Knox and Pyper (1986) scale up studies.

If the low loading fraction is maintained constant (0.3 %) during scale up to a 100 litres column, 305 ml would be processed each run. Using half the superficial velocity used in analytical experiment and a sugar concentration of 5 mM it would be possible to process 1.5 g/d, running 6 injections per day and washing and regenerating overnight.
A Chromaflow column designed and commercialised by Amershan Pharmacia biotech. could provide a suitable solution: it permits packing, operation, unpacking and cleaning in

situ (no need to lift the lid). This has evident practical advantages and has shown excellent performance and reproducibility (Williams, 2002).

Two factors have not yet been considered: the purity required, which can completely change column design and operating condition, and the real nature and amount of impurities in the desired feed. The significance of these factors can be reduced by including the affinity chromatographic step as late as possible in the purification scheme (Janson and Hedman, 1982).

Higher productivity can be achieved by increasing the sorbent capacity or the flow rate (Robinson, 1974), the first option seems to be more realistic with fragile matrices. Increasing flow rate could be the best solution if the pressure drop (ΔP) could be kept low by stacking shorter columns or using an alternative column design known as radial flow chromatography, where samples flows across rather than down the axial length of the bed (Saxena *et al.*, 1988).

Chapter VI

Low Affinity Pair Size Exclusion Chromatography

6.1 Summary

The two sections of this chapter describe a novel approach for monosaccharide separations: Low Affinity Pair Size Exclusion Chromatography (LAPSEC) which uses the specificity of free lectin in solution within a size exclusion column. In the first section, LAPSEC is described and its effectiveness investigated through qualitative and quantitative analysis of the separation achievable, carrying out simulations with a simple multi-sectional equilibrium model. The second part is focused on the experimental application of LAPSEC with ConA and LTA –monosaccharide systems. The potential of this technique for downstream L-fucose recovery is demonstrated and in particular the ease, economics and versatility of process set up and operation, compared with immobilised lectin chromatography, suggests that LAPSEC could provide a viable alternative to traditional Affinity Chromatography.

6.2 Introduction

Although immobilised low molecular weight ligands can be used effectively to recover high molecular weight proteins, the converse is not usually true. The adverse molecular weight ratio and practical limitations will rarely be cost effective for the recovery of low molecular weight species. This is particularly true for weak lectin-monosaccharides interactions. Despite these practical constraints, affinity separations are potentially attractive as they can allow a high degree of optical or regio-selectivity not easily achieved with other approaches.

In 1962 Hummel and Dreyer first used gel filtration to separate ligand macromolecule complexes from free species to allow calculation of both bound and free concentrations. Using similar principles this technique could also be exploited for chromatographic separation of weakly bound species. This size exclusion based protocol removes the need for macromolecule immobilisation hence allowing the use of higher macromolecule concentrations and offering significant potential for cost reduction.

6.3 Protocol

In the absence of specific interaction between large and small molecules, a size exclusion chromatographic column would operate in a desalting mode when is loaded with gel which allows a partition coefficient of one for molecules of interest (e.g. MW<1 kDa) and zero for the macromolecules (e.g. MW>20 kDa). The macromolecules would elute after an eluent volume equal to the void volume and the small molecules after a volume of eluent equivalent to the total column volume. If one of the components of a mixture of small molecules is reversibly bound by the macromolecule-receptor its effective partition coefficient is reduced and it will elute earlier than unbound material providing a basis for separation. When the affinity interaction is weak there is the additional advantage that conditions can be engineered such that the macromolecule elutes as a pure component, that is easily recycled and reconcentrated. The low molecular weight sample would be mixed with the high molecular weight receptor and applied to the column as a discrete sample, this is followed by a period of elution with buffer containing receptor and then the remaining elution is conducted with buffer without receptor.

6.4 Practical issues

Feed concentration in SEC is limited by viscosity and macromolecule aggregation constraints; this effectively limits protein concentration to be lower than approximately 10 mg/ml. Depending on the sample volumes used and stochiometry of the interaction, the low molecular weight ligand concentration can be higher than that of the macromolecule. The sample volume is also limited by the need to ensure adequate column length for

excluded material introduced at the trailing edge of the sample to pass included material introduced at the leading edge of the sample. In an affinity pair application the applied volumes for sample and receptor can be different such that an increased elution volume of receptor solution can be used to compensate for the concentration limitations. Finally in terms of interaction strength; the lower the dissociation constant the higher the fractional binding will be for a given set of ligand-receptor concentrations. This will magnify the apparent reduction in the partition coefficient for the bound ligand, however tighter binding will increase the degree to which ligand is co-eluted with receptor and will limit the potential for direct recycle of receptor.

6.5 Potential benefits

This is a highly selective potentially viable separation technique for preparative scale recovery of low molecular weight products offering low resin costs, efficient use of affinity receptor, no requirement for specific eluents and process flexibility. In fact the same resin can be used with different affinity pairs for different separations, the affinity pair can be replaced once denatured without replacing the support matrix, and the matrix can be sterilised without risk to the affinity pair.

6.6 Model development

The plate model has proved extremely useful in chromatography, in that it provides a convenient means of evaluating and comparing column performance from a determination of height of a theoretical plate under operating conditions. The assumption that each plate is at equilibrium requires that the governing rate processes, adsorption/desorption and mass transfer, are rapid compared with the liquid velocity through the column. This means that with equilibrium plate models, predicted performance will be independent of column feed rate. The magnitude of discrepancy will depend on the balance of the rate processes and the column feed rate achievable in a given application.

The more rigorous approach taken in the application of rate models overcomes the inherent limitation of stage models. However, the mathematical complexity of these models usually

necessitates a number of simplifying assumptions as described in Chapter II and the requirement to numerically solve the partial differential equation describing column concentration as a function of both time and position imposes large computational burdens (Arve and Liapis, 1988). In this work a multistage approach is adopted, rate equations neglected and equilibrium assumed throughout each stage in which the column is composed.

Given the fragile structure of the gels employed for these kinds of applications, flow rates must usually be lower than 10-20 cm/hour and that makes the equilibrium hypothesis viable.

In the plate theory, equilibrium between gel and liquid is implicitly assumed such that the number of theoretical plates can be calculated from the response of the column. Hence given the column length, the height equivalent to a theoretical plate (HETP) can be calculated and used as a comparative index of performance. The column is divided into a number of sequential stirred tanks where fluid elements are stepped from stage to stage as elution proceeds (Wankat, 1974). Within each stage, the system is modelled as a batch reactor, the reaction is assumed to reach equilibrium instantaneously and the model is essentially identical to the plate theory.

6.6.1 Model structure

Once that the column is described as a series of N equilibrium stages, the material balance equation for each species involved must be solved at every stage and for every loading step, the input and initial conditions specified and the output conditions calculated. This is achieved by taking the initial conditions for the gel as those at the current stage for the previous step, and the initial conditions for the liquid phase as those at the previous stage at the previous step. The conditions are updated at the end of each sequence of stage calculations. Column loading is determined by setting a loading volume fraction f, as a function of total bed volume; f_p for the volume of protein injected and f_a for the sugar mixture.

$$f = \frac{V_{injected}}{V_{bed}} \tag{6.1}$$

therefore the number of loading steps L_s is calculated using the stage volume and column voidage;

$$L_s = \frac{f \cdot N}{\varepsilon} \tag{6.2}$$

Hence for this number of steps the feed to the first stage is set at the specified feed concentration, thereafter the feed to the first stage is set to zero.
This protocol simulates the addition of an ideal square pulse to the column but any desired pulse shape could be generated.

6.6.2 LAPSEC theory and algorithm

Two low molecular weight species A and B are considered; A specifically binds to the higher molecular weight receptor P while B does not. A and B species can partition between liquid (V_e) and gel (V_s) phases of a size exclusion column on the other hand P is completely excluded. Depending on the partition coefficients the concentration of A will be higher in the liquid phase V_e, representing the column voidage and hence A will move faster than B throughout the column. In the following the subscripts s and e indicate respectively quantities belonging to stationary and mobile phase, K_p (as defined with equation (2.1)) is the partition coefficient and the species are indicated with the subscripts A, B and P. The total column volume is $V_{bed} = V_s + V_e$, the voidage ε was defined with equation 2.2 and the equilibrium partition expressions follow,

$$C_{As} = K_{pA} \cdot C_{Ae} \tag{6.3}$$

$$C_{Bs} = K_{pB} \cdot C_{Be} \tag{6.4}$$

$$C_{Ps} = K_{pP} \cdot C_{Pe} \tag{6.5}$$

Conditions will be chosen such that $K_{pA} = K_{pB} = 1$, $K_{pP} = 0$ and assuming that only A binds to the receptor protein P. In the stage model the liquid element in the current stage is transferred to the following stage and is replaced by the liquid element coming from the previous stage. Since the protein P is only in the mobile liquid phase, all adsorbed A is transferred to the next stage. Figure 6.1 shows an i^{th} equilibrium stage during loading step.

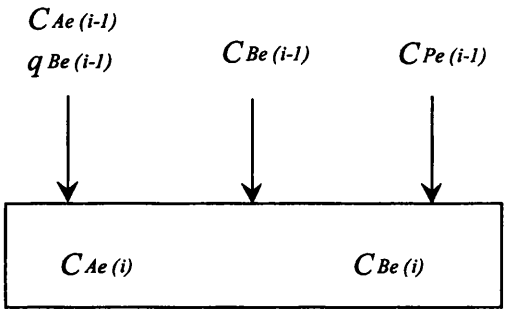

Figure 6.1: The i^{th} equilibrium stage during a loading step.

The A, B and P material balances for each equilibrium stage *i* are:

$$C_{A,tot(i)} = \varepsilon \cdot \left(C_{Ae(i-1)} + q_{Ae(i-1)}\right) + (1-\varepsilon) \cdot C_{Ae(i)} \tag{6.6}$$

$$C_{B,tot(i)} = \varepsilon \cdot C_{Be(i-1)} + (1-\varepsilon) \cdot C_{Be(i)} \tag{6.7}$$

$$C_{P,tot(i)} = \varepsilon \cdot C_{Pe(i-1)} \tag{6.8}$$

Assuming mutual depletion the binding expression in terms of dissociation constant is

$$K_d = \frac{\left(C_{A,tot} - q_{Ae}\right) \cdot \left(C_{P,tot} - q_{Ae}\right)}{q_{Ae}} \tag{6.9}$$

and solving for q_{Ae},

$$q_{Ae} = \frac{\left(K_d + C_{A,tot} + C_{P,tot} - \sqrt{K_d^2 + 2 \cdot C_{A,tot} \cdot K_d + 2 \cdot C_{P,tot} \cdot K_d + C_{A,tot}^2 - 2 \cdot C_{A,tot} \cdot C_{P,tot} + C_{P,tot}^2}\right)}{2} \tag{6.10}$$

while liquid phase concentration of A at equilibrium is

$$C_{Ae} = \left(C_{A,tot} - q_{Ae}\right) \tag{6.11}$$

The model based on this mathematical approach was written in Power Basic and listed in Appendix A and a flow chart for this algorithm is given in Figure 6.2

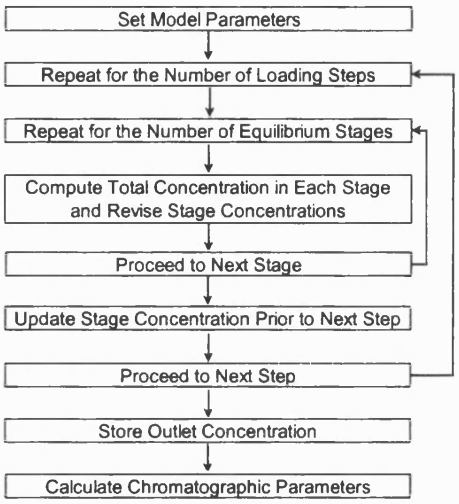

Figure 6.2: Flow chart describing the model algorithm.

The concentration of A (C_A), B (C_B) and P (C_P) with dissociation constant (K_d) for A-P interaction, the number of loading steps (*Nstep*) and stages (*Nstage*), column voidage (ε) and injection volume fractions (f_A for A-B mixture, f_P for P) are all input values.

The concentration elution profiles of A, B and P normalised to the input values and some chromatographic performance parameters, such as A-B resolution (R), retention volume for A (normalised to the total bed volume V_{bed}), purity, dilution factor and peak asymmetry (A_s) for A are generated as programs outputs. The purity for the target component A is calculated as a percentage of overlapping peak A over peak B, and the dilution factor as the ratio of the initial number of loading steps and the real number of loading steps with which peak A is totally eluted. Retention Volume, Resolution, and peak asymmetry are typical chromatographic parameters used for separation evaluation, defined in Chapter II.

6.6.3 Model predictions

The first set of simulations is run with the macromolecule carrier- receptor P at constant concentration in the mobile phase ($f_p=1$). Good resolution between P and A can be achieved over a wide range of C_A concentrations of A injected, as shown in Figure 6.3. In the following chromatograms, peaks are always normalised over the initial injected molecule concentration as C/C_o.

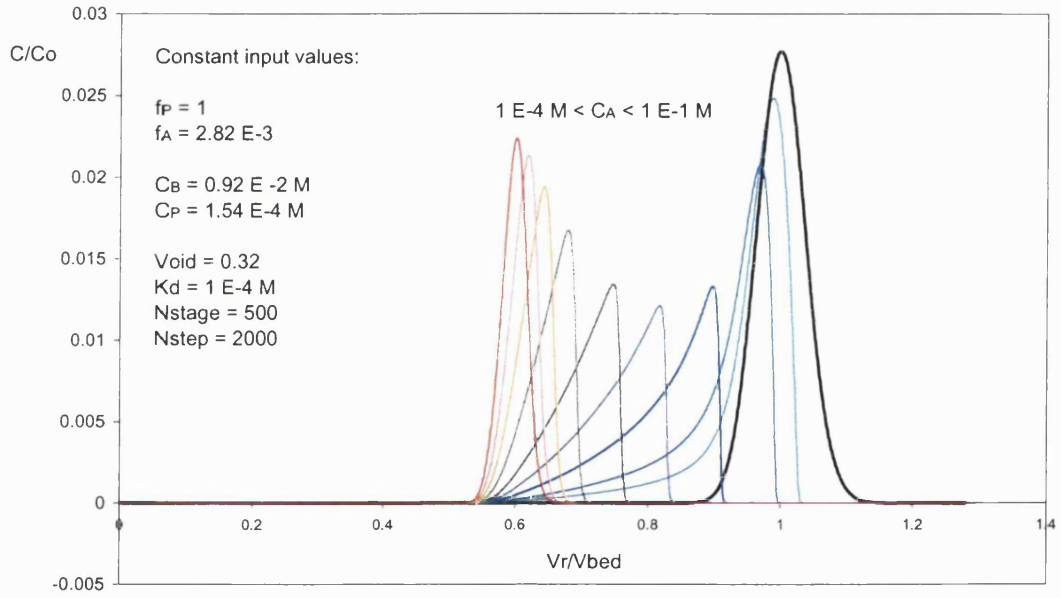

Figure 6.3: Elution profiles of mixtures of impurities B (black peak) and a number of target A concentrations (coloured peaks) injected when the mobile phase contains receptor P.

This clearly represents a limit situation where the maximum lectin capacity achievable on the edge of protein solubility can be totally exploited throughout the whole column bed to optimise A-B separation and maximise throughput. Of course this is unlikely to be achievable since $f_p<1$ and P, A, B should ideally elute as pure components. Calculated chromatographic parameters and relative trend lines are summarised, as a function of

concentration of A injected, in Figure 6.4, over the range where 100 % purity for A was obtained.

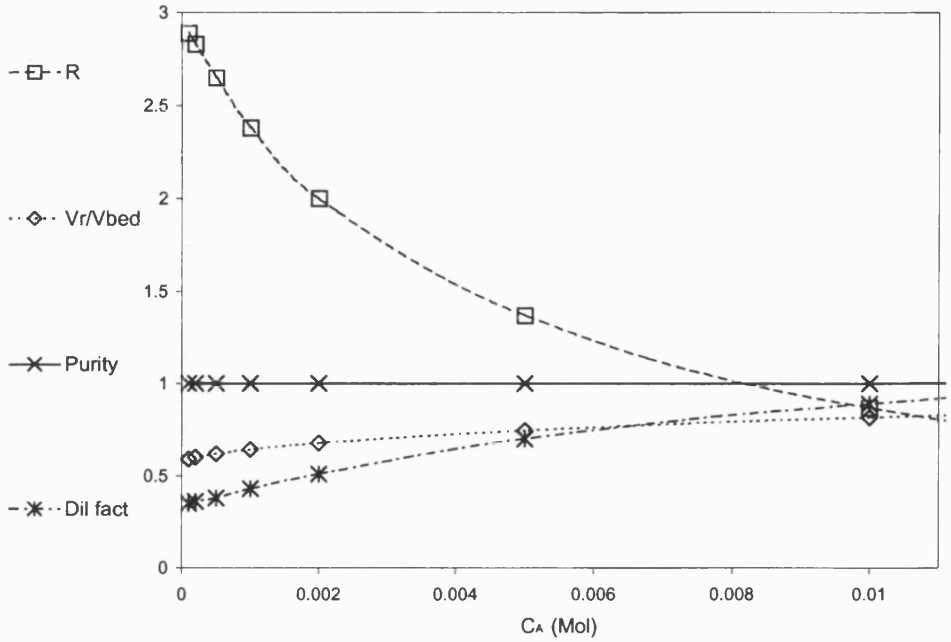

Figure 6.4: Resolution R, retention volume fraction V_r / V_{bed}, Purity and Dilution factor for A. Points are calculated from the elution profiles relative to the simulations of Figure 6.3.

Within this concentration range for A, the second set of simulations (Figure 6.5) shows that a smaller finite amount of protein receptor can be injected, eluted as a pure component while generating a decent separation of A from the impurities B. However the range of A concentrations which can be injected while maintaining reasonable separation becomes smaller. Figure 6.6 highlights a drop in Purity and Resolution above a critical value of C_A.

When the injected P concentration is increased 3 fold, the simulation shown in figure 6.7 clearly shows that A is always co-eluted partially or totally with P. Similarly K_d, values can affect the separation; a high affinity A-P pair makes A partially or totally co-eluted with P, while too weak interaction does not effectively separate A from B (Figure 6.8).

Trends, describing chromatographic parameters dependence on the strength of binding (K_d), are in Figure 6.9.

The last simulations (Figure 6.10) investigated the effect of the number of equilibrium stages on the model elution peaks shape. As expected from equilibrium theory, peaks spread when *Nstage* is decreased but in terms of A-B separation performance, the resolution *R* seemed not to be greatly affected for *Nstage* > 150 (Figure 6.11).

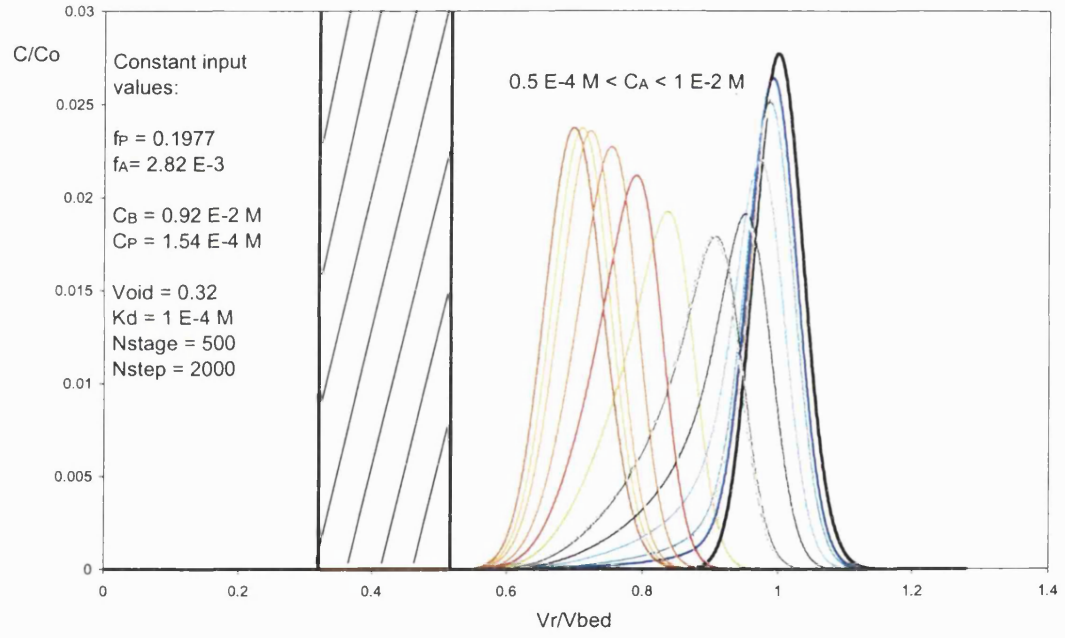

Figure 6.5: Elution profiles of mixtures of impurities B (black peak) and a number of targets concentrations of A (coloured peaks) injected together with a finite volume containing P (shaded area square pulse).

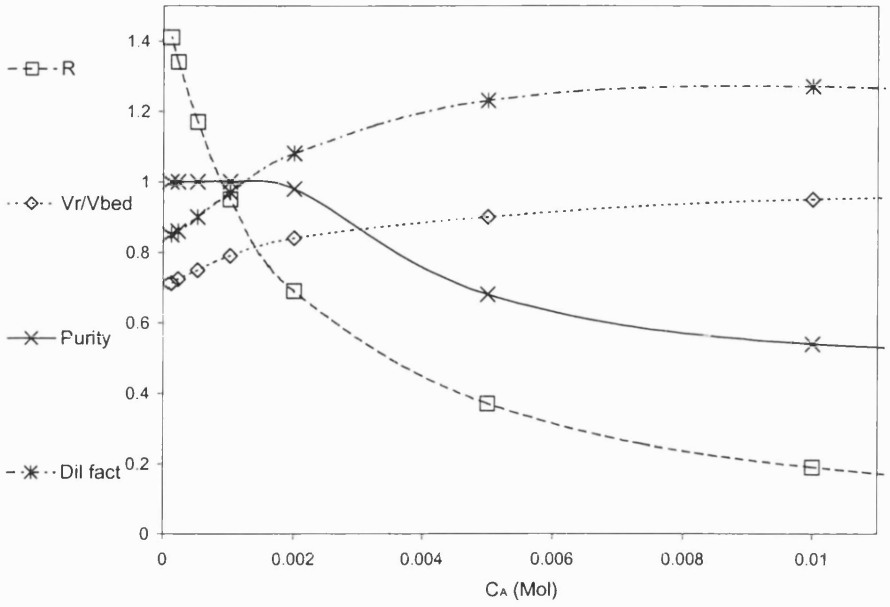

Figure 6.6: Resolution R, retention volume fraction V_r / V_{bed}, Purity and Dilution factor for A. Points are calculated from the elution profiles relative to the simulations of Figure 6.5.

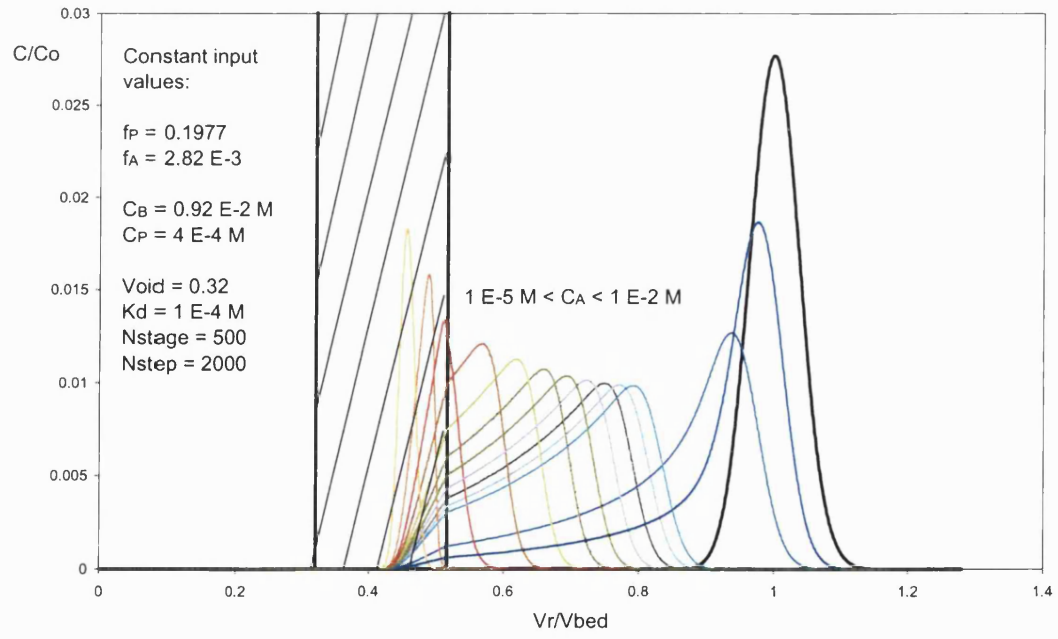

Figure 6.7: Elution profiles of mixtures of impurities B (black peak) and a number of targets concentrations of A (coloured peaks) injected together with a finite volume containing P (shaded area square pulse) 3 times more concentrated than in Figure 6.5.

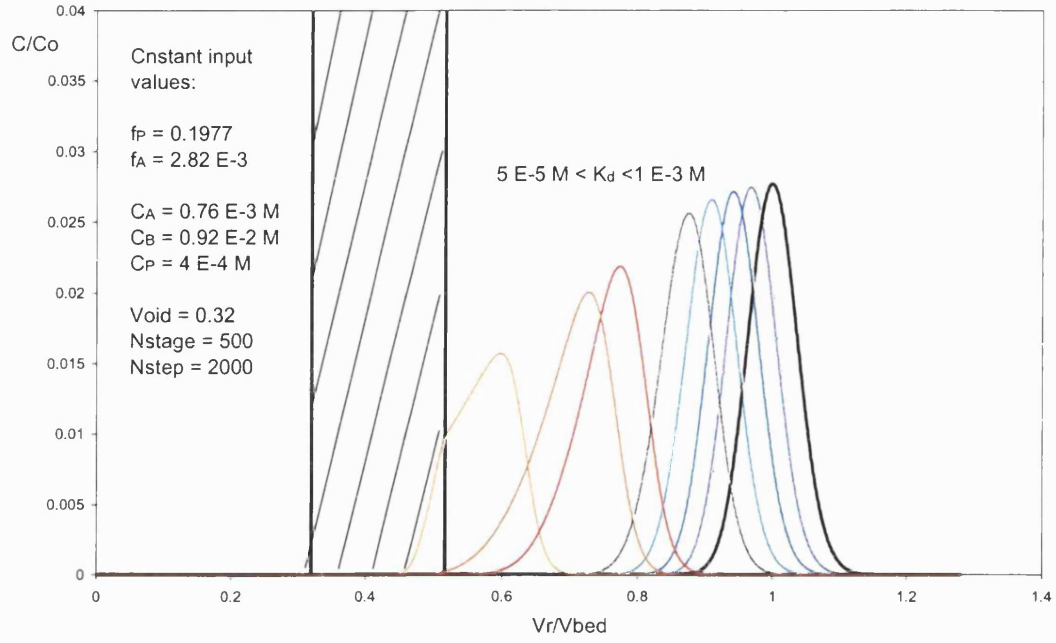

Figure 6.8: Effect of strength of interaction on elution profiles of mixtures of impurities B (black peak) and target component A (coloured peaks). P (shaded area square pulse) concentration is as for Figure 6.5.

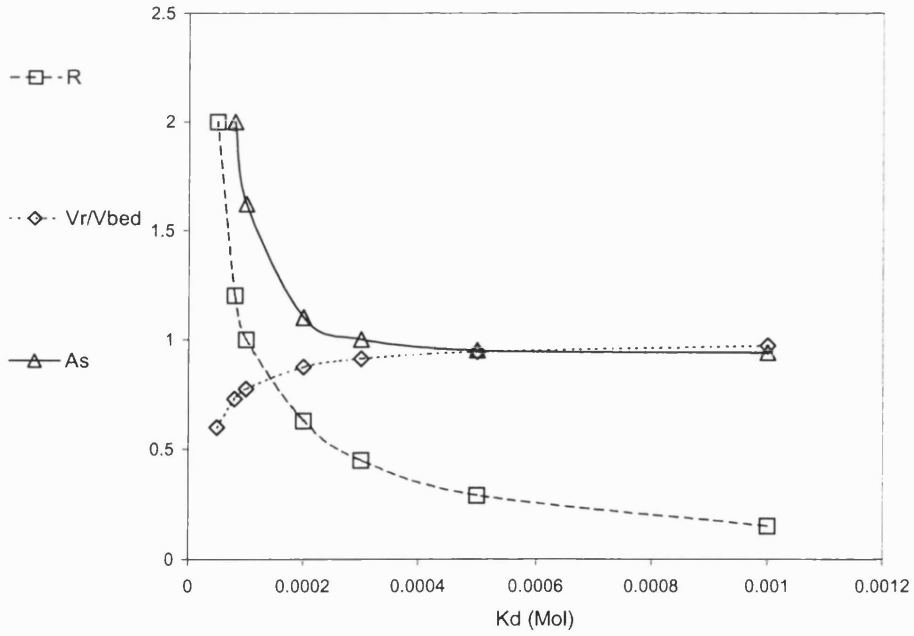

Figure 6.9: Resolution R, retention volume fraction V_r / V_{bed}, and Asymmetry factor A_s for A against A-P affinity changes. Points are calculated from the elution profiles relative to the simulations of Figure 6.8.

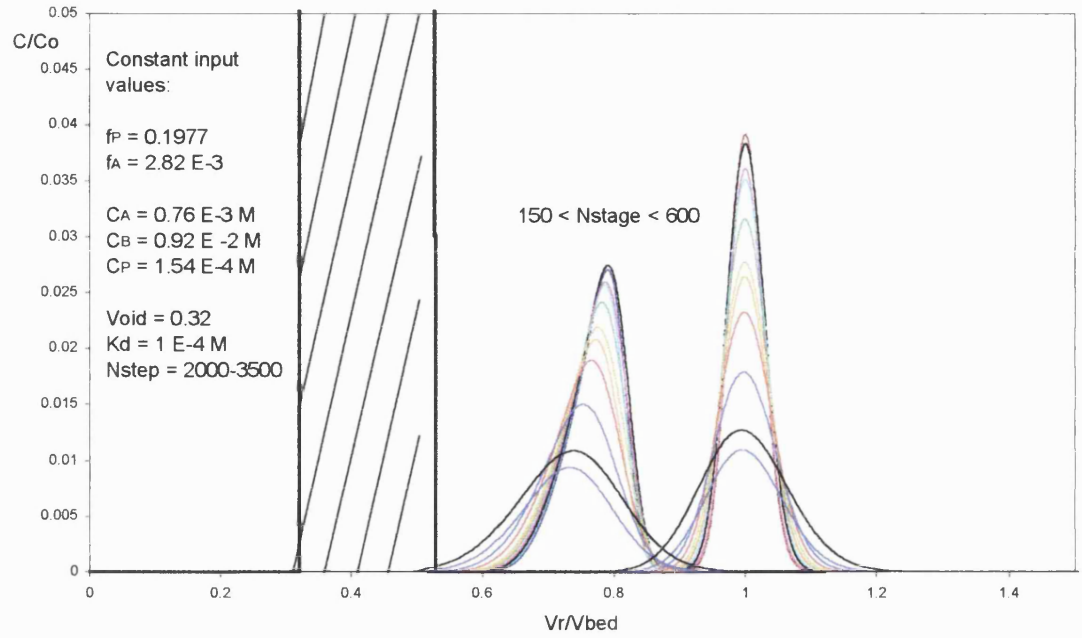

Figure 6.10: Effect of the number of equilibrium stages on the elution profiles of mixtures of impurities B and target component A. Macromolecule receptor P eluting within the shaded square pulse.

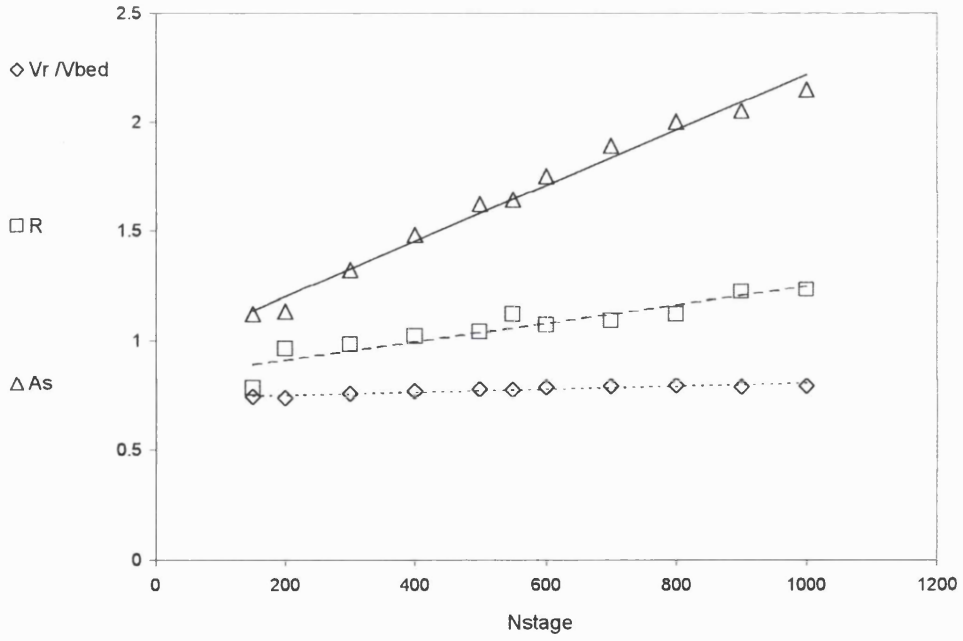

Figure 6.11: Effects of the number of equilibrium stages on retention volume V_r / V_{bed}, Asymmetry A_s and A-B resolution *R*.

6.7 Introduction to experimental LAPSEC investigation

Results with commercial immobilised lectins on agarose gel show that specific monosaccharides separation can be achieved using this system but both the possibility of scale up and the applicability to a real process stream containing target monosaccharides must be further investigated. Unfortunately costs, poor stability and short lifetime of these materials make further process scale up less attractive.

Lectin/monosaccharide weak affinity interactions and their difference in size represent an ideal target for a LAPSEC application. This combination of Affinity and Size Exclusion Chromatography for monosaccharide separations has been studied. This was preferred to further investigation of immobilised LTA system mainly because this new approach avoids lectin immobilisation, is easy and straightforward to perform and the model predictions were promising.

6.8 Materials

General reagents, sugars, p-nitrophenyl-α-D-mannopyranoside (pnpm), -α-D-glucopyranoside (pnpg), -α-L-arabinopyranoside (pnpa), -α-L-fucopyranoside (pnpf), Concanavalin A type IV highly purified and cellulose dialysis tubes (12 kDa cut off) have been commercially obtained from Sigma Ltd. (Poole, England). Polyethylene syringe filters 0.22 μm were obtained from Millipore (Watford U.K.)
Ultrapure water from an ELGA Purelab Option Unit (Bucks, U.K.) was used throughout.
Lotus Tetragonolobus lectin (LTA) purified, as described in Chapter IV, from winged beans (Thompson and Morgan, Ltd., Ipswich, UK) was used and dry size exclusion BioGel P-6 was purchased from BioRad (Hertfordshire, England).

6.9 Equipment

A schematic diagram of the chromatographic equipment operating in LAPSEC mode is outlined in Figure 6.12; injection loops for macromolecule (lectin) solution P, target

monosaccharides A and impurities B mixture are represented respectively with syringes (3) and (4) and are realised experimentally with two manual Rheodyne 7010 valves (Supelco, Poole U.K.). The detector (7) is a Gilson UV 116 (Anachem, Luton U.K.) or RID-10A Refractive Index from Shimadzu (Wolverton, U.K.), depending on the nature of the sugars to be detected. Chromatogram data are visualised and collected with VisiDAQ Acquisition Card (Captec Ltd. Hampshire, England) on a common PC and exported as excel files.

The back pressure regulator (8) is essential to prevent trapped bubbles in the detector cell and improve baseline stability (max 75 psi) especially with the Gilson 306 HPLC pump (2) working at extremely low flow rates (0.01-0.02 ml/min).

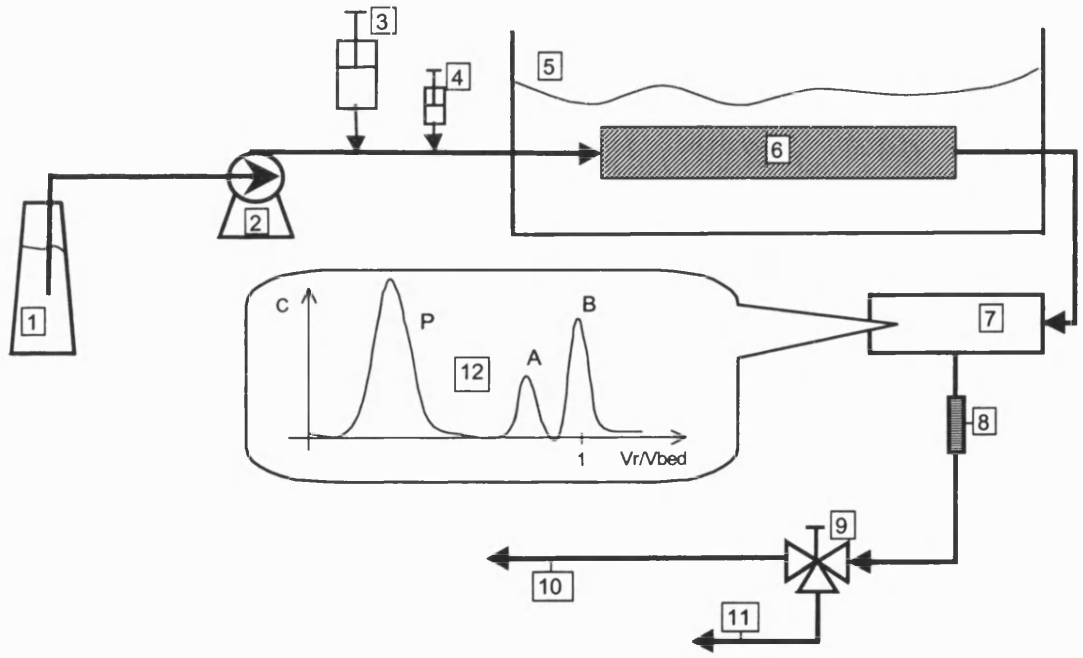

Figure 6.12: Schematic diagram of the LAPSEC equipment; (1): buffer reservoir, (2): delivery pump, (3): injection loop for protein solution, (4): injection loop for sugar mixture, (5): water bath, (6): chromatographic size exclusion column, (7): detector, (8): back pressure regulator, (9): valve, (10): recycle line, (11): product and waste line, (12): typical chromatogram.

6.10 ConA tests: Methods

The ConA sample is made by dissolving the lectin in Tris Buffer; after a few hours dialysis against the same buffer and filtration throughout 0.22 μm polyethylene syringe filters, the final concentration is adjusted to 5 mg/ml. Dry BioGel P-6 was hydrated and allowed to swell in the chromatographic buffer (75% v/v of buffer) at operating temperature for 3-4 hours. An analytical glass column 3 × 250 mm was slurry packed with the wet gel under vacuum. The system equilibrated at 20°C with 20 mM Tris Buffer pH 7.2-7.4, containing 0.5 mM $CaCl_2$, 0.5 mM $MgCl_2$, 0.5 mM $MnCl_2$, 150 mM NaCl, 0.02% Thimerosal as preservative and 5 mg/ml of Concanavalin A. The mobile phase is recycled at a flow rate of 0.02 ml/min and 5 μl injections of L-Ara and D-Man single or mixed together have been performed, the monosaccharides detected with a Shimadzu RID-10A and passed to waste.

A second set of three experiments was carried out with same column but lower flow rates, 0.01 ml/min. This time ConA was injected with a 100 μl loop containing 5 mg/ml rather than included in the mobile phase. 5 μl injections of pnpm (0.1 mM), pnpa (0.37 mM) or a mixture of both were performed. The absorbance of eluted material was recorded at 305 nm. The wavelength was chosen as before to exploit the higher absorbance of sugar derivatives rather than protein at this wavelenght.

6.11 ConA-D-Mannose low affinity pair: Results and Discussion

When ConA is immobilised on the chromatographic gel, separation of injected monosaccharides is based on their partition coefficient ($K_p>1$).
On the other hand in the LAPSEC system with ConA in the mobile excluded phase, separation is still based on K_p but this time $K_p<1$. Figure 6.13 (left) shows the results of single monosaccharide injections; since L-Arabinose is not a specifically bound by ConA, its elution was not affected by the lectin dissolved in the mobile phase and it was eluted after one bed volume (black peak).

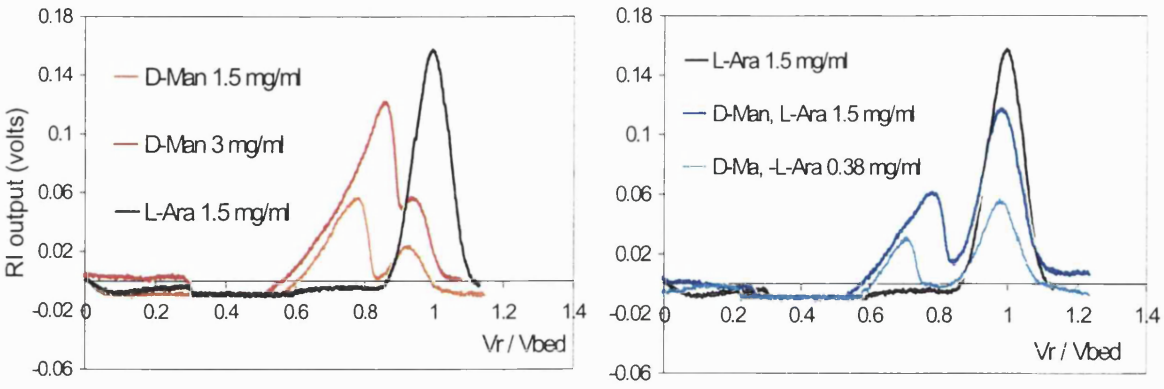

Figure 6.13: Performance of 3×250 mm BioGel P6 column with mobile phase containing ConA. Elution profile detected with Differential Refractor Index, 5 µl injection loop.

Figure 6.13 (left) shows the elution of D-Man at concentration of 3 and 1.5 mg/ml and the effectiveness of ConA in reducing the apparent sugar partition coefficient is evident. The second peak appearing in these chromatograms could be explained in terms of impurities present in the sugar solution, or depending on the unfavourable ratio of maximum binding capacity to sample applied, part of the D-Man sample could be left behind (not predicted by the model). The two chromatograms in Figure 6.13 (right) represent a mixture of D-Man and L-Ara both at 1.5 and 0.375 mg/ml.

Obviously having lectin receptor free in the mobile phase works as well as the immobilised lectin; although the specific target sugar is eluted contaminated with the protein while with the standard affinity chromatography mode is eluted pure. The possibility of achieving the same results using a small finite volume of ConA injected and eluted alone was proved with the model simulations and tested. Results are shown in Figure 6.14. A total number of approximately 20 nmoles of ConA monomer are injected with 0.5 nmoles of pnpm, 1.85 nmoles of pnpa respectively both together and separately. The separation of pnpm is evident when compared with the control experiments also shown in Figure 6.14. For that achieved separation, dialysis and filtration of the lectin sample is crucial to remove impurities which otherwise would have contaminated the products.

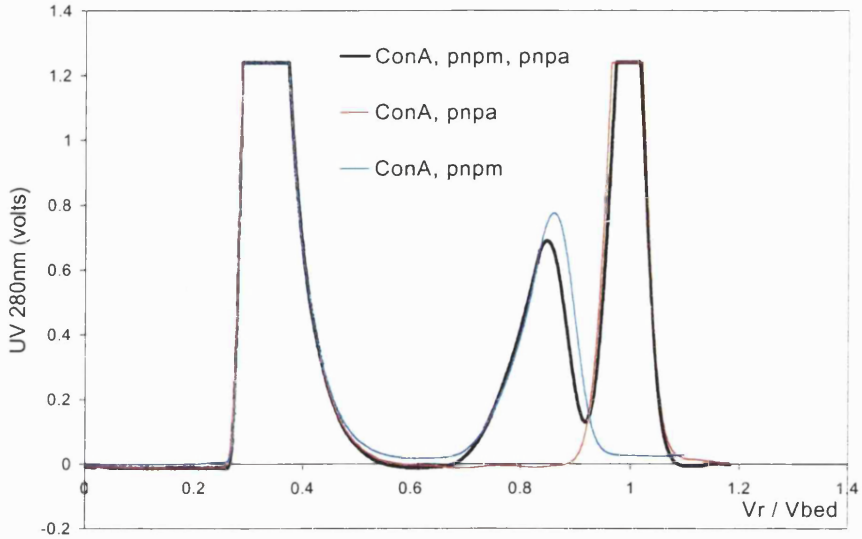

Figure 6.14: Three chromatograms relative to 100 µl of ConA (5 mg/ml) samples injected with: 5 µl solutions containing 0.1 mM pnpm (blue line), 0.37 mM pnpa (red line) and the two of them together (black line).

6.12 LTA tests: Methods

LTA was purified by affinity chromatography of winged beans extract, as in details reported in Chapter IV and used in LAPSEC mode with the same equipment and column used for ConA tests (at 5°C). Injections loops of 150 and 350 µl for LTA solutions (1 mg/ml, concentration determined by SPR and UV measurements) were used for respectively two sets of three experiments each. The Lotus lectin solution was injected at the same time as 5 µl solution containing 0.2 mg/ml, 0.04 mg/ml and 0.008 mg/ml of pnpf and pnpg. The mobile phase (0.02 ml/min) comprised of phosphate buffer pH 7.2-7.4 (50 mM) containing 150 mM NaCl and 0.02 % sodium azide as preservative. The chromatograms are obtained with on line UV detector (305 nm) increasing sensitivity for more diluted sugar samples, data acquired and stored on PC with VisiDaq acquisition data card. A final test was run, using 4 mg/ml of LTA injected with 350 µl injection loop and 0.2 mg/ml of pnpf and 2.8 mg/ml of pnpg injected with 5 µl loop.

6.13 LTA-L-Fucose low affinity pair: Results and Discussion

As demonstrated with ConA, a small finite pulse of Lectin can realise the separation of its specific ligand from a mixture of monosaccharides in a BioGel P6 column. Figures 6.15, 6.16 and 6.17 show the same approach when the target monosaccharide is L-fucose and the carrier-receptor is the Lotus lectin, purified from winged beans. The effect of injected volume of LTA on the elution of a mixture of pnpf and pnpg is highlighted when compared with the sugar control injection (blue line). Increasing the lectin injection loop from 150 to 350 µl made the separation feasible. As expected for this low capacity system the lower the injected ligand-impurities concentration the better their resolution. In fact in Figures 6.16 and 6.17, better resolution is achieved when sugars samples were diluted 5 and 25 times.

The last set of chromatograms in Figure 6.18 demonstrate how 350 µl of a 4 times more concentrated LTA sample can pull out the same amount of pnpf as the conditions used in Figure 6.15 although impurities (pnpg) were 10 times more concentrated.

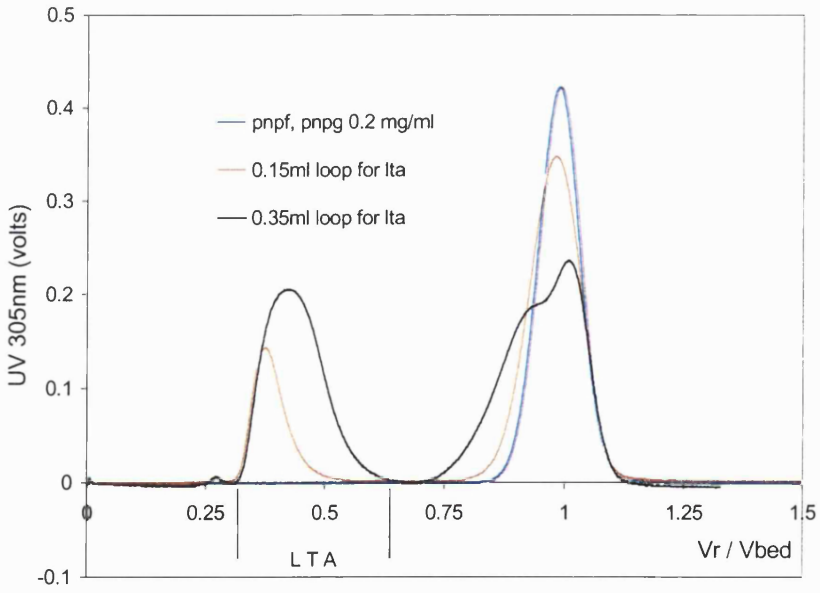

Figure 6.15: LTA (1 mg/ml) volume effect on the elution of 5 µl sugar mixture, containing pnpf and pnpg, injected alone (blue), with 0.15 ml (red) and 0.35 ml (black) of LTA containing solution.

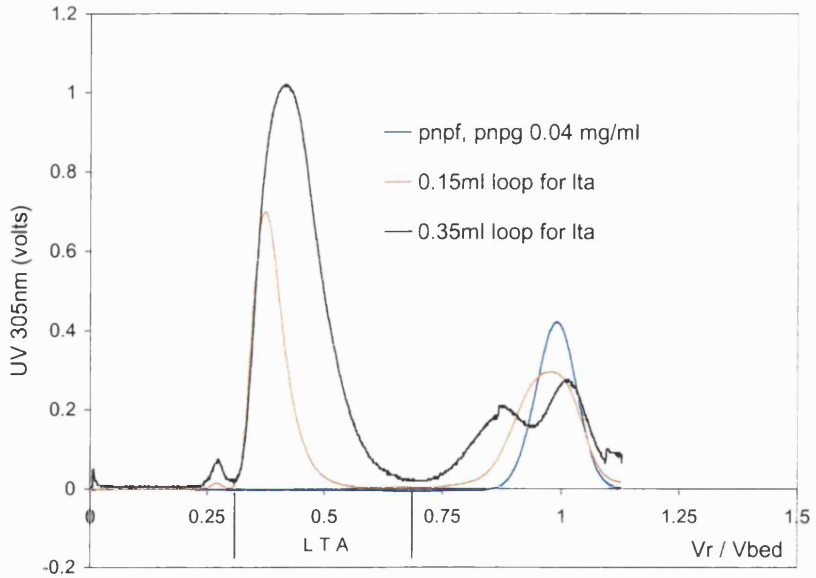

Figure 6.16: LTA (1 mg/ml) volume effect on the 5 times diluted 5 µl sugar mixture, containing pnpf and pnpg, injected alone (blue), with 0.15 ml (red) and 0.35 ml (black) of LTA containing solution.

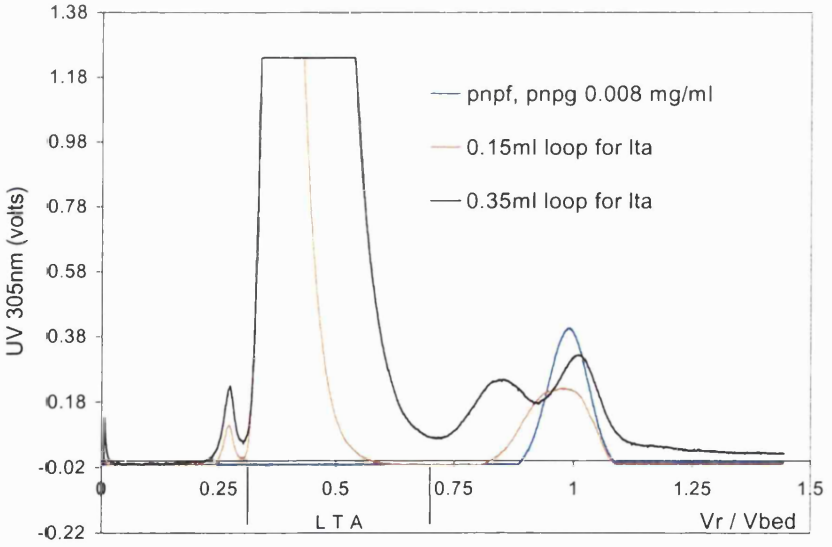

Figure 6.17: LTA (1 mg/ml) volume effect on the 25 times diluted 5 µl sugar mixture, containing pnpf and pnpg, injected alone (blue), with 0.15 ml (red) and 0.35 ml (black) of LTA containing solution.

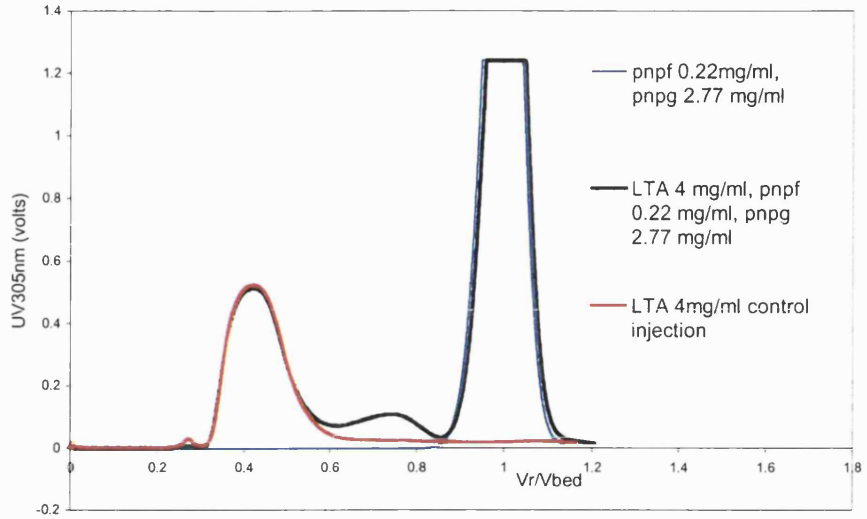

Fig. 6.18: Sugar control injection (blue chromatogram), LTA control injection (red chromatogram) and the two injections performed together (black chromatogram). On the x-axis the retention volume is normalised on the total bed volume which include column and extra-column contribution.

6.14 Comparisons with the model predictions

In the design of those experimental conditions described in ConA and LTA LAPSEC systems, the multi-sectional model proved to be very useful. During model simulation, constant input values such as the Number of Theoretical Stages (*Nstage* = 250 ± 30) and Voidage (ε= 0.33 ± 0.02) were found experimentally for the 3 × 250 mm BioRad P6 column injecting sugar and protein alone. Another constant input value was the injection volume for the sugars which was always kept at 5 µl, while depending on the application, lectin injection volume varied from 100, 150, 350 µl to total bed volume when dissolved in the buffer. In the ConA simulation with monosaccharides the dissociation constant (K_d = 6×10^{-4} M) found during D-Man isothermal titration experiment (Chapter III) was used while in the tests with sugar derivatives the value (K_d = 3.5×10^{-5} M) found during FC experiment (Chapter III) with pnpm was adopted. Experimental results and model prediction in terms of retention volume fraction and resolution are summarised in Table 6.1.

Table 6.1: Retention Volume fraction and Resolution obtained experimentally and using the multisectional model for Con A in LAPSEC applications. P is the lectin, A the specific monosaccharide, B the impurities

C_P (mg/ml)	C_B (mM)	C_A (mM)	V_A/V_{bed}	V_A/V_{bed} (MODEL)	R	R (MODEL)
5, in buffer	-	16.6	0.868	0.895	0.46	0.43
5, in buffer	-	8.3	0.784	0.875	0.9	0.52
5, in buffer	8	8	0.780	0.875	0.8	0.52
5, in buffer	2	2	0.720	0.855	1.3	0.61
5 in 100 µl	0.37	0.1	0.839	0.724	0.85	0.9

Table 6.2 shows values obtained for LAPSEC tests and simulation when 350 µl of LTA was injected. In this case the model input value for the dissociation constant (K_d=1.5× 10^{-4} M) was assumed as the average value obtained between ITC and FC tests (Chapter IV).

Table 6.2: Retention Volume fraction and Resolution obtained experimentally and using the multisectional model for LTA in LAPSEC applications. P is the lectin, A the specific monosaccharide, B the impurities

C_P (mg/ml)	C_B (mM)	C_A (mM)	V_A/V_{bed}	V_A/V_{bed} (MODEL)	R	R (MODEL)
1, in 350 µl	0.772	0.772	0.930	0.931	0.191	0.346
1, in 350 µl	0.154	0.154	0.863	0.909	0.557	0.465
1, in 350 µl	0.031	0.031	0.846	0.903	0.704	0.500
4, in 350 µl	9.2	0.772	0.757	0.703	0.930	1.3

Although mass transfer and kinetics limitation are neglected as well as other bands broading factors such as extra-column effects, the simple multisectional model gave a useful picture of the separation achievable with a LAPSEC approach and it could provide an important starting point for further scale up investigations.

6.15 LAPSEC tests with less pure LTA on a larger scale

Lotus lectin activity in the crude extract can potentially be used in L-fucose separation in LAPSEC mode if just partially purified and adequately concentrated. This approach would eliminate the greatest effort in LTA affinity purification and could be exploited collecting the higher SPR response fractions eluted from a size exlusion column overloaded with winged beans crude extract and injecting them into the BioRad P6 column with the monosaccharides mixture.

6.15.1 Materials and Method

Materials and suppliers have been listed previously. The system used was a BioRad semi-automated FPLC; a schematic layout is shown Figure 6.19.

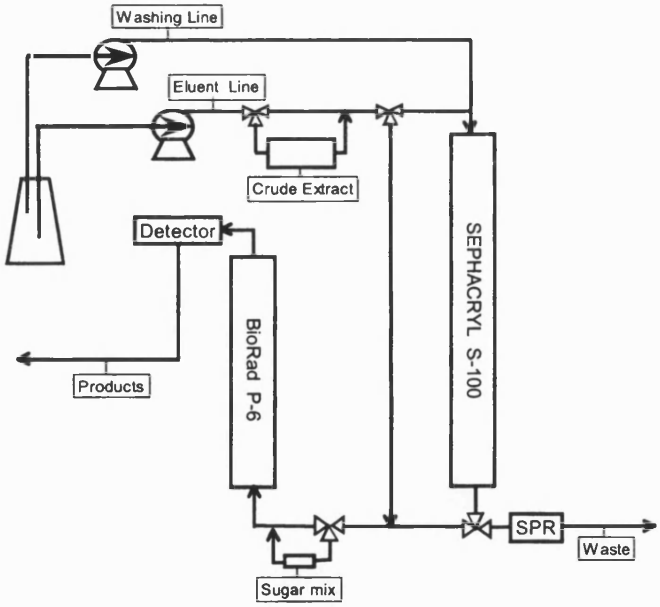

Fig. 6.19: Schematic layout for the FPLC system adopted in LAPSEC L-Fucose separation using partially purified LTA.

Concentrated and filtered crude extract (14 ml) was injected into the first column 26 × 600 mm packed with Sephacryl S-100 kept at room temperature, 10 ml elution fractions collected, diluted and analysed with SPR equipped with a papf activated CM5 micro chip The highest activity fractions were also assayed at 5 °C with 12.2 mM L-fucose titrant solution in the ITC. The chromatographic eluent was 50 mM Phosphate buffer pH 7.2-7.4 containing 150 mM NaCl, 0.02 % NaN_3 and flowing at 0.8 ml/min. Two higher activity fractions were identified and in a second run automatically injected with 150 µl, containing 0.35 mM pnpf and 0.33 mM pnpg, into a second column; 26 × 270 mm packed with BioRad P-6 gel and thermostated at 5°C. When the two LTA rich fractions eluted completely, the first column was by-passed and washed from the remaining impurities with a second pump.

6.15.2 Results and Discussion

The overloaded Sephacryl S-100 column eluted material showed significant spread of LTA, however the highest activity was found in the 12^{th} and 13^{th} fraction. Total concentration of Lotus lectin in those fractions was determined with a calibrated SPR assay and by Isothermal Titration Calorimetry, exploiting a double data fitting procedure as described previously and assuming one to one binding between LTA monomer (MW=17 kDa) and L-fucose. Final active concentration results were in reasonable agreement, an example is reported in Figure 6.20, where 12^{th} and 13^{th} fractions together resulted containing 0.6 mg/ml from SPR analysis and 0.7 mg/ml from isothermal titration. Even with highly concentrated crude extract the final concentration of LTA in 12^{th} and 13^{th} fractions did not go over 1 mg/ml this value and K_d result from titration calorimetry were used as inputs in the multisectional LAPSEC model. Injection loops were then designed so that the final injection fraction was close to the one used during small scale studies, but 3 times smaller for the sugar mixture. The BioRad P-6 column efficiency appeared to be maintained from small to larger scale (N = 200-300) column as measured with single sugar injections. Unfortunately with such a design the model predicted appreciable separation (R=0.6) only with LTA concentrations over 2 mg/ml. In fact experimental results did not show sign of separation and are not reported. Moreover the two fraction containing LTA showed also too

large amount of smaller molecular weight impurities, contaminating the elution of the monosaccharides mixture with a number of obvious process limitation.

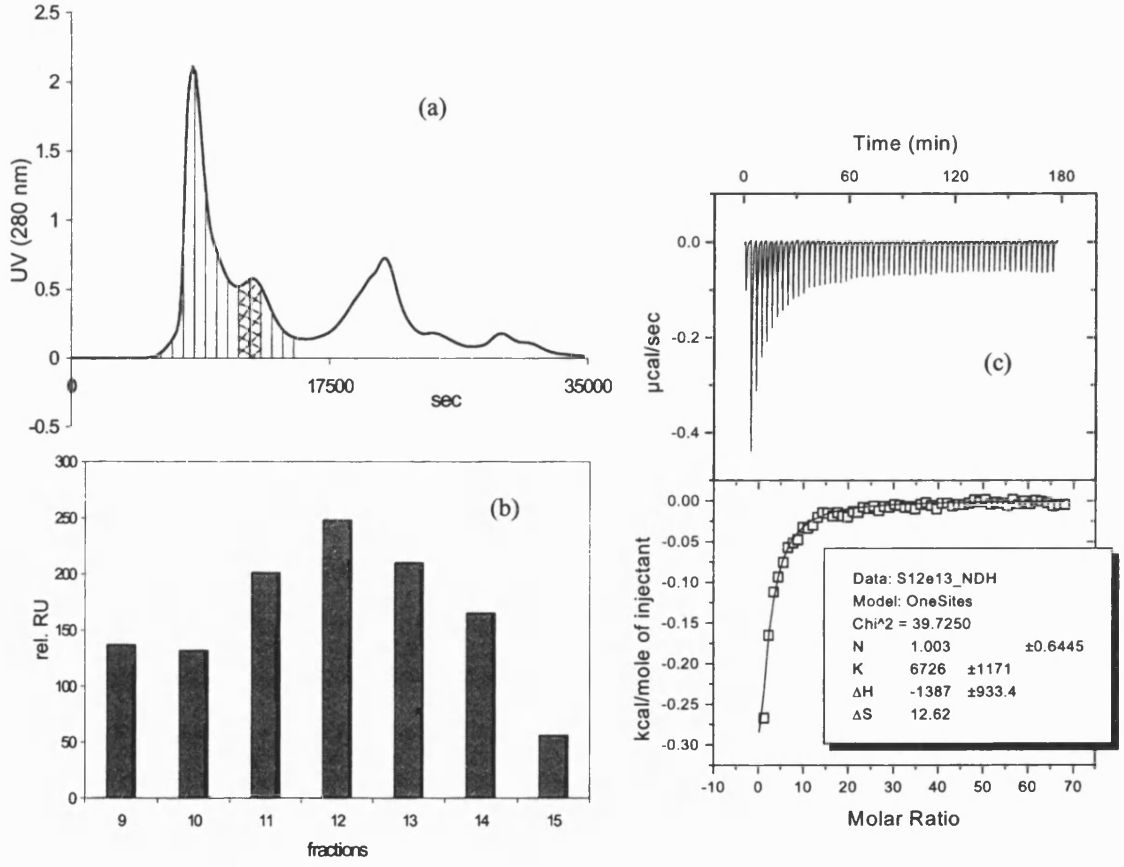

Fig. 6.20: (a): elution profile of 14 ml of crude extract from Sephacryl S-100 column, collected fractions are indicated, the 12th and 13th fractions area is shaded. (b): SPR relative response of pooled fractions. (c): fraction 12 and 13 titrated with L-Fucose with thermodynamic results.

However the system could be improved by pre-fractionating the crude extract with ultrafiltration modules and optimising the size exclusion column or testing other partial purification chromatographic techniques which could fit the process on line, e.g.: ion exchange chromatography. This could be the subject of further investigation.

Chapter VII

Conclusion and Future work

7.1 Lectins: a powerful tool in bio-refining

The exploitation of lectin specificity to a particular sugar structure in chromatographic separation of monosaccharides was demonstrated to be effective on a laboratory scale, using model solutions containing the target solute. The goal of this work is to show the possibility of using this technique, applied to a specific high value low volume carbohydrate. The novelty consists in the WAC application to monosaccharides that has not been investigated before and in introducing a new chromatographic approach LAPSEC as a combination of two well established techniques, Affinity and Size Exclusion Chromatography. These processes based on lectins can be considered in bio-refining of industrial side streams, containing the sugar target mixed with other similar molecules, when high selectivity is required.

7.2 The applications

The experimental work conducted at the beginning on Concanavalin A has been extremely useful to identify the main features and constraints involved in lectin based WAC and LAPSEC separation of monosaccharides. This led to the real project objective, L-fucose separation, with a better understanding of system performance. The most suitable L-fucose binding lectin was identified (LTA) and purified using AC, characterised using a number of techniques such as chromatography, ITC and SPR. Compared to ConA, LTA is smaller and more selective for L-fucose; this increased the potential chances of the lectin being successfully employed.

In fact LTA was an effective tool in realising highly targeted L-fucose separation, either immobilised onto an affinity media (WAC) or as a carrier for the specific sugar in LAPSEC mode. The main limitation of these applications was the low capacity, although ConA as well as LTA showed unsuspected higher capacity in their relative monosaccharide moiety binding.

7.3 The process productivity

A conclusive quantification of the potentials of these techniques can be made in terms of Productivity *P*, defined in Chapter II with equation (2.32). Within the range of experimental application tested, achieved productivity during WAC and LAPSEC, are summarised with the following graphs in Figures 7.1 and 7.2, reporting the amount of fucose separable with the two approaches in function of the injected concentration. Immobilised LTA gives higher productivity (Figure 7.1), when the latter is calculated on the base of one chromatographic cycle time, since LAPSEC is a much slower process. However over a column life time estimated to be 3 months for LTA-agarose column and one year for the BioRad P-6 gel column, LAPSEC can achieve higher productivity (around 260 g with 100 litre column) than WAC (160g with 100 litre column) as shown on the left hand side of Figure 7.2. On the other hand the separable range of injected concentration tested is higher in WAC and the achieved Productivity is obviously larger (up to 570 g) as in Figure 7.2 (right).

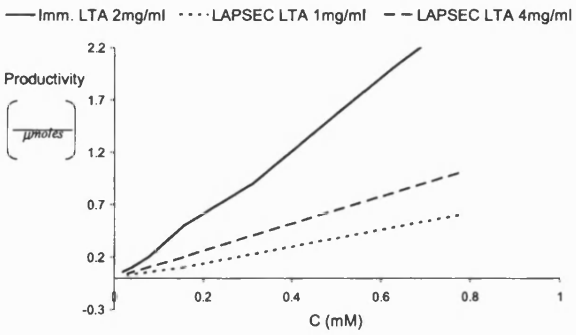

Figure 7.1: Trends in Productivity for the two systems; Immobilised LTA and LAPSEC.

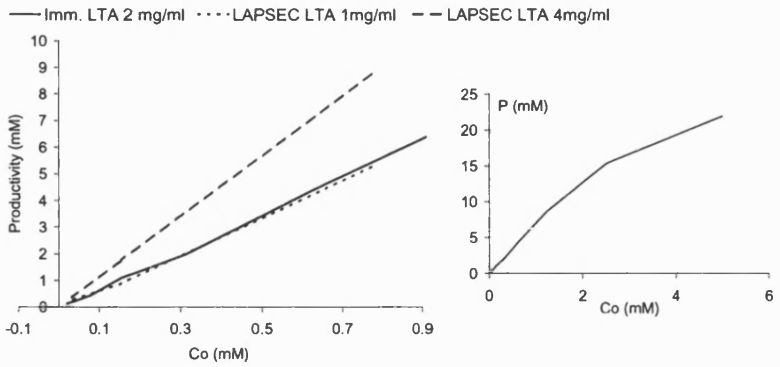

Figure 7.2: Left: Trends in Productivity for the two systems; immobilised LTA and LAPSEC. Right: Trends in Productivity for immobilised LTA over the full range of possible injected mixture concentration.

7.4 Future work

Regarding WAC, future investigation should focus on the development of an inexpensive immobilised lectin affinity media, chemically and mechanically more stable, with high degree of porosity and with the highest active lectin density possibly achievable. Simple mathematical model for WAC have been presented in literature and their feasibility should be investigated with this and further experimental data.

LAPSEC is at a very early stage of study, therefore several parameters should be further investigated. First of all, to increase throughput, higher flow rates could be tested within the limit of bed compressibility, as well as new size exclusion stationary phase. Porous glass could be used. Different combinations between concentration and injection loop should be examined. In particular the real potential of this method has to be identified yet, this means that for a given system, lectin concentration should increase to the limit of aggregation and injection loops adapted to obtain the best separation and purity among the components involved.

In both approaches costs could be drastically reduced if the lectin required is cloned and produced in culture rather than purified from natural plant sources.

7.5 Conclusions

- Lectins can be used as a tool in Chromatography for sugar separation; in particular exploiting the weak but specific interaction with monosaccharides.

- The process is based on a balance of dynamic equilibrium and mass transfers phenomena with which the target is separated from the rest of impurities under isocratic conditions.

- Once that the target is identified a possible specific and highly selective binding lectin can be purified from a natural source.

- Novel technologies such as ITC and SPR are extremely useful in the purification and characterisation process.

- Despite the unfavourable MW ratio between the sugar target and lectin receptor, the latter, in both immobilised and soluble form, has shown large molar capacity for monosaccharide. In fact, due to possibly cooperative, secondary non specific or specific interactions, relatively high binding capacities in mol terms have been measured.

- It is difficult to identify exactly the mechanism of weak interactions since in this range other side effects are energetically significant and influence the overall results, although this does not affect the specificity.

- Langmuir and Adair equilibrium isotherms and the equilibrium plate approach to model column chromatographic applications have shown to be simple and provide reasonable approximations.

- LTA can be used for L-fucose purification;

    - ➢ either immobilised onto a stationary phase following the classic elution chromatography approach.

- or free in solution as a carrier throughout a size exclusion column operating in desalting mode.

- Both the two approaches have low productivity and low throughput, particularly the second one.

- For the first approach, the use of LTA for the commercial purification of L-fucose will depend primarily on the development of a high capacity column of immobilised lectin.
  - Issues like costs, stability and lifetime of those commercial materials make scale-up investigation difficult.
  - When relying on analytical results alone, possible larger scale applications must be based on very high added-value products.

- The LAPSEC approach can be a valid alternative for L-fucose purification despite the lower throughput, as it yields higher productivity than AC within the same injected sugar concentration range.
  - LAPSEC is easy to perform on small and large scale.
  - In direct comparison with a standard LAC approach, LAPSEC represents a more economical solution for the separation process of small molecules i.e. monosaccharides, using lectins.
  - LAPSEC can be well simulated with a column multi-sectional equilibrium model, which could provide the basis of preparative or semi-preparative separation protocols.

- Further studies are required.
  - The effectiveness of lectin AC and LAPSEC with real complex feed streams has to be proved. These approaches should be included at the latest stage possible along the bio-refining process.
  - AC scale up could be investigated with larger batch chromatographic column operating in plug or radial flow.

- The requirements of large amount of lectins could be satisfied cloning the suitable lectin for microbiological production, cutting down the process major cost.
- LAPSEC can be further optimised in terms of column lengths, packing materials, injection volumes and concentrations.
- The use of fractionated and concentrated crude extracts directly in L-fucose separation remains a low cost possibility and should be investigated further.

REFERENCES

Adair, G. S. (1925). The haemoglobin system. VI. The Oxygen dissociation curve of Hemoglobin. *Journal of Biological Chemistry*, **63**, pp. 529-545.

Agrawal, B. B. L. and Goldstein I. J. (1968). Protein-Carbohydrate Interaction. VII. Physical and Chemical Studies on Concanavalin A, the Hemagglutinin of the Jack Bean. *Archives of Biochemistry and Biophysics*, **124**, pp. 218-229.

Allen, H. J., Johnson E. A. Z. and Matta, K. L. (1977). Comparison of the binding specificities of Lectins from Ulex europaeus and Lotus Tetragolobus. *Immunological Communications*, **6**, (6), pp. 585-602.

Allen, H. J. and Johnson E. A. Z. (1977). A simple procedure for the isolation of L-Fucose-binding lectins from Ulex europaeus and Lotus tetragonolobus. *Carbohydrate Research*, **58**, pp. 253-265.

Anderson, D. J., Anhalt J. S. and Walters R. R. (1986). High-performance affinity chromatography of divalent Concanavalin A on matrices of variable ligand density. *Journal of Chromatography*, **359**, pp. 369-382.

Anderson, D. J. and Walters R. R. (1986). Equilibrium and rate constant of immobilised Concanavalin A determined by high-performance affinity chromatography. *Journal of Chromatography*, **376**, pp. 69-85.

Andrews, P., Kitchen B. J. and Winzor D. J. (1973). Use of affinity chromatography for the quantitative study of acceptor-ligand interactions: The lactose syntheses system. *The Biochemical Journal*, **135**, (4), pp. 897-900.

Arnold, F. H., Blanch, H. W., and Wilke, C. R. (1985a). Analysis of affinity separations I: Predicting the performance of affinity adsorbers. *Chemical Engineering Journal*, **30**, pp. B9-B23.

Arnold, F. H., Blanch, H. W. and Wilke, C. R., (1985b). Analysis of affinity separations II: The characterisation of affinity columns by pulse technique. *Chemical Engineering Journal*, **30**, pp. B25-B36.

Arnold, F. H., Schofield S. A. and Blanch H. W. (1986). Analytical affinity chromatography. I. Local equilibrium theory and the measurement of association and inhibition constants. *Journal of Chromatography*, **355**, pp. 1-12.

Arnold, F. H. and Blanch H. W. (1986). Analytical affinity chromatography. II. Rate theory and the measurement of biological binding kinetics. *Journal of Chromatography*, **355**, pp. 13-27.

Avre, B. H. and Liapis A. I. (1988). Biospecific Adsorption in Fixed and Periodic Countercurrent Beds. *Biotechnology and Bioengineering*, **32**, pp. 616-627.

Belter, P. A., Cussler E. L. and Hu W. S. (1988). *Bioseparation. Downstream processing for Biotechnology.* Chichester: John Wiley & Sons.

Bernasconi, C. F. (1976). *Relaxation Kinetics*. New York: Academic Press.

Bracewell, D. G., Brown R. A., Gill A. and Hoare M. (2001). Monitoring and control of bioproducts from conception to production in real-time using an optical biosensor. *Chemical Engineering and Technology*, **24**, (7), pp. 25-31.

Bradford, M. (1976). A rapid and sensitive method for the quantification of microgram quantities of protein utilizing the principle of protein-dye binding. *Analytical Biochemistry*, **72**, pp. 248-254.

Castillo, J. R., Cepria G., Demarcos S., Galban J., Mateo J. and Ruiz E. G. (1993). Surface-plasmon resonance sensor as detector in HPLC and specific Lactate determination. *Sensor and Actuators A-Physical*, **37**, (8), pp. 582-586.

Cepria, G. and Castillo J. R. (1997). Surface plasmon resonance-based detection. An alternative to refractive index detection in high-performance liquid chromatography. *Journal of Chromatography A*, **759**, pp. 27-35.

Chapman, V. J. and Chapman D. J. (1980). *Seaweeds and their uses*. London: Chapman and Hall.

Chase, H. A. (1984). Prediction of the performance of preparative affinity chromatography. *Journal of Chromatography*, **297**, pp. 179-202.

Christensen, L. L. H. (1997). Theoretical analysis of protein concentration determination using biosensor technology under conditions of partial mass transport limitation. *Analytical Biochemistry*, **249**, pp. 153-164.

Clegg, R. M., Loontiens F. G., Vanlandschoot A. and Jovin T. M. (1981). Binding-kinetics of methylalpha-D-Mannopyranoside to ConcanavalinA-temperature-jump relaxation study with 4-methylumbelliferyl alpha-D-Mannopyranoside as a florescence indicator ligand. *Biochemistry*, **20**, (16), pp. 4687-4692.

Connelly P. R. (1994). Acquisition and use of calorimetric data for prediction of the thermodynamics of ligand-binding and folding reaction of proteins. *Current Option in Biotechnology*, **5**, pp. 381-388.

Cornish-Bowden, A. (1979). *Fundamentals of Enzyme Kinetics*. London: Butterworths.

Coulson, J. M. and Richardson J. F. (1968). *Chemical Engineering. Vol. 2* Fourth edition, Oxford: Pergamon.

Cozzi, R., Protti P. and Ruaro T. (1987). Analisi chimica moderni metodi strumentali. Teoria-strumentazione. *ESU spa.*

Creighton, T. E. (1993). *Proteins Structure and Molecular Properties*. New York: W. H. Freeman and Company.

Cuatrecasas, P., Wilchek M. and Anfinsen C. B. (1968). Selective enzyme purification by affinity chromatography. *Proceedings of the National Academy of Sciences of the United States of America*, **61**, (2), pp. 636-643.

Dantigny, P., Wang Y, Hubble J. and Howell J. A. (1991). Optimisation of frontal chromatography by partial loading. *Journal of Chromatography*, **545**, pp. 27-42.

Dean, P. D. G., Johnson W. S. and Middle F. A. (1985). *Affinity chromatography: a practical approach.* Oxford: IRL Press.

Derewenda, Z., Yariv J., Helliwell J. L., Kalb A. J., Dodson E. J., Papiz M. Z., Wan T. and Campbell J. (1989). The structure of the saccharide-binding site of concanavalin A. *EMBO Journal*, **8**, (8), pp. 2189-2193.

Desai, P. R. and Springer G. F. (1972). Eel Serum Anti-Human Blood-Group H(O) Protein. *Methods in Enzymology*, **28**, pp. 383-388.

Disley, D. M., Morrill P. R., Sproule K. and Lowe C. R. (1999). An optical biosensor for monitoring recombinant proteins in process media. *Biosensors & Bioelectronics*, **14**, (5), pp. 481-493.

Elgavish, S. and Shaanan B. (1997). Lectin-carbohydrate interactions: different folds, common recognition principles. *TIBS*, pp. 462-467.

Flory, P. J. (1953). *Principles of Polymer Chemistry*. London: Cornell University Press.

Fornstedt, N. and Porath J. (1975). Characterisation studies on a New Lectin Found in Seeds of Vicia Ervilia. *FEBS Letters*, **57**, (2), pp. 187-191.

Freire, E., Obdulio L. M. and Straume M. (1990). Isothermal Titration Calorimetry. *Analytical Chemistry*, **62**, (18), pp. 950-959.

Freitag, R. (1999). Displacement chromatography for biopolymer separation. *Nature Biotechnology*, **17**, pp. 300-303.

Gemeiner, P., Polakovic M., Mislovicova D. and Stefuca V. (1998). Cellulose as a (bio) affinity carrier: properties, design and applications. *Journal of Chromatography B-biomedical Application*, **715**, pp. 245-271.

Gibbs R. V. (1992). *Recognition of N-Acetyl-α-D-Galactosamine by the seed lectin from Dolichos Biflorus.* Ph.D. Thesis, University of Portsmouth.

Giddings, J. C. (1965). *Dynamics of Chromatography-I- Principles and Theory.* London: Edward Arnold Ltd.

Green, R. J., Frazier R. A., Shakesheff K. M., Davies M. C., Roberts C. J. and Tendler S. J. B. (2000). Surface plasmon resonance analysis of dynamic biological interactions with biomaterials. *Biomaterials*, **21**, pp. 1823-1835.

Grubisic, Z., Rempp P. and Benoit H. (1967). A Universal Calibration for gel Permeation Chromatography. *Polymer Letters*, **5**, pp. 753-759.

Gupta, D., Dam T. K., Oscarson F. and Brewer C. F. (1997). Thermodynamics of Lectin-Carbohydrate Interactions. *Journal of Biological Chemistry*, **272**, (10), pp. 6388-6392.

Harris, E. L. V. and Angal S. (1989). *Protein Purification Method A practical approach.* New York: IRL-Press.

Heikkilä, H. (1983). Separating sugar and amino acids with chromatography. *Chemical Engineering*, **24**, pp. 50-52.

Herbert, N. R. (1991). Comparison between analytical and preparative liquid chromatography. **In:** *Preparative and Process-scale liquid chromatography*, (G. Subramanian, ed.), pp. 9-38. Chichester: Ellis Horwood.

Hill, A. V. (1910). The possible effect of the aggregation of the molecules of hemoglobin on its dissociation curves. *Journal Physiological Society (Proceedings)*, **40**, pp. iv-vii.

Holdgate G. A. (2001). Making Cool Drugs Hot: Isothermal Titration Calorimetry as a Tool to Study Binding Energetics. *BioTechniques*, **31**, pp. 164-184.

Homola, J., Yee S. S. and Gaublitz G. (1999). Surface plasmon resonance sensors: review. *Sensors and Actuators B*, **54**, pp. 3-15.

Hořejší V. and Kocourek J. (1978). Studies on Lectins. Properties of some lectins prepared by Affinity Chromatography on O-Glycosyl Polyacrylamide gels. *Biochimica et Biophysica Acta*, **539**, pp. 299-315.

Horvath, C. and Lin H. J. (1976). Movement and band spreading of unsorbed solutes in liquid chromatography. *Journal of Chromatography*, **126**, pp. 401-420.

Horvath, C. and Lin H. J. (1978). Band spreading in liquid chromatography. General plate hight equation and a method for the evaluation of the individual plate hight contributions. *Journal of Chromatography*, **149**, pp. 43-70.

Hubble, J. (2001). Competition and intrinsic displacement effects in overloaded weak affinity chromatography. *Separation Science and Technology*, **36**, (4), pp. 541-554.

Hummel, J. P. and Dreyer W. J. (1962). Measurement of protein-binding phenomena by gel-filtration. *Biochimica Biophysica Acta*, **63**, pp. 530-532.

Hupe K. P. and Hoffmann B. (1989). Optimum Condition in Preparative Liquid Chromatography. II. Selection of Column Dimensions. **In:** *Preparative-Scale Chromatography* (E. Grushka, ed.) **46**, pp. 77-88, New York: Marcel Dekker.

Janson, J. C. and Hedman P. (1982). Large-scale chromatography of proteins. **In:** *Advances in Biochemical Engineering* (A. Fiechter, ed.), **25**, pp. 43-99.

Jaulmes, A. and Vidal C. (1989). Theoretical aspects of quantitative affinity chromatography: an overview. **In:** *Advances in Chromatography* (J.C. Giddings, E. Grushka, J. Gazes, P.R. Brown, ed.) **28**, pp. 1-64, New York: Marcel Dekker.

Jelesarov I. and Bosshard H. R. (1999). Isothermal Titration Calorimetry and Differential Scanning Calorimetry as Complementary tools to investigate the energetics of Bimolecular Recognition. *Journal of Molecular Recognition,* **12**, pp. 3-18.

Johnson, M. L. and Faunt L. M. (1992). Parameter Estimation by Least-Squares Methods. *Methods in Enzymology*, **210**, pp. 1-37.

Johnsson, B, Lofas S. and Lindquist G. (1991). Immobilisation of Proteins to carboxymethyldextran-modified gold surface for biospecific interaction analysis in Surface-Plasmon Resonance sensors. *Analytical Biochemistry*, **198**, (2), pp. 268-277.

Jonsson, J. A. (1987). *Chromatographic theory and basic principles.* New York: Marcel Dekker.

Jungbauer, A. (1993). Preparative chromatography of Biomolecules. *Journal of Chromatography*, **639**, pp. 3-16.

Jungbauer, A. (2000). Workshop: Biochromatography, **In:** *The International Symposium on Preparative and Industrial Chromatography and Allied Techniques*, ETH Zurich, October 2000.

Kalb, A. J. (1968). The Separation of Three L-Fucose-binding proteins of Lotus Tetragonolobus. *Biochimica et Biophysica Acta,* **168**, pp. 532-536.

Kaltenbrunner, O., Jungbauer A. and Yamamoto S. (1997). Prediction of the preparative chromatography performance with a very small column. *Journal of Chromatography A*, **760**, pp. 41-53.

Karlsson, R., Fägerstam L., Nilshans H. and Persson B. (1993). Analysis of active antibody concentration. Separation of affinity and concentration parameters. *Journal of Immunological Methods*, **166**, pp. 75-84.

Kasai, K. I. and Oda Y. (1986). Frontal Affinity Chromatography: theory for its application to studies on specific interactions of biomolecules. *Journal of Chromatogrphy*, **376**, pp. 33-47.

Kelly, C. (1984). Physiochemical properties and N-terminal sequence of eel lectin. *Biochemical Journal*, **220**, pp. 221-226.

Kieda, C. and Monsigny M. (1986). Involvement of membrane sugar receptors and membrane glycoconjugates in the adhesion of 3 LL cell subpopulations to cultured pulmonary cells. *Invasion Metastasis*, **6**, pp. 347-366.

Knox, J. H. and Pyper H. M. (1986). Framework for maximising throughput in preparative liquid chromatography. *Journal of Chromatography*, **363**, pp. 1-30.

Kobata, A. and Endo T. (1992). Immobilized lectin columns: useful tools for the fractionation and structural analysis of oligosaccharides. *Journal of Chromatography*, **597**, pp. 111-122.

Kochibe, N. and Furukawa K. (1980). Purification and Properties of a Novel Fucose-Specific Hemagglutinin of Aleuria aurantia. *Biochemistry*, **19**, pp. 2841-2846.

Kochibe, N. and Furukawa K. (1982). Aleuria aurantia Hemagglutinin. *Methods in Enzymology,* **83**, pp. 373-377.

Konami, Y., Yamamoto K. and Osawa T.(1990). The primary structure of the Lotus tetragonolobus seed lectin. *FEBS letters,* **268**, (1), pp. 281-286.

Konami, Y., Yamamoto K. and Osawa T. (1991). The primary structure of two types of the Ulex europeus Seed Lectin. *Journal Biochemistry,* **109**, pp. 650-658.

Laemmli, U. K. (1970). Cleavage of Structural Proteins during the Assembly of the Head of Bacteriophage T4. *Nature*, **227**, pp. 680-685.

Lapidus, L. and Amundson N., R. (1952). Mathematics of Adsorption in beds. VI. The effect of longitudinal diffusion in ion exchange and chromatographic columns. *Journal of Physical Chemistry*, **56**, pp. 984-988.

Laurent, T. C. and Killander J. (1964). A theory of gel filtration and its experimental verification. *Journal of Chromatography,* **14**, pp. 317-330.

Leickt, L., Bergstrom M., Zopf D. and Ohlson S. (1997). Bioaffinity Chromatography in the 10 mM Range of K_d. *Analytical Biochemistry*, **253**, pp. 135-136.

Levy, P. F., Sanderson J. E., Kispert R. G. and Wise D. L. (1981). Biorefining of Biomass to liquid fuels and organic chemicals. *Enzyme and Microbial Technology*, **3**, (3), pp. 207-215.

Liener, I. E., Sharon N. and Goldstein I. J. (1986). *The Lectins. Properties, Functions, and Applications in Biology and Medicine*. London: Academic Press.

Lineweaver, H. and Burk D. (1934). The Determination of Enzyme Dissociation Constant. *Journal of American Chemical Society*, **56**, pp. 658-666.

Listinsky, J. J., Listinsky C. M., Alapati V. and Siegal G. P. (2001). Cell surface fucose ablation as a therapeutic strategy for malignant neoplasms. *Advances in Anatomic Pathology,* **8**, (6), pp. 330-337.

Lonnerdal, B., Borrebaeck C. A. K., Etzler M. E. and Ersson B. (1983). Dependence on cations for the binding activity of lectins as determined by affinity electrophoresis. *Biochemical and Biophysical Research and Communications*, **115**, (3), pp. 1069-1074.

Loris, M., Hamelryck T., Bouckaert J. and Wyns L. (1998). Legume lectin structure, *Biochimica Biophysica Acta*, **1383**, pp. 9-36.

Lowe, C. R. and Dean P. D. G. (1974). *Affinity Chromatography*, London: John Wiley & Sons.

Lowe, C. R., Yon Hin B. F., Cullen D. C., Evans S. E., Stephens L. D. G. and Maynard P. (1990). Biosensors. *Journal of Chromatography*, **510**, pp. 347-354.

Mammem, M., Choi S. K. and Whitesides G. M. (1998). Polyvalent interactions in Biological Systems: Implications for design and use of multivalent ligands and inhibitors. *Angewandte Chemie-International edition*, **37**, pp. 2754-2794.

Marquardt, D.W. (1963). An Algorithm for Least-Squares Estimation of NonLinear Parameters. *Journal Society Industrial Application Math*, **11**, (2), pp. 431-441.

Marquardt, T., Luhn K., Srikrishna G., Freeze H. H., Harms E. and Vestweber D. (1999). Correction of Leukocyte Adhesion Deficiency Type II With Oral Fucose. *Blood*, **94**, (12), pp. 3976-3985.

Martin, A. J. P. and Synge R. L. M. (1941). A new form of chromatogram employing two liquid phases. 1. A theory of Chromatography. 2. Application to the micro-determination of the higher monoamino-acid in proteins. *Biochemical Journal*, **35**, pp. 1358-1368.

Matthies, H., Schroeder H., Smalla K. H. and Krug M. (2000). Enhancement of glutamate release by L-fucose changes effects of glutamate receptor antagonists on long-term potentiation in the rat hippocampus. *Learning & Memory*, **7**, (4), pp. 227-234.

Merkle, R. K. and Cummings R. D. (1984). Lectin affinity chromatography of glycopeptides. *Methods in Enzymology*, **138**, pp. 232-259.

Michaelis, L. and Menten M. L. (1913). The kinetics of invertase activity. *Biochemische Zeitschrift*, **49**, pp. 333-369.

Mislovicova, D., Chudinova P. G. and Docolomansky P. (1995). Affinity chromatography of invertase on Concanavalin A-bead cellulose matrix: the case of an extraordinary strong binding glycoenzyme. *Journal of Chromatography*, **664**, pp. 145-153.

Muller, A. J. and Carr P. W. (1984). Chromatographic study of the thermodinamic and kinetic characteristics of silica-bound Concanavalin A. *Journal of Chromatography*, **284**, pp. 33-51.

Muller, A. J. and Carr P. W. (1986). Examination of the thermodynamic and kinetic characteristic of microparticulate affinity chromatography supports. Application to Concanavalin A. *Journal of Chromatography*, **357**, pp. 11-32.

Nichol, L. W., Ogston A. G., Winzor D. J. and Sawyer W. H. (1974). Evaluation of Equilibrium Constants by Affinity Chromatography. *Biochemical Journal*, **143**, pp. 435-443.

O'Carra, P., Barry S. and Griffin T. (1973). Spacer-Arms in Affinity Chromatography: the Need for a More Rigorous Approach. *Biochemical Society Transactions*, **1**, pp. 289-290.

Oda, Y., Kasai K. and Ishii S. (1981). Studies on the Specific Interaction of Concanavalin A and Saccharides by Affinity Chromatography. Application of Quantitative Affinity Chromatography to a Multivalent System. *Journal Biochemistry*, **89**, pp. 285-296.

Ohlson, S., Bergstrom M., Leickt L. and Zopf D. (1998). Weak affinity chromatography of small saccharides with immobilised wheat germ agglutinin its application to monitoring of carbohydrate transferase activity. *Bioseparation*, **7**, pp. 101-105.

Ohlson, S., Lundblad A. and Zopf D. (1988). Novel Approach to Affinity Chromatography Using "Weak" Monoclonal Antibodies. *Analytical Biochemistry*, **169**, pp. 204-208.

Ohyama, Y., Kasai K., Nomoto H. and Inoue Y. (1985). Frontal affinity chromatography of Ovalbumin Glycoasparagines on a Concanavalin A-Sepharose Column. A quantitative study of the binding specificity of the lectin. *Journal Biological Chemistry*, **260**, (11), pp. 6882-6887.

Osawa, T. and Matsumoto I. (1972). Gorse (Ulex europeus) Phytohemagglutinins. *Methods in Enzymology*, **28**, pp. 323-327.

Pazur, J. H., Scrano R. E. and Perloff M. D. (1996). Comparision of the properties of Concanavali A and anti-α-D-Glucose antibodies. *Journal of Protein Chemistry*, **15**, (4), pp. 329-335.

Pereira, M. E. A. and Kabat E. A. (1974). Discussion Paper: Blood Group Specificity of the Lectin from Lotus Tetragolobus. *Annals New York Academy of Sciences*, pp. 301-305.

Pereira, M.E.A., Kisailus E. C., Gruezo F. and Kabat E. A. (1978). Immonuchemical Studies on the Combinig Sites of the Blood Group H-Specific Lectin 1 from Ulex europaeus seeds. *Archives of Biochemistry And Biophysics*, **185**, (1), pp. 108-115.

Rathi, R. C., Kopeckova P. and Kopecek J. (1997). Biorecognition of sugar containing N-(2-hydroxypropyl)methacrylamide copolymers by immobilised lectin. *Mcromolecular Chemistry and Physics*, **198**, (4), pp. 1165-1180.

Rich, R. L. and Myszka D. G., (2000). Advances in surface plasmon resonance biosensor analysis. *Current Opinion in Biotechnology*, **11**, pp. 54-61.

Richalet-Secordel, P. M., Rauffer-Bruyere N., Christensen L. L. H., Ofenloch-Haehnle B., Seidel C. and Van Regenmortel M. H. V. (1997). Concentration Measurement of Unpurified Proteins Using Biosensor Technology under Conditions of Partial Mass Transport Limitation. *Analytical Biochemistry*, **249**, pp. 165-173.

Robinson, P. J., Wheatley M. A., Janson J. C., Dunnil P. and Lilly M. D. (1974). Pilot Scale Affinity Chromatography of β-Galactosidase. *Biotechnology and Bioengineering,* **16,** pp. 1103-1112.

Ross, P. D. and Subramanian S. (1981). Thermodynamics of Protein Association Reactions: Forces Contributing to Stability. *Biochemistry,* **20,** pp. 3096-3102.

Ruthven, D. M. (1984). *Principles of Adsorption and Adsorption Processes,* New York: John Wiley & Son.

Sampaio, A. H., Rogers D. J. and Barwell C. J. (1998). Isolation and Characterisation of the Lectin from the Green Marine Alga Ulva lactuca L. *Botanica Marina,* **41,** pp. 427-433.

Sarbajna, S., Das S. K. and Roy N. (1995). A novel synthesis of L-Fucose from D-Galactose. *Carbohydrate Research,* **270,** pp. 93-96.

Saxena, V., Weil A. E., Kawahata R. T. and McGregor W. C., Chandler M. (1988). Applications of Radial flow columns for fast affinity chromatography. *International Laboratory,* Jan/Feb., pp. 50-57.

Scatchard, G. (1949). The Attraction of Proteins for Small Molecules and Ions. *Annals of New York Academy of Science,* **51,** pp. 660-672.

Schmid, A. and Flodin P. (1992). Porosity determination of Poly[(trimethylolpropane trimethacrylate)-co-(methyl methacrylate)] gels. *Makromolekulare Chemie-Macromolecular Chemistry and Physics,* **193,** pp. 1579-1589.

Schmid, A., Kulin L. I. and Flodin P. (1991). Porosity determination of Poly(trimethylolpropane trimethacrylate) gels. *Makromolekulare Chemie-Macromolecular Chemistry and Physic,* **192,** pp. 1223-1234.

Scopes, R. K. (1994). *Protein Purification Principles and Practice.* New York: Springer-Verlag Inc.

Sharon, N. and Lis H. (1990). Legume lectins – a large family of homologous proteins. *FASEB Journal,* **4,** pp. 3198-3208.

Sharon, N. and Lis H. (1998). 110 years of lectin research. *Charbohydrate in Europe,* **23,** pp. 12-17.

Sheehan, D. (2000). *Physical Biochemistry: Principles and Applications.* Chichester: John Wiley and Sons, Ltd.

Sigurskjold, B. W., Altman E. and Bundle D. R. (1991). Sensitive titration microcalorimetric study of the binding of Salmonella O-antigenic oligosaccharides by a monoclonal antibody. *European Journal of Biochemistry.* **197,** pp. 239-246.

Singh, R. S., Tiwary A. K. and Kennedy J. F. (1999). Lectins: Sources, Activities, and Applications. *Critical Reviews in Biotechnology,* **19,** (2), pp. 145-178.

Srinivas, V. R., Reddy G. B. and Surolia A. (1999). A predominant hydrophobic recognition of H-antigenic sugars by winged bean acidic lectin: a thermodynamic study. *FEBS Letters* **450,** pp. 181-185.

Stenberg, E., Persson B., Roos H. and Urbaniczky C. (1991). Quantitative determination of Surface concentration of Proteins with Surface-Plasmon-Resonance using Radiolabeled Proteins. *Journal of Colloidal and Interface Science,* **143** (2), pp. 513-526.

Strandh, M., Ohlin M., Borrebaeck C. A. K. and Ohlson S. (1998). New approach to steroid separation based on low affinity IgM antibody. *Journal of Immunological Methods,* **214,** pp. 73-79.

Swaminathan C. P., Surolia N. and Surolia A. (1998). Role of Water in the Specific Binding of Mannose and Mannoligosaccharides to Concanavalin A. *Journal of American Chemical Society,* **120,** pp. 5153-5159.

Takemura, M., Lijima B., Tateno Y. and Kataura K. (1988). *Production of L-Fucose.* Jp. Pat. 63027496 A.

Thomas, C. J. and Surolia A. (2000). Mode of molecular recognition of L-Fucose by Fucose-binding legume lectins. *Biochemical and Biophysical Research Communication*, **268**, pp. 262-267.

Thomas, H. G. (1944). Heterogeneous ion exchange in a flowing system. *Journal of the American Chemical Society*. **66**, pp. 1664-1666.

Thompson, K. C. (2000). Pharmaceutical applications of calorimetric measurements in the new millennium. *Thermochimica Acta*, **355**, pp. 83-87.

Tien, C. (1994). *Adsorption Calculation and modelling*. London: Butterworth-Heinemann.

Treybal, R. E. (1968). *Mass-Transfer Operation*. London: McGraw-Hill.

Van Damme, J., P., Peumans W. J., Pusztai A. and Bardocz S. (1998). *Handbook of plant lectins: Properties and Biomedical Applications*. Chichester: Wiley.

van Deemter, J. J., Zuiderweg F. J. and Klinkenberg A. (1956). Longitudinal diffusion and resistance to mass transfer as causes of non-ideality in chromatography. *Chemical Engineering Science* **5**, pp. 271-289.

Vanhooren, P. T. and Vandamme E. J. (1999). L-Fucose: occurrence, physiological role, chemical, enzymatic and microbial synthesis. *Journal of Chemical Technology and Biotechnology*, **74**, pp. 479-497.

Van Thorre, D. (2002). Sweet Beet Incorporated. *Process for obtaining stereoisomers from biomass*. U.S. Pat. 6,365,732.

Vermeulen, T., LeVan M. D., Hiester N. K. and Klein G. (1973). Adsorption and Ion Exchange. **In:** *Perry's Chemical Engineers' Handbook 6th edition* (R. H. Perry, ed.), Section 16, pp. 1-46. New York: McGraw-Hill.

Wang, J. L. and Edelman G. M. (1978). Binding and functional properties of Concanavalin A and its derivatives. *Journal of Biological Chemistry*, **253**, (9), pp. 3000-3007.

Wankat, P. C. (1974). Theory of Affinity Chromatography Separations. *Analytical Chemistry*, **46**, (11), pp. 1400-1408.

Wankat, P. C. (1986). *Large Scale Adsorption and Chromatography Volume 1 and 2*. Boca Raton: CRC Press, Inc.

Wikstrom, M. and Ohlson S. (1992). Computer simulation of weak affinity chromatography. *Journal of Chromatography*, **597**, pp. 83-92.

Wilchek, M. and Miron T. (1999). Thirty years of affinity chromatography. *Reactive & Functional Polymers*, **41**, pp. 263-268.

Williams, B. A., Chervenak M. C. and Toone E. J. (1992). Energetics of Lectin-Carbohydrate Binding. *Journal of Biological Chemistry*, **267**, (32), pp. 22907-22911.

Williams, A., Taylor K., Dambuleff K., Persson O. and Kennedy R. M. (2002). Maintenance of column performance at scale. *Journal of Chromatography A*, **944**, pp. 69-75.

Wiseman, T., Williston S., Brandts J. F. and Lin L. N. (1989). Rapid measurement of Binding Constants and Heats of Binding Using a New Titration Calorimeter. *Analytical Biochemistry*, **179**, pp. 131-137.

Wong, C., Alajarin R., Moris-Varas F., Blanco O. and Garcia-Junceda E. (1995) Enzymatic synthesis of L-Fucose and analogs. *Journal of Organic Chemistry*, **60**, pp. 7360-7363.

Yamamoto, S. (1988). *Ion Exchange Chromatography of Protein*, New York: Marcel Dekker.

Yamamoto, S. and Sano Y. (1992). Short-cut method for predicting the productivity of affinity chromatography. *Journal of Chromatography*, **597**, pp. 173-179.

Yamashita, K., Kochibe N., Ohkura T., Ueda I. and Kobata A. (1985). Fractionatiuon of L-Fucose-containing Oligosaccharides on Immobilised Aleuria aurantia Lectin. **260**, (8), pp. 4688-4693.

Yan, L., Wilkins P. P., Alvarez-Manilla G., Do Su-II. I., Smith D. F. and Cummings R. D. (1997). Immobilised Lotus tetragonolobus agglutinin binds oligosaccharides containing the Le(x) determinant. *Glycoconjugate Journal* **14**, (1), pp. 45-55.

Yang, C. M. and Tsao G. T. (1982a). Packed-Bed Adsorption Theories and Their Applications to Affinity Chromatography. **In:** *Advances in Biochemical Engineering* (A. Fiechter, ed.), **25**, pp. 1-18.

Yang, C. M. and Tsao G. T. (1982b). Affinity Chromatography. **In:** *Advances in Biochemical Engineering*, (A. Fiechter, ed.), **25**, pp. 19-41.

Yariv, J., Klab A. J. and Blumberg S. (1972). Lotus tetragonolobus L-Fucose-Binding Proteins, *Methods in Enzymology*, **28**, pp. 356-360.

Yariv, J., Klab A. J. and Katchalski E. (1967). Isolation of an L-Fucose Binding Protein from Lotus tetragonolobus Seed. *Nature*, **215**, (19), pp. 890-891.

Yarmush, M. L. and Colton C. K. (1985). Affinity Chromatography. **In:** *Comprehensive Biotechnology*, (Moo-Young Murray, ed.), **2**, pp. 507-519. Oxford: Pergamon.

Zeder-Lutz, G., Benito A. and Van Regenmortel M. A. V. (1999). Active concentration measurements of recombinant biomolecules using biosensor technology. *Journal of Molecular Recognition*, **12**, (5), pp. 300-309.

Zieler, K. (1989). Misuse of non linear Scatchard plots. *TIBS*, **14**, pp. 314-317.

Zopf, D. and Ohlson S. (1990). Weak-affinity chromatography, *Nature*, **346**, pp. 87-90.

Appendix A

'Sectional model of an affinity column
'Equilibrium Langmuir

```
DEFDBL a-z
FUNCTION PBMAIN()
CLS
DIM c(2,500),q(2,500)
co=0.0000259      'Feed concentration
qm=0.00078        'Maximum resin capacity
nstage=30         'Number of equilibrium sections
cvol=10           'Column length
kd=3.68e-5        'Association constants
void=.32          'Column voidage
PRINT "Filename?"
LINE INPUT filename$
OPEN filename$ FOR OUTPUT AS #1
alpha=(1-void)
ht=cvol/nstage
FOR i=1 TO nstage
q(1,i)=0
c(1,i)=0
NEXT i
c(1,0)=co
j=0
WHILE c(1,nstage)/co <=.999
FOR i=1 TO nstage
ctot=void*c(1,i-1)+alpha*(q(1,i)+c(1,i))
c(2,i)=1/2*ctot-1/2*kd-1/2*alpha*qm+1/2*SQR(ctot^2+2*ctot*kd-
2*ctot*alpha*qm+kd^2+2*kd*alpha*qm+alpha^2*qm^2)
q(2,i)=(ctot-c(2,i))/alpha
NEXT i
FOR k=1 TO nstage
c(1,k)=c(2,k)
q(1,k)=q(2,k)
NEXT k
PRINT #1, j*ht*void/cvol,c(2,nstage)/co
PRINT  j*ht*void/cvol,c(2,nstage)/co
j=j+1
WEND
qsum=0
FOR k=1 TO nstage
qsum=qsum+q(1,k)
NEXT k
qsum=qsum/nstage
PRINT "c","q"
PRINT co,qsum
CLOSE #1
END FUNCTION
```

'Sectional model of an affinity column
'equilibrium assumption and 2 sites Adair binding equation

```
DEFDBL a-z
FUNCTION PBMAIN()
CLS
DIM c(2,500),q(2,500)
co=0.0000259      'Feed concentration
```

```
qm=7.8e-4        'Maximum resin capacity
nstage=30        'Numer of sections
cvol=10          'Column length
fr=2.359e-2      'Flow rate
k1=23435     'Association constants
k2=33038
'Products of association constants
a=k1
b=a*k2
void=.32         'Column voidage
PRINT "Filename?"
LINE INPUT filename$
OPEN filename$ FOR OUTPUT AS #1
alpha=(1-void)
ht=cvol/nstage
FOR i=1 TO nstage
q(1,i)=0
c(1,i)=0
NEXT i
c(1,0)=co
j=0
WHILE c(1,nstage)/co <=.999
FOR i=1 TO nstage
ctot=void*c(1,i-1)+alpha*(q(1,i)+c(1,i))
IF ctot>1e-5*co THEN 'if nothing in stage bypass calculation
CALL bisect(ctot,alpha,qm,a,b,c,d,cl) 'use bisection algorithm to find cl
ELSE
cl=0
END IF
c(2,i)=cl
q(2,i)=(ctot-cl)/alpha
NEXT i
FOR k=1 TO nstage
c(1,k)=c(2,k)
q(1,k)=q(2,k)
NEXT k
PRINT #1, ht*j*void/cvol,c(2,nstage)/co
PRINT  j*ht*void/cvol,c(2,nstage)/co
j=j+1
WEND
qsum=0
FOR k=1 TO nstage
qsum=qsum+q(1,k)
NEXT k
qsum=qsum/nstage
PRINT "c","q"
PRINT co,qsum
CLOSE #1
END FUNCTION
'Bisection root finding routine
SUB bisect(ctot,alpha,qm,a,b,c,d,cx)
x1 = ctot        'Set maximum possible value of c = ctot
x2 = 0           'Set minimum possible value of c = 0
CALL func(x2,ctot,alpha,qm,a,b,c,d,fmid)
CALL func(x1,ctot,alpha,qm,a,b,c,d,f)
IF f * fmid >= 0 THEN
PRINT "Root not bracketed"
END IF
IF f < 0 THEN   'Orients search
```

```
cx = x1
dx = x2 - x1
ELSE
cx = x2
dx = x1 - x2
END IF
'Bisection loop
acc = .0001 * (x1 + x2) / 2
FOR ii = 1 TO 50
dx = .5 * dx
xmid = cx + dx
CALL func(xmid,ctot,alpha,qm,a,b,c,d,xr)
IF xr <= 0 THEN
cx = xmid
END IF
IF ABS(dx) < acc THEN GOTO 200
NEXT ii
PRINT "too many bisections"
200    END SUB
SUB func (ci,ctot,alpha,qm,a,b,c,d,x)
'adair equation
y=(a*ci+b*ci^2)/(1+2*a*ci+b*ci^2)
'fn(ci) to equal zero
x=(ctot-alpha*qm*y)-ci
END SUB
```

Low Affinity Pair Chromatography Model (LAPSEC)
Partition coefficient for sugars = 1
Partition coefficient for proteins = 0

```
DEFDBL a-z
FUNCTION PBMAIN()
CLS
DIM ca(2, 5000), qa(2, 5000),cb(2, 5000), qb(2, 5000),cp(2,5000)
DIM qp(2,5000),ao(5000),bo(5000),po(5000)
'Initial conditions
'Feed concentration for a & b
PRINT "Feed concentration of a?"
LINE INPUT cao$
cao = VAL(cao$)
PRINT "Feed concentration of b?"
LINE INPUT cbo$
cbo = VAL(cbo$)
PRINT "Feed concentration of p?"
LINE INPUT cpo$
cpo = VAL(cpo$)
'Number of stages
PRINT "Number of plates"
LINE INPUT nstage$
Nstage = VAL(nstage$)
'Dissociation constant for each component
PRINT "Kd for a"
LINE INPUT kd$
Kd = VAL(kd$)
'Column voidage
PRINT "Voidage"
LINE INPUT void$
void = VAL(void$)
'Loading fraction
```

```
PRINT "Loading fraction for a"
LINE INPUT f$
fa = VAL(f$)
PRINT "Loading fraction for p"
LINE INPUT fp$
fp = VAL(fp$)
'Number of loading steps
ls = INT(fa*nstage/void)
lsp = INT(fp*nstage/void)
'Number of steps simulated
PRINT "Number of steps"
LINE INPUT nstep$
Nstep = VAL(nstep$)
print"ls & lsp",ls,lsp
print"nstep",nstep"
'Alpha
a = (1 - void)
'Set initial stage concentrations to zero for both components
FOR i = 1 TO nstage
qa(1, i) = 0
ca(1, i) = 0
qb(1, i) = 0
cb(1, i) = 0
cp(1, i) = 0
qp(1, i) = 0
NEXT i
'Set feed concentration to first stage for loading steps
ca(1, 0) = cao
cb(1, 0) = cbo
cp(1, 0) = cpo
'Column routine
zz=TIMER
FOR l=1 TO nstep
'Once loading steps exceeded set feed to first stage to zero
IF l>ls THEN
ca(1, 0) = 0
cb(1, 0) = 0
cp(1, 0) = cpo
END IF
IF l>lsp THEN
cp(1,0)=0
END IF
'Step through the column
FOR i = 1 TO nstage
'Compute the total concentration in each stage
'i.e. liquid conc from previous stage + adsorbed from current stage
ctota = void*(ca(1, i - 1) + qa(1, i-1))+a*ca(1,i)
ctotb = void*cb(1, i - 1) + a * cb(1, i)
ctotp = void*cp(1, i - 1)
'Solution routine for revised liquid phase concentrations
CALL eqn(ctota,ctotp,kd,qa)
'Revised stage concentrations
cb(2, i) = ctotb
ca(2, i) = ctota-qa
qa(2, i) = qa/void
cp(2,i)= ctotp/void
NEXT i
'Update stage concentrations prior to next step
FOR k = 1 TO nstage
```

```
ca(1, k) = ca(2, k)
qa(1, k) = qa(2, k)
cb(1, k) = cb(2, k)
cp(1,k)=cp(2,k)
NEXT k
'Set column effluent equal to liquid phase conc in last stage
ao(l)=ca(1,nstage)/cao
bo(l)=cb(1,nstage)/cbo
po(l)=cp(1,nstage)/cpo
NEXT l
PRINT "time s", TIMER-zz
'Data output
PRINT "Filename?"
LINE INPUT filename$
OPEN filename$ FOR OUTPUT AS #3
'count number of steps containg a
astep=0
'determine conc of b in a steps
bcont=0
amax=0
bmax=0
lmax=0
lbmax=0
lwa1=0
lwa2=0
lwb1=0
lwb2=0
wa1=0
wa2=0
wb1=0
wb2=0
FOR l=1 TO nstep
print#3,l*void/nstage,ABS(ao(l)),ABS(bo(l)),ABS(po(l))
asum=asum+ao(l)
bsum=bsum+bo(l)
psum=psum+po(l)
IF ao(l)>0.001 THEN
astep=astep+1
IF bo(l) >0.001 THEN
bcont=bcont+bo(l)
END IF
END IF
IF ao(l)>amax THEN
amax=ao(l)
lmax=l
END IF
IF bo(l)>bmax THEN
bmax=bo(l)
lbmax=l
END IF
NEXT l
FOR l=1 TO lmax
IF (ABS(ao(l)-amax/1000))<=0.001 THEN
lwa1=l
wa1=ao(l)
END IF
NEXT l
FOR l=1 TO lbmax
IF (ABS(bo(l)-bmax/1000))<=0.001 THEN
```

```
lwb1=l
wb1=ao(l)
END IF
NEXT l
FOR l=lmax TO nstep
IF(ABS(ao(l)-amax/1000))<=0.001 THEN
lwa2=l
wa2=ao(l)
GOTO 1111
END IF
NEXT l
1111 FOR l=lbmax TO nstep
IF(ABS(bo(l)-bmax/1000))<=0.001 THEN
lwb2=l
wb2=ao(l)
GOTO 1112
END IF
NEXT l
1112  CLOSE #3
PRINT "a loaded",cao*ls*void,"a eluted",asum*cao*void
PRINT "b loaded",cbo*ls*void,"b eluted",bsum*cbo*void
PRINT "p loaded",cpo*lsp*void,"p eluted",psum*cpo*void
PRINT ""
PRINT "Dilution factor",astep/ls,"Purity",asum*100/(asum+bcont)
PRINT ""
'retention for a
FVra=lmax*void/nstage
PRINT "Fract.Vra=", FVra, "Camax/Cao", amax
wa=(lwa2-lwa1)*void/nstage
'peak wight for A
PRINT "Wa=", wa
FVrb=lbmax*void/nstage
PRINT ""
'retention for B
PRINT "Fract.Vrb=", FVrb, "Cbmax/Cbo", bmax
'peak widht for B
wb=(lwb2-lwb1)*void/nstage
PRINT "Wb=", wb
PRINT ""
'resolution
PRINT "R=", 2*(FVrb-FVra)/(wb+wa)
'asimmetry
PRINT "As=", (lwa1-lmax)/(lmax-lwa2)
END  FUNCTION
SUB eqn(ctota,ctotp,kd,qa)
qa = (kd+ctota+ctotp-SQR(kd^2+2*ctota*kd+2*kd*ctotp+ctota^2-2*ctota*ctotp+ctotp^2))/2
END SUB
```

Appendix B

UV Calibration

UV calibration is done using BSA and ConA standards and absorbance measurement at 280 nm and 595 nm with Bradford assay. Absobance is compared in scanning wavelength mode for 10 μM pnpg (continuous line) and 1 mg/ml Con A (dotted line) solution.

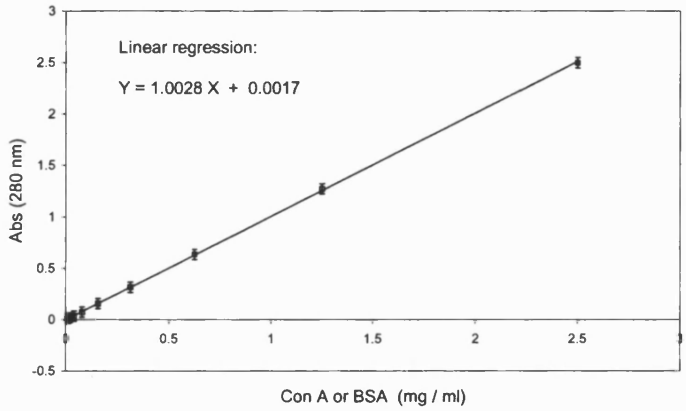

Figure B.1: UV calibration for ConA and BSA standards

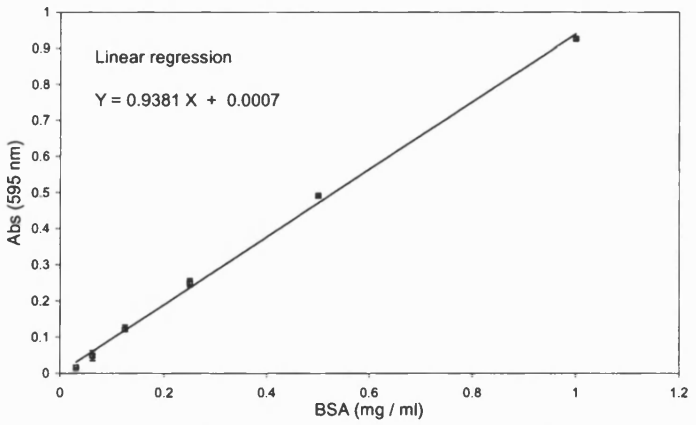

Figure B.2: UV calibration with BSA standards using Bradford Method

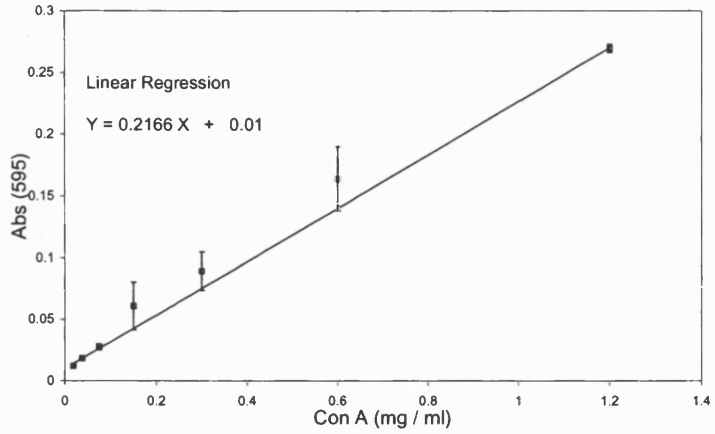

Figure B.3: UV calibration with ConA standards using Bradford Method, the three points with large errors are excluded during linear regression.

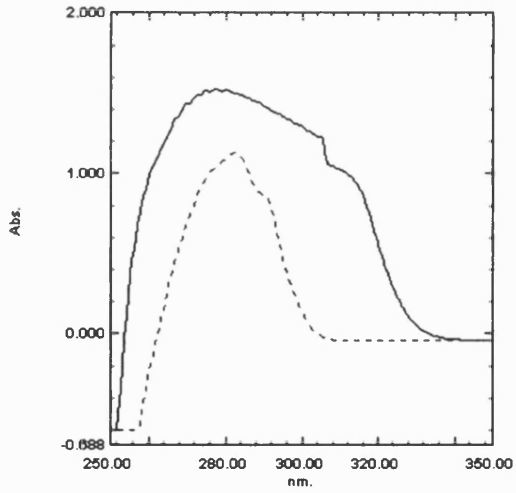

Figure B.4: Absorbance profile in wavelength scanning mode for 10 μM pnpg (continuous line) and 1 mg/ml Con A (dotted line).

SDS-Gel Electrophoresis Calibrations

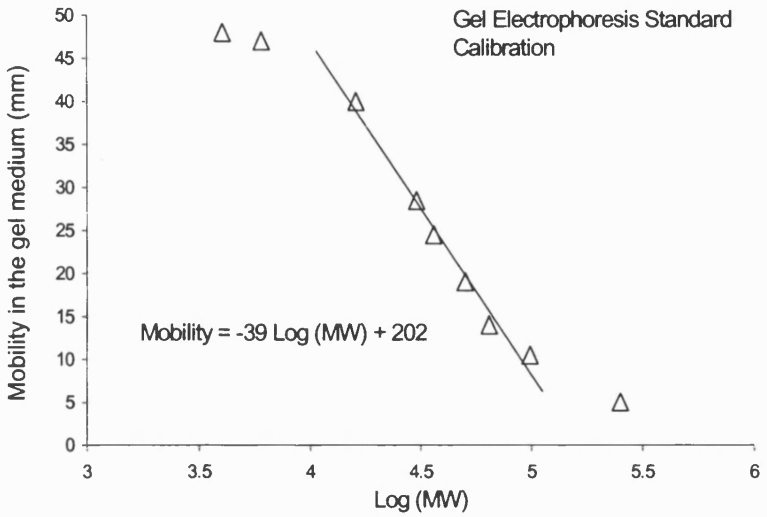

Mobility (mm)	Log (MW)	MW
5	5.39794	250000
10.5	4.991226	98000
14	4.80618	64000
19	4.69897	50000
24.5	4.556303	36000
28.5	4.477121	30000
40	4.20412	16000
47	3.778151	6000
48	3.60206	4000

	ConA	LTA
Mobility =	29.5	31
MW(Da)=	26489.69	24244.62

Figure B.5: Calibration data, linear regression and results relative to the SDS-Tris Glycine gel of Figure 4.13 (b). The first two points and the last one were not considered for the linear fit.

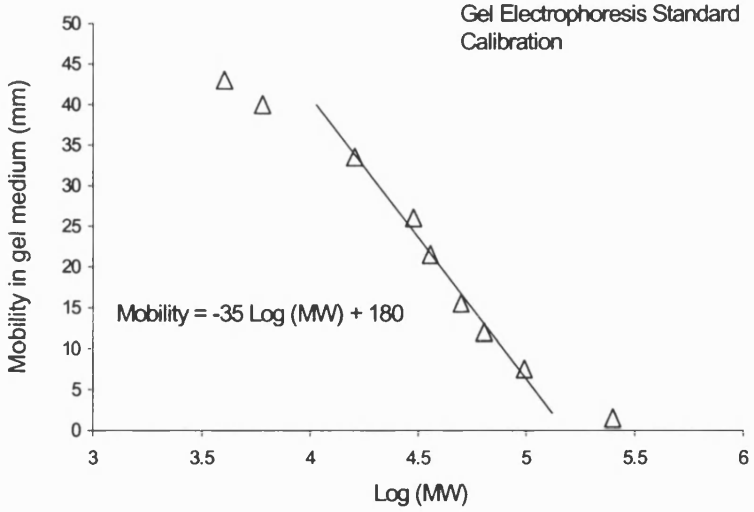

Mobility (mm)	Log (MW)	MW
1.5	5.39794	250000
7.5	4.991226	98000
12	4.80618	64000
15.5	4.69897	50000
21.5	4.556303	36000
26	4.477121	30000
33.5	4.20412	16000
40	3.778151	6000
43	3.60206	4000

	ConA	LTA
Mobility =	25	27.5
MW(Da)=	26826.96	22758.46

Figure B.6: Calibration data, linear regression and results relative to the SDS-Tris Glycine gel of Figure 4.13 (a). The first two points and the last one were not considered for the linear fit.

An average value for the lectins monomers MW, obtained from the two gels are respectively 26660 Da for ConA and 23500 Da for LTA.

Adsorption equilibrium data and calculation

Breakthrough curves, during FC loading of solution at concentration C_o, are stored as C_i, concentration in the outlet, in function of time of elution.

The breakthrough curve is integrated to obtain the breakthrough retention volume (V_r) as described with equation 2.22. Practically with the excel file containing the succession of C_i/C_o values in function of time, V_r is numerically obtained as follows,

$$V_r = F_r \cdot \left[n \cdot a - a \cdot \frac{\sum_{j=1}^{n} C_i}{C_o} \right] \qquad \text{(B.1)}$$

where F_r is the flow rate, n the number of sample readings, a the time interval between samples.

Table B.1: Experimental ionic adsorption equlibrium data of ConA on a DEAE-cellulose (GDG resin).

C(mg/ml)	0.04	0.11	0.13	0.18	0.21	0.27	0.32	0.38	0.48	0.58	0.65	0.68	0.76
q(mg/ml)	2.91	4.67	8.6	11.1	14.5	16.7	19.1	20.8	22.9	23.8	25.3	25.8	27.1

Table B2: FC results and calculation for pnpm adsorption onto ConA Sepharose 4B affinity media

Co [M]	Vr [ml]	q (M)	q / Co		
1.66E-03	1.062534761	0.000743012	4.48E-01		
0.00083	1.28401508	0.000754147	9.09E-01		
0.000415	1.702305331	0.000738404	1.78E+00	Kd =	3.65E-05 M
0.0002075	2.401187212	0.000671059	3.23E+00	Vbed =	0.7065 ml
0.00010375	3.646389127	0.000604439	5.83E+00	qmax =	7.83E-04 M
5.1875E-05	5.092974957	0.00045842	8.84E+00	void =	0.32 -
2.5938E-05	6.880559461	0.00032572	1.26E+01	Vnr =	0.8475 ml

Table: B3: FC results and calculation for pnpg adsorption onto ConA Sepharose 4B affinity media

Co [M]	Vr [ml]	q (M)	q / Co			
1.38E-03	1.15204819	0.00068152	0.495292			
6.88E-04	1.37413894	0.00065881	0.9575766			
3.44E-04	1.66347967	0.00053659	1.5598428			
1.72E-04	2.1171857	0.00043073	2.5042373	Kd =	1.70E-04	M
8.60E-05	2.29733333	0.00024761	2.8792168	Vbed =	0.7065	ml
4.30E-05	2.54003766	0.00014553	3.3844088	qmax =	7.80E-04	M
2.15E-05	2.7011236	7.9974E-05	3.7197111	void =	0.32	-
1.08E-05	2.8839	4.4077E-05	4.1001624	Vnr =	0.9141	ml

Table B4: FC results and calculation for pnpf adsorption onto LTA-Agarose affinity media (20°C)

Table B4: FC results and calculation for pnpf adsorption onto LTA-Agarose affinity media (5°C)

Co [M]	Vr [ml]	q [M]	q / Co			
0.0005	0.9200542	6.0881E-05	0.121761948			
0.00025	0.9747701	6.06903E-05	0.242761252			
0.000125	1.0605136	5.40469E-05	0.432375437			
6.25E-05	1.18505	4.4236E-05	0.707776399			
3.13E-05	1.2934573	2.96097E-05	0.947509561			
1.56E-05	1.4219599	1.92142E-05	1.229710866	Kd =	3.30E-05	M
7.81E-06	1.5589461	1.197E-05	1.532158951	Vbed =	0.7065	ml
3.91E-06	1.6814113	7.0412E-06	1.802546601	qmax =	6.60E-05	M
1.95E-06	1.7949653	4.01027E-06	2.053259402	void =	0.36	-
9.77E-07	1.9857359	2.41646E-06	2.474456581	Vnr =	0.8477	ml

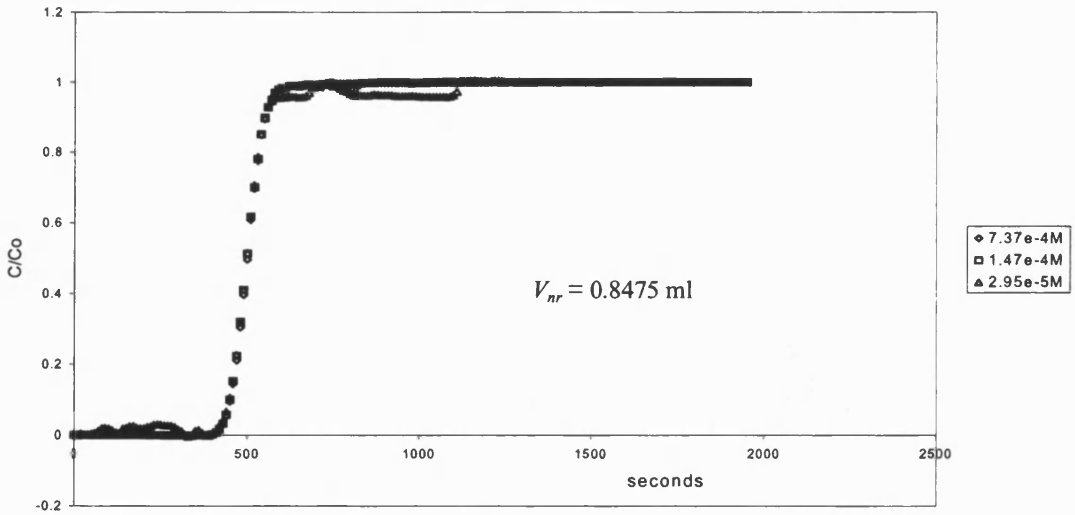

Figure B7: Three different concentrations breakthroughs of pnpa non retained sugar into LTA-Agarose 3×100 packed column operating with FPLC system.

Appendix C

From the MicroCal Origin software, the data worksheets contain:

DH	Experimental heat change per injection *i*	µcal/injection
INJV	volume of titrant injected	µl
X_t	Total Concentration of ligand before each injection	mM
M_t	Total Concentration of receptor before each injection	mM
XM_t	Total ligand-receptor molar fraction	-
NDH	Normalised heat change for injection i per mole of injected	cal/mol
Fit	Results of fitting data model	cal/mol

The amount of ligand bound during each injection (q) is related to the heat evolved *DH* by the expression:

$$q = \frac{DH}{\Delta H^{o} \cdot V_{cell}} \qquad \text{C.1}$$

Where V_{cell} is the working volume of the titration cell and ΔH^{o} is the molar heat of binding. From the initial concentration value for the receptor M_t^{o}, concentration is therefore recalculated every injection (ΔV_i) based on the conservation of mass:

$$M_t = \frac{M_t^{o}\left(2 \cdot V_{cell} - \Delta V\right)}{\left(2 \cdot V_{cell} + \Delta V\right)} \qquad \text{C.2}$$

where ΔV is the cumulative volume change and the average receptor concentration displaced in ΔV is the mean of the two concentration before and after the volume change. Assuming that the injected ligand stays in V_{cell}, the hypothetical concentration would be

$$X_t^{o} = \sum_{i=1}^{n-1} \frac{\Delta V_i \cdot X_i}{V_{cell}} \qquad \text{C.3}$$

but considering again the displaced volume effect the corrected total titrant concentration in the cell is

$$X_t = X_t^o \cdot \left(1 - \frac{\Delta V}{2 \cdot V_{cell}}\right) \qquad \text{C.4}$$

Before the displaced volume leaves the working volume V_{cell}, it contributes to the heat effect as much as the equivalent volume remaining in the cell, therefore the heat released after i^{th} injection defined in equation 2.41 is corrected as

$$\Delta Q_i = Q_i + \frac{dV_i}{V_o}\left(\frac{Q_i + Q_{i-1}}{2}\right) - Q_{i-1} \qquad \text{C.5}$$

Q is a quantity which applies only to the working volume V_{cell}.

When ΔH^o is known, from the experimental heat of binding the amount of ligand bound during each injection (q_i) is calculated with C.1.

The total bound titrant would then be $\sum_{i=1}^{n} q_i$ and with X_t and M_t data, Scatchard plots of bound fraction/free ligand (Y/F) versus bound ligand fraction (Y) can be analysed.

The bound ligand fraction Y is the concentration of bound ligand q over the total concentration of acceptor (M_t) identified in this work as lectin monomer concentration. The free ligand X is calculated as (X_t - q) after each injection.

The following table C.1 reports the kind of data obtained during an ITC experiment for ConA D-Mannose titration as an example.

Table C.1: ITC data from origin worksheet and calculated values for Scatchard plot evaluation relative to Con A titrated with D-Mannose at 20°C.

DH	INJV	Xt	Mt	XMt	NDH	Fit One	Fit Two	q	Y	Y/X
-16.7998	2.004	0	0.15	0.08378	-888	-1065.76	-1050.92	2.92731E-06		
-48.295	4.993	0.01255	0.14979	0.29303	-1031.2	-1020.72	-1012.5	1.13425E-05	0.075987	2345.456
-44.9261	4.993	0.04374	0.14927	0.503	-956.226	-959.47	-957.908	1.91708E-05	0.128879	2315.919
-42.1886	4.993	0.07482	0.14875	0.71369	-895.302	-901.921	-903.756	2.6522E-05	0.178912	2256.773
-39.7433	4.993	0.1058	0.14824	0.92511	-840.882	-847.951	-851.56	3.34471E-05	0.226422	2193.742
-37.9583	4.993	0.13666	0.14772	1.13726	-801.155	-797.42	-801.965	4.00612E-05	0.272137	2136.772
-35.5904	4.993	0.16742	0.14721	1.35013	-748.456	-750.171	-753.562	4.62627E-05	0.315356	2077.483
-33.7103	4.993	0.19806	0.1467	1.56373	-706.612	-706.037	-709.042	5.21367E-05	0.356636	2021.022
-31.9333	4.993	0.2286	0.14619	1.77805	-667.061	-664.844	-667.267	5.77009E-05	0.39608	1967.326
-30.0097	4.993	0.25903	0.14568	1.9931	-624.25	-626.418	-628.537	6.293E-05	0.433462	1914.416
-28.4382	4.993	0.28935	0.14518	2.20887	-589.273	-590.587	-590.355	6.78853E-05	0.469242	1864.479
-27.0271	4.993	0.31956	0.14467	2.42537	-557.866	-557.181	-556.225	7.25946E-05	0.503535	1817.322
-25.6191	4.993	0.34967	0.14417	2.64259	-526.529	-526.037	-526.091	7.70587E-05	0.536359	1772.494
-24.2208	4.993	0.37966	0.14367	2.86054	-495.407	-496.998	-495.955	8.12791E-05	0.56771	1729.449
-23.0823	4.993	0.40954	0.14317	3.07921	-470.066	-469.917	-467.544	8.53011E-05	0.597891	1688.867
-21.9264	4.993	0.43932	0.14267	3.29861	-444.337	-444.652	-442.666	8.91217E-05	0.626823	1650.106
-20.8955	4.993	0.46899	0.14218	3.51873	-421.392	-421.073	-419.26	9.27627E-05	0.654734	1613.49
-19.845	4.993	0.49855	0.14168	3.73958	-398.009	-399.055	-397.199	9.62206E-05	0.681497	1578.346
-19.0767	4.993	0.528	0.14119	3.96116	-380.907	-378.485	-376.375	9.95447E-05	0.707496	1545.441
-18.152	4.993	0.55734	0.1407	4.18345	-360.322	-359.255	-356.693	0.000102708	0.732527	1513.915
-17.3316	4.993	0.58657	0.14021	4.40648	-342.06	-341.266	-339.968	0.000105728	0.756656	1483.719
-16.3607	4.993	0.6157	0.13973	4.63023	-320.449	-324.427	-322.304	0.000108578	0.779793	1454.48
-15.989	4.993	0.64471	0.13924	4.8547	-312.172	-308.652	-307.421	0.000111364	0.802568	1427.408
-15.3321	4.993	0.67362	0.13876	5.0799	-297.549	-293.864	-291.493	0.000114036	0.824734	1401.693
-14.6719	4.993	0.70242	0.13827	5.30583	-282.851	-279.991	-278.194	0.000116592	0.846161	1376.951
-14.0178	4.993	0.73111	0.13779	5.53248	-268.289	-266.966	-265.592	0.000119035	0.866907	1353.157
-13.5565	4.993	0.75969	0.13731	5.75985	-258.018	-254.727	-255.437	0.000121397	0.887147	1330.528
-12.8386	4.993	0.78816	0.13684	5.98795	-242.039	-243.219	-242.275	0.000123634	0.906675	1308.55
-12.5788	4.993	0.81652	0.13636	6.21678	-236.251	-232.388	-231.488	0.000125826	0.925941	1287.918
-11.903	4.993	0.84477	0.13589	6.44633	-221.206	-222.188	-221.23	0.0001279	0.94454	1267.805
-11.5679	4.993	0.87292	0.13541	6.6766	-213.743	-212.574	-211.466	0.000129916	0.962767	1248.67
-11.3335	4.993	0.90095	0.13494	6.90761	-208.522	-203.505	-203.868	0.000131891	0.980818	1230.654
-10.7648	4.993	0.92888	0.13447	7.13933	-195.86	-194.944	-194.97	0.000133766	0.998256	1213.046
-10.4602	4.993	0.9567	0.134	7.37178	-189.078	-186.856	-186.482	0.000135589	1.015344	1196.181
-10.113	4.993	0.98441	0.13354	7.60496	-181.344	-179.209	-180.024	0.000137351	1.032172	1180.086
-9.81589	4.993	1.01201	0.13307	7.83886	-174.727	-171.974	-172.252	0.000139062	1.048651	1164.6
-9.36976	4.993	1.0395	0.13261	8.07349	-164.794	-165.123	-166.429	0.000140694	1.064655	1149.493
-9.06779	4.993	1.06689	0.13215	8.30884	-158.068	-158.632	-159.292	0.000142274	1.080372	1134.981
-8.72893	4.993	1.09416	0.13169	8.54492	-150.521	-152.477	-152.463	0.000143795	1.09575	1120.932
-8.54516	4.993	1.12133	0.13123	8.78172	-146.426	-146.637	-147.471	0.000145284	1.11099	1107.55
-8.17033	5	1.14839	0.13077	9.01958	-137.825	-141.088	-142.673	0.000146708	1.125837	1094.467
-8.02285	5	1.17537	0.13031	9.25817	-134.541	-135.812	-136.604	0.000148106	1.140504	1081.924
-7.70459	5	1.20225	0.12986	9.49749	-127.463	-130.795	-130.783	0.000149448	1.154933	1069.806
-7.58947	5	1.22902	0.1294	9.73753	-124.899	-126.022	-128.143	0.000150771	1.169219	1058.203
-7.43135	5	1.25568	0.12895	9.9783	-121.379	-121.479	-122.721	0.000152066	1.18339	1047.095
-7.40032	5	1.28223	0.1285	10.2198	-120.684	-117.151	-117.515	0.000153355	1.197619	1036.617
-6.90078	5	1.30867	0.12805	10.46202	-109.577	-113.025	-113.931	0.000154558	1.211266	1026.112
-6.76392	5	1.335	0.1276	10.70497	-106.53	-109.09	-110.495	0.000155736	1.224726	1015.962
-6.48776	5	1.36122	0.12716	10.94865	-100.387	-105.334	-107.199	0.000156867	1.237997	1006.123
-6.33094	5	1.38733	0.12671	11.19306	-96.8963	-101.748	-102.666	0.00015797	1.251047	996.5564
-6.40378	5	1.41334	0.12627	11.43819	-98.5088	-98.3217	-99.6552	0.000159086	1.26429	987.6149
-6.0997	5	1.43923	0.12583	11.68405	-91.7456	-95.0458	-96.7627	0.000160148	1.277203	978.7956
-5.9873	5	1.46502	0.12539	11.93064	-89.2418	-91.9122	-92.6607	0.000161192	1.29005	970.3208
-5.69781	5	1.4907	0.12495	12.17795	-82.8026	-88.9132	-91.3195	0.000162185	1.302582	961.9646
-5.80936	5	1.51627	0.12451	12.426	-85.2755	-86.0413	-87.4556	0.000163197	1.315361	954.174
–		1.54173	0.12407	–						

Appendix D

Chromatograms relative to ConA-Sepharose packed columns

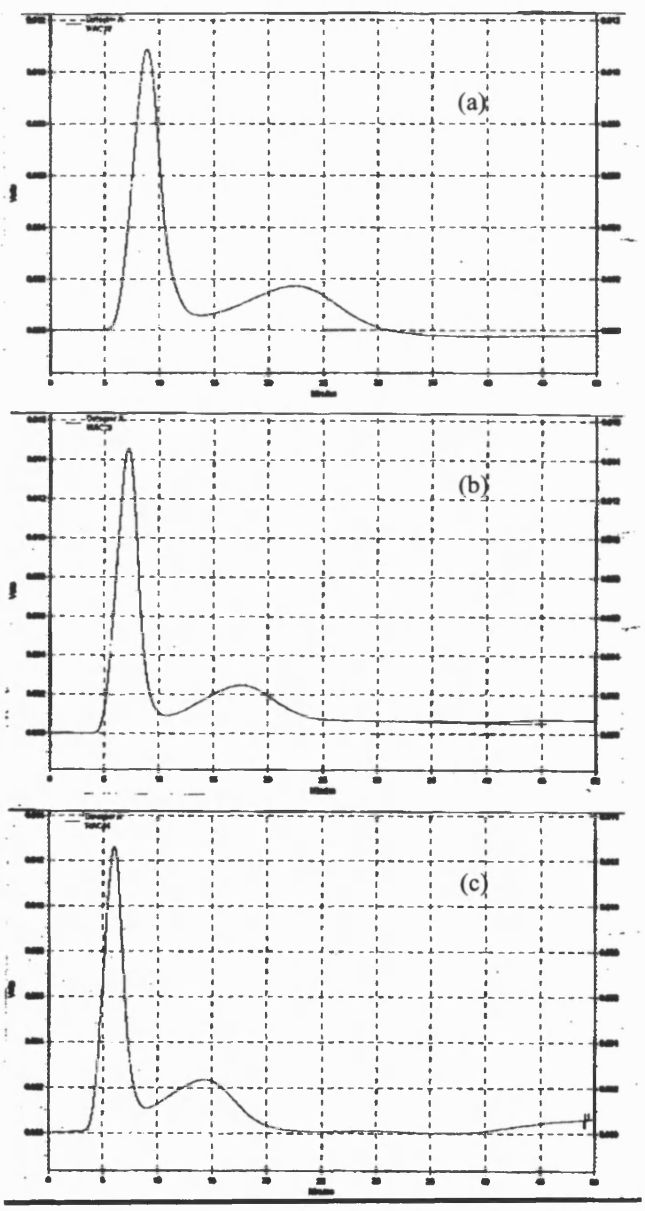

Figure D.1: Affinity chromatography of L-Fucose (1 mg/ml) and D-Mannose (1 mg/ml) in order of elution. (a): 0.2 ml/min, Y-axis range 0 - 0.012 volts. (b): 0.25 ml/min, Y-axis range 0 - 0.016 volts. (c): 0.3 ml/min, Y-axis range 0 - 0.014 volts. Column 4 × 114 mm.

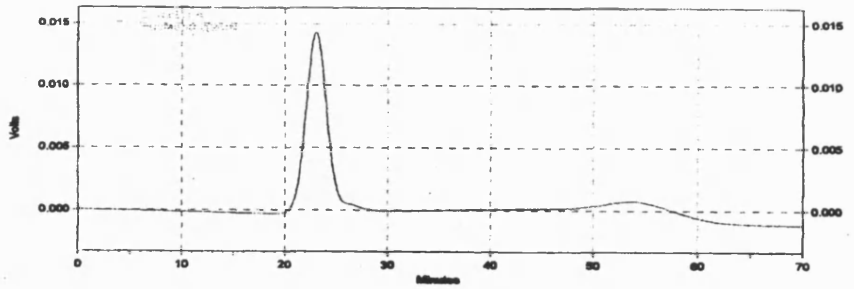

Figure D.2: Injection of 5 µl with 1mg/ml Fucose (first peak) and 1 mg/ml Mannose (second peak). Flow rate 0.2 ml/min. Column 4.4 × 250 mm.

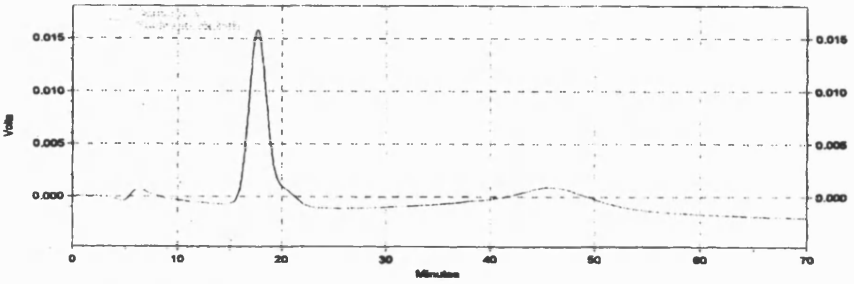

Figure D.3: Injection of 5 µl with 1mg/ml Fucose (first peak) and 1 mg/ml Mannose (second peak). Flow rate 0.25 ml/min. Column 4.4 × 250 mm.

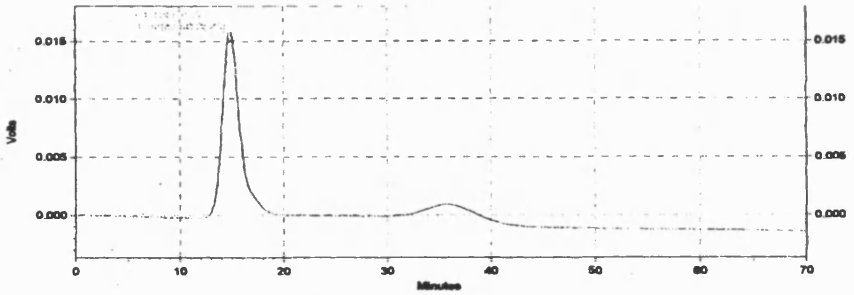

Figure D.4: Injection of 5 µl with 1mg/ml Fucose (first peak) and 1 mg/ml Mannose (second peak). Flow rate 0.3 ml/min. Column 4.4 × 250 mm.

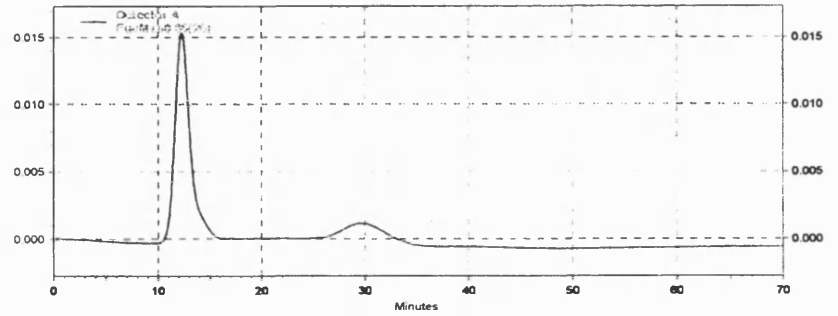

Figure D.5: Injection of 5 µl with 1mg/ml Fucose (first peak) and 1 mg/ml Mannose (second peak). Flow rate 0.35 ml/min. Column 4.4 × 250 mm.

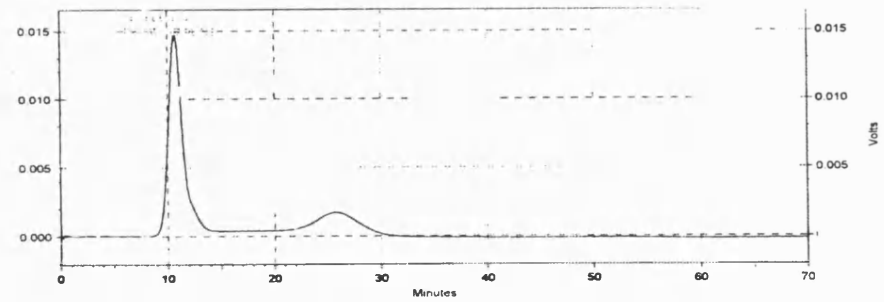

Figure D.6: Injection of 5 µl with 1mg/ml Fucose (first peak) and 1 mg/ml Mannose (second peak). Flow rate 0.4 ml/min. Column 4.4 × 250 mm.

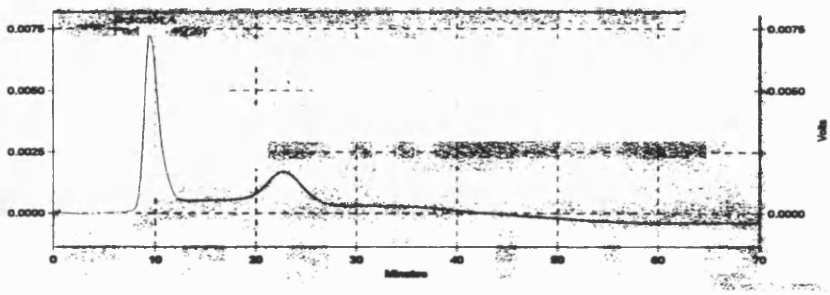

Figure D.7: Injection of 5 µl with 1mg/ml Fucose (first peak) and 1 mg/ml Mannose (second peak). Flow rate 0.45 ml/min. Column 4.4 × 250 mm.

Appendix E

Presentation

"Do Lectin monomers show 1:1 binding with monosaccharides?"
Presented (poster) at The 19th International Lectin Meeting, (INTERLEC 19th), Fortaleza, Brazil 25–30th, March, 2001.

Poster presentation recognised as prize-winning contribution by the organiser.

Do Lectin monomers show 1:1 binding with monosaccharides ?

Fabio Sartori & John Hubble

Department of Chemical Engineering, University of Bath, UK

ABSTRACT

Legume lectins generally consist of two or more subunits in a multimeric arrangement with each monomer usually considered to bind one specific oligosaccharide molecule. In this study results obtained for Concanavalin A (ConA) using a frontal chromatography approach suggest that in the case of monosaccharides each monomer may be capable of binding more than one sugar molecule.

In frontal chromatographic systems, once breakthrough is complete, adsorbate in solution will be in equilibrium with the immobilised lectin allowing the partition isotherm of a specific sugar to be characterised. In this work affinity chromatography was conducted with ConA immobilised on Sepharose4B with experiments carried out over a range of feed concentrations using pnp-D-Glucopyranoside as the adsorbing species. The results obtained showed the maximum binding capacity observed gave a ratio of adsorbate to immobilised monomer significantly greater than 1.

Analysis of the binding data obtained suggests that each ConA monomer is capable of binding 2 pnp-D-Glucopyranoside molecules. The binding isotherms and breakthrough curves obtained are best described in terms of a two site Adair equation where the association constant for the second sites greater than the first, i.e. positively cooperative. The results of the chromatographic study are supported by data obtained using an isothermal titration calorimeter which also showed binding stoichiometrys greater than one.

BACKGROUND

Concanavalin A (ConA) is a legume which, at ambient temperature and neutral pH, comprises of four non-glycosylated subunits of 26 kDa, held together by non-covalent interaction. Each subunit or monomer, is considered to contain a single specific sugar binding site.

ConA will bind both terminal ~linked D-glucose and N-acetylglucosammine [1]; however, higher affinity is exhibited for D-Mannose and its glycosides in ~anomeric form Man•1-6(Man•1 3)Man). In 1989 Derewenda *et al.* [2] and Loris *at al.* [3] elucidated, at atomic resolution, the crystal structure of both ConA-methyl-~D-mannopyranoside and ConA-trimannoside complexes.

These results identifyied all the key features of binding in terms of the linkages between sugar carbons and lectin aminoacids.

This raises an interesting question: since the binding site can accomodate a trimannoside molecule, is it possible that more than one small monosaccharide molecule could be bound with weaker affinity?

Evidence for this possibility is provided by HPLC studies conducted by Ackerson *et al.* [4] where immobilised ConA showed a greater than theoretical capacity leading the authors to consider the possibility of a second population of non-specific binding sites.

Similarly, an isothermal calorimetric titration study with ConA carried out by Williams *et al.* [5] suggests that binding can occur through a number of n distict sites instead of a single high affinity site.

OBJECTIVE

To investigate the binding stoichiometry of monosaccharide/monomer interactions for Concanavalin A, both immobilised on Sepharose 4B, and in free solution.

MATERIALS & METHODS

ConA immobilised on Sepharose 4B, obtained from SIGMA Chemicals Ltd, was slurry packed in a 3×10 mm glass column. P-nitrophenil- D-Glucopiranoside, D-Glucosio, lyophilized ConA, salts and buffer all of high purity were purchased from SIGMA Chemicals Ltd.

Experiments were all carried out in Tris Buffer 20 mMol, pH 7.2-7.4, containing 150 mMol NaCl, 0.5 mMol $CaCl_2$, $MnCl_2$, $MgCl_2$, and 0.02% Thimerosal.

Frontal loading of pnp-Glucopiranoside at different concentrations throughout the ConA-Sepharose column was performed at 0.1 ml/min. From each breakthrough curve the retention volume is calculated from,

$$V_r = \frac{1}{C_0}\int_0^{C_0} V(C)\,dC$$

V_r, the retention volume for an unretained solute, was determined from the breakthrough curve of pnp-arabinopiranoside solutions.

B_m, the amount of pnp-D-Glc specifically bound to the stationary phase each run can be determined from,

$$B_m = C_0\,(V_r - V_0)$$

The equilibrium partition isotherm of a specific ligand between mobile and stationary phase can be calculated using this method. [6]

The experimental equilibrium points obtained (adsorbed solute, (q) vs mobile phase concentration, (C)) were then fitted using both single site (Langmuir) and two sites model (Adair [7]) models using a commercial package (Scientist Micromath ltd).

$$q = \frac{q_{max}\cdot C}{K_d + C} \qquad \text{(Langmuir)}$$

$$Y = \frac{K_{a1}C + K_{a1}K_{a2}C^2}{1 + 2K_{a1}C + K_{a1}K_{a2}C^2} \qquad \text{(Adair)}$$

where q is the number of moles of adsorbed pnp-Glc per liter of gel, K_d is the dissociation constant and q_{max} is the gel maximum binding capacity, Y is the fraction of occupied sites and K_{a1} and K_{a2} are the two microscopic association constants in the case of Adair model for two sites.

The equilibrium constants calculated from the best fitting of the experimental results have been adopted in a multistage model to describe the original experimental breakthrough curves.

In this model the column is treated as a series of N equilibrium stages in which the mass balance for each stage is;

$$C_{wi} = \varepsilon\cdot C_{i,i-1} + \alpha\cdot(C_{i,j} + q_{i,j})$$

$j = 1,\ldots N$ stages

$i = 1, 2$

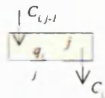

The subscript i indicates the loading step for each stage: 1 before, 2 after equilibrium, • is the external void volume fraction and • is the stationary phase volume fraction.

A thermodynamic assessment of ConA-D-Glc interactions has also been conducted using a MicroCal VP Isothermal Titration Calorimetry System. In this case, ConA solution (0.385 mM, monomer concentration) was titrated with 56 injections 5+l each of D-Glc solution (15,56 mM). One binding site per monomer and a reaction stoichiometry equal to 1 have been assumed to interpret the calorimetric data with Origin Software package.

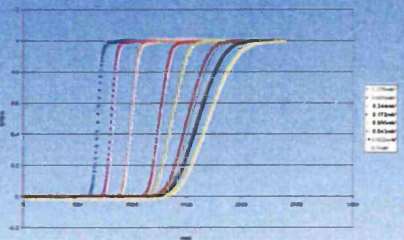

Fig.1: Normalised breakthrough curves, representing the experimental elution profile of pnp-D-Glc solutions at different feed concentration throughout the ConA-Sep. column.

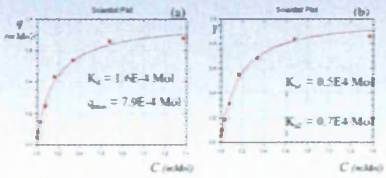

Fig.2: Experimental adsorption equilibrium points for the system ConA-Sep., pnp-Glc, fitted by (a) Langmuir equation, (b) Adair model two binding sites.

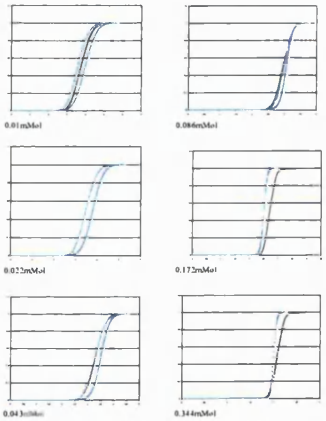

Fig.3: Multistage equilibrium model description of experimental breakthrough. ___ : Experimental, ■ : Langmuir, ▲: Adair 2 binding sites.

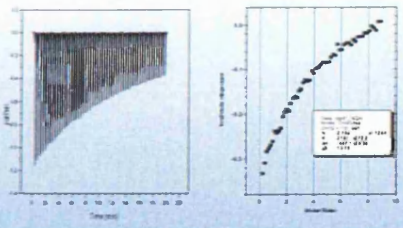

Fig.4: Micro-calorimetric titration of ConA solution with D-Glucose as ligand. Results shown are calculated assuming unitary binding stechiometry and considering monomer concentration.

RESULTS & DISCUSSION

- Figure 1 shows the concentration dependence of pnp-D-Glc breakthrough front (non-retained solute breakthrough curves are not reported but showed similar shape and the expected V_r value over a wide range of concentrations.
- A sdorption equilibrium points calculated using the frontal chromatography approach are well described by a Langmuir equation (Figure 2.a) but the calculated maximum binding capacity of 8E-4 Mol is much higher than the theoretical value (4E-4 Mol), calculated from the manufacturer's data on immobilised ConA concentration (10 - 15 mg/ml).
- This excess capacity could be explained by the existence of multiplet binding site on each monomer. Taking the simplest case of two sites per monomer figure 2 shows the experimental points and the fits obtained to the Langmuir model (a) and Adair model (b) and reports the respectives association constants. In the Adair case $K_{a2} > K_{a1}$ indicating positive homotopic cooperativity. However, there is little to distinguish the quality of the fits obtained and on this data alone it would be difficult to justify the introduction of the extra parameter required by the Adair model.
- While the multi-stage equilibrium model used to predict breakthrough curves shows little difference between Adair and Langmuir models at high concentration. The Adair based model gives significantly better predictions when low feed concentrations are used. In both cases some discrepancy between experimental data and prediction is inevitable as the models do not consider mass transfer limitations.
- The results of the ITC measurements reported in Figure 4 show an inconsistency with the assumption of a single site per monomer for the interaction of ConA-D-Glc.

REFERENCES

1. Van Damme, E.J.P., Peumans, W.J., Pusztai, A., Bardocz, S. Handbook of plant lectins: Properties and Biomedical Applications, Wiley, 1998.

2. Derewenda Z., Yariv J., Helliwell J.R., Kalb A.J., Dodson E.J., Papiz M.Z., Wan T., Campbell J., EMBO J., 8, 2189-2193 (1989).

3. Loris, M., Hamelryck, T., Bouckaert, J., Wyns, L., Biochim. Biophys. Acta 1383, 9-36, (1998).

4. Ackerson, D.S., Wallace, R.R., J. Chrom., 376, 49-60, (1986).

5. Williams S.-K., Townsend M. C., Jones R. L., J. Biol. Chem., 267, No.32, 22967-22970, (1992).

6. Kasai Kan-ichi, Yoko-Oka, J. Chrom., 376, 33-47, (1986).

7. Adair G. S., J. Biol. Chem. 63, 529-545, (1925).

ACKNOWLEDGEMENTS

Financial support from Bioresources (Biotechnology) is gratefully acknowledged.